Studies on the Mode of Action of a Class of Antimicrobial Peptide Mimetics

---

Dissertation

zur

Erlangung der naturwissenschaftlichen Doktorwürde
(Dr. sc. nat.)

vorgelegt der

Mathematisch-naturwissenschaftlichen Fakultät

der

Universität Zürich

von

Peter Jetter

aus

Deutschland

Promotionskomitee

Prof. Dr. John A. Robinson (Vorsitz)

Prof. Dr. Leo Eberl

Prof. Dr. Nathan W. Luedtke

Zürich 2007

For Sonya

1 Introduction

Antimicrobial research is driven by the contributions of many different disciplines such as medicine, chemistry, biochemistry, microbiology, bacteriology, and pharmaceutical chemistry. Arguably only few areas of research have had such a profound influence upon human society as the introduction of antibiotics into clinical practice. At present, the vast majority of known microbial infections are amenable to antibiotic therapy and around 250 different antibacterial compounds, plus an increasing number of antimycobacterial, antiviral, antiretroviral, antifungal, antiprotozoal, and anthelmintic agents are available for their treatment.[1] Notwithstanding the tremendous success of past and present antimicrobial chemotherapy, factors such as the increase of widespread bacterial resistance, the emergence of new pathogens, or the increase in human life expectancy, together with increased susceptibility of the elderly to infectious diseases, lead to the continued demand for developing future antimicrobial agents.

1.1 Antibiotics and chemotherapy

The notion of antibiotic action (*antibiosis*) was first introduced by Vuillemin, a pupil of Pasteur, in 1889 to describe an antagonism between micro-organisms: "*principe actif d'un organisme vivant qui détruit la vie des autres pour protéger sa propre vie*".[2] Already in the previous decade of the same century - and over fifty years before the discovery of penicillin by Fleming in 1928[3] - Pasteur and Joubert described an antagonism involving the anthrax bacterium[4] and Tyndall noted the retarding effect of a mould on bacterial growth.[5] It is noteworthy in this respect that the first commercially available antibiotic to find therapeutic use was an extract of *Pseudomonas aeruginosa*, called pyocyanase.[6] In 1942 the term antibiotic was redefined by Waksman to denote substances produced by micro-organisms antagonistic to the growth or life of other micro-organisms in high dilution.[7]

Antimicrobial chemotherapy is generally defined as the administration of a compound with systemic action, meaning that the compound reaches the infected area via the bloodstream.[1] Traditional remedies which are capable of systemic action include quinine from cinchona bark and emetine from the ipecacuanha root.[8] The

concept of chemotherapy was coined by Paul Ehrlich at the beginning of the twentieth century, founded on his belief that infectious diseases could be treated with synthetic chemicals.[9] Other concepts introduced by Ehrlich into the field of antimicrobial research include (a) that antimicrobial agents should be toxic compounds which bind to micro-organisms - by means of chemical receptors - and that the binding of the micro-organism relative to the host determines the effectiveness of the compound, (b) the use of screening processes to aid in drug discovery, (c) the chemical modification of existing compounds to improve their pharmacological properties, and (d) the notion that drugs can be activated by metabolism in the host organism. Furthermore, Ehrlich proposed that bacteriostatic action of a compound, that is the inhibition of bacterial growth instead of direct killing, can be sufficient for the immune system of the host to cope with the infectious disease.[10]

The beginning of modern chemotherapy was marked by the introduction of the sulfa drugs, and their forerunner prontosil rubrum, by Domagk in 1935,[11] followed by the antibiotic revolution set off by the re-evaluation of penicillin through Chain and Florey in 1940.[12] Inspired by their tremendous success, the screening of microbial cultures lead to the discovery of most of the classes of antibiotics that are in current use, such as the aminoglycoside, macrolide or glycopeptide antibiotics. Following a period of extensive screening programmes, both the synthetic- and discovery-based approaches have converged by introducing chemical variations into the scaffolds of established antibiotics, as exemplified by the development of four generations of semi-synthetic cephalosporins.[13]

1.2 Bacterial targets of antimicrobial action

As already noted by Ehrlich, the fundamental basis of antimicrobial chemotherapy is the selective toxicity of antibiotics towards micro-organisms. Fortunately, there exist sufficient differences in the structure and organisation of microbial and mammalian cells to allow for selective drug action.[14] Probably the most prominent example of this principle is manifested in the bacterial cell-wall, which is absent from higher organisms and thus a natural target of several antibiotics in current use. Other important processes that are targeted by antibiotics include bacterial protein synthesis, replication and transcription of DNA, or folate synthesis.

Table 1.1 Site of antibacterial action and primary targets of antibiotics frequently used for the systemic treatment of infectious diseases.

Site of action	(Class of) Antimicrobial agent	Primary Target(s)
Cell wall	β-Lactams and cephalosporins	Transpeptidases / transglycosylases (PBPs)[a]
	Glycopeptides	D-Alanyl-D-alanine of peptidoglycan / lipid II
	Cycloserine	Alanine racemase / D-alanine synthetase
	Fosfomycin	Pyruvyl transferase
Protein synthesis	Chloramphenicol	Peptidyl transferase
	Aminoglycosides	Initiation complex / translation
	Tetracyclines	Ribosomal A-site
	Macrolides	Translocation
	Oxazolidinones	Formation of 70S initiation complex
Cell membrane	Colistimethate sodium[b]	Bacterial phospholipids
Folate synthesis	Sulfonamides	Pteroate synthetase
DNA replication	Quinolones	DNA gyrase
	Novobiocin	DNA gyrase
RNA synthesis	Rifampicin	RNA polymerase

[a] PBPs ≡ penicillin binding proteins; [b] colistimethate consists of poly-sulfomethylated polymyxins.

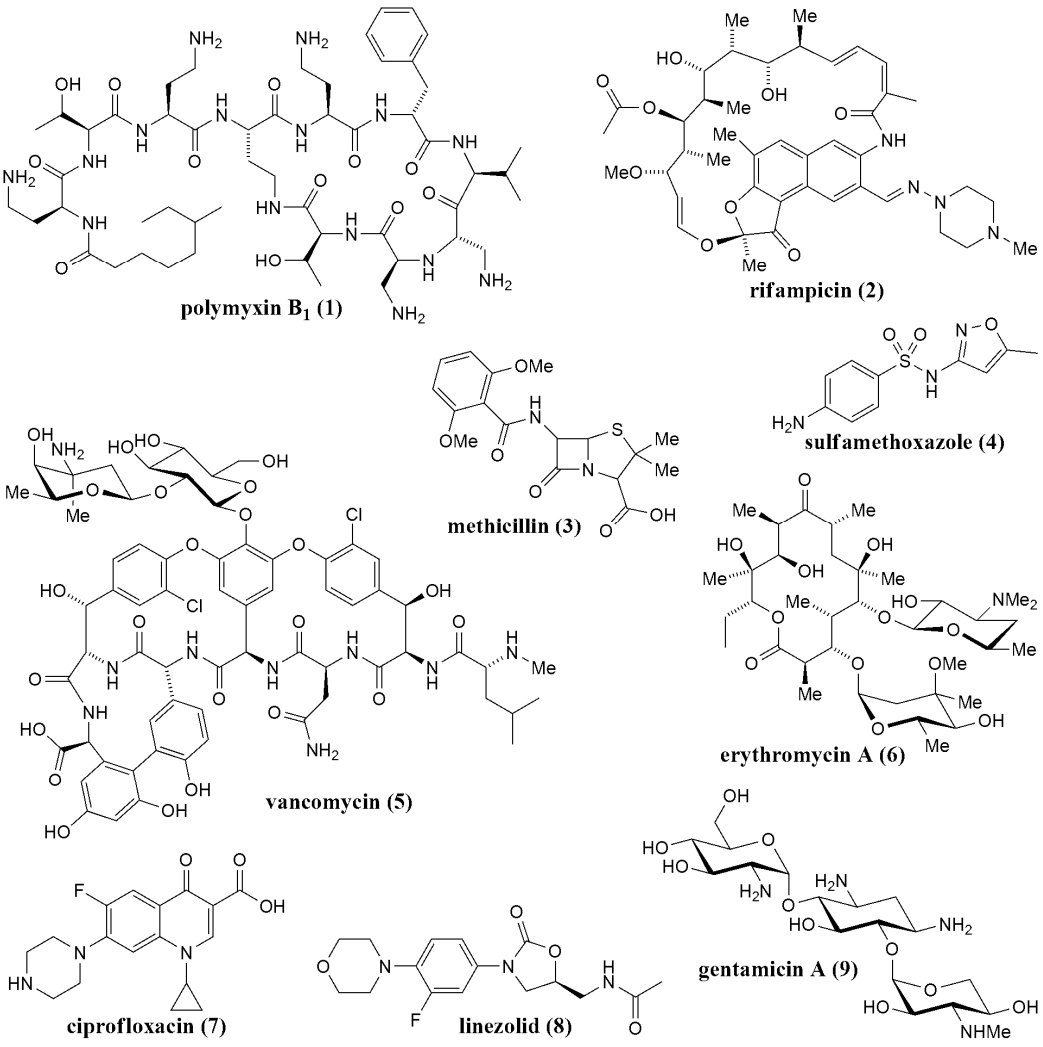

Figure 1.1: Structural diversity of various antibiotics in current clinical use. Polymyxins are generally confined to topical applications.

A summary of currently used antibiotics and their bacterial targets is given in **Table 1.1** and the structural diversity of some of these compounds is indicated in **Figure 1.1**.

1.3 Bacterial resistance and the need for new antibiotics

Antibiotic resistance is an increasing problem associated with, and endangering the use of, clinically relevant antibiotics as frequently accentuated in the literature.[15] Several mechanisms exist by which micro-organisms evade the action of antibiotics and the most common of these are:

- Enzymatic inactivation of drugs (e.g. through β-lactamases, chloramphenicol acetyl transferase, aminoglycoside inactivating enzymes).
- Modification of the bacterial cell envelope (e.g. alterations in membrane composition or the expression of porin proteins).
- Drug removal from the microbial cell (e.g. multidrug efflux pumps).
- Modification of the antibiotic target (e.g. mutations in penicillin binding proteins or RNA polymerase).
- Metabolic bypass (e.g. replacement of the D-alanyl-D-alanine terminus in enterococci).

Resistance is due to the genetic flexibility of micro-organisms in combination with the large populations encountered in typical infections, and their short generation times.[14] Three important genetic bases exist for the development of bacterial resistance. Firstly, bacteria such as *P. aeruginosa* show a high degree of intrinsic resistance which is caused by a combination of decreased antibiotic uptake and the prevalence of multidrug efflux systems.[16] These free-living soil organisms have evolved under exposure to antibiotics in the environment for aeons and were probably already resistant to many antibiotics when they became available for treatment. Secondly, spontaneous mutations affecting genes – especially those encoding target sites of antimicrobial drug action - can lead to resistance. While spontaneous mutation is an important mechanism for the development of resistance in bacterial populations it is thought to be the main mechanism in viral populations since the DNA replication machinery of these pathogens lacks sophisticated proof-reading abilities. In contrast, for bacteria, the most important origin of drug resistance is horizontal gene transfer via conjugation, transduction, or transformation.[17] A well-

studied mechanism for the spreading of resistance genes in Gram-negative bacteria consists of cellular conjugation mediated by so-called R-plasmids.[18]

Several approaches exist to preserve the usefulness of existing antibiotics and to minimise the effects of bacterial resistance. Foremost amongst these are the rational use of antibiotics and improved efficiency in treating microbial infections by the right choice of drugs or combinations thereof. For decades, resistance was successfully fought by introducing chemical modifications into semi-synthetic derivatives but the increased pressure of resistance leads to increased effort to find drugs with new targets and/or belonging to new chemical classes. Different strategies exist for antimicrobial drug discovery such as target-based high throughput screening.[19] In addition to phenotypic screening and due to the availability of more than 300 microbial genome sequences (September 2006), functional genomic approaches play an increasing role in various aspects of antimicrobial research.[20] For instance, the comparison of human and pathogen genome sequences can be used for the selection and validation of antibacterial targets, and transcriptome and proteome expression profiling can help in elucidating antimicrobial modes of action.[21] Nevertheless, it has to be mentioned that targets identified by such methods are not necessarily viable for drug development, since the screening conditions generally ignore important aspects such as cell permeability.[22]

1.4 Antimicrobial peptides (AMPs)

One class of compounds that shows considerable promise for development into novel antimicrobial agents and which has therefore recently received an increased amount of interest are the so-called antimicrobial peptides (AMPs). These are short peptides of typically less than 50 amino acids found widespread throughout all kingdoms of life; representatives have been isolated from such diverse sources as mammals, fish, molluscs, amphibians, insects, and plants. AMPs typically show broad spectra of activity against Gram-positive as well as Gram-negative organisms and they also frequently display antifungal, antiprotozoal, and antiviral properties.[23] AMPs are thought to be part of the innate immune system,[24] and although they show large structural diversity in primary sequences as well as with respect to their secondary structures, they share common physico-chemical parameters. Most prominently, due to the high abundance of lysine and arginine residues, virtually all

AMPs bear multiple positive charges at physiological pH; hence they are sometimes collectively referred to as cationic AMPs. Furthermore, most of them are able to form amphipathic structures, at least after interaction with membranous systems. It has to be mentioned that some negatively charged AMPs such as dermcidin from human sweat glands have been described,[25] but their antimicrobial activity is often only modest.

The main mechanism of action for the vast majority of these compounds is thought to be the disturbance and/or disintegration of membrane structures. A detailed discussion of these and alternative mechanisms of AMP action will be deferred until **Chapter 2**, but it is indicated at this point to emphasise that the targeting of the microbial membrane is far from being unprecedented in either research or clinical applications. For example, polymyxin B (**1**) and colistin, two peptide antibiotics, are often included in topical applications and colistimethate sodium, a polymyxin derivative, finds systemic use in combination therapies directed against *P. aeruginosa* (c.f. **Table 1.1**).[26] However, it is in the field of AMPs that such agents reach a level of discrimination between mammalian and microbial membranes that is sufficient for conceivable systemic use on a broader therapeutic scale.

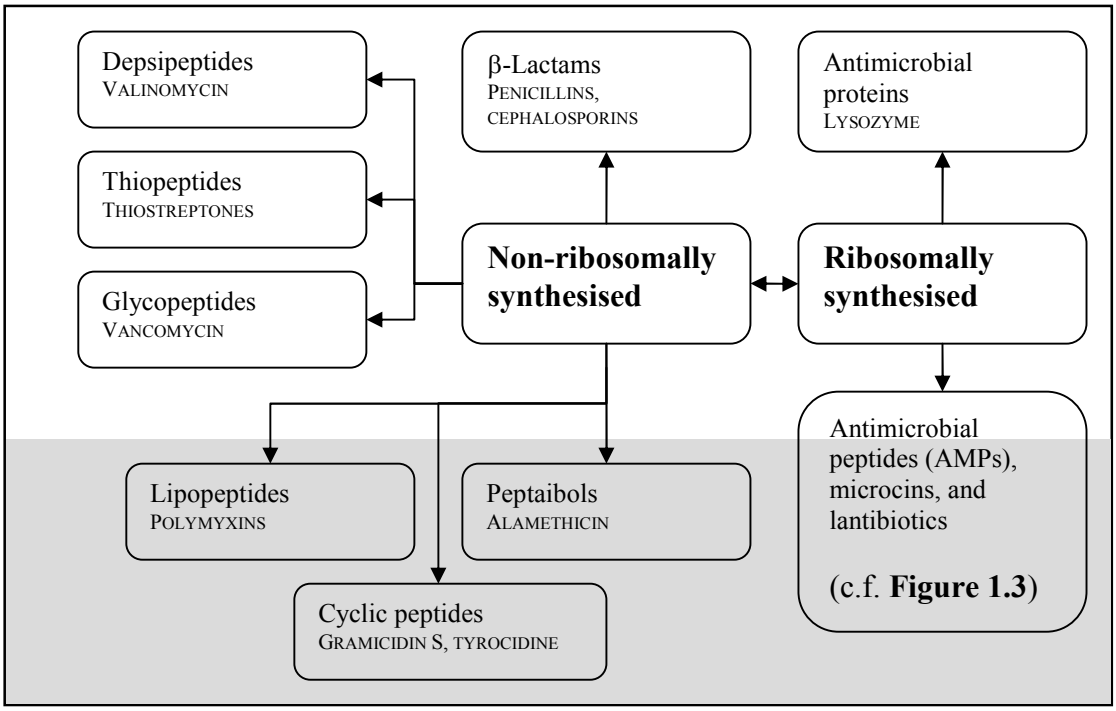

Figure 1.2 An overview of major classes of antimicrobial compounds that contain peptide bonds (peptide antimicrobial agents). The grey box highlights similarity in the presumed and/or proven membrane-active mechanisms of the contained (classes of) compounds.

Because there is occasionally some confusion in the literature, it is desirable to give a more rigorous definition of the term AMP and of the way it will be used throughout this work. A superficial definition of a peptidic compound with antimicrobial activity will not do, since this does not differentiate them from compounds of such paramount clinical importance as the glycopeptide antibiotics.[27] These and other antibiotics, such as the already mentioned polymyxins, are generally referred to in the literature as peptide antibiotics.[28, 29] A natural way of distinguishing AMPs from these compounds is provided by their biosynthetic origins (**Figure 1.2**). All peptidic antibiotics (peptide antimicrobial agents) that are in current clinical use are of non-ribosomal origin, and this holds also for β-lactams and cephalosporins, although they are not generally termed peptide antibiotics. In addition to the principal classes of peptide antibiotics depicted on the left side of **Figure 1.2**, various compounds that share features of more than one class have been described. Well-studied examples of such composite peptide antibiotics comprise teicoplanin (lipoglycopeptide), daptomycin (lipodepsipeptide), or ramoplanin (lipoglycodepsipeptide).[30]

In contrast to these peptide antibiotics, AMPs are exclusively of ribosomal origin. They are gene-encoded, i.e. one gene encodes for one peptide and they are synthesised as prepropeptides containing an N-terminal signal sequence, a highly conserved pro-region, and a highly variable C-terminal cationic peptide region.[31] After the signal sequence is removed by signal peptidases,[32] the release of the AMP in its active form depends on further proteolytic processing.[33] Different proteases are involved in different species to cleave off the propeptide region. Additionally, the C-terminus of the AMP is frequently amidated by the action by peptidylglycine α-amidating monooxygenase (PAM).[34] The majority of ribosomally synthesised peptides with antimicrobial activities is of eukaryotic origin but three classes of peptides are produced by prokaryotes, namely the class I and II bacteriocins from Gram-positive and the microcins from Gram-negative species. Extensive post-translational modifications occur in the biosynthesis of class I bacteriocins (often better known as lantibiotics) and microcins; for example, the nisin gene cluster consists of 11 distinct gene products.[35] Therefore it seems justifiable to exclude them from a classification as AMPs. Class II bacteriocins, on the other hand, are unmodified polypeptides consisting of 20 to 60 amino acids and thus will be treated as

AMPs, although the gene clusters of these peptides are more complex than those of their eukaryotic counterparts.[36]

Extensive post-translational modifications are not confined to micro-organisms. Primate θ-defensin (RTD-1) is initially processed like a normal defensin, but is subsequently backbone-cyclised.[37] Moreover, two distinct genes are responsible for the amino acid sequence of the mature peptide. Other backbone-cyclic peptides such as the plant cyclotides,[38] have been described to display antimicrobial activity, and as in the case of RTD-1 little is known about the mechanisms of their cyclisation.[39] Analogously to the lantibiotics and microcins, these compounds will therefore not be regarded as genuine AMPs.

Finally, anionic AMPs and several cationic AMPs such as buforin or lactoferricin B are products of the proteolytic processing of larger peptides/proteins that have a distinct function in the cell apart from the independent antimicrobial activity of their processing products. It is noteworthy that the parental proteins might even display antimicrobial activity on their own, as is the case for lysozyme. These fragments were first proposed to constitute a distinct subclass of AMPs by Boman.[40]

In the following discussions, the term AMPs will be used to describe those ribosomally derived polypeptides from eukaryotic organisms and the class II bacteriocins that are capable of exerting their antimicrobial action without distinct post-translational modifications, i.e. modifications that require the presence of tailoring enzymes whose function(s) are only associated with the synthesis of the (class of) antimicrobial agent (c.f. **Figure 1.3**).

1.4.1 Classification of AMPs

At present, more than 1000 different AMPs have been isolated from natural sources, not to mention the large number of derivatives synthesised in order to optimise their biological properties. Several comprehensive online databases of AMPs are available, which can be searched according to primary sequences, secondary structures or reported activity spectra.*

* See for example: http://www.bbcm.units.it/~tossi/pag1.htm, http://research.i2r.astar.edu.sg/Templar/DB/ANTIMIC/, and http://aps.unmc.edu/AP/main.php.

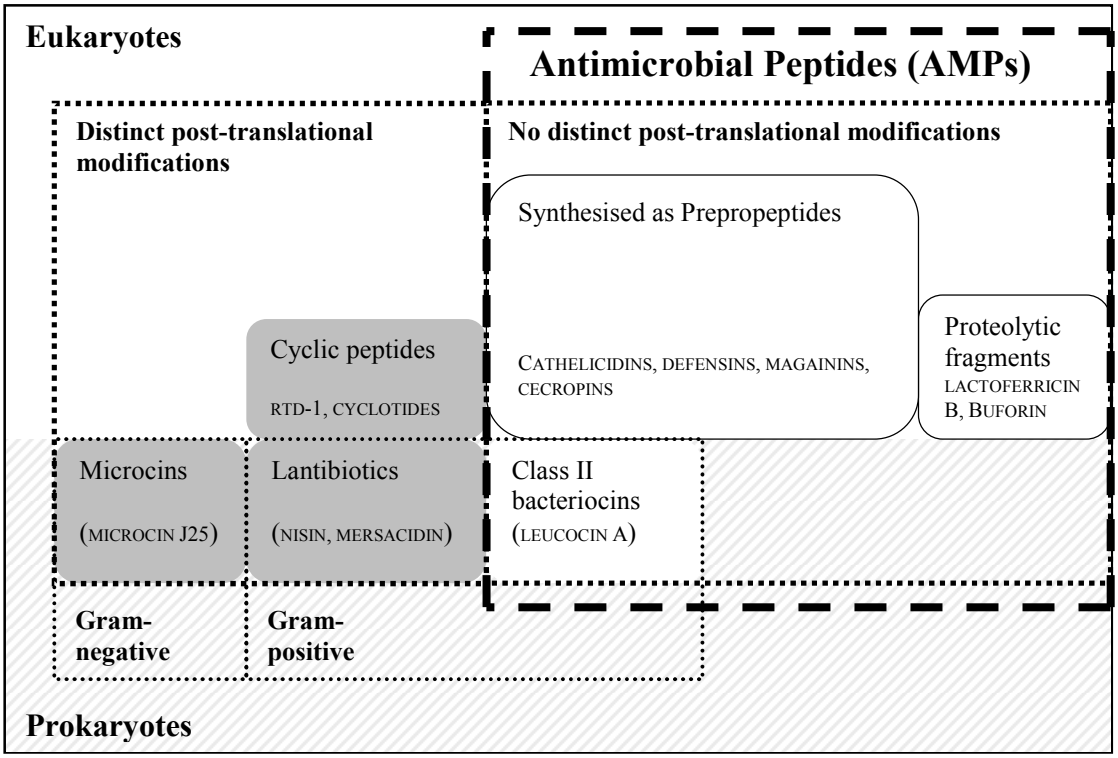

Figure 1.3 Classification of ribosomally synthesised peptide antimicrobial agents apart from antimicrobial proteins (c.f. **Figure 1.2**). Compounds treated as genuine AMPs in this work are indicated by the broken line (see text). Note that the compounds in the shaded area fulfil all requirements of Waksman's antibiotic definition.

Due to the large number of AMPs it is desirable to classify them further. Various classification schemes exist, for instance they can be grouped according to which organism or class of organisms they originate from, which kind of tissue they are expressed in, or on the basis of their antimicrobial spectra. However by far the most common approach adopted in the literature for organising the multitude of AMPs consists of classifying them according to their (secondary) structural features. As mentioned, most AMPs are able to adopt a defined secondary structure, at least upon interaction with membranous systems, and they are accordingly grouped into four different structural classes.[41] The two largest classes are comprised of linear α-helical and β-sheet/β-hairpin AMPs. Among the latter, subclasses are often introduced, for example according to how many disulfide bonds are involved in constraining the peptide conformation; compounds containing between two and five disulfide bonds have been described. The third important class of AMPs consists of peptides enriched in certain amino acids such as the Trp-rich, His-rich or Pro/Arg-rich AMPs. Only limited structural data for this class of AMPs is available, although

those peptides with an unusually high proportion of proline in their sequence are sometimes described to possess a type II poly-L-proline helix, based on CD and FTIR spectroscopic data.[42] They are therefore sometimes alternatively denoted extended helical peptides.[41] The fourth class, which contains only a small number of AMPs, is made up of compounds containing loop structures, such as thanatin or bactenecin. Looped structures are often defined as possessing only one disulfide bridge,[43] although this criterion might seem rather arbitrary and especially thanatin could also be classified as a β-sheet/β-hairpin peptide. Due to the large number of AMPs described in the literature no attempt can or will be made here to digress into an exhaustive description of the different classes, sequences, structures, sources, and activities of these substances. Rather **Table 1.2** and **Figure 1.4** serve to hint at these aspects of AMPs. A multitude of review articles focusing on all aspects of AMP chemistry and biology is available (for recent reviews, see [23, 44-47]).

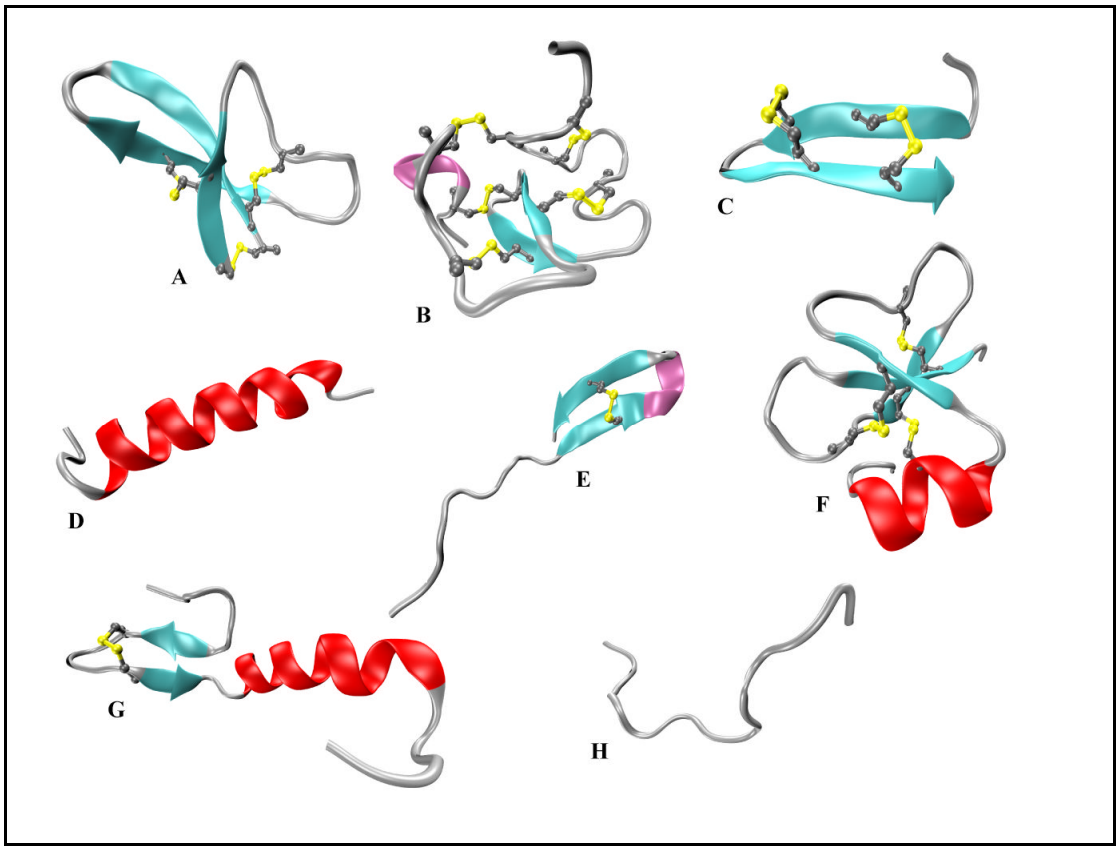

Figure 1.4: Structural diversity of antimicrobial peptides. (**A**) HBD-2 [PDB code 1FD3];[48] (**B**) EAFP-2 [PDB code 1P9Z];[49] (**C**) protegrin-1 (**11**) [PDB code 1PG1];[50] (**D**) pleurocidin [PDB code 1Z64];[51] (**E**) thanatin [PDB code 8TFV];[52] (**F**) HNP-2 variant [PDB code 1ZMH];[53] (**G**) leucocin A [PDB code 1CW6];[54] (**H**) indolicidin [PDB code 1G89].[55] The illustrations have been prepared with the VMD software package;[56] disulfide bonds are indicated in yellow.

Table 1.2: Sources, sequences and activity spectra of selected AMPs, grouped according to classes described in the text.

AMP	Source	Primary sequence[a]	Spectrum[b]	Ref.[c]
		α-helical		
LL-37	Human	**H**-LLGDFF**RK**S**K**E**K**IG**K**EF**KR**IVQ**R**I**K**DFL**R**… ...NLVP**R**TES-OH	G^-, G^+, F, V	[57-59]
Magainin-2	Amphibian	**H**-GIG**K**FLHSA**KK**FG**K**AFVGEIMNS-OH	G^-, G^+, F, P	[60]
Dermaseptin	Amphibian	**H**-ALW**K**TML**KK**LGTMALHAG**K**AALGAAA… …DTISQGTQ-OH	G^-, G^+, F, P	[61, 62]
Pleurocidin	Fish	**H**-GWGSFF**KK**AAHVG**K**HVG**K**AALTHYL-OH	G^-, G^+	[63]
		β-sheet / β-hairpin		
Protegrin-1	Pig	**H**-**R**GG**R**LC$_1$YC$_2$**RRR**FC$_2$VC$_1$VG**R**-NH_2	G^-, G^+, F, V	[64-66]
Androctonin	Scorpion	**H**-**R**SVC$_1$**R**QI**K**IC$_2$**RRR**GGC$_2$YY**K**C$_1$TN**R**PY-OH	G^-, G^+, F	[67]
Tachy-plesin-1	Crab	**H**-**K**WC$_1$F**R**VC$_2$Y**R**GIC$_2$Y**RK**C$_1$**R**-NH_2	G^-, G^+, F, V	[68, 69]
Poly-phemusin	Crab	**H**-**RR**WC$_1$F**R**VC$_2$Y**R**GFC$_2$Y**RK**C$_1$**R**-NH_2	G^-, G^+, F, V, P	[69-71]
α-defensin (HNP-1)	Human	**H**-AC$_1$YC$_2$**R**IPAC$_3$IAGE**RR**YGTC$_2$IYQG**R**… …LWAFC$_3$C$_1$-OH	G^-, G^+, F, V, P	[72-75]
β-defensin (HBD-2)	Human	**H**-GIGDPVTC$_1$L**K**SGAIC$_2$HPVFC$_3$P**RR**Y**K**QIGTC$_2$G… …LPGT**K**CC$_3$**KK**P-OH	G^-, G^+, F, V, P	[76-79]
θ-defensin (RTD-1)	Monkey	GFC$_1$**R**C$_2$LC$_3$**RR**GVC$_3$**R**C$_2$IC$_1$T**R**[d]	G^-, G^+, F, V	[37, 80]
MGD-1	Mussel	**H**-GFGC$_1$PNNYQC$_2$H**R**HC$_3$**K**SIPG**R**C$_4$GGYC$_1$GGW… …H**R**L**R**C$_2$TC$_3$Y**R**C$_4$G-OH	G^-, G^+	[81]
Ee-CBP	Bark	**H**-QQC$_1$G**R**QAGN**RR**C$_2$ANNLC$_3$C$_1$SQYGYC$_2$G**R**TN… …EYC$_3$C$_4$TSQGC$_5$QSQC$_5$**RR**C$_6$G-OH	F	[82]
		Enriched in certain amino acids		
PR-39	Pig	**H**-**RRR**P**R**PPYLP**R**P**R**PPPFFPP**R**LPP**R**IPPG… …FPP**R**FPP**R**FP-NH_2	G^-, G^+	[83]
Pyrr-hocoricin	Insect	**H**-V**D**KGSYLP**R**PT[e]PP**R**PIYN**R**N-OH	G^-, G^+, F	[84, 85]
Drosocin	Insect	**H**-G**K**P**R**PYSP**R**PT[f]SHP**R**PI**R**V-OH	G^-, G^+, F	[86, 87]
Apidaecin	Insect	**H**-GNN**R**PVYIPQP**R**PPHP**R**I-OH	G^-, G^+	[88]
Histatin 5	Human	**H**-DSHA**KR**HHGY**KRK**FHE**K**HHSH**R**GY-OH	G^-, G^+, F	[89]
Indolicidin	Bovine	**H**-ILPW**K**WPWWPW**RR**-NH_2	G^-, G^+, F, V	[90-92]
		Looped structures		
Thanatin	Insect	**H**-GS**KK**PVPIIYC$_1$N**RR**TG**K**C$_1$Q**R**M-OH	G^-, G^+, F	[93]
Bactenecin	Bovine	**H**-**R**LC$_1$**R**IVVI**R**VC$_1$**R**-OH	G^-, G^+, F	[94, 95]
		Derived from larger precursor molecules		
Buforin	Frog	**H**-AG**R**G**K**QGG**K**VRA**K**A**K**T**R**SS**R**AGLQFPVG**R**... ...VH**R**LL**RK**GNY-OH	G^-, G^+, F	[96]
Lacto-fericin B	Bovine	**H**-F**K**C$_1$**RR**WQW**R**M**KK**LGAPSITC$_1$V**RR**AF-OH	G^-, G^+, F, V, P	[97-100]

[a] To emphasise the charged nature of AMPs, basic residues are depicted in boldface and acidic residues are underlined; the positive charge of the free N-termini is indicated by **H** and the negative charge of the free C-termini by OH; The disulfide bonding patterns are indicated by subscripts; [b] G^- ≡ active against Gram-negative species; G^+ ≡ active against Gram-positive species; F ≡ antifungal activity; V ≡ antiviral activity; P ≡ antiprotozoal activity; [c] References; [d] backbone-cyclisation of RTD-1 is indicated by a solid line; [e] the threonine residue of pyrrhocoricin is glycosylated with *N*-acetyl-α-D-galactosamine; [f] the threonine residue of drosocin is glycosylated with β-D-galactopyranosyl-(1 → 3)-α-*N*-acetyl-D-galactosamine.

1.4.2 Selectivity of AMPs

As mentioned already, selective toxicity towards microbial cells is crucial for any antibiotic compound to be of therapeutic use. Compounds such as the polymyxins suffer from poor selectivity and it is this property that greatly hampers their utility in systemic applications. One of the main reasons for the microbial selectivity of AMPs is thought to lie in the different make-up of various cell membranes.[24] In contrast to mammalian membranes, for instance, the outer layer of the bacterial plasma membrane contains a high density of negatively charged phospholipids such as phosphatidylglycerol (PG) and cardiolipin (CL).[101] Additionally, the outer membranes of Gram-negative organisms are composed of negatively charged lipopolysaccharides (LPS) which are thought to interact electrostatically with the positively charged AMPs.[102] However, electrostatic forces on their own are unlikely to be the sole parameter of selectivity since on the one hand mammalian cells are also decorated with macromolecules bearing negative charges,[103] and on the other hand anionic polypeptides are also able to insert into negatively charged phospholipid bilayers.[104] The interactions of several AMPs with model membranes of different compositions have been studied and it is generally found that they selectively bind to or permeabilise negatively charged membrane systems. AMPs for which such selectivity has been demonstrated include magainin-2,[105] tachyplesin-I,[106] peptide G15 from granulysin,[107] or PGLa.[108] In contrast, closely related peptide venoms (often also referred to as AMPs) such as melittin and mastoparan, which display a more hydrophobic character, are able to permeabilise both zwitterionic and anionic model membranes.[105] It has been reported that supplementary membrane compounds such as cholesterol can confer additional protection from attack by AMPs, at least when introduced into zwitterionic model membranes.[105] However, a recent publication ascribes only a secondary role to cholesterol in influencing the interaction of cationic AMPs with anionic model membranes.[109]

1.4.3 AMPs and bacterial resistance

It has been proposed that AMPs are less prone to generate bacterial resistance than currently used antibiotics. An argument in favour of this notion is the fact that these compounds are still active despite their evolutionary ancient lineage.[24]

Mechanisms of resistance to AMPs do exist however, comprising expression of proteases, secretion of proteins that bind AMPs, extrusion of AMPs by multidrug efflux systems and especially the reduction of the net anionic charge of the microbial cell walls and/or membranes.

Several factors have been described to account for the putative ability of AMPs to counteract these measures.[110] Firstly, many AMPs lack unique epitopes for recognition by bacterial proteases. Secondly, the ability of bacteria to lower the negative charge at their surfaces seems to be limited and thirdly, a reduced anionic nature of the microbial surface might be counterbalanced by the introduction of higher positive charge into the peptide scaffolds. Additionally, it has been argued that AMPs might act by multi-hit mechanisms (c.f. **Section 2.2**);[111] the simultaneous interaction with diverse targets would of course greatly diminish the possible emergence of resistance. Moreover, bacteria are expected to encounter a wide array of different AMPs at the source of infection, which could further explain a decreased propensity to generate bacterial resistance. This effect may be even increased by the fact that AMPs are released at high concentrations directly at the site of infections, contrary to the low concentrations typically encountered in antibiotic chemotherapy. They have therefore been described as ‘dirty’ antibiotics that, by virtue of their antimicrobial mechanisms, are able to affect a wide range of antimicrobial pathogens simultaneously.[112] Noteworthy, more recently, so-called ‘dirty’ drugs, i.e. drugs acting by multiple mechanisms, and/or addressing possessing multiple targets, are receiving increased attention for various therapeutical applications.[113]

1.5 Antimicrobial peptide mimetics (AMPMs)

As outlined in the previous section, AMPs show considerable potential as candidates for development into new therapeutically useful antimicrobial agents. The increased interest in this class of compounds originates mainly from their hitherto possibly underappreciated main mechanism of action, which is associated with differential features of prevailing cell membranes (c.f. **Chapter 2**).[24] Two factors which are intricately related to this mechanistic aspect account largely for the appeal of AMPs as prospective drugs. Firstly, membrane-active mechanisms of action are associated with the broad spectrum of antimicrobial activities of AMPs and secondly, these mechanisms could account for the presumably low potential of AMPs to generate bacterial resistance. Notably, AMPs often show good activities against multidrug resistant pathogens such as multidrug (methicillin) resistant *S. aureus* (MRSA) and *P. aeruginosa*. Dichotomously, membrane-active mechanisms also account for one of the major drawbacks of naturally occurring AMPs, undermining their therapeutic potential. That is, they frequently display high toxicity, as exemplified, for instance, in an ability to lyse red blood cells. Thus, an important pre-requisite for their further development, at least for systemic applications, is an increase of their selectivity towards micro-organisms.

Several approaches for uncoupling the toxic and antimicrobial properties of AMPs, thereby increasing this selectivity, have been described in the literature. A commonly employed strategy consists of taking naturally occurring AMPs as scaffolds for the construction of novel derivatives, typically by incorporation of alternative amino acid residues into the molecular framework. Yet another virtue of AMPs lies in their amenability to combinatorial chemistry based approaches, due to the modular principle of peptides in general. Not surprisingly, extensive structure-activity relationship (SAR) studies aimed at improving their biological activity have been carried out on a variety of AMP scaffolds. The parameters generally varied in these studies comprise overall size, primary sequence, secondary structure, hydrophobicity, amphipathicity, and charge.[114] The result of such an approach is illustrated by the development of IB-367, a protegrin analogue with improved antimicrobial activity, albeit with undiminished haemolytic activity.[115]

An extension to this approach of modifying the peptide sequence consists of the deletion or addition of residues, or in the truncation of the naturally occurring

peptide sequence. For example, an N-terminally shortened derivative of dermaseptin shows improved activity compared to its parent compound, and a C-terminal fragment of LL- 37 was found to display cytotoxic activity towards both microbial and cancer cells.[116, 117] This truncation of AMPs can not only provide an insight into minimal structural motifs necessary for biological activity, but also leads to shorter peptide fragments that are more attractive for possible large scale synthesis.

Furthermore, AMPs have been designed *de novo* either by methods relying on general structural requirements such as the presence of amphipathicity and α-helical structure,[118] or by template-assisted methods. In template-assisted methods, patterns of different amino acids in connection with their physico-chemical parameters such as charge or hydrophobicity are assembled into sequence-templates which can then be used for the designed synthesis of AMP(M)s.[119] Moreover, template-assisted methods are not confined to the above mentioned sequence-templates. Additionally, structural templates can be used to constrain linear peptides into defined conformations such as β-hairpins or α-helices. For example, Tam et al. introduced additional cystine or backbone cyclisation constraints into the framework of tachyplesin and Andreu and co-workers likewise used a cystine link to induce an amphipathic α-helical conformation in short linear peptide fragments derived from thionin.[120, 121]

1.5.1 D-Pro-L-Pro as a structural template

The approach employed by our group for the development of antimicrobial peptide mimetics with improved biological activities is based on the introduction of organic templates into a peptidic backbone in order to stabilise β-hairpin conformations.[122] Several organic templates have been developed for achieving such stabilisation, but of particular interest for this work is the D-Pro-L-Pro template (**10**) depicted in **Figure 1.5**. It has been demonstrated that the heterochiral **10** promotes the formation of regular hairpin conformations,[123, 124] and this has been exploited by our group in the synthesis of β-turn mimetics that are obtained by grafting the sequences of naturally occurring β-hairpin folds onto the template. This methodology has been successfully applied to the design of inhibitors of the p53-HDM2 interaction,[125] trypsin inhibitors,[126] human antibody Fc-binding peptidomimetics,[127] and ligands that bind to viral TAR RNA regulatory elements.[128]

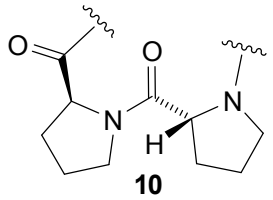

10

Figure 1.5 The D-Pro-L-Pro template (**10**); attachment points to the peptide backbone are indicated by wavy lines.

1.5.2 AMPMs derived from naturally occurring β-hairpin AMPs

There exist a variety of naturally occurring AMPs with β-hairpin folds which present auspicious starting points for AMPMs based on the D-Pro-L-Pro template (**10**). A selection of these compounds is depicted in **Figure 1.6** along with schematic drawings emphasising their β-hairpin folds. As can be seen, the β-hairpin of naturally occurring AMPs is typically constrained by disulfide bonds. An additional constraint of backbone-cyclisation can be found in RTD-1, a mammalian AMP isolated from a monkey species.[37] While other AMPs, especially the α-helical subclass, often adopt their secondary structure only upon interaction with membranous systems, β-hairpin AMPs generally already display their secondary structure in an aqueous environment. These compounds were isolated from a variety of sources and they have been studied extensively because of their interesting antimicrobial activities, and as model compounds for mechanistic studies. The extensive SAR studies on protegrin-1 (**11**), resulting in the development of IB-367, have been mentioned already. Additionally, this peptide has been used frequently as a model compound for solid-state NMR and computational studies directed towards understanding its interaction with membranous systems. Further interest in β-hairpin AMPs originates from the antiviral properties that some of these compounds display. Most notably amongst those are the tachyplesins and polyphemusins, which have been isolated from various crab species.[129, 130]

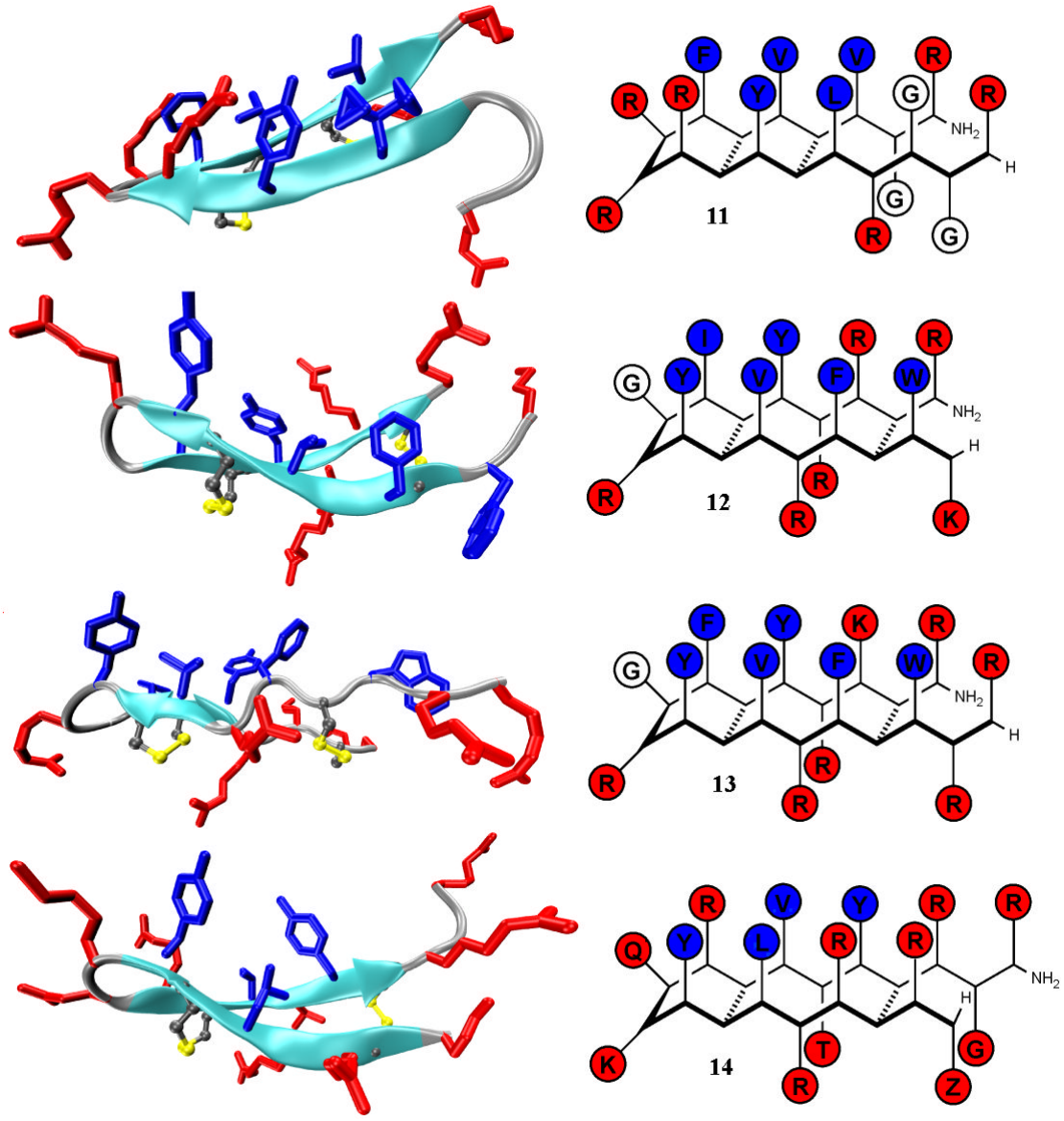

Figure 1.6 NMR structures of naturally occurring β-hairpin AMPs together with schematic drawings emphasizing their β-hairpin folds. Disulfide bonds are depicted in yellow, or as broken lines, and the clustering of polar (red) and apolar residues (blue) is indicated. From top: Protegrin-1 (**11**) [PDB code 1PG1],[50] tachyplesin-1 (**12**) [PDB code 1WO0], polyphemusin-1 (**13**) [PDB code 1RKK],[131] and gomesin (**14**) [PDB code 1KFP].[132] The illustrations have been prepared with the VMD software package.[56]

A further incentive for the use of this class of molecules as sequence templates in the design of AMPMs derives from findings that underline the importance of the well-defined β-hairpin conformation in naturally occurring AMPs for their antimicrobial activity. For example, it has been shown that linear derivatives of protegrin-1 displayed diminished antimicrobial as well as membrane-lytic

properties,[133] and similar results have also been reported for tachyplesins and polyphemusins.[131, 134] Furthermore, disulfide constrained peptide-mimetics of the β-hairpin region of mammalian and mussel defensins retain antimicrobial activity, once again highlighting the importance of this structural motif.[135, 136]

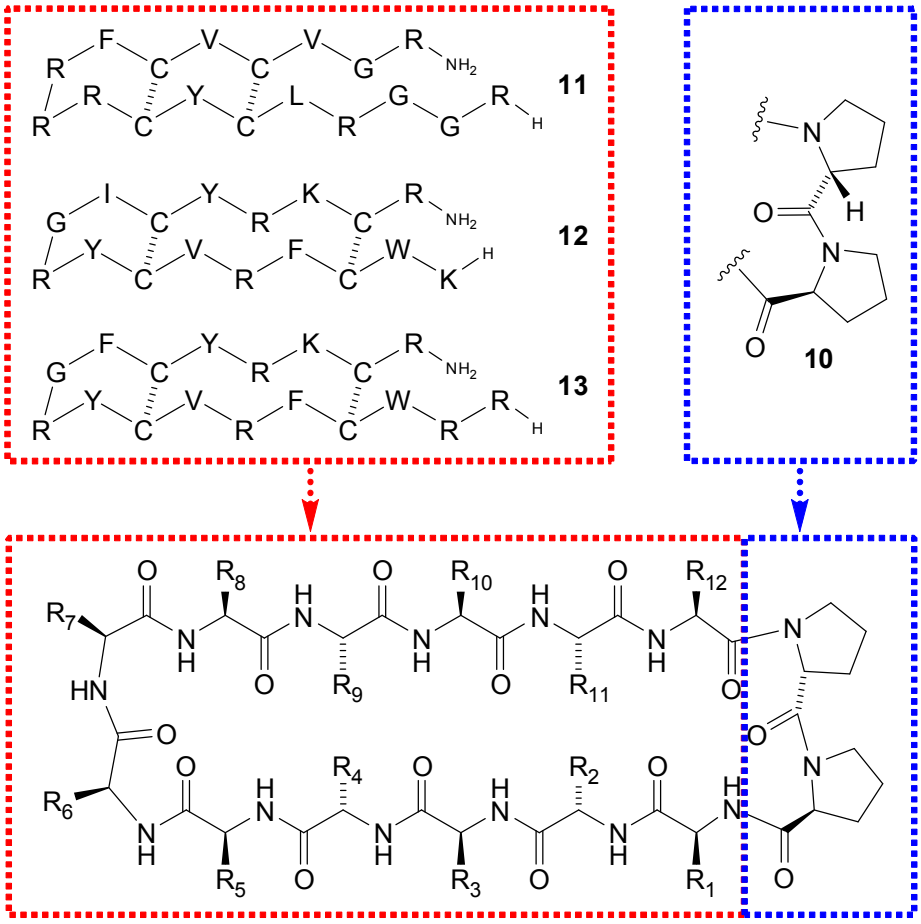

Figure 1.7 Grafting of sequences of naturally occurring antimicrobial β-hairpin peptides (**11** = protegrin-1; **12** = tachyplesin-1; **13** = polyphemusin-1) onto the D-Pro-L-Pro template (**10**).

Motivated by these findings, several series of AMPMs based on the above mentioned naturally occurring β-hairpin structures and the D-Pro-L-Pro dipeptide (**10**), as well as other organic templates, have been synthesised by our group.[137-140] The AMPMs were designed by grafting the sequences onto the organic template as indicated in **Figure 1.7**. Since this work is only concerned with experiments directed at AMPMs employing the D-Pro-L-Pro (**10**) template, I will focus solely on compounds containing this template. An additional possible advantage of the organic template approach lies in the fact that the hairpin inducing template relaxes the

requirement for the cystine bridges, thereby creating free slots for additional amino acid side-chains.

1.5.3 Project outline

The biological activities of selected representatives of four generations of AMPMs are reproduced in **Table 1.3**. It is evident from this table that the first library of β-hairpin mimetics, of which mimetics **15** and **16** are shown in **Table 1.3**, was successful in separating the antimicrobial and haemolytic activities of the parent AMP(s). While mimetic-**15** still showed an appreciable amount of haemolytic activity towards human red blood cells (hRBC), compound **16** retained good antimicrobial activity against Gram-positive as well as Gram-negative organisms but almost completely lost the haemolytic properties.

Extensive SAR studies have been conducted with the scaffold of mimetic-**16**, the most attractive compound of the first library with respect to its low haemolytic activity,[138] which demonstrated that the antimicrobial activity is tolerant to a large number of the over 100 single site substitutions tested. Several other AMPMs based on **16** have been developed in our laboratory and in cooperation with Polyphor Ltd.† Of particular interest was the discovery of mimetic **17**, which in addition to non-detectable haemolytic properties under standard assay conditions (with a peptide concentration of 100 μg/mL), displayed an increased selectivity towards the Gram-negative organism *P. aeruginosa*. Remarkably, the haemolytic activity of **17** amounted to only 1% at a peptide concentration of as high as 1 mg/mL. Subsequent modifications in two further rounds of optimisation lead to the AMPMs **18** and **19** with a concomitant increase in activity and selectivity towards *P. aeruginosa* (c.f. **Table 1.3**). During the course of development of these newer generations of AMPMs, several clues such as differences in their killing kinetics and the remarkable selectivity towards *P. aeruginosa*, accumulated, indicating that some representatives might exert their antibacterial action by a mechanism that differs fundamentally from the membrane-active models generally proposed for the naturally occurring β-hairpin AMPs from which they were ultimately derived.

† **Polyphor Ltd.** Gewerbestrasse 14, CH-4123 Allschwil

Table 1.3 Antimicrobial and haemolytic activities of AMPMs derived from protegrin-1. The values for mimetics **15** and **16** and for **11** are taken from [137]; other values are taken from [139].

ID[a]	sequence[b]	MIC[c] [μg/mL]						%H[d]
		E. coli	*P. aeruginosa*		*S. aureus*		*C. albicans*	hRBC[e]
		25922[f]	27853[f]	PAO1[f]	25923[f]	29213[f]		
15	**LRLQYRRFQYRVpP**	6	12	n.d.[g]	12	n.d.	6	27
16	**LRLKKRRWKYRVpP**	12	6	n.d.	12	n.d.	12	1
17	**RWLKKQRWKYYRpP**	16	0.25	n.d.	> 64	> 64	n.d.	0
18	**TWLKKRRWKKVKpP**	64	0.03	0.06	32	>64	n.d.	0
19	**TWLKKRRWKKAKpP**	64	0.015	0.004	>64	>64	n.d.	0
11	**Protegrin-1**[h]	3	3	n.d.	6	n.d.	6	37

[a] Substance identifier; [b] peptides are cyclised by a peptide bond between the terminal residues; [c] minimal inhibitory concentration (for a definition, refer to **Section 3.3**) [d] % Haemolysis at a peptide concentration of 100 μg/mL; [e] hRBC ≡ human red blood cells; [f] strain or ATCC number; [g] n.d. ≡ not determined; [h] the sequence of **11** is shown in **Figure 1.7**.

Therefore, it was decided to investigate the possible modes of action of these compounds. To this end, a variety of biophysical, bacteriological and biochemical methods were employed and these experiments will be described in subsequent sections following a review of mechanistic aspects of AMP(M)s.

Finally, it should be mentioned that the mechanistic studies and the development of new AMPMs progressed to a large extent in parallel. Therefore, certain experiments have not been conducted with all mimetics of **Table 1.3**. Nonetheless, all experiments always include at least a representative of those mimetics that show the characteristic selectivity towards *P. aeruginosa*, and which are therefore assumed to share the same underlying mechanistic behaviour.

2 Modes and mechanisms of AMP action

Since the preliminary studies on AMPMs derived from protegrin-1 (**11**) led to the presumption that some of these compounds might exert their antibacterial activity by mechanisms differing from the ones commonly associated with AMPs, it seems desirable at this point to summarise what is currently known about the modes and mechanisms of AMP action. Both expressions "mode of action" and "mechanism of action" are generally used interchangeably in the literature, but for the purpose of this work they will be associated with different concepts. The term mode of action will be used in a phenomenological sense, which is independent from the underlying mechanism(s) that will be denoted as mechanisms of action. For example, the mode of action of chloramphenicol is the inhibition of protein biosynthesis; mechanistically it does so by binding to the 50S subunit of the bacterial ribosome.

With increased research efforts directed towards the *in vivo* antimicrobial action of AMPs it becomes increasingly evident that this action can be divided into two different modes. Firstly, AMPs might act by directly killing or inhibiting the growth of micro-organisms. These direct effects are the defining feature of AMPs as implied by their name, and are used for the isolation of AMPs from natural sources. Antimicrobial activity is typically assessed by *in vitro* assays (c.f. **Section 3.3**), and in an *in vitro* setting any antimicrobial effect has necessarily to be mediated directly through the AMP. These considerations hold even for the conceivable case where the active principle might be derived from the AMP by metabolic processing through the target organism.

In contrast, the antimicrobial action of an AMP, or that of any antimicrobial agent in general, in an *in vivo* setting cannot *per se* be attributed to a direct effect on the microbial cells. Complications arise due to the inevitably increased complexity of the system and therefore a second mode of antimicrobial action, functioning by exerting immuno-modulatory effects on the host, as opposed to the abovementioned direct mode of action, is well conceivable. The proposed contribution of such immuno-modulatory effects to the antimicrobial action of AMPs has led to the coining of the term host defence peptides (HDPs) as an alternative to the commonly used term AMPs. Although AMPs are increasingly referred to as HDPs by some authors,[141, 142] I will continue to use the former term, since this work is concerned

with AMPMs of distinct antibacterial activity *in vitro*, which thus evidently display a direct mode of antibacterial action.

Notwithstanding the accumulating evidence for immuno-modulatory effects of AMPs on the host immune system, the vast majority of AMPs is thought to act mainly, if not exclusively, by a direct mode of action. For these AMPs, another distinction with respect to the underlying mechanisms of the antimicrobial action can be made. On the one hand, a large majority of AMPs that have been studied with mechanistic aspects in mind are thought to, or have been shown to act by targeting and impairing the function of the microbial cell membrane and/or cell wall. The importance of such mechanisms in motivating AMP research was pointed out in the introduction. On the other hand, there is an increasing number of AMPs for which mechanisms of direct antimicrobial action have been suggested which would not primarily depend on fundamental features of membranous systems. To emphasise the unusual behaviour of such AMPs, they are often described as possessing an "alternative", or "different" mechanism of action.

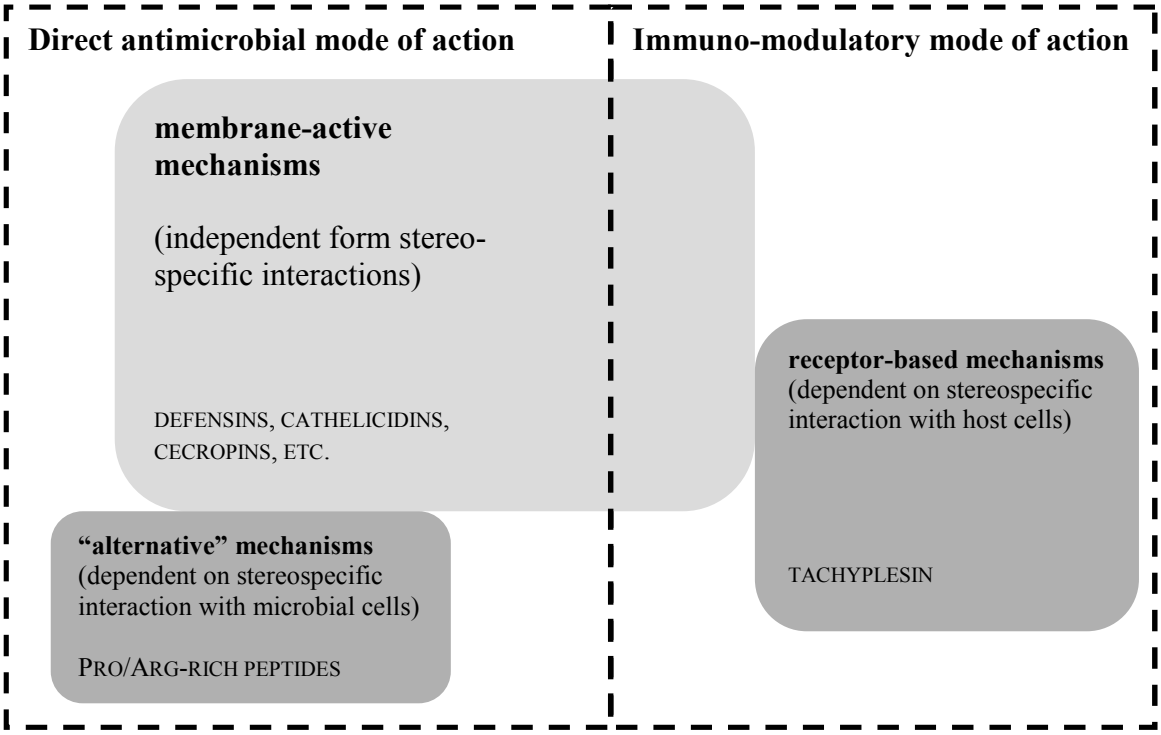

Figure 2.1 Modes and mechanisms of antimicrobial action displayed by AMPs. Note that several compounds might act by a combination of different modes of action. Some examples of well-studied AMPMs are given.

A graphical representation of the different modes and mechanisms of AMP action is shown in **Figure 2.1**. The following discussion is based on this division into different modes as well as mechanisms of action, and special emphasis will be given to AMPs with alternative mechanisms of direct antimicrobial action, due to the experimental behaviour of our AMPMs.

2.1 Direct modes of action

Regardless of the concrete models that are used to rationalise the direct action of AMPs, several steps must occur in order to bring about bacterial killing. These steps comprise: (1) attraction of the AMP to the microbial species (possibly mediated by electrostatic interactions); (2) attachment to the microbial plasma membrane which might, in the case of bacteria, be preceded by permeation of the cell wall (outer membrane and/or peptidoglycan layer); (3) permeabilisation of the target plasma membrane and/or translocation across it; resulting in (4) the bacterial killing, mediated by various effects which might include action on intra-cellular targets.

First of all, AMPs must be attracted to the microbial membrane, or to the bacterial cell wall. The latter is composed largely of a peptidoglycan layer (Gram-positive species), or of the outer membrane (OM) together with a smaller peptidoglycan layer (Gram-negative species). Attraction of AMPs to the surface of microbial targets is intimately related to the issue of selectivity (c.f. **Section 1.4.2**), and a major role in this first step is generally attributed to electrostatic interactions, especially with LPS,[143] or with other negatively charged components of bacterial cell walls.[144] Following attraction to the bacterial targets, the peptides have to pass through the outer membrane in Gram-negative species. HNP-1, for instance, was shown to effectively disrupt the OM, as demonstrated by the release of a periplasmic β-lactamase.[145] The release of this enzyme is thought to be brought about by destabilisation of the OM via displacement of divalent cations during the binding of peptide to LPS.[146] In the case of Gram-positive bacteria, the bacterial cell-wall generally represents no barrier for AMPs as suggested, for example, by the size exclusion limit of 30 to 57 kDa for polysaccharides.[147] The preference of AMPs to attach to microbial membranes is thought to originate mainly from the differing phospholipid compositions of host and target plasma membranes (vide supra).

After penetration of the cell wall and attachment to the membrane, several events have been suggested to be responsible for killing the target organism. Such events have been proposed to include dissipation of trans-membrane potential and the pH gradient,[148, 149] caused, for example, by formation of ion-channels,[150] disturbance of the osmotic regulation,[151] efflux of metabolites, and the uncoupling of respiration,[152] although various AMPs vary considerably in their ability to depolarise cytoplasmic membranes with respect to a membrane sensitive dye.[43] Additionally, the interaction with intra-cellular targets or the inhibition of enzymatic processes of the target cells have been suggested. The latter effects touch on the border between membrane-active and alternative mechanisms of action, but first we will be concerned with membrane-active mechanisms, in which the killing events are solely dependent on disruption of membrane integrity and function.

2.1.1 Membrane-active mechanisms

It seems appropriate to begin a mechanistic discussion with this category for several reasons. Firstly, in spite of increasing reports of AMPs to which other mechanisms of action are attributed, the vast majority of AMP(M)s described to date is still thought to belong in this category. Also, historically the various hypotheses, theories, and models explaining the antimicrobial action and selectivity of these compounds were originally concerned with membrane-active mechanisms, which might be partially attributable to the fact that early mechanistic research in this field was stimulated by peptide venoms that had long been expected to disrupt cellular membranes. Most importantly, though, it has to be kept in mind that an important question for any antibiotic substance is concerned with its uptake into the target organism, unless it is acting on extracellular or surface compounds alone. Therefore, even if AMPs employ alternative mechanisms in the killing or the growth-inhibition of micro-organisms the models derived for a more direct action on the membrane remain an important aspect of AMP action.

Several indications point to a membrane-active mechanism being best suited to account for the antimicrobial action of the majority of AMP(M)s. Firstly, these compounds usually possess similar activity ranges, typically in the low micromolar range. They also display broad-spectrum antimicrobial activity towards Gram-negative, Gram-positive, and fungal species. The similar activities and activity

patterns of AMPs, despite large differences in their structures and sequences, can be satisfactorily explained by membrane-active mechanisms. These are able to provide an underlying mechanistic framework which, in accordance with the observations, is insensitive to variations in the peptide structures as long as certain physico-chemical parameters are adhered to (vide infra). The same holds true for the rapidity with which many of these compounds exert their (mostly bactericidal) action. Often a decrease in the viable cell count of several orders of magnitude is observed within minutes of induction with the AMP (c.f. **Section 3.3**), and such rapid action would be expected from an impairment of membrane function.

Of paramount importance, and one of the main arguments for the development of the different models of cell permeabilisation, is the identical behaviour of various enantiomeric pairs of AMP(M)s (c.f. **Section 3.4**), which strongly suggests mechanisms that are not dependent on topological recognition of chiral entities such as protein or nucleic acid receptors. Indeed, these findings rather point to an involvement of peptide/lipid interactions in the mode of action of these peptides.

Furthermore, morphological studies on the effects of AMPs on bacterial cells, typically employing scanning and/or transmission electron microscopy, often show the formation of compromised membrane structures, such as the formation of blebs on the membrane surface,[153] or the swelling of the bacterial cell concomitant with detachment of the outer membrane in *E. coli*.[154] It has to be mentioned though, that such morphological changes have also been interpreted as secondary effects that occur only after the cells have been damaged irreversibly.

2.1.1.1 Parameters of membrane-active mechanisms

Several interdependent structural determinants have been examined for their influence on antimicrobial action according to membrane-active modes of action.[155] For example, the overall charge of the AMP might be important in the initial electrostatic interaction with the cell wall, and contribute to the selectivity for certain phospholipids. Indeed, most AMPs are positively charged, and several studies emphasise a relationship between increased cationic charge and increased antimicrobial activity.[156, 157] Other important parameters that have been studied systematically include the hydrophobic moment μ_H,[158] which is used as a measure for the amphipathicity, especially in α-helical AMPs.[159] It has been found that a

modification of the hydrophobicity can increase the selectivity of AMPM gramicidin S derivatives towards micro-organisms.[160] Related to the hydrophobic moment is the peptide hydrophobicity, which is defined as the percentage of hydrophobic residues in the peptide. Hydrophobicity seems to be necessary for insertion of the peptides into the membrane, and it is thus not surprising that AMPs possess a hydrophobicity of around 50%. Additionally, it has been shown that increasing hydrophobicity can lead to an increase in haemolytic activity.[159] Another important parameter for α-helical peptides is the polar angle (Θ), which describes the relative angles subtended for the polar and the apolar faces, as best demonstrated in a helical wheel projection.[161] A smaller polar angle has been linked to an increased capacity for pore formation and membrane permeabilisation.[162] It has to be emphasised that all these parameters are interconnected, and subtle variations in one of them can lead to quite drastic changes in the activity and selectivity of the AMP.[155]

2.1.1.2 Models of pore-formation and membrane permeabilisation

As mentioned above, killing events caused by membrane-active peptides are associated with permeabilising effects on the cytoplasmic target membrane. Several models have been devised for this process; a graphical representation of the three most common models is shown in **Figure 2.2**. These models have been proposed based on biophysical experiments with artificial and natural membranes, computational studies, and bacteriological data (e.g. activity spectra).

An important factor in all models is the orientation of the peptide molecules with respect to the bilayer surface. It has been found that the most important variable for this orientation is the peptide concentration, generally expressed as the peptide to lipid ratio [P]/[L]. According to OCD (orientated circular dichroism), AMPs are typically bound parallel to the lipid bilayer if this ratio remains below a certain threshold concentration [P]/[L]*, above which increasing amounts of the peptide are found perpendicular to the lipid bilayer. The threshold concentration has been found to depend essentially on membrane composition and temperature.[163]

The state of an AMP in which it is bound parallel to the membrane surface is commonly referred to as the S state, while the inserted peptide is denoted as being in the I-state. Generally, peptides in the S-state lead to a thinning of the membrane, as found for example by X-ray diffraction studies.[164] This thinning effect is also

thought to facilitate pore-formation, and originates in the expansion of the membrane surface by the insertion of the peptides between the headgroups of the phospholipids.[165, 166]

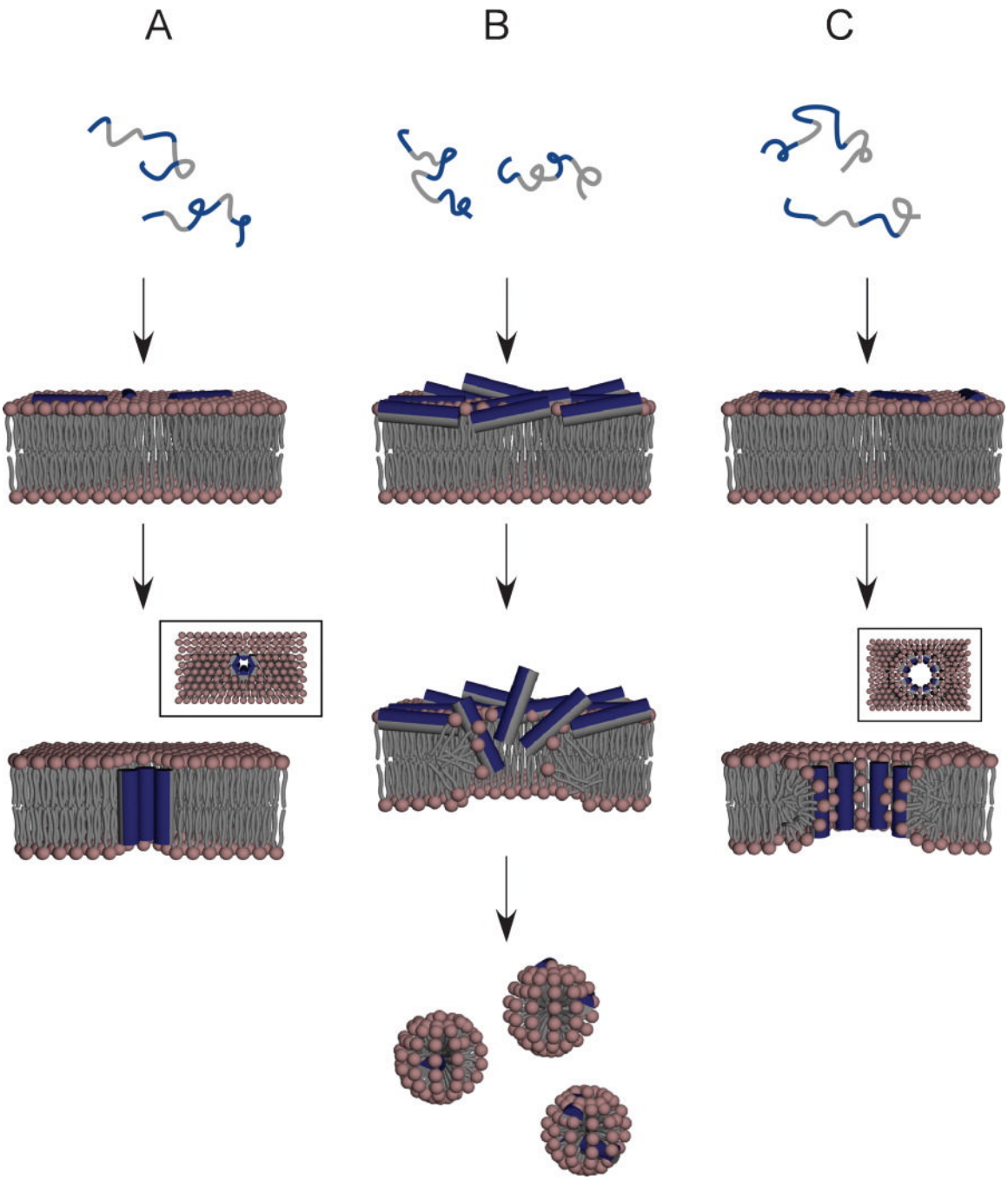

Figure 2.2 Three common models of membrane-permeabilisation by AMP(M)s. (**A**) barrel-stave model; (**B**) carpet-model; (**C**) toroidal-pore model. Note the different diameters of the membrane pores predicted by the barrel-stave or the toroidal-pore model shown in the insets, and the orientation of the peptides with respect to the bilayer normal in the different models. The amphipathic nature of the peptide molecules and the adoption of secondary structure upon interaction with the membrane is indicated.

BARREL-STAVE MODEL The barrel-stave model (**Figure 2.2A**) postulates the formation of discrete pores in the phospholipid bilayer and was in its essentials first proposed by Baumann and Mueller in 1974.[167] In this model, amphipathic compounds first bind to the surface of the membrane, possibly with concomitant adoption of secondary structure. Subsequently, they self-assemble on the surface and insert into the bilayer, thus creating the pore structure(s). The multimerisation of monomers before the insertion into the membrane is necessary because it would be energetically unfavourable for a single amphipathic molecule to insert into the apolar region of the membrane, due to the unfavourable interactions between the apolar interior of the phospholipid bilayer and the polar face of the amphipathic molecule.[168] Recruitment of additional peptide monomers could then successively increase the pore size until a stable configuration was achieved. For amphipathic peptides, the inside of the pore is lined with their hydrophilic faces, whilst their hydrophobic faces are in contact with the membrane interior.[169] Therefore, compounds for which a barrel-stave mechanism seems plausible are thought to be generally more hydrophobic than the majority of AMPs.[170]

The geometrical layout of the pores is such that the long axis of the inserted molecules is parallel to the normal of the bilayer at all times. This gives the pore the appearance of a barrel whose shape is lined with peptidic staves. Notably, in the barrel-stave model, the molecules are not always entirely in contact with the phospholipid head groups,[163] and this is a major criterion that differentiates it from the other models of pore-formation. An additional feature of the barrel-stave model is illustrated by the fact that peptides need a certain length to span the membrane in its entirety. In the case of AMPs, those belonging to the α-helical subclass are most-likely to fulfil this requirement, although they need a minimum of at least 20 amino acids to achieve the necessary length.[171]

One of the few peptide antimicrobial agents for which the applicability of the barrel-stave model seems secure, is the peptaibol alamethicin. This wide acceptance is based on experimental evidence, such as the reproducible discrete states of single-channel ion conduction,[172] indicating the presence of discrete aggregates of alamethicin monomers in the pore, and neutron in-plane scattering experiments. The scattering experiments suggest a pore-size of 4 nm outside diameter and 1.8 nm inside diameter, giving a calculated diameter of 1.1 nm for the lining peptides.[173] This is in

good agreement with the diameter of the alamethicin helix found in crystal structures, and indicates that the pores are composed of 8 peptide monomers.[174] A membrane pore composed of 8 peptidic monomers, that is reminiscent of alamethicin pores, has also been described for the lantibiotic nisin (vide infra).

A relatively recent example of a genuine AMP (according to the definitions given in the introduction) is ceratotoxin A, a 36 residue α-helical insect AMP that has been reported to form voltage-dependent ion channels in lipid bilayers, and which is thought to form pores consisting of five to six peptide monomers according to the barrel-stave mechanism.[175]

CARPET MODEL In the carpet model, the target cell membrane is thought to become covered by AMPs in a carpet-like fashion (**Figure 2.2B**).[176] The peptides orient themselves in such a way that their hydrophilic face is in contact with the polar head groups of the phospholipids, while their hydrophobic face is in contact with, or respectively inserts into, the apolar environment of the membrane. After reaching a certain threshold concentration, the peptides are believed to impair the membrane integrity, for example by influencing the bilayer curvature.[168, 170] For example, the expansion of the hydrophilic head group region by AMPs leads to perturbation of the membrane integrity by introduction of positive membrane curvature strain; these effects can be studied by differential scanning calorimetry (DSC) which measures the effect of AMPs on the phase transition temperature of the change from the lamellar to the hexagonal phase.[177] Examples of peptides that are reported to introduce positive membrane curvature strain include the AMP magainin-2 and the wasp venom mastoparan.[178, 179] Generally, vesicle lysis, i.e. the complete breakdown of the membrane, accompanied by formation of micellar structures, is associated with a classical carpet model. Therefore, this model is closely associated with the concept of detergent-like action and these effects have also been aptly described as membrane solubilisation. An important feature of the carpet model is that the AMPs are in constant contact with the hydrophilic head groups of the phospholipids, instead of inserting parallel to the bilayer normal as is the case for the barrel-stave model. Important experimental support for this geometry comes from solid state NMR experiments determining the orientation of peptides in the lipid bilayer. For example, piscidins, AMPs from fish,[180] or cecropin A[181] are found to be oriented

perpendicular to the bilayer normal in solid-state NMR experiments throughout the process of membrane permeabilisation.

The carpet model is attractive for rationalising the action of a variety of AMPs, including those that are too short to span the lipid bilayer in its entirety. This model is also in agreement with the broad activity spectra of AMPs; the MIC values of these compounds are usually in a range that is well explicable with the need to reach a certain threshold concentration such as is necessary in the carpet model. It was first proposed by Shai and co-workers for the 34 residue AMP dermaseptin,[182] based on biophysical experiments employing fluorescently labelled AMPs, that indicated that dermaseptin and other peptides, such as magainin, only achieved very shallow penetration into the membrane bilayer. It has since been used to account for the action of a variety of AMPs other than the ones noted above, such as androctonin,[183] diastereomeric AMPs derived from naturally occurring AMPs,[184, 185] LL-37,[186] and mastoparan X,[187] to mention but a few.

TOROIDAL PORE MODEL This model is also synonymously known as the wormhole model, and in analogy to the carpet model, one of its major features is that the molecules remain associated with the polar headgroups throughout the permeabilisation process.[188] In contrast to the carpet model, it postulates the transient formation of the eponymous pores, instead of the disintegration of the membrane bilayer. The toroidal pores are lined with both peptides and phospholipid headgroups, resulting in a high curvature of the phospholipid bilayer (c.f. **Figure 2.2C**). The curvature of the membrane results in a thinning of the headgroups at the surface of the pore, and the peptide molecules also act by filling this space. The toroidal pore model can also account for the phenomenon of lipid flip-flop, i.e. the redistribution of phospholipids between the outer and inner layers of a membrane.[189] AMPs can reduce the half-life time for lipid flip-flop from days to minutes, and additionally, lipid flip-flop has been found, in dye-leakage experiments, to be correlated with membrane permeabilisation, suggesting an interrelation with pore-formation.[190] Since the pores are thought to be only of temporary existence, the same principle of redistribution between inside and outside layers of the membrane is also conceivable for the AMPs themselves. Accordingly, the toroidal pore model can also lend itself to account for the translocation of AMPs across target membranes.

Another distinction from the barrel-stave model, apart from the orientation of the peptides, can be found in the overall pore size in this model. The toroidal pores are expected to be larger than the typically penta- to octameric pores of the barrel-stave model. Estimates of pore-sizes can be obtained via dye-leakage experiments and indeed, pores formed by AMPs such magainin-2 are found to be significantly larger than those formed by alamethicin.[191] Additionally, the characteristics of ion-channel formation, for instance voltage independence, have been reported to favour a toroidal pore mechanism.[192]

MISCELLANEOUS MODELS Apart from the three common models depicted in **Figure 2.2**, others have been described occasionally. For example, Miteva et al. proposed, based on calculations of the electrostatic potential of the AMP NK-lysine bound to the membrane surface, that the formation of pores could be due to *molecular electroporation*, i.e. the formation of pores due to the presence of an electrical field caused by the AMPs surrounding the target membrane.[193]

A *sinking-raft* model was proposed by Pokorny et al. for the pore forming action of δ-lysine, in which α-helical peptides form trimers on the membrane surface that sink through the membrane, whereby they keep their hydrophilic faces in contact, and allow pore formation when the trimer is half-way across the bilayer.[194]

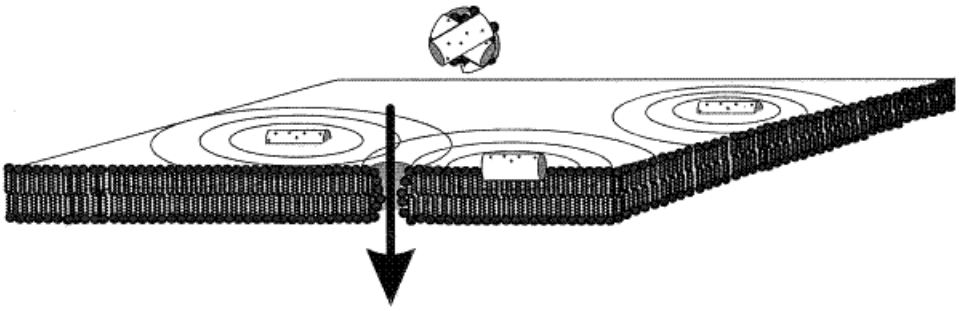

Figure 2.3 The in-plane diffusion model of membrane permeabilisation. The amphipathic character of the permeabilising compound is indicated.

Yet another model is the *in-plane diffusion model*, which postulates that the insertion of peptides into the surface induces curvature strain into the membrane within a diameter of about 100 Å around the peptide (**Figure 2.3**). These disturbances are suggested to diffuse in the plane of the membrane and allow for the formation of

transient pores in overlapping areas. The in-plane diffusion model has been suggested to explain the findings that the membrane-association of many AMPs is not cooperative.[195]

2.1.1.3 Final remarks concerning membrane-active mechanism(s)

The models of membrane permeabilisation have been developed to rationalise the killing of micro-organisms mediated by effects on the integrity of their membrane structures. On the one hand, such effects can be brought about by pore-formation, independent of whether the pores are only of transient existence, as in the toroidal-pore or in-plane diffusion models, or of a more stable nature, as is the case for the barrel-stave model. On the other hand, membrane-active killing of microbes might be associated with complete disintegration of the target membrane, which is, for example, suggested for the carpet model. It should be noted though, that a major difference between the carpet and toroidal pore models only exists for the final stages of membrane permeabilisation.

The classical carpet model is associated with a detergent-like action and an important experimental methodology that can be used to distinguish it from the toroidal pore model is the use of oriented lipid bilayers in ^{31}P-NMR.[196] In such experiments, the presence of isotropic peaks indicates the presence of smaller bilayer, or respectively micellar fragments. Additionally, the β-hairpin AMP protegrin-1 (**11**) has been proposed to disrupt membranes under the formation of small, disk-shaped fragments, instead of micellar aggregates.[197] The formation of micelles has been found to occur for certain peptides such as melittin,[198] or mastoparan,[199] two insect venoms that have often been described to possess detergent-like properties and whose mechanisms of action are in full agreement with the carpet model. Accordingly, Ladokhin and White showed that melittin induced the release of fluorescently labelled markers of different sizes from model membrane systems in an unselective, i.e. detergent-like, fashion.[200] In contrast to these peptides, micellisation has not been found for LL-37,[196] which has been traditionally associated with the carpet model (vide supra). Another experimental result in favour of a toroidal pore model consists of the findings that there is often no complete dissipation of membrane potential at concentrations below the MIC.

It has been suggested that the carpet model could be an extreme case of the toroidal pore model, viz. it is well conceivable that the simultaneous formation of too many transient pores leads to the disintegration of the target membrane. A decisive factor concerning which of both models is more adequate in a given situation could therefore consist of the overall peptide-to-lipid ratio. Consequently, the term Shai-Matsuzaki-Huang model (SMH model) is sometimes used to unite both models.[24] Like the toroidal pore model, the SMH model is also attractive to account for the translocation of AMPs across microbial membranes in such mechanisms as propose interaction with intra-cellular targets.[111]

2.1.2 Alternative mechanisms of direct antimicrobial action

The postulation of alternative mechanisms of AMPM action originates from experimental findings that are difficult to account for within the mechanistic framework of membrane-activity. Foremost, on investigation of the biological activities of some enantiomeric pairs of AMPs, a diminished activity was displayed for the unnatural all-D forms. This is a very powerful argument for the involvement of stereospecific receptors in the corresponding mechanism (c.f. **Section 3.4**). Additionally, some AMPs show antimicrobial activities at concentrations that are much lower than necessary for the killing of microbes according to a carpet mechanism, and they often display a concomitant selectivity for certain microbial species (c.f. **Section 3.3**).

Not surprisingly, the border between alternative and membrane-active mechanisms is not clear-cut. For instance, mechanisms that depend on stereospecific binding to a receptor molecule on the membrane surface before exerting a principally unspecific permeabilising effect are conceivable. Indeed, lantibiotics such as nisin and mersacidin have been shown to bind to a so-called docking molecule in the bacterial membrane. This docking molecule has been identified as lipid-II, a precursor of peptidoglycan biosynthesis.[201] But whereas mersacidin is thought to directly inhibit the cell-wall biosynthesis,[202] nisin forms pores in the lipid bilayer in a targeted fashion, involving a pore complex of eight nisin molecules and four lipid-II moieties.[203] It is thought that after binding to lipid-II on the membrane surface, a part of the molecule is inserted into the membrane to achieve pore-formation similar to the barrel-stave model.[204] This notion is further supported by findings that nisin

displays membrane-permeabilising properties even in model systems lacking lipid-II, but only at higher concentrations, which are comparable to those typically encountered for membrane-active AMPs.

Conversely, unspecific binding of peptides to membranes could induce secondary structure that might be necessary for stereospecific interaction with a membrane-bound receptor molecule. Alternatively, the membrane-active properties of an AMP might enable it to translocate efficiently through the membrane and interact stereospecifically with an intra-cellular target. In addition to the lantibiotics, the microcins from Gram-negative bacteria also show interesting mechanistic features.[205] For example, microcin B17 impairs the function of bacterial DNA gyrase,[206] and microcin J25 is suggested to interact with the β-subunit of bacterial RNA polymerase, thus affecting RNA synthesis.[207]

The following discussion will focus on AMPs as defined in the introduction, and special emphasis will be given to two well-studied cases. This serves not only as a background for comparison with our AMPMs but also to review the experimental methodology used in the delineation of alternative mechanisms of antimicrobial action. Despite increased effort directed towards the study of alternative mechanisms, it is fair to mention that unambiguous examples are rare. Not surprisingly, most studies have been directed at AMPs that show promise for future clinical applications, such as the human AMP histatin 5.[185]

2.1.2.1 Interaction with discrete macromolecules

HISTATIN-5 Histatins are relatively small, (3-4 kDa) cationic histidine-rich peptides, found as components of human saliva. They possess bactericidal and fungicidal properties, although their antibacterial activities are only modest.[208, 209] Histatins play an important role in the control of fungal infections of the oral cavity via the innate immune system. Histatin-5, which is formed by processing of its histatin-3 precursor, displays the most potent antifungal activity of all histatins. In addition to their antimicrobial activity, they have been described to possess other biological activities, such as binding to tannins, hydroxyapatite, or metal ions, and the inhibition of cytokine induction, of certain proteases involved in periodontal disease, or of leukotoxin activity. For more information about these activities, the reader is

referred to a recent review by de Smet and Contreras.[44] Apart from these effects, the direct fungicidal activity of histatin-5 in an *in vitro* setting has been studied extensively, and the fungicidal mechanism of this compound has been suggested to involve binding to a receptor on the cell surface, followed by cell cycle arrest, efflux of ATP, inhibition of respiration, and production of reactive oxygen species (ROS).[44, 210] Due to the large body of publications directed towards it, histatin-5 serves as an excellent case-study for the elucidation of alternative mechanisms of AMP action.

The story of histatin-5 as an AMP with an alternative mode of action began in 1998 with a report from Edgerton and co-workers, who described saturable binding of ^{125}I-histatin 5 to *C. albicans* cells.[211] This binding could be competed with histatins-3 and -4, and was not detected for spheroblasts created from the same organism, the latter of which are also less susceptible to histatin-5. The latter result is somewhat contradictory to the report of Driscoll et al, who described that *C. albicans* spheroblasts are as susceptible to histatins as the wild type cells.[212] In addition, it was observed that dye-release from calcein loaded *C. albicans* was not correlated with microbial killing, suggesting that the loss of cell integrity is a secondary effect, occurring after cell death, rather than the primary source of the antifungal action. Blot overlays and chemical cross-linking experiments with ^{125}I-histatin 5 led to the isolation of a proteinaceous compound of around 70 kDa in the cell lysate and in crude membrane preparations.[211] This putative receptor was later identified by MALDI mass spectrometric analysis as either Ssa1p or Ssa2p, both heat-shock proteins from C. albicans.[213] Ssa1p/2p are conserved members of the yeast HSP70 heat-shock protein family and are major immunogens of the fungal cell-wall in *C. albicans*. Fungicidal studies with SSA1/SSA2 mutants showed a reduced activity of histatin-5 and suggest a function of Ssa1p/Ssa2p as binding receptors for histatins that could be involved in their translocation across the membrane.[213] Recently, this functional role was attributed to Ssap2 alone.[214]

Fluorescently-labelled histatin-5 is taken up into the cell, as has been shown by fluorescence microscopy, and the uptake was correlated to the metabolic state of the cell. *C. albicans* cells treated with sodium azide showed diminished uptake, and they were found to be less susceptible to histatins in a candidacidal assay. The labelled compound co-localised with mitochondria and was proposed to dissipate the trans-membrane potential of the mitochondrion, based on dye-efflux experiments. Interestingly, the uptake of labelled histatin-5, as well as the killing of the fungal cells,

is reduced under high ionic strength conditions,[215] especially under high calcium conditions,[216] and translocation of the peptide is accompanied with influx of propidium iodide. Both findings suggest an involvement of membrane-permeabilisation during the uptake of histatin-5, contrary to the above mentioned dye-leakage experiments. It has also been shown that the release of histatins can be brought about intracellularly, i.e. by expressing histatins inside *C. albicans* cells.[217] Based on these results, energized mitochondria were proposed to be the cellular target of histatin-5, for example via perturbation of the mitochondrial membrane.[215] That the metabolic state of *C. albicans* cells has an influence on the killing by histatin 5 was also reported by Gyurko et al. who found that mutants of *C. albicans* that are incapable of respiration are also less susceptible to histatins than wild-type cells. The same reduced susceptibility has been found for cells treated with the respiratory inhibitor sodium azide or with the proton gradient uncoupler CCCP,[218, 219] and the accumulation of the peptide in the cytosol and subsequent killing was correlated with the inhibition of mitochondrial ATP synthesis.[218]

This notion is corroborated by the finding that *S. cerevisiae,* grown under conditions at which they perform fermentation, are less susceptible towards histatin 5.[220] Koshlukova et al. reported on the loss of intracellular ATP induced by histatin-5 via a proposed non-lytic mechanism,[219] and they suggested that extra-cellular ATP can activate putative purinergic P2 receptors on the surface of *C. albicans*, that could lead to cell death via alteration of the membrane permeability,[221] or by lysis.[222] It has been shown that ATP efflux alone is not sufficient to cause cell death, and that the incubation of *C. albicans* cells with ATP analogues increased the killing, while removal of extra-cellular ATP decreased it.[223] Interestingly, anaerobically grown cells were not susceptible to extra-cellularly added ATP.

Also seemingly related to this loss of intra-cellular ATP could be the disruption of the *C. albicans* cell cycle by halting the cells in the G1 phase, which is also a marker of cell apoptosis. This is thought to be caused by a decrease in cell volume mediated by histatin-5, which causes rapid efflux of potassium and magnesium ions leading to parallel movement of water out of the cell. It is noteworthy that the increase of the cell size is thought to be critical for progression through the cell cycle.[224] A recent publication from Baev et al. suggests that the potassium transporter TRK1 is involved in the release of ATP and potassium by

histatin-5,[225] and the uptake of propidium iodide into the cells caused by histatin-5 has also been associated with the presence of Trk1p.[77]

Helmerhorst et al. on the other hand, correlated the formation of intracellular reactive oxygen species (ROS), by means of the oxygen radical sensitive probe dihydroethidium, with cell death and proposed that ROS formation, resulting from an impaired mitochondrial function, is the key event in the killing of fungal cells mediated by histatin-5.[226] Contrary to this proposal, recent publications claim that ROS formation is only a secondary effect of histatin-5 action. These experiments are based on the use of a cell-permeant ROS scavenger and on the lack of certain markers of apoptosis such as protein carbonyl formation, cytochrome c release or chromosomal fragmentation.[227, 228]

Despite increased experimental effort, it still remains unclear by which mechanisms a non-lytic efflux of ATP and other metabolites from the cell occurs. Of special interest is the study by Den Hertog et al, who investigated the binding to, and the peptide-induced leakage of trypsin from PC/PS liposomal systems, caused by histatin-5 and two derivatives. These authors suggest that peptide translocation occurs via peptide-phospholipid interactions and they found the translocation rate of histatin-5 in these artificial systems was much slower than observed for *C. albicans*, suggesting that other components of the fungal cell membrane might be involved in the process.[229] The candidacidal effects of LL-37 and histatin-5 were compared, and although effects were less pronounced for histatin-5, efflux of nucleotides such as ATP or NAD could be observed.[230]

To conclude, the mechanism of candidacidal action of histatin-5 is still a matter of debate. The currently proposed mechanism consists of binding to a specific receptor, presumably Ssa1p (Hsp 70), followed by translocation into the cytoplasm and targeting of mitochondria. Further events might comprise non-lytic release of ATP leading to cell death via activation of purinergic receptors, or the formation of reactive oxygen species (ROS) due to histatin-5 mediated out-of-sequence electron transfer from a carrier in the respiratory chain to molecular oxygen, which could lead to damage of macromolecular cell components, and ultimately to cell death.

To complicate matters, P113, a synthetic linear peptide containing a sequence of 12 of the 24 amino acids of histatin-5, possesses good antibacterial activity against *P. aeruginosa*, *S. aureus*, and *H. influenza*.[231] Of special interest are the findings that P113D, the enantiomer of P113, is as active against *C. albicans* as the parent

compound.[232] P113 has been demonstrated to be taken up into *C. albicans* cells and the activity of both P113 and P113D is abolished by pre-incubation with sodium azide, exactly as is the case for histatin-5.[233] This is an experimental result which is difficult to bring into accordance with the proposed specific binding events proposed for histatin-5, even if P113 is only a shortened derivative. It could nevertheless point to the fact, that the interaction of histatin-5 with Ssa2p might either not be stereospecific, or not primarily involved in the killing events caused by histatin-5. Intriguingly, the undiminished activity of P113D is not mentioned in any studies on histatin-5, and there has been no attempt to test fungicidal activity of an enantiomeric histatin-5, although the synthesis of a linear 24-mer consisting only of standard amino acids poses no conceptual difficulties. Indeed, all-D histatin-5 has been synthesised and was reported to be a selective inhibitor of the pro-protein convertases furin and PC7, but no data for the antimicrobial activity of all-D histatin-5 or histatin-5 was given.[234]

PRO/ARG-RICH PEPTIDES The class of short Pro/Arg-rich insect AMPs contains to-date the best characterised examples of AMPs with evidence for an alternative mechanism of action. Strong indications thereof originated again in the findings that the enantiomer of apidaecin proved to be practically inactive towards several strains of *E. coli*.[235] This turned out to parallel the behaviour of other proline-rich AMPs from invertebrates, namely drosocin and pyrrhocoricin, further highlighting their close relationship and attractiveness from a mechanistic point of view.[87, 236]

Other clues pointing to an alternative mechanism were reported, for instance the ability of formaecin to affect only growing cells.[237] Such behaviour is often taken as an indication that active metabolism is required for the antimicrobial action, but on the other hand it has been argued that membrane-active peptides might need a sufficiently high trans-membrane potential for translocation and active metabolism is required to generate such a potential. Additionally, the action of Pro/Arg-rich peptides is associated with being independent from lysis of the target cells. Indeed, apidaecin Ib and drosocin have been shown to possess no ability to induce dye-leakage from artificial liposomes containing lipid A analogues, and they have not been found to adopt amphipathic structures.[238]

The incorporation of radioactively labelled D- and L-apidaecin into eukaryotic cells has been studied, and it was found that the uptake is stereospecific and energy-driven, suggesting translocation of apidaecin through a transporter-, or permease-mediated mechanism.[239] It has been remarked that the data could also be interpreted in a way that both enantiomers transverse the outer membrane non-specifically, whilst during the washing process employed in the experiment, only the L-form is specifically retained, for example by a putative intra-cellular target. It was also concluded, that another target might be involved in the mechanism of action of apidaecin, based on the fact that some radioactively labelled peptides with modified sequences which were taken up into the bacterial cell, failed to kill them. Experiments on the incorporation of radioactively labelled biosynthetic precursors suggested that inhibition of bacterial protein synthesis is a likely mode of action for apidaecins.[239]

Further studies on the mechanism of action of Pro/Arg-rich AMPs were carried out by Otvos and co-workers, mostly with pyrrhocoricin. Based on the fact that a biotinylated pyrrhocoricin analogue only lost one order of magnitude in activity towards *E. coli* D22,[236] an affinity chromatography approach employing anti-biotin monoclonal antibodies coupled to agarose for the immobilisation of the biotinylated probe molecule, was developed. Eluates from affinity chromatography experiments carried out with *E. coli* cell lysates were subjected to SDS-PAGE analysis and led to the discovery of two protein bands corresponding to 60 and 70 kDa respectively.[240] A modified Western-blot protocol using biotinylated pyrrhocoricin instead of a primary antibody, and horseradish peroxidase conjugated to streptavidin, led to strong labelling of these bands, confirming an interaction between the labelled probe molecule and the two proteinaceous compounds. Additionally, two low molecular weight bands were detected, which did not respond to protein-selective staining methods. One of these bands was found to arise from unspecific labelling when checked with a biotinylated negatively charged control peptide. Tryptic digestion of the two proteinaceous compounds, followed by MS/MS analysis, led to their identification as DnaK and GroEL. Interestingly, LPS preparations from *E. coli* and *S. typhimurium* could not be detected with this modified Western blot, and biotinylated all-D pyrrhocoricin showed significantly lower binding to DnaK in the Western blot assay, suggesting a correlation of antimicrobial activity and binding to DnaK. In a further set of experiments, the authors studied the binding of fluorescently

labelled pyrrhocoricin, as well as drosocin and apidaecin, to heat shock proteins and LPS via fluorescence polarization assays.[240] In these experiments, the fluorescently labelled pyrrhocoricin was found to bind to DnaK as well as to GroEL. The fact that GroEL did not bind biotinylated pyrrhocoricin under Western blot conditions might originate from elimination of GroEL-ligand interaction during the denaturing conditions of the SDS page or during binding to the blotting membrane. The binding of the biotinylated probe molecule to DnaK under these conditions was explained by the authors as possibly originating from a mechanism that does not depend on the native global fold of the protein, or from partial re-naturation on the blotting membrane. Additionally, it was found that LPS bound strongly to all employed fluorescently labelled peptides. From the fact that a negative control peptide also bound to GroEL, it was concluded that this interaction was unspecific. Further competition binding assays, using unlabelled pyrrhocoricin as the competitor together with either DnaK or GroEL, were conducted. These experiments led the authors to propose that the interaction with DnaK involves two independent fragments of DnaK, in contrast to GroEL.

In a subsequent study by the same group, it was found that pyrrhocoricin inhibited the ATPase activity of recombinant DnaK in contrast to all-D pyrrhocoricin and the control peptides magainin-2 and cecropin A.[241] To study the effect of pyrrhocoricin on the re-folding of proteins (a biological function of DnaK), the group assayed the activity of two bacterial enzymes, namely alkaline phosphatase and β-galactosidase *in vivo,* and similar results were obtained. Based on dot-blot and fluorescence polarisation assays it was suggested that pyrrhocoricin binds in the hinge region of DnaK, forming a multi-helical lid over the peptide binding region of DnaK. The inhibition of ATPase activity was located in the N-terminal residues 2-10 of pyrrhocoricin whilst the C-terminal half of the molecule was described to be involved in its ability to translocate across cellular membranes as studied by confocal laser microscopy using fluorescently labelled analogues.[85] It should be mentioned though, that Chesnokova et al. reported that L-pyrrhocoricin binds to DnaK like a conventional peptide substrate, and does not inhibit DnaK mediated ATP hydrolysis.[242] It is also noteworthy that pyrrhocoricin showed similar effects on the ATPase activity of a wild type as well as a lidless mutant of DnaK.

Based on these experimental data, the following model for the action of pyrrhocoricin, apidaecin and drosocin is currently accepted as most likely: (1) The

peptides interact unspecifically with an outer-membrane component of Gram-negative bacteria, presumably LPS; (2) after accessing the periplasmic space they bind to a docking molecule, for example a component of a permease-type transporter system and are translocated into the cell; (3A) final targeting of an intracellular component, presumably DnaK and inhibition of its ATPase and/or other functions in refolding proteins. Alternatively (3B), the peptides might bind to macromolecular compounds corresponding to a molecular weight of around 15 kDa or to bacterial DNA, which were both found in the blot-overlay experiments.

2.1.2.2 Inhibition of macromolecular biosynthesis

In contrast to the reported binding to proteinaceous compounds by Pro/Arg- and His-rich peptides, a variety of AMPs are also suggested to exert their antimicrobial action through another type of binding to macromolecules, which might be independent from the exact sequence of the constituent monomeric units. In these cases, an interaction would rather be associated with recurring structural motifs, such as the DNA double helix.

In particular, there are several AMPs for which an alternative mechanism of action has been proposed to comprise the inhibition of the target organisms' macromolecular biosynthetic machinery. Typically, such mechanisms are inferred from the effects of AMPs on the patterns of incorporation of radioactively labelled precursor molecules into the micro-organismal macromolecular fractions (c.f. **Section 3.6**). Additionally, these data are often correlated with studies on the membrane-permeabilising properties of the AMPs in liposomal model systems, and with kinetic data of their antimicrobial action.

PR-39 In 1993, Boman et al. reported on the mechanism of antibacterial action of PR-39, a Pro-/Arg-rich antimicrobial peptide isolated from the small intestine of the pig.[243] These authors described an 8 minute lag phase in the killing of *E. coli* D21 which they attributed to a barrier in the outer membrane since, this lag phase was absent in a strain with a defective OM barrier. Furthermore, it was concluded from measurements of the time course of the optical density of PR-39 treated cell suspensions, that no lysis occurred during PR-39 mediated killing of *E. coli* D21, because there was no apparent drop in the optical density of the bacterial

suspension. Kinetic studies of the antibacterial action, which were carried out in parallel, showed that after the short lag phase an immediate drop of more than three orders of magnitude in the viable cell counts occurred, pointing to a rapid bactericidal action of PR-39.

Experiments with radioactively labelled precursor molecules of macromolecular biosynthesis, namely [^{3}H]-thymidine and [^{3}H]-leucine showed that their incorporation ceased within three to nine minutes after addition of PR-39, followed by degradation of cellular protein and DNA. Based on this data it was suggested that PR-39 kills bacteria by a non-lytic mechanism which selectively arrests DNA and protein biosynthesis, and leads to degradation of these macromolecules.

From my point of view it is important to comment on this report, because PR-39 is cited in virtually every review article that touches on modes and mechanisms of AMP action, and it is typically taken as a prototype for an AMP that acts by an alternative mechanism. Judging from the experimental data given in the original publication and outlined above, this seems rather astonishing. The observed rapid killing, coupled with rapid cessation of incorporation of biosynthetic precursor molecules, bears all the hallmarks of a membrane-active mode of action. Additionally, effects on the biosynthesis of other macromolecules, especially RNA were not studied, thus the statement that PR-39 kills bacteria through a mechanism that stops selectively DNA and protein biosynthesis lacks any firm experimental foundation. Furthermore, Merrifield and co-workers synthesized all-D PR-39 and found that this compound is comparable in activity to the natural all-L form with respect to *E. coli* (which was employed in the experiments described by Boman et al.) and *B. subtilis*, leading them to propose that both isomers lyse the bacteria by a mechanism other than the one proposed by Boman and colleagues.[244] Ironically, the all-D form was reported in this study to be significantly more active towards *P. aeruginosa* and *S. aureus*, the latter of which is 1000-fold more susceptible towards the all-D PR-39, as judged by determination of lethal concentrations (LC).

P-DER This peptide is a synthetic hybrid of the AMPs pleurocidin and dermaseptin and has been shown to translocate across membranous systems at sub-MIC concentrations, without inducing concomitant dye-leakage. Based on the incorporation of radioactively labelled precursor molecules it was suggested that this peptide exerts a selective inhibitory effect on RNA biosynthesis around its MIC,[245]

although this interpretation of the experimental data might seem rather bold at closer inspection. Additionally, at concentrations above the MIC, P-Der clearly showed behaviour in accordance with a membrane-active mechanism. Interestingly, these findings for P-Der were interpreted by Brogden in his review article as indications that pleurocidin and dermaseptin act by inhibiting bacterial macromolecular biosynthesis.[47]

INDOLICIDIN This short AMP isolated from bovine neutrophils contains an unusually high amount of tryptophan residues. The incorporation of radioactively labelled precursors of macromolecular synthesis showed inhibition of DNA and RNA at concentrations at which protein synthesis was not affected.[246] *E. coli* cells treated with indolicidin showed filamentation, and this has been compared to the inhibition of DNA synthesis by other antibiotics, such as nalidixic acid,[247] further supporting the notion that inhibition of DNA synthesis might be involved in the antibacterial mechanism of indolicidin.

CAP10A CAP10A is a synthetic indolicidin derivative, in which all proline residues are replaced by alanines. This peptide was suggested to impair protein, RNA, and DNA biosynthesis in *S. aureus* without killing the bacterial cells when treated with twofold MIC concentrations of peptide.[248] Nevertheless, incorporation of radio-labelled precursors for all studied classes of macromolecules stops simultaneously, a fact that is generally assumed to be best explained by a membrane-active mechanism.

BUFORIN-2 Buforin-2 is a condensed variant of a naturally occurring amphibian AMP which was reported to cross membranes following a toroidal pore model in which the pores are postulated to possess such a short lifetime that no significant impairment of membrane functions occurs. This has been inferred from dye-leakage experiments and the absence of lipid flip-flop, i.e. the scrambling of phospholipids between the inner and outer layers of the plasma membrane.[249] Buforin-II has been suggested to kill by binding to DNA and RNA, mostly based on gel-retardation experiments.[96]

TACHYPLESIN-I This β-hairpin AMP from the horseshoe crab has been reported to bind to the minor groove of the DNA duplex helix, based on DNA footprinting analysis.[250] Anti-parallel β-sheets have been identified as DNA binding motifs,[251] and the reduction of the disulfide bonds in tachyplesin-I or their replacement with alanines in an analogue indeed leads to a strongly reduced interaction. Therefore, the binding to DNA has been suggested to be involved in the antibacterial mechanism of tachyplesin-I. Interestingly, several compounds that bind to the DNA minor groove, such as pyrrole tetramides, show potent antimicrobial activity.[252]

2.1.2.3 Final remarks concerning alternative mechanisms

To summarise, it can be noted that although a variety of AMPs have been suggested to act by an alternative mechanism of antimicrobial action, these claims often do not withstand closer inspection, as has been argued for PR-39. The experimental data does suggest interaction with nucleic acids for some AMPs but it is questionable as to how specific these interactions might be, not least because no reports on enantiomeric forms of these peptides (except for PR-39) are available. Not surprisingly, the binding of buforin-II to nucleic acids is referred to as unspecific in recent publications, the same might very well apply to indolicidin and its congener Cap10A. Moreover, and this is an important aspect that distinguishes these compounds from the Pro/Arg-rich peptides, all of them have been demonstrated to be capable of interacting with, or permeabilising, membrane structures. Thus, it is conceivable that these effects are mediated by unspecific, for example electrostatic, interactions between the cationic AMPs and components of the biosynthetic machinery, notably with negatively charged molecules such as ribosomes, nucleic acids in general, or proteins which are negatively charged at physiological conditions. Support for such a notion comes, for example, from the finding that indolicidin-derived AMPs inhibit aminoglycoside acyltransferase and phosphotransferase, enzymes that show stretches of high negative charge at physiological pH. A variety of structurally different AMPs can inhibit these enzymes, indicating the lack of specificity for this inhibition.[253] Unspecific interaction can lead to an additive or synergistic effect caused by the impairment of several processes inside the target cell. It is very likely that such combined effects are operative, and this is sometimes

referred to as a multi-hit mechanism.[23] Another hypothesis in this respect is that a given AMP might act preferentially on one or more intracellular targets, also depending on the bacterial species and the exact nature of the AMP.[254]

It is therefore important for a mechanistic classification of AMPs to consider whether an unspecific interaction with intracellular components represents a primary or rather a secondary effect leading to the death of the target organism. Yet, even if an AMP primarily kills or inhibits the growth of micro-organisms by unspecific interaction with intracellular targets, it can do so only by translocating into the target cell. The requirement of reaching a putative intracellular target has been commented on before.[24] However, if the uptake depends on membrane-active properties of the AMP, I suggest that these should be regarded as membrane-active peptides, instead of ascribing alternative mechanisms to them. The ability to interact with and to translocate across target membranes is the underlying mechanistic feature of such AMPs. Without this ability, no antimicrobial activity could be observed.

2.2 Indirect (immuno-modulatory) modes of action

The second main mode of AMP action is concerned with their immuno-modulatory properties (c.f. **Figure 2.1**). The existence of such a mode of action for certain AMPs, which is at least partially independent from the direct killing of micro-organisms, has been suggested by experimental observations that link their *in vitro* and *in vivo* activities. Many AMPs, especially defensins and cathelicidins are thought not to be capable of directly killing micro-organisms either at concentrations corresponding to their natural abundance in the host, or with respect to the physiological conditions that they are likely to encounter at the sites of infection, i.e. the high salt concentrations, especially of the divalent cations of magnesium and calcium.[255] For example, LL-37 displays MIC values in the range of 1-30 μg/mL under routine assay conditions (low ionic strength), whereas in the presence of tissue culture medium it is completely inactive against *S. aureus* and *S. typhimurium* at concentrations up to 100 μg/mL.[256] Nevertheless, there is strong evidence that AMPs play an important role in host immunity. For instance, the expression of AMPs in cells of the immune system is induced by inflammatory stimulants such as LPS,[257] and *in vivo* studies involving transgenic or knockout animal models have shown that defensins significantly contribute to the clearing of bacterial infections.[258-260] Accumulating evidence points to the fact that many of these peptides might exert their beneficial action through activation and modulation of cells of the host immune defence. Indeed, a variety of AMPs have been demonstrated to confer beneficial effects on the host organism other than the direct killing of invading micro-organisms.

2.2.1 Immuno-modulatory effects displayed by AMPs

The immuno-modulatory effects of AMPs can be grouped into three classes, namely immune activation, immune suppression, and enhancement of the immune response. Studies on the immuno-modulatory effects of AMPs have largely been carried out with α- and β-defensins or with cathelicidins, and an overview of their properties is given here.

IMMUNE ACTIVATION Several AMPs have been described to be involved in the recruitment of cells of both the innate and the adaptive immune system to areas of infection. This attraction might take place either directly by a chemotactic activity of these compounds, which has been demonstrated for a variety of AMPs, (**Table 2.1**) or indirectly, via the induction of chemokines such as IL-8, or by stimulating the release of other mediators of inflammation such as the degranulation of histamine from mast cells (c.f. **Table 2.2**). It is noteworthy though, that no correlation between antimicrobial activity and histamine releasing potency has been found for several defensins.[261] Other effects of defensins involved in the inflammatory response comprise the modulation of neutrophil activity, for example by the up-regulated expression of adhesion molecules, the enhancement of phagocytosis,[262, 263] modulation of the classical pathway of complement activation, [264, 265] and induction of the production of reactive oxygen species (ROS) which might aid in the killing of micro-organisms.[266] Interestingly, an activating function on the complement pathway was also reported for the β-hairpin peptide tachyplesin-I.[267]

Table 2.1 Chemotactic effects on various cells of the immune system associated with AMP action.

Cell type	AMP	Reference(s)
monocytes/macrophages	human neutrophil peptides 1 & 2 (HNP-1/-2)	[268]
	human β-defensins 3 & 4 (HBD-3/-4)	[269, 270]
	proBac7	[271]
	Bac2A	[256]
	LL-37	[272]
	CRAMP	[273]
T-lymphocytes (and subsets)	human neutrophil peptides 1 & 2 (HNP-1/-2)	[274, 275]
	CAP37	[274]
	human β-defensin 2 (HBD-2)	[276]
	LL-37	[272, 277]
immature DCs[a]	human neutrophil peptide 2 (HNP-2)	[275]
	human β-defensin 2 (HBD2)	[276]
	murine β-defensins 2 & 3 (MBD-2/-3)	[278]
mast cells	human β-defensin 2 (HBD-2)	[279]
	LL37	[280]
neutrophils	PR-39	[281]
	LL-37	[272]
	CRAMP	[273]
PML[b]	LL-37	[277]

[a] DC ≡ dendritic cells; [b] PML ≡ polymorphonuclear leukocytes

IMMUNE SUPPRESSION A variety of AMPs have been shown to protect animals from the severe effects of septic shock which are associated with the killing of Gram-negative micro-organisms and the release of LPS. Septic shock can also be caused by the induction of high levels of pro-inflammatory cytokines such as TNF-α, IL-1β, and IL-6. Indeed, it has been found that LL-37 inhibits macrophage stimulation by LPS with concomitant up-regulation of several cytokines, but not the pro-inflammatory TNF-α.[282] An analogous inhibition of the release of TNF-α was found for LL-37 in human monocytes challenged with LPS, [283] or for PR-39 in a murine model.[284] Other AMPs have been found to neutralise the detrimental effects of LPS *in vitro* as well as in various animal models, for example CAP18,[285] indolicidin,[256] and synthetic $LALF_{31–52}$.[286] Additional effects of AMPs that could help to attenuate the negative effects accompanying inflammatory response on the host have been found to include the enhancement of angiogenesis, an important aspect of wound repair, by PR-39 and by LL-37.[287, 288]

Table 2.2 Differential expression and release of mediators of inflammation induced by AMPs.

Effect(s)[a]	AMPs	Reference(s)
histamine release from mast cells	various rabbit, guinea pig, and human defensins	[261]
	human β-defensin 2 (HBD-2)	[289]
	LL-37	[289]
induction of PGD_2	human β-defensin 2 (HBD-2)	[289]
induction of IL-6	human neutrophil peptides 1 – 3 (HNP-1/-2/-3)	[290, 291]
induction of IL-8 synthesis	human neutrophil peptides 1 – 3 (HNP-1/-2/-3)	[290, 291]
	LL-37	[256, 292, 293]
	indolicidin	[256]
up-regulated expression of TNF-α and IL-1β	human neutrophil peptides 1 - 2 (HNP-1/-2/-3)	[294]
down-regulation of IL-10	human neutrophil peptides 1 - 2 (HNP-1/-2/-3)	[294]
up-regulation of IL-8 and several chemokine receptors	LL-37	[282]
induction of IFN-α, IFN-γ, IL-2, and IL-13	$LALF_{31-52}$	[295]
induction of TNF-α	LL-37	[296]
	murine β-defensin 2 (MBD-2)	[297]
induction of IL-1β	murine β-defensin 2 (MBD-2)	[297]

[a] IL ≡ interleukin; PGD_2 ≡ prostaglandin D_2; IFN ≡ interferon; TNF ≡ tumour necrosis factor.

Furthermore, defensins have been reported to promote proliferation of epithelial cells and fibroblasts,[298, 299] indicating a role in wound healing.[300] Finally, the AMP precursor proBac5 has been reported to inhibit cathepsin L, a protease that is present in inflammatory cells and might contribute to damage of the host tissue.[271]

ENHANCEMENT OF ADAPTIVE IMMUNITY AMPs can bridge the innate and adaptive immune systems by chemo-attracting iDC (to take up antigens) and by influencing the differentiation of DCs. For example, LL-37 enhances the phagocytotic properties of iDCs, which can increase the density of antigen presentation and thus subsequently the T-cell stimulation.[296] Likewise, murine β-defensin 2 has been found to stimulate the maturation of DCs via the Toll-like receptor 4 (TLR4).[297] Defensins can enhance the systemic antibody response,[301, 302] and have been shown to induce anti-tumour immunity in mice when fused to a non-immunogenic tumour antigen.[278] Analogously, LL-37 showed adjuvant effects in a genetically fused vaccine.[303]

2.2.2 Mechanisms of immuno-modulatory effects *in vivo*

Inasmuch as it is of interest to understand how the direct antimicrobial action of AMPs is mediated on the molecular level, it is also of interest to elucidate how AMPs exert their immuno-modulatory functions. Generally, the interaction of AMPs with immune cells has been related to the involvement of specific receptors. For example, human β-defensins have been proposed to interact with CC chemokine receptors, based on the fact that HEK293 cell lines transfected to express this receptor were chemo-attracted by HDB-2.[276] Additionally, chemotactic effects of HDB-2 could be inhibited by pertussis toxin, which is generally regarded as indicating the involvement of a receptor coupled to $G_{i\alpha}$ protein.[276] Other receptors that have been suggested to be involved in the action of AMPs include formyl peptide receptor-like 1 (FPRL1),[272, 273] epidermal growth-factor receptor (EGFR),[304] or the P2X(7) receptor.[305] Further, α-defensins have been reported to bind to fibronectin, thus affecting endothelial cell adhesion and angiogenesis,[300] and LL-37 has been documented to induce phosphorylation and activation of extracellular kinases such as p38 and the mitogen activated protein kinase (MAPK).[306]

The effect of AMPs on modulating the immune response towards LPS is thought to be mediated by binding of the AMP to the LPS, which in turn could abolish the binding of LPS to LPS binding protein (LBP).[307] Strong evidence for such a mechanism comes from the fact that certain AMPs such as HNP-1 and HBD-2/-3 show an additive behaviour with indolicidin or LL-37 with respect to the anti-endotoxin properties.[256] On the other hand, the combination of LL-37 and indolicidin displays a synergistic effect in anti-endotoxin activity,[256] and the AMP Bac2a is less effective at inhibiting LPS mediated release of TNF-α than indolicidin, despite its stronger binding to LPS,[307] thus suggesting the involvement of other mechanisms in these activities.

It is interesting to note in this context that the diverse effects elicited by α-defensins have been classified into two groups according to the required dose of the AMP. Disruption or permeabilisation of cell membranes (vide supra), inhibition of NADPH activation,[308] and modulation of the complement system all require higher concentrations of α-defensins (in the micromolar range), [264, 265] whereas chemotactic activities of these peptides are detectable at nanomolar concentrations.[275] Thus, it might seem tempting to associate a membrane-active mechanism with the interactions depending on a high peptide concentration, especially if one considers that the membrane-activity of defensins in this concentration range has been well documented. Along these lines, it has been found that the classical pathway of complement activation was induced by α-defensins in their native state, as well as when their disulfide bonds were reduced, and even when the corresponding cysteine residues were acetylated. In contrast, activities at low nanomolar concentrations are often associated with receptors, especially with G-protein coupled receptors.

However, of particular importance in this respect is a report by Braff et al, in which immuno-modulatory effects of LL-37 and its enantiomer D-LL-37 were studied.[293] The authors found that the stimulating effect of D-LL-37 on the induction of IL-8 in keratinocytes was even greater than for naturally occurring LL-37, and this was attributed to increased proteolytic stability of D-LL-37. The induction of IL-8 by both antipodes could be inhibited by pertussis toxin, indeed suggesting an involvement of G-protein coupled receptors in the process, but it has to be concluded that these receptors are not (stereo)specifically inhibited by LL-37. It has been speculated that LL-37 might activate membrane-receptors by inducing conformational

changes associated with its interaction with the plasma-membrane. The example of LL-37 serves as a vivid illustration of the problems in assigning receptors to the immuno-modulatory function of AMPs. In fact, many of these effects could be mediated by the underlying membrane-activity of AMPs. It would therefore be of great interest to examine the immuno-modulatory effects of other enantiomeric pairs of AMPs, or of chemokines in general.

Finally, arguments brought forward in favour of a membrane-active direct mode of action, like the tolerance to large variations in sequences and structures of AMPs of diverse origins, increasingly apply to immuno-modulatory functions as well (inasmuch as more different AMPs are studied). The fact that all of these substances have been shown to be capable of displaying membrane-active properties has been mentioned already. Interestingly, there are several reports on the antibacterial activity of several chemokines, and these activities are in the same concentration range as found for defensins.[309] These findings could lead to the notion of a possibly similar underlying mechanism for both the immuno-modulatory and the antimicrobial actions of these compounds, and a membrane-active mechanism poses the no conceptual difficulties to accommodate both functions. A mechanism of bacterial killing displayed by the chemokines, apart from a membrane-active mechanism is only difficult to imagine, especially at the observed concentration regime.

2.3 Final remarks on modes and mechanisms of AMP action

As has been elaborated, mechanistic aspects of a variety of AMPs have been studied, and they are usually distinguished in the literature as following either a membrane-active or alternative mechanism, in a sense that these are mutually exclusive. Arguments have been presented in this section that this distinction is (a) often not unambiguous and that (b) the membrane-active principle of AMPs can serve as a unifying theme for almost all AMPs described to date.

More precisely, the described activities of various peptides are likely to be ultimately dependent on membrane-interactions of these compounds, and it is also likely that many of the immuno-modulatory effects described for AMPs are no exception. The possibility that compounds impair the function of membrane-receptors mechanosensitively, i.e. by disturbing their function via alteration of

membrane properties of the embedding membrane, has been mentioned (vide supra, c.f. also **Section 3.4**).

To conclude, it has been pointed out that the permeabilising activity of AMPs might be overestimated due to the facts that (a) studies on model membranes cannot lead to the detection of alternative mechanisms, (b) these studies are often carried out under conditions that are not physiologically relevant, and (c) amphipathic peptides will disturb any membranous system, if their concentration is high enough (i.e. not necessarily reflecting the MIC).[23] On the other hand, it could also be remarked that reports on the action of AMPs by an alternative mechanism are overemphasised because of the attractiveness of discovering unusual mechanisms, and because the term alternative mode of action is often (mis-)interpreted in a sense that equates membrane-activity with a detergent-like action.

3 Mechanistic studies on AMPMs

3.1 Synthesis of AMP(M)s

All antimicrobial peptide mimetics (AMPMs) used in this work were synthesised according to a mixed solid-phase solution-phase strategy developed in our group (**Scheme 1**).[124] Briefly, the first amino acid was coupled to freshly activated, acid-labile 2-chlorotrityl chloride resin (**20**) with 4 equivalents DIEA in DCM. Generally, Fmoc-L-Pro-OH was chosen as the first amino acid to be attached to the resin, since this allowed for the synthesis of larger batches of preloaded resin (**21**) that could be used for the synthesis of all AMPM(s). The linear, fully side-chain protected precursors (**22**) were synthesised employing standard SPPS Fmoc-chemistry on an Applied Biosystems model 433A peptide synthesizer on a 0.25 mmol scale.[310] Generally, 4 equivalents of the appropriately side-chain protected *N*-Fmoc amino acids are activated with HBTU, HOBt and DIEA in DMF. Fmoc-deprotection was achieved with 20% piperidine in NMP.

Linear, fully side-chain protected precursors (**22**) were cleaved from the resin with 0.6 to 0.8% TFA in DCM and the excess of acid was neutralized with an appropriate amount of 10% pyridine in MeOH. Linear peptide solutions were concentrated to 5% of the original volume under vacuum, and precipitated with water, followed by washing with $NaHCO_3$ and $NaHSO_4$ solutions. Crude **22** was dried overnight in a vacuum desiccator over KOH. Cyclisation reactions were carried out in freshly distilled DMF at room temperature at peptide concentrations ranging from 1 to 2.5 mg/mL of crude **22**.

The C-termini of the linear peptides was activated with 1.25 equivalents of both HATU and HOAt and with 2.5 equivalents of DIEA based on the crude yield of **22**, and the progress of the cyclisation reactions was monitored by LC/MS via the disappearance of the peak corresponding to the starting material, and was typically completed after 30 minutes. Deprotection reactions were run until LC/MS analysis showed the absence of any by-products containing residual protecting groups.

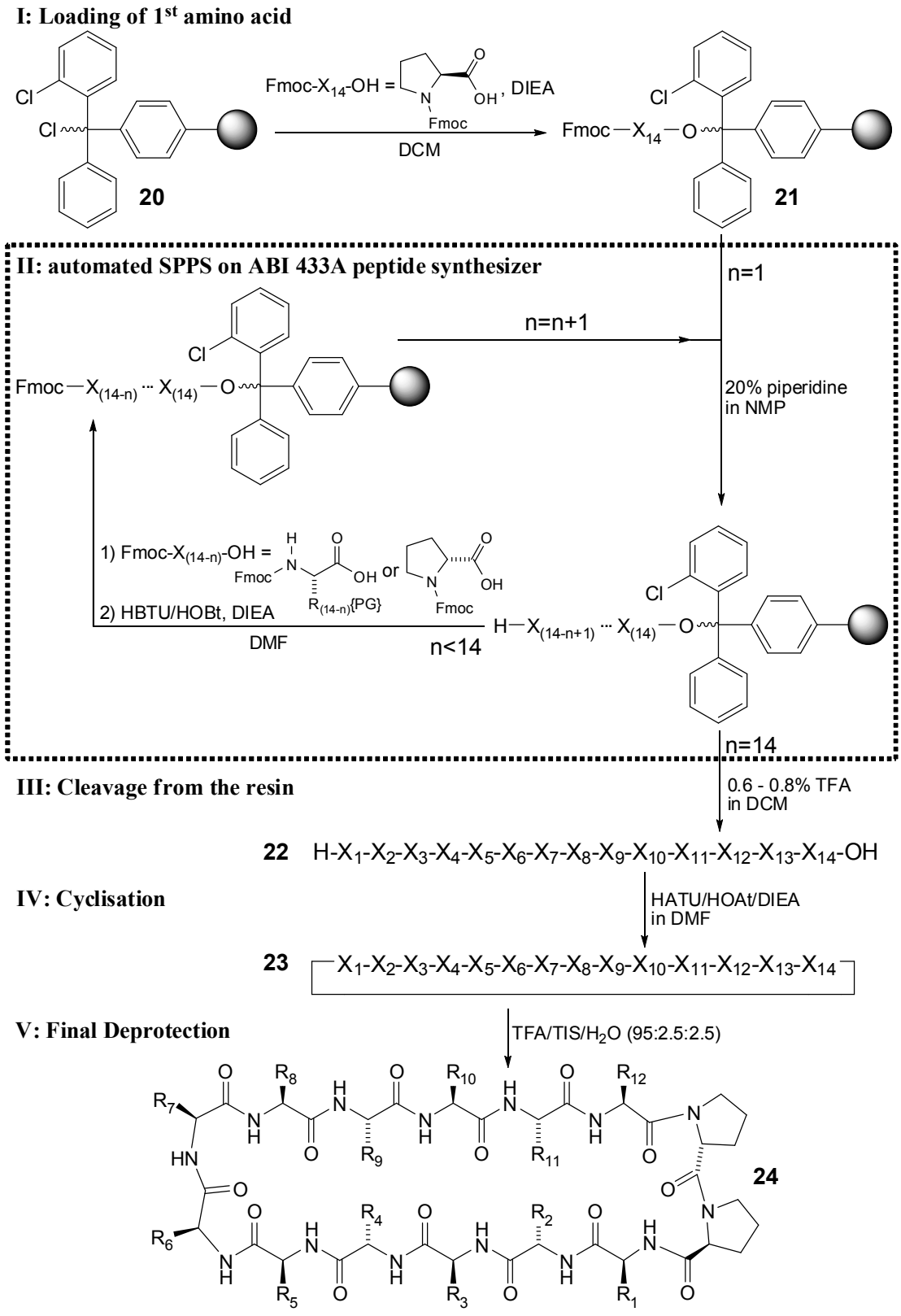

Scheme 1 Synthesis of AMPM(s)

The crude, cyclic and fully side-chain protected peptides (**23**) were evaporated to dryness followed by deprotection with TFA/H_2O/TIS (95:2.5:25 v/v/v) as an odourless deprotection cocktail. Typically, all deprotection reactions were finished after 2 to 3 hours. The crude cyclic peptides (**24**) were precipitated with ice-cold diethyl ether, centrifuged and washed three times with ether. After air-drying, the crude peptide products were purified by preparative reversed phase HPLC using H_2O/aetonitrile with added 0.1% of TFA as solvent system. The purified AMPMs were characterised by LC/MS, MS, analytical HPLC and ^{1}H NMR (c.f. **Appendix 2**).

3.3.1 Chromatographic behaviour and purification of mimetic 17

Mimetic **17** displays an unusual, characteristic two-peak pattern when analysed by HPLC chromatography; a representative chromatogram illustrating this pattern is shown in **Figure 3.1**. Identical patterns were also obtained for other AMPMs developed in our group, most notably, when position-12 of the amino acid sequence (N-terminal to the D-Pro-L-Pro template) is occupied by an arginine residue. Direct evidence for the influence of this position on the chromatographic pattern of the AMPMs is given by the fact that replacement of Arg-12 by Val-12 in an otherwise unchanged sequence leads to the recurrence of a normal single peak pattern.[139]

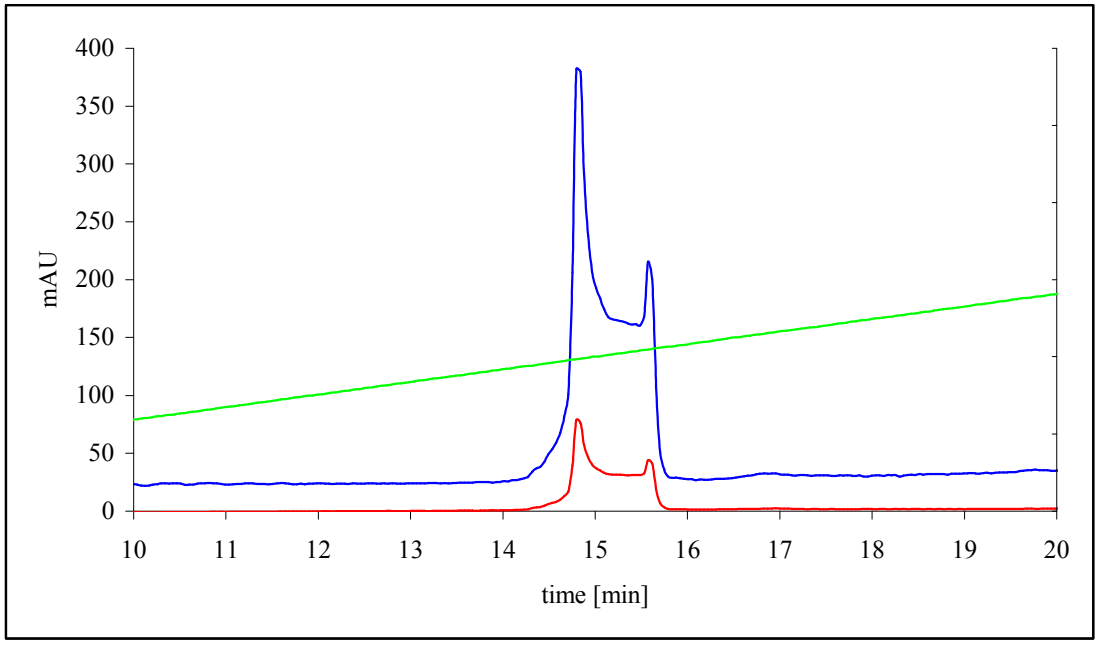

Figure 3.1 Characteristic two-peak pattern of purified mimetic-**17**. Conditions: Vydac218TP54 C18 analytical column; 5 to 100% acetonitrile in water (+0.1% TFA) in 7 column volumes; flow 1 ml/min; blue trace=226 nm; red trace=278nm.

Due to this peak pattern, a two-step purification protocol was needed to obtain pure **17**. Typically, three fractions (F_1 to F_3) as depicted in **Figure 3.2** were collected and re-subjected to a second round of purification. Pure **17** was obtained by collecting fraction F_1(2^{nd} purification) of re-injected fraction F_3 and vice versa. Fortunately, both AMPMs **18** and **19** showed normal single peak patterns, greatly simplifying their purification protocols.

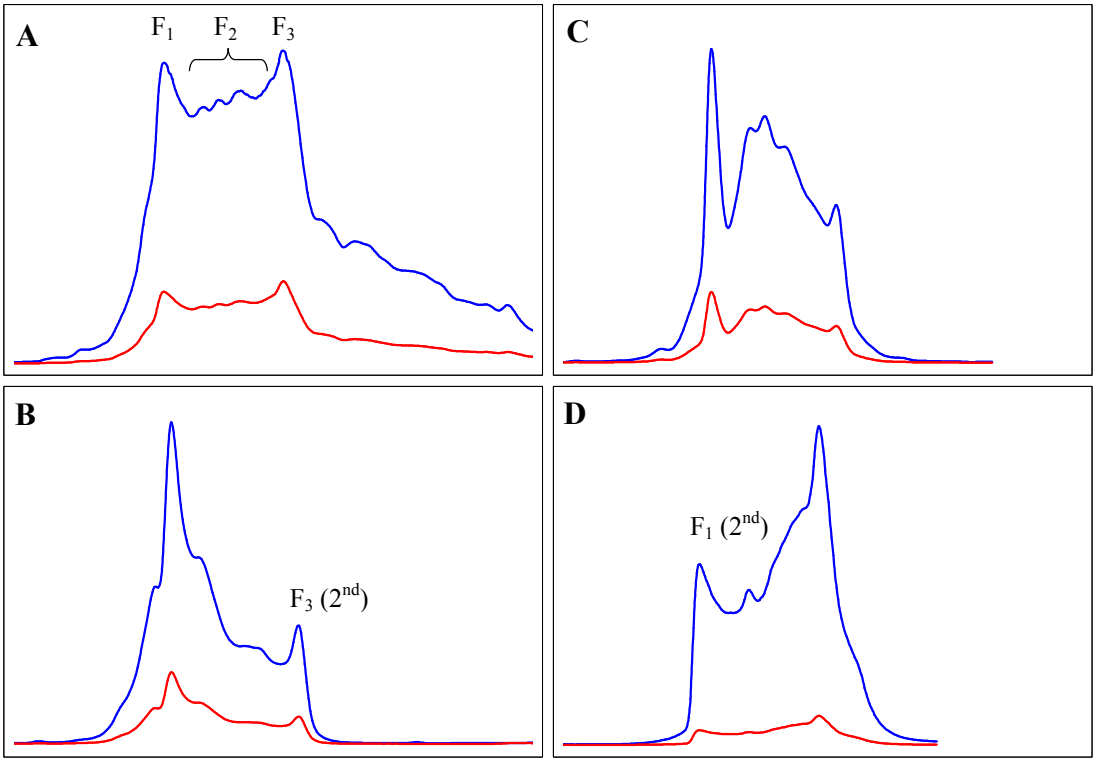

Figure 3.2 HPLC patterns in the two-step purification of mimetic **17**. (**A**) crude **17**, fractions F_1 to F_3 were collected as indicated; (B) re-purification of fraction F_1; (C) re-purification of fraction F_2; (D) re-purification of fraction F_3. Pure **17** was obtained by collecting fractions F_1(2^{nd}) and F_3(2^{nd}). Purification conditions: Vydac218TP1022 C18 preparative column; 10 to 50% acetonitrile in water (+0.1% TFA) in 30 minutes; 15 ml/min; blue trace=226 nm; red trace=278nm.

3.3.2 Synthesis of protegrin-1

As a control AMP possessing a well-studied mechanism of action, protegrin-1 (**11**) has been synthesised, using standard Fmoc-SPPS methodology. Briefly, crude, linear protegrin-1 was assembled on a rink amide MBHA resin, which allows for the routine synthesis of C-terminal amides. The automated peptide synthesis was carried out analogously to the protocol described for the AMPMs, followed by simultaneous

cleavage from the resin and deprotection of the side-chain protecting groups with TFA/phenol/thioanisole/ethanedithiol 82.5:5:5:2.5 (v/v/v/v), to yield a fully deprotected linear precursor.

The oxidation of the linear precursor was carried out as air oxidation in 0.1M NH_4/HCO_3 solution at a crude peptide concentration of 0.1 mg/mL until LC/MS analysis showed complete consumption of the linear precursor. The absence of free thiols was checked by an Ellman test, and crude **11** was purified by preparative HPLC. The identity of the final product could be confirmed by comparison of the ^1H NMR spectrum with a published literature example,[311] and additionally, the antimicrobial activity of pure **11** was in excellent agreement with reported values.[312]

3.2 NMR experiments

NMR studies with mimetic **16** in aqueous solution and bound to perdeuterated dodecylphosphocholine (DPC-d_{38}) micelles have been described previously.[137] It was found that this compound was largely unstructured in aqueous solution, as indicated by $^{3}J_{HN\alpha}$ scalar coupling constants around 7 Hz and the absence of a significant number of cross-strand NOEs in NOESY spectra (**Figure 3.3A**). In the presence of DPC-d_{38} micelles, however, **16** adopted a regular hairpin structure; containing a type-II' β-turn at the tip of the hairpin (**Figure 3.3B**). Such behaviour, namely the induction of secondary structure upon transition from an aqueous to a more apolar environment, is frequently encountered with many amphipathic AMPs, especially those belonging to the α-helical subclass.[155] Additionally, solvent mixtures such TFE/water or HFIP/water are often used as membrane mimicking environments as an alternative to micellar systems.[313]

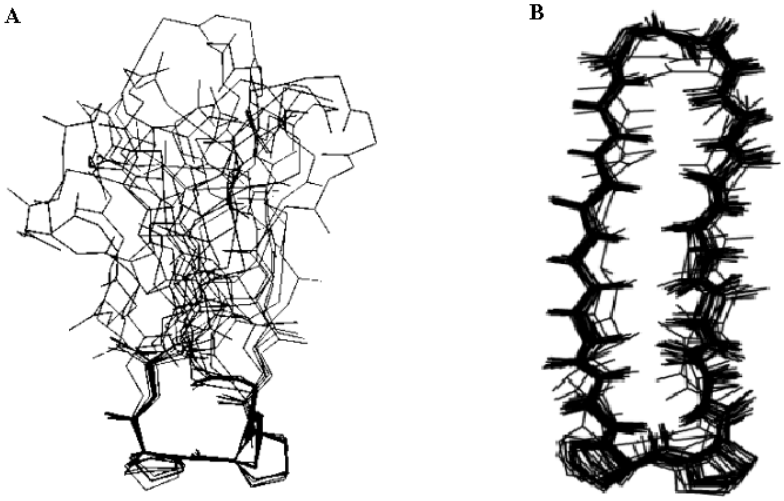

Figure 3.3 (**A**) Superimposition of 13 low energy average solution structures over the backbone heavy atoms of the D-Pro-L-Pro template (calculated for mimetic **16** in water at pH 2.3). (**B**) Superimposition of 18 low energy average solution structures over the backbone heavy atoms (calculated for **16** in the presence of DPC-d_{38} micelles). Taken from ref [137].

3.2.1 NMR structures of 17 and 18 bound to DPC-d_{38} micelles

1D ^{1}H-NMR spectra of **17** as well as 1D and 2D ^{1}H-NMR spectra of **18** were recorded at 600 MHz in aqueous solution (H_2O/D_2O 9:1, pH 5, 300K) at a typical peptide concentration of approximately 10 mg/mL. The narrow range of the chemical shifts of the amide proton resonances of these compounds, suggested that neither mimetic **17** nor mimetic **18** adopted any preferred conformations in aqueous solution (**Figure 3.4**).

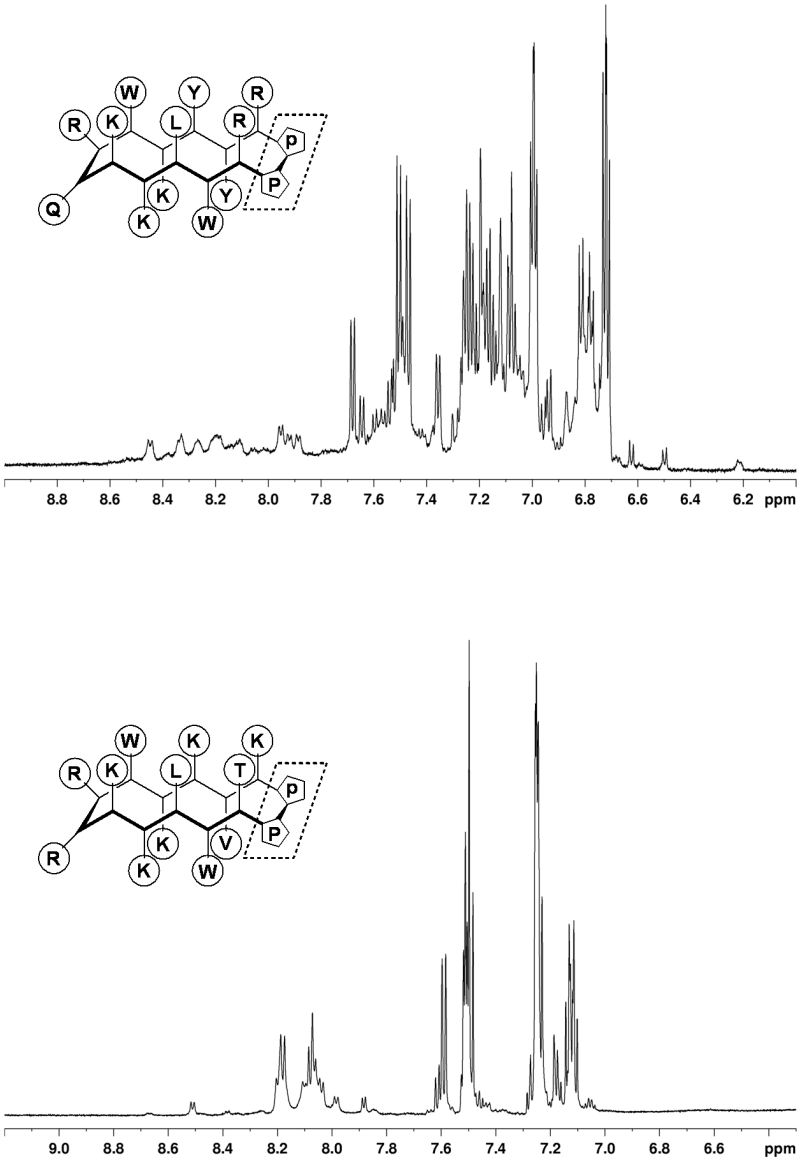

Figure 3.4 Expansions of the amide proton regions of the 600 MHz ^{1}H-NMR spectra of mimetic **17** (top) and mimetic **18** (bottom); recorded at peptide concentrations of 10 mg/mL in H_2O/D_2O (9:1) at pH 5 and 300K.

In addition, the number of observed amide proton resonances suggests that both mimetics contain at least two molecular species, at ratios of approximately 3:1, which interconvert slowly on the NMR timescale. This parallels the situation found for mimetic **16**, where NMR analysis also showed the presence of different molecular species in aqueous solution. Although signal overlap in the NMR spectra of mimetic **16** in aqueous solution precluded the assignment of two of the minor conformational isomers, it was suggested that at least one of these isomers arose through *cis-trans* isomerism of the peptide bond between Val-12 and D-Pro-13.[137] In contrast to all other naturally occurring amino acids, only proline has a significant propensity to form Xaa-Pro (Xaa = arbitrary amino acid) *cis* peptide bonds, and these bonds are often found in turn regions of water-soluble proteins.[314]

It is of interest to note, in this respect, that a derivative of mimetic **16** into which the additional constraint of a disulfide bridge had been introduced, formed an unusual loop structure containing a *cis* amide bond N-terminal to the D-Pro-L-Pro template, as well as a short 3_{10}-helical stretch.[137] Furthermore, the presence of an Xaa-D-Pro bond in other β-hairpin mimetics based on the D-Pro-L-Pro template, such as a Fc-binding peptide mimetic, has been reported.[127] It is also of interest to recall the peculiar HPLC profile observed for mimetic **17** (c.f. **Section 3.1**); a plausible explanation of such a profile is offered by the presence of *cis-trans* peptide bond isomers of this compound.

To study the AMPMs in a membrane mimetic environment, spectra were recorded in 300 mM DPC-d_{38} in H_2O/D_2O 9:1 at pH 5 and 300K, and at a peptide concentration of 2 mM (approximately 4 mg/mL). From the 1D ^{1}H-NMR spectra (**Figure 3.5**, **Appendix 4**) it could be seen that the amide proton resonances corresponding to both **17** and **18** covered a wider range of chemical shift values than in the spectra measured in aqueous solution. This finding was indicative of the adoption of preferred conformations upon interaction with the perdeuterated micellar system.

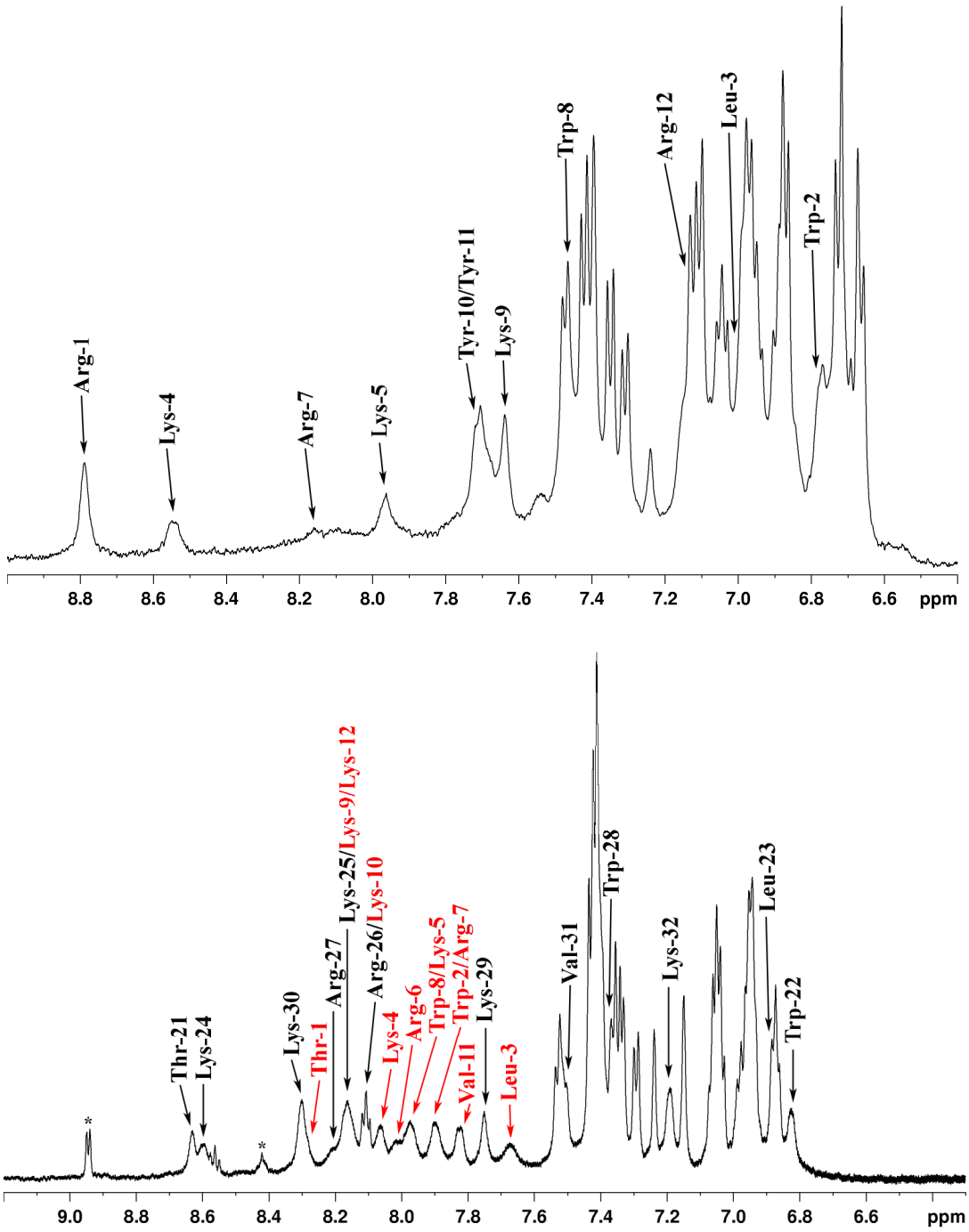

Figure 3.5 Expansions of the amide proton regions of the 600 MHz ^{1}H-NMR spectra of **17** (top) and **18** (bottom); recorded at peptide concentrations of 4 mg/mL in 300 mM solutions of DPC-d_{38} in H_2O/D_2O (9:1) at pH 5 and 300K. The amide resonances, as determined from 2D TOCSY experiments, are indicated (**c.f. Appendix 4**). For mimetic **18**, the resonances corresponding to the *cis*- or the *trans*-isomer are depicted in black and red, respectively. The numbering for the *cis*-isomer is derived from the normal numbering system by the addition of the value 20. * denote artefacts from the DPC-d_{38} preparation (c.f. reference [315]).

The spectral assignment of DQF-COSY and TOCSY spectra of **17** and **18** bound to DPC-d_{38} micelles was performed according to standard methods.[316] Distance restraints were obtained from NOESY spectra with a mixing time of 120 ms, and the large number of observed NOEs made structure calculations possible (c.f. **Appendix 4**), by applying a simulated annealing (SA) protocol implemented in the DYANA software package.[317] These calculations were carried out by Dr. K. Möhle.

MIMETIC-17 In addition to the network of sequential NOE connectivities, a variety of medium- and long-range NOEs were observed, indicating a defined structure of **17** in the presence of DPC-d_{38} micelles; these connectivities are depicted in **Figure 3.6**. In particular, many side-chain to side-chain and backbone to side-chain contacts were found between Leu-3/Trp-8, Leu-3/Tyr-11, and Trp-8/Tyr-11, illustrating that **17** is furnished with a hydrophobic core.

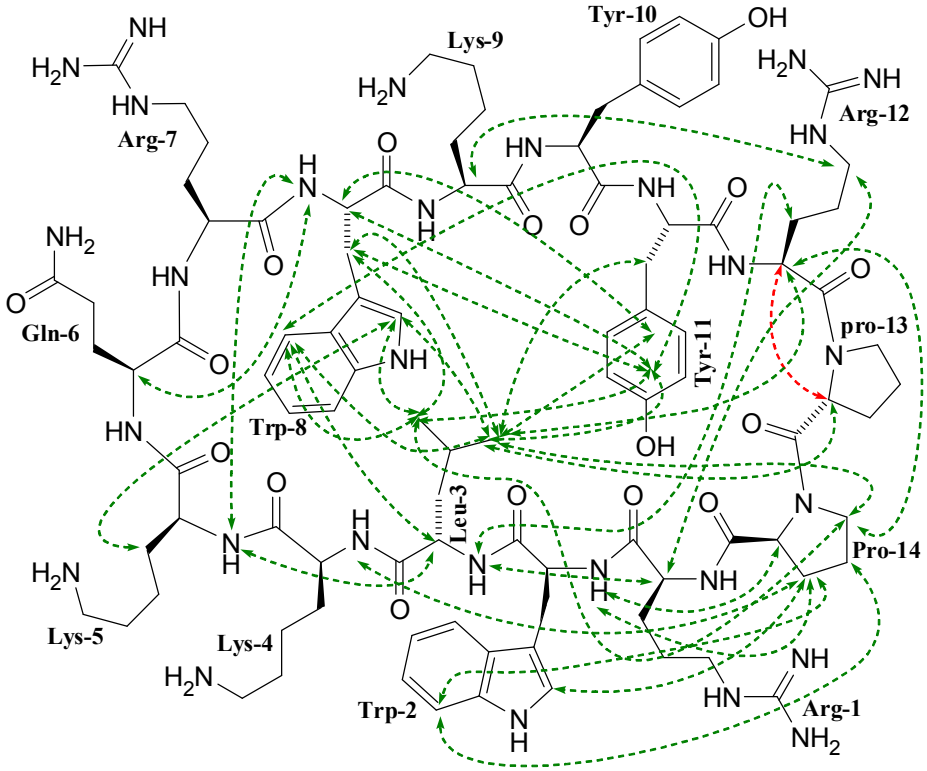

Figure 3.6 Medium- and long-range NOE connectivities observed for mimetic **17** bound to DPC-d_{38} micelles. The sequential NOE indicating the presence of a *cis*-amide bond is included and highlighted in red.

An interesting structural feature of mimetic **17**, which is indicated by the $d_{\alpha N}(i, i+2)$ NOE connectivity between Gln-6/Trp-8, as well as by the $d_{\alpha N}(i, i+3)$ NOE connectivity between Lys-9/Trp-12, is the formation of a 3_{10}-helical stretch N-terminal to the template. Moreover, the presence of a *cis*-amide bond N-terminal to the D-Pro-L-Pro template was deduced from a strong NOE between the H_α protons of Arg-12 and D-Pro-13 (c.f. also **Figure 3.6A**), confirming again the involvement of *cis*/*trans* isomerism. It should, however, be noted that in the case of **17**, the *cis*-isomer is the only molecular species found to be present in DPC-d_{38} micellar solution.

The ensemble of structures calculated by the SA protocol converged to a well-defined amphipathic structure with a pairwise rmsd of 1.03 Å for all backbone atoms (**Table 3.1**). A superimposition of the 20 calculated structures of mimetic **17** with the lowest target energy function, emphasising the amphipathic nature of these molecules in the presence of micelles, is given in **Figure 3.7**.

Table 3.1 Input of conformational constraints and statistics of the structure calculation for mimetics **17** and **18** with the Program DYANA

	Mimetic	**17**	**18**
NOE upper-distance limits	Total	153	155
	Intra-residue	63	65
	Sequential	54	46
	Medium- and long-range	36	44
Residual target function value [Å^2]		0.62 ± 0.08	0.97 ± 0.08
Mean rmsd values [Å]	All backbone atoms	1.03 ± 0.37	0.81 ± 0.22
	All heavy atoms	2.47 ± 0.65	2.10 ± 0.56
Residual NOE violation	Number > 0.2 Å	21	23
	Maximum (Å)	0.34	0.30

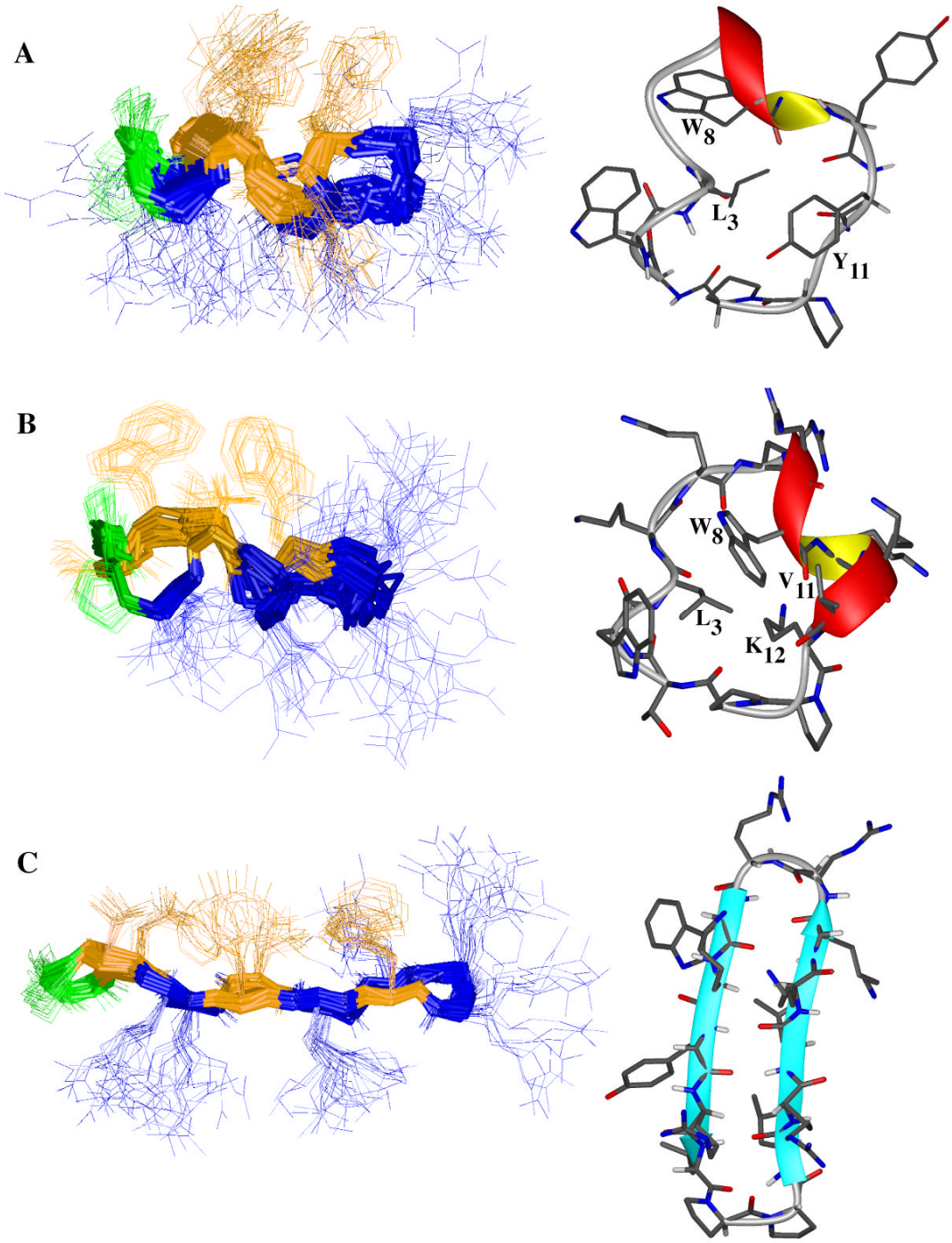

Figure 3.7 Comparison of the average solution NMR structures of the major (or exclusive) conformational isomers of mimetics **17** (**A**), **18** (**B**), and **19** (**C**) bound to DPC-d_{38} micelles. On the left, superimpositions of the 20 average solution structures with the lowest energy target functions over the backbone heavy atoms are shown (18 for mimetic **17**). Polar residues, apolar residues and the D-Pro-L-Pro template are depicted in orange, blue, and green respectively. On the right, ribbon representations of the corresponding average solution structures with the lowest energy target function are given, shown with the amino acid side-chains.

MIMETIC 18 In contrast to **17**, two conformational isomers were observed for **18** in micellar solution, at a ratio of approximately 5:3. The spectral assignment made it possible to identify the major and the minor isomer as containing a Lys-12/pro-13 *cis*- or *trans*-amide bond, respectively. Since the minor *trans*-isomer was characterised by the absence of medium- and long range NOE contacts, it was not surprising that the resulting low-energy structures showed little convergence to a defined three-dimensional conformation (**Figure 3.8**, c.f. also the narrow range of amide resonances in **Figure 3.5**).

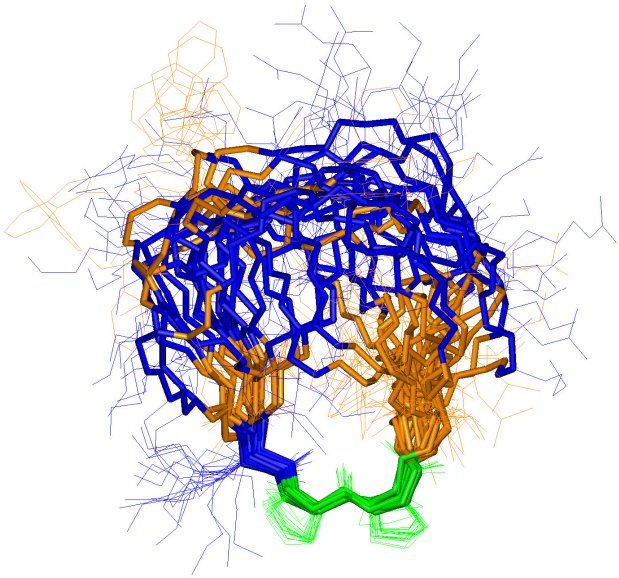

Figure 3.8 (**A**) Superimposition of 20 average solution structures with the lowest energy target function over the backbone atoms of the D-Pro-L-Pro template (calculated for mimetic **18** in 300 mM solution of DPC-d_{38} at pH 5).

For the major isomer, however, the presence of a network of sequential NOE connectivities, as well as a variety of observed medium- and long-range NOEs (c.f. **Appendix 4**) pointed to the adoption of a preferred three-dimensional structure in the presence of DPC-d_{38} micelles. The obtained medium- and long-range NOEs are depicted in **Figure 3.9**. In particular, a variety of side-chain to side-chain contacts were found between Leu-3/Trp-8, and Trp-8/Val-11, indicating a hydrophobic core for **18**, comparable to that of mimetic **17**. Another similarity to **17** is the presence of a 3_{10} helical stretch N-terminal to the D-Pro-L-Pro template, as deduced from the presence of $d_{\alpha N}(i, i+2)$ NOE connectivities between Trp-8/Lys-10, Lys-9/Val-11, and

Lys-10/Lys-12. The *cis*-configuration of the Lys-12/pro-13 amide bond was deduced from a strong NOE between their H_α protons (c.f. also **Figure 3.11**).

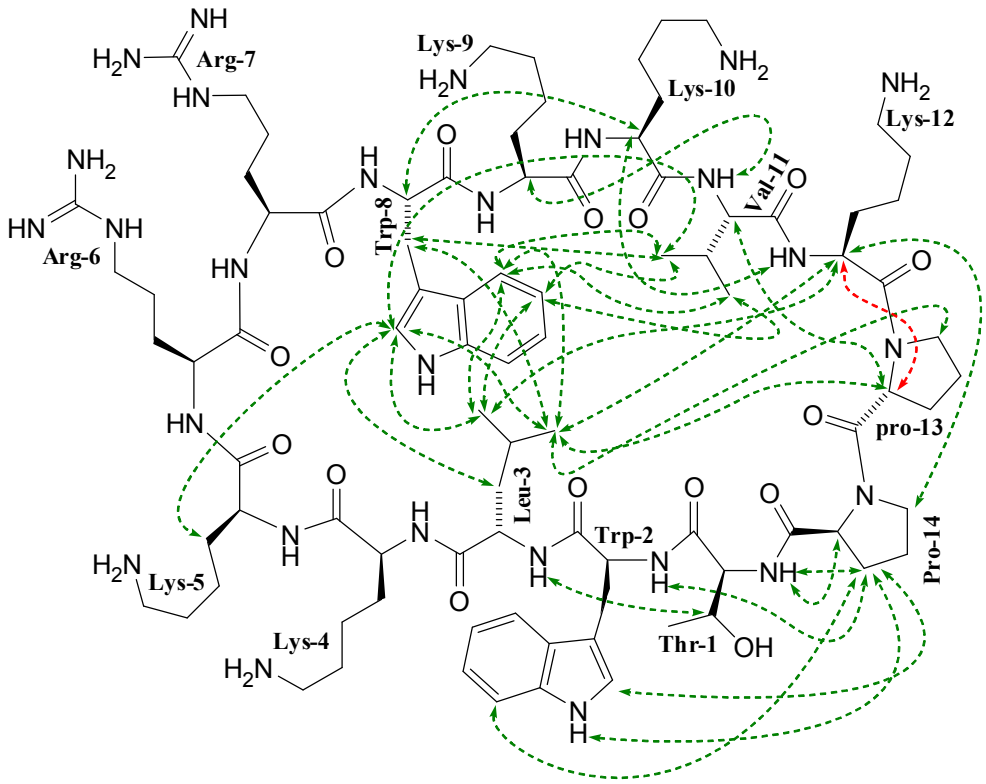

Figure 3.9 Medium- and long-range NOE connectivities observed for mimetic **18** bound to DPC-d_{38} micelles. The sequential NOE indicating the presence of a *cis*-amide bond is included and highlighted in red.

The ensemble of structures calculated by the SA protocol converged to a well-defined amphipathic structure with a pairwise rmsd of 0.81 Å for all backbone atoms (**Table 3.1**). A superimposition of the 20 calculated structures of mimetic **18** with the lowest target energy function, emphasising the amphipathic nature of these molecules in the presence of micelles, is given in **Figure 3.7**.

COMPARISON OF 16, 17 AND 18 An amphipathic distribution of the amino acid side-chains is found for all three compounds, but it can be seen from **Figure 3.7** that the structures employed to accommodate this distribution differ fundamentally between **16** on the one hand, and **17** and **18** on the other. Whereas in mimetic **16** a regular β-hairpin fold is able to spatially separate residues of different polarity, despite the introduction of a charged residue on the apolar face of the idealised hairpin

structure, both **17** and **18** are characterised by the formation of 3_{10}-helical stretches and the presence of a *cis*-amide bond N-terminal to the D-Pro-L-Pro template.

The formation of these unusual structural elements might be necessary in order to accommodate hydrophobic interactions between Leu-3, Trp-8, and Tyr-11 in **17**, or between Leu-3, Trp-8, and Val-11 in **18**, thus generating the hydrophobic cores of these molecules. The calculated average solution structures of **17** and **18** with the lowest energy target functions are superimposed in **Figure 3.10** so as to emphasise their close structural relationship.

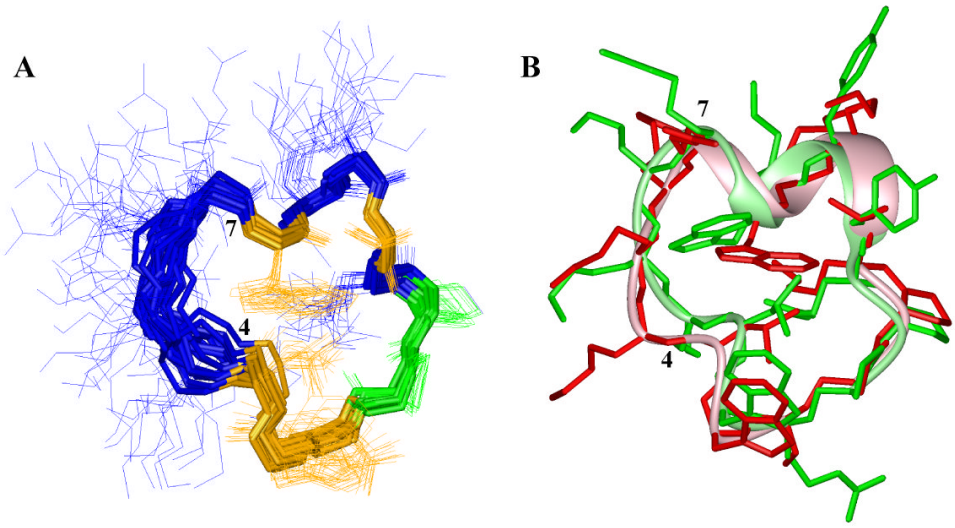

Figure 3.10 (**A**) Superimposition of the 20 average solution structures with the lowest energy target function of mimetic **18** over the backbone heavy atoms of the D-Pro-L-Pro template (calculated in the presence of DPC-d_{38} micelles). (**B**) Superimposition of the two calculated structures with the lowest energy target function of **17** (green) and **18** (red), calculated in the presence of DPC-d_{38} micelles.

As can be seen from the bundle of 20 superimposed average solution structures with the lowest energy target function (**Figure 3.10**), as well as from the network of medium- and long-range NOE connectivities (c.f. **Figure 3.6** and **Figure 3.9**), the structure of **18** is more ambiguous in the polar region of the molecule, opposite to the D-Pro-L-Pro template comprising residues Lys-4 to Arg-7, when compared to **17**. In particular, several long-range NOEs observed in this region for **17** (Leu-$3_{H\alpha}$/Lys-5_{NH}, Glu-$6_{H\alpha}$/Trp-8_{NH}, and Lys-5_{NH}/Trp-8_{NH}) had no counterparts in the spectra of mimetic **18**.

With respect to the *cis*/*trans* isomerism, it is noteworthy that, starting from a *cis*/*trans* ratio of approximately 1:3 in aqueous solution for both **17** and **18**, the introduction of micelles leads to an exclusive population of the *cis*-isomer in the case of **17**, whereas for mimetic **18** the ratio is only shifted to approximately 5:3 in favour of the *cis*-isomer (**Figure 3.11).**

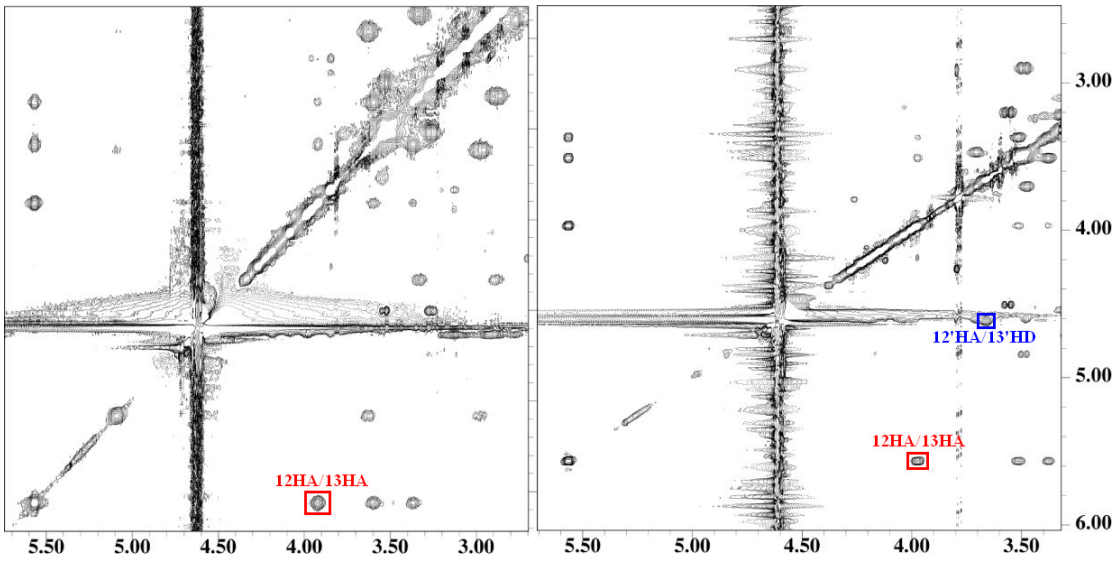

Figure 3.11 Sections of NOESY spectra of mimetic **17** (left) and mimetic **18** (right) in the presence of DPC-d_{38} micelles. Cross peaks indicating the presence of a Xaa-D-Pro *cis* peptide bond (red), or a Xaa-D-Pro *trans*-peptide bond (blue) are highlighted.

3.2.3 Conclusions

It was found that **16**, **17** and **18** adopt amphipathic structures in the presence of DPC-d_{38} micelles, albeit with different secondary structures. The formation of secondary structure upon interaction with membranous systems is often regarded as a general property of many AMPs, and most notably, the commonly employed classification scheme of AMPs is built upon such secondary structural features. It should be borne in mind, however, that such behaviour does not necessarily imply bacterial killing via a membrane-active mechanism. Nevertheless, it has to be concluded from the NMR experiments that **16**, **17** and **18** show the ability to form amphipathic structures upon interaction with a model membrane system, and thus these AMPMs become at least *potentially* membrane-active. It is further noted that the formation of amphipathic structures in a micellar environment does not implicitly indicate an involvement in the binding of the AMPM to a putative receptor, or that the

AMP is able to (efficiently) permeabilise membrane systems. Last but not least, it should be remembered that the use of micellar systems in the NMR experiments will possibly select for the formation of amphipathic structures.

Recently, proline residues have received attention as molecular switches. For instance, *cis*/*trans* isomerism of a Xaa-Pro bond has been reported to be responsible for opening and closing a neurotransmitter-gated ion-channel,[318] or to be involved in the regulation of lysine methylation in histone H3.[319] Interestingly, the antimicrobial activity of a histone H1 fragment was also described as being dependent on the configuration of the Xaa-Pro bond(s).[320]

It is, therefore, also conceivable that two different conformational isomers of an AMPM might be involved in its antimicrobial mechanism(s). For example, one conformer could permit membrane interaction (e.g. to translocate across the membrane) whereas a different conformer could be involved in the interaction with other (specific) targets (e.g. DNA, c.f. β-hairpins as DNA minor groove binding motifs). Along these lines, indolicidin has recently been proposed to exert its antimicrobial action via a combination of different conformations that are formed when the peptide is bound either to membranes, or to DNA.[321]

3.3 Biological Activities and Selectivities

As mentioned in **Section 1.5**, the evaluation of the biological activities of AMPMs derived from protegrin-1 (**11**) pointed towards the involvement of alternative mechanisms of antibacterial action for several members of this class of mimetics. A variety of bacteriological experiments have been carried out on the AMP(M)s that have been synthesised in this work (**11**; mimetics **16** to **19**;) in order to (a) verify the notion of alternative antibacterial action and (b) gain further insights into the basis of the putative alternative mode of action. Therefore, in the following discussion of the experiments, special emphasis will be given to those aspects that can aid in the inference of mechanistic features, as well as to the comparison of the results obtained with the behaviour of AMPs described the literature.

3.3.1 Minimal inhibitory concentrations and haemolytic activities

The primary criterion for the evaluation of the AMPMs is their activity against micro-organisms. Several methods exist for the quantification of this activity *in vitro*, which is generally referred to as susceptibility testing. Such tests are routinely performed on isolated micro-organisms, in order to predict the *in vivo* success of antibiotic chemotherapy, and three different approaches are commonly used. In broth- or agar dilution methods, serial dilutions of the test compounds are prepared in the corresponding medium and inoculated with a defined quantity of test organisms.[322] The amount of test compound that inhibits bacterial growth after a defined incubation period, typically taken to be between 16 and 20 hours, is defined as the minimal inhibitory concentration (MIC). The MIC is used as a direct measure of the *in vitro* susceptibility of the test organism towards the test compound. The second most commonly used method is the so-called disc diffusion test (Kirby-Bauer disc diffusion), in which filter discs impregnated with test compounds are placed on agar plates which have been inoculated to give confluent growth of the test organism, and the size of the zone of growth inhibition after overnight incubation is used as a measure for the bacterial susceptibility.[323] Finally, the E-test is a diffusion method based on a pre-formed gradient of the antibacterial agent on a plastic strip; the MIC value is obtained from the intersection of the growth inhibition zone with the gradient strip.[324]

Routine testing of the antibacterial activity of the AMPMs, via determination of their MIC values, was implemented as a broth micro-dilution method in 96 well-plates, according to published guidelines. Since it has been shown that the MIC values obtained for cationic AMPs can depend drastically on adsorption effects, the protocol of Steinberg et al. was adapted, in which bovine serum albumin (BSA) is added at a final concentration of 0.01% in order to counteract these effects.[312] Briefly, two-fold serial concentrations of the AMPM were prepared in Mueller-Hinton (MH) broth and inoculated with a final concentration of approximately 5×10^5 CFU/mL of the appropriate test organism. The MIC values were recorded as those dilutions of test compound that completely inhibited bacterial growth after an incubation period of 20 hours, as judged by visual inspection.

A second important criterion for the AMPMs, with respect to their potential usefulness as therapeutic agents, consists of their haemolytic activity, i.e. their ability to lyse red blood cells. Such activity is often used as an indicator for the toxicity of AMPs towards (mammalian) host cells, and a low extent of haemolysis is naturally a pre-requisite for any systemic applications. The haemolytic activity of our AMPMs was determined by their ability to lyse human red blood cells (hRBC), typically at a peptide concentration of 100 μg/mL. The results of these experiments are expressed as % haemolysis relative to 0.1% Triton-X 100™, which is taken as reference corresponding to complete lysis of the blood cells. **Table 3.2** summarises the MIC values obtained for a panel of five test organisms, as well as the haemolytic activities of the AMPMs that have been synthesised in this work for studying their modes and mechanisms of action. For comparison, protegrin-1 (**11**), the prototypal AMP of our AMPMs, polymyxin B (**1**, c.f. **Figure 1.1**), a structurally related bactericidal agent, and tobramycin (**25**, c.f. **Figure 3.31**) an aminoglycoside displaying good activity against *Pseudomonas spp.* are also included.

Table 3.2 MIC values and haemolytic activity of AMPMs (**16**-**19**) and control antimicrobial agents (**1**, **11**, **25**).

ID[a]	MIC[b] [μg/mL]					% H[c]
	E. coli ATCC 25922	*P. aeruginosa* ATCC 27853	*P. aeruginosa* PAO1	*S. aureus* ATCC 25923	*S. aureus* ATCC 29213	hRBC[d]
16	4	2	2	16	16	1
17	16	0.25	1	16	> 64	0
18	32	0.03	0.03	4	> 64	0
19	64	0.008	0.015	> 64	> 64	0
1	< 0.06	< 0.06	0.125	4	32	4.4
11	0.25	0.5	0.5	0.25	1	37
25	1	0.5	0.5	0.06	0.125	n.d.[e]

[a] substance identifier; [b] minimal inhibitory concentration; [c] % haemolysis at a peptide concentration of 100 μg/mL; [d] human red blood cells; [e] not determined.

3.3.2 Selectivity and activity spectra of AMPMs

An interesting trend that can be extracted from **Table 3.2** is the increased selectivity of the later generations of AMPMs, most notably of mimetic **19**, towards the two strains of *Pseudomonas aeruginosa*. The selective growth inhibition of this Gram-negative, opportunistic pathogen by **19** is highlighted in **Table 3.3**, and is to be contrasted with the absence of comparable selectivity for **16**, a member of the first generation of AMPMs, and for protegrin-1 (**11**), one of the β-hairpin AMPs from which these mimetics were ultimately derived.

The absence of selectivity, i.e. a broad-spectrum of antimicrobial action is generally regarded as one of the hallmarks of AMPs. The lack of selectivity encountered in most AMPs is readily explicable in mechanistic terms, on the basis of a membrane-active mode of action. It is evident that AMPs which follow a membrane-active mechanism also depend on characteristic features of membranes to display any kind of selectivity. Variations in membrane composition, for instance, are intimately related to the selectivity of AMPs towards bacterial membranes (c.f. **Section 1.4.2**). Although it has been shown that variations in the membrane composition can also provide at least a rudimentary explanation of the selectivity of some AMPs towards different bacteria,[150] the reported selectivities are orders of magnitude less pronounced than observed for mimetic **19**.

Table 3.3 Selectivity of antimicrobial peptides towards *P. aeruginosa* strains PAO1 and ATCC 27853. The selectivity is expressed as the ratio of the corresponding MIC values taken from **Table 2.5**

Substance	Selectivity Ratios			
	E. coli ATCC 25922 vs.		*S. aureus*[a] vs.	
	P. aeruginosa ATCC 27853	*P. aeruginosa* PAO1	*P. aeruginosa* ATCC 27853	*P. aeruginosa* PAO1
16	2	2	4	4
17	64	16	128	32
18	1100	1100	2100	> 2100
19	4300	8000	> 4300	> 8000
11	0.5	0.5	1.5	1.5

[a] values averaged for strains ATCC 25923 and ATCC 29213.

In addition to the remarkable degree of selectivity demonstrated by mimetic **19** (three to four orders of magnitude higher activity towards *P. aeruginosa* as compared to both *E. coli* and *S. aureus*), further aspects suggest that the selectivity of our AMPs may have a more fundamental origin than mere discrimination between different bacterial membranes. To begin with, it is especially instructive to consider the pair of Gram-negative test organisms, which show a comparable composition of phospholipids in their plasma membranes.[325] Moreover, protegrin-1 (**11**),[312] as well as other β-hairpin AMPs, such as polyphemusin-1 (**13**),[326] tachyplesins,[327] RTD-1,[327] or a cyclic 18 residue peptide mimetic of the β-hairpin region of HNP-2[135], all display broad-spectrum activity against *E. coli*, *P. aeruginosa*, and *S. aureus,* despite several structural differences between them. Both findings suggest that the change in selectivity from **16** to **17,** and the later generation mimetics **18** and **19,** is caused by something more than a subtle alteration of structural parameters such as hydrophobicity, amphipathicity, and charge. It is noteworthy in this respect, that the estimated positive charge of the AMPMs at physiological pH remains constant for mimetics **16**, **18**, and **19** and is even reduced from +7 to +6 for mimetic-**17**.

A comparable high selectivity towards certain bacterial species has been found for leucocin A, a type IIa bacteriocin produced by lactic acid bacteria, which has been shown to depend on a stereo-specific interaction for its antibacterial activity (c.f. **Section 3.4**).[328] The involvement of a stereospecific receptor has been proposed to account for the potency, as well as for the narrow activity spectrum of this compound. Accordingly, large differences in the activity spectra of other type IIa bacteriocins

have been described, despite their high sequence homology and have been attributed to differences in their modes of action.[329, 330]

It is important to note that the increase in selectivity for mimetics **17**-**19** derives both from an improvement in the activity towards *P. aeruginosa* and from a loss of activity against other bacterial species. This loss of activity could originate from an associated loss of a membrane-active mechanism pathway, which could operate for the complete panel of test organisms. The improvement in activity towards *P. aeruginosa* in this scheme would then be mediated by (specific) interaction with a target absent from both *E. coli* and *S. aureus*.

Finally, it should be emphasised that although the AMPMs lose their broad-spectrum of activity, this does not diminish their potential as therapeutically useful antibacterial agents. Foremost, mimetic-**19** possesses a very potent activity against *P. aeruginosa,* which is both an important opportunistic pathogen of humans and a plant pathogen. As a nosocomial pathogen, it causes infections of the urinary tract and the respiratory system as well as bacteraemia and a variety of systemic infections, especially in immuno-compromised patients such as burns victims. Additionally, *P. aeruginosa* plays an important role as a pathogen in cystic fibrosis patients. To further capitalise on this selectivity, the MIC values of **16**, **18**, and **19** for a variety of species belonging to the genus *Pseudomonas*, as well as against *Burkholderia cepacia*, a related Gram-negative bacterium, were determined; the results are shown in **Table 3.4**. It can be seen from this table that all tested mimetics, as well as protegrin-1 (**11**), displayed satisfactory activity against most tested species, except *P. chlororaphis* and *B. cepacia*. The latter finding is not surprising, since this species is notorious for its resistance towards antibacterial agents.[331] It is also noteworthy that the later generation mimetics **18** and **19** generally possess higher activity towards the susceptible *Pseudomonas* species, when compared to **16** and **11**, thus further underlining their potential as anti-pseudomonal agents.

Furthermore, highly selective antibiotics are attractive since they are less prone to disrupt the natural flora of the host, which plays an important part in host immunity by preventing colonization by pathogens,[332] and they can help to decrease the selective pressure on non-targeted bacteria, thereby decreasing the development of resistance by horizontal gene transfer.[333] Therefore, it is not surprising that attempts are being made to develop highly selective antibacterial compounds, for example by including a *Pseudomonas*-specific target sequence into an antimicrobial peptide,[334]

by fusing antibiotics to monoclonal antibodies specific for certain bacteria,[335] or by fusing a bacterial pheromone to the antibacterial domain of colicin Ia.[336] Nevertheless, further advances in rapid aetiological diagnosis and determination of the susceptibility patterns of the pathogen to be treated might be needed in order to increase the applicability of narrow spectrum antibiotics.[337]

Table 3.4 MIC values of mimetics **16**, **18**, **19** as well as **11** towards *Pseudomonas spp.* and *B. cepacia*.

Species	MIC[a] [μg/mL]			
	mimetic-**16**	mimetic-**18**	mimetic-**19**	protegrin-1 (**11**)
P. aeruginosa[b]	2	0.03	0.015	0.5
P. aeruginosa[c]	2	0.03	0.008	0.5
P. putida	0.25	0.13	≤ 0.008	0.25
P. aureofaciens	1	0.06	0.015	0.25
P. syringae	0.13	≤ 0.03	≤ 0.008	≤ 0.03
P. fluorescence[d]	16	4	0.06	0.125
P. fluorescence	2	0.5	0.06	0.125
P. chlororaphis	> 64	> 64	> 64	32
B. cepacia	> 64	> 64	> 64	> 64

[a] minimal inhibitory concentration; [b] PAO1; [c] ATCC 27853; [d] strain III.

3.3.3 Bactericidal effects of the AMPMs

In principle, there are two fundamentally different ways by which antimicrobial substances can exert their biological activity. Bactericidal agents do so by directly killing their bacterial target, whereas bacteriostatic agents only inhibit the growth of bacterial cells. Examples of both types are widespread and well documented. For instance, linezolid, an oxazolidinone antibiotic that inhibits the initiation of protein synthesis in susceptible bacteria, is a bacteriostatic agent with a broad-spectrum activity,[338] whereas β-lactam antibiotics such as the penicillins are well known for their bactericidal action.[339] Nevertheless, the distinction is not always clear-cut, and bacteriostatic agents can become bactericidal at higher concentrations.[340] For example, antibiotics such as the macrolides, which are generally considered bacteriostatic, also show bactericidal activity against some Gram-positive species.[341] It should be emphasised that bacteriostatic action of an antibacterial agent does not impair its usefulness in antimicrobial chemotherapy, since

the uncompromised immune system can generally cope with an infection that is prevented from getting out of control.[342] Also, for many infections by Gram-negative pathogens, a rapid lysis of bacteria, with the concomitant release of LPS, can lead to serious complications, namely septic shock, and these conditions can be attenuated by the use of bacteriostatic agents.[343] An important parameter used to discriminate between bactericidal and bacteriostatic action is the minimum bactericidal concentration (MBC) (or minimum lethal concentration, if other organisms such as fungi are to be included). The definition of the MBC is not as unambiguous as for the MIC, and varies according to the source. Generally, the MBC is taken to be the minimum concentration of a test compound that results in a reduction of at least $3\log_{10}$ (99.9%) in the viable cell count - as compared to the inoculum - after incubation for 24 hours.[344] Comparable to the MIC, the inoculum is typically chosen to have a value of around 5×10^5 CFU/mL and can greatly influence the results obtained (vide infra). The MBCs for **16** and **18** have been determined in parallel to their MICs and are shown in **Table 3.5**. The MBC values obtained show that both mimetics display a bactericidal action against *P. aeruginosa* PAO1 at concentrations that are comparable, respectively identical, to their MIC values. It must therefore be concluded that these two AMPMs exert a bactericidal action towards *P. aeruginosa* PAO1.

Table 3.5 Comparison of the MBC and MIC values obtained for **16** and **18** with respect to *P. aeruginosa* PAO1. Values obtained from two independent experiments are shown.

substance	MBC [μg/mL]	MIC [μg/mL]
mimetic-**16**	8 / 8	4 / 4
mimetic-**18**	0.125 / 0.25	0.06 / 0.06

3.3.4 Kinetics of bacterial killing

Whereas the determination of the MBC value allows for discrimination between bacteriostatic and bactericidal action, its usefulness is limited by the fact that it is only concerned with effects that manifest themselves during the 24 hours incubation period. More interesting from a mechanistic point of view, however, is the recording of so-called killing curves (time-kill analysis), which permit the analysis of the kinetics of antibacterial action. Killing curves are an extension to the MBC concept inasmuch as the decrease of viable cells is sampled more frequently during a time-period of interest, instead of relying solely on one endpoint. Therefore, multiple subcultures of the samples are evaluated for their viable cell count in order to study the rate of bactericidal action. For the following experiments, a spread-plate method on MH-agar plates was used to determine the number of viable cells. The bacterial samples were serially diluted in MH-broth to achieve a count range between 30 and 300 colonies; the number of required dilutions was typically determined by preliminary experiments.

One of the indications that mimetic **17** might act by an alternative mode of action, mentioned above, came from the recording of killing curves, which was carried out by Polyphor Ltd.[‡] with **17**. The results of the time-kill analysis of *P. aeruginosa* with mimetic **17** and with protegrin-1 (**11**), which was used as a control, are shown in **Figures 3.12** and **3.13**. From these experiments it was evident that although **16** and **11** were bactericidal at or above their MIC values, **16** showed a significantly slower onset of the antibacterial action than the naturally occurring, reportedly membrane-active AMP, **11**. For example, bacterial suspensions induced with **11** at 1×, 4×, and 8× the MIC showed a reduction of $3\log_{10}$ or higher in the viable cell count during the first 30 minute incubation period, whereas the same reduction for 4× and 8× the MIC of mimetic-**17** occurred only after 3 to 4 hours. The re-growth of the *P. aeruginosa* induced with 1×MIC of **17** after crossing the $3\log_{10}$ threshold is probably caused by the uncertainty in the determination of the MIC values, which can typically vary about a factor of two and was probably not reached in this experiment.

Prompted by these results, the kinetics of antibacterial action of AMPMs were studied, with special emphasis on the effects caused in the first two hours after induction.

[‡] See footnote †, page 19

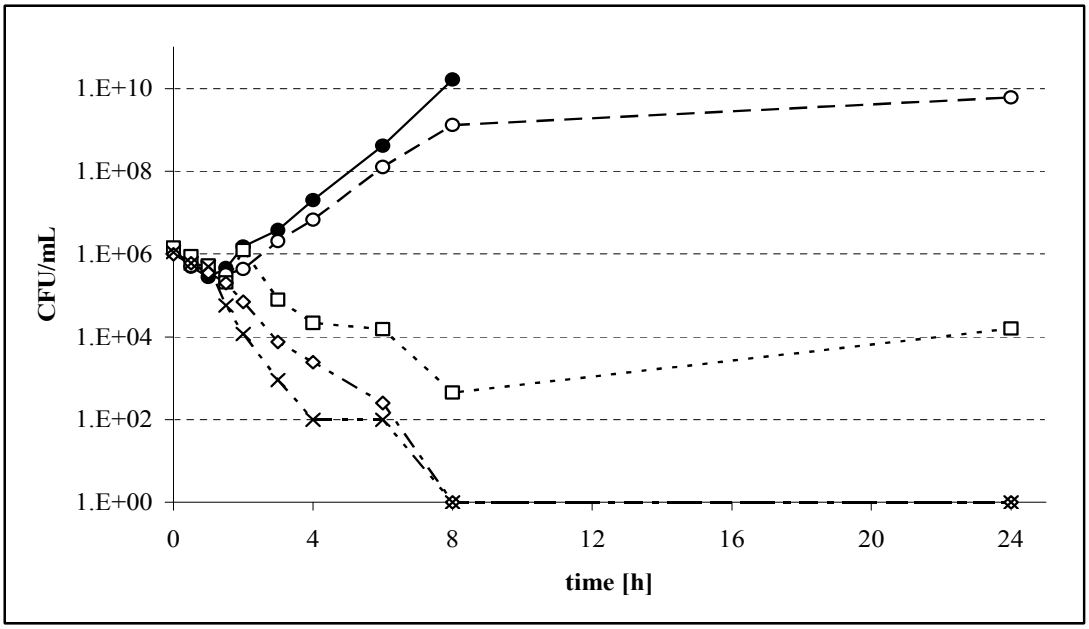

Figure 3.12 Time-kill analysis of *P. aeruginosa* ATCC 27853 with mimetic-**17**; (●): control; (○): 0.5×MIC; (□): 1×MIC; (◊): 4×MIC; (×): 8×MIC.

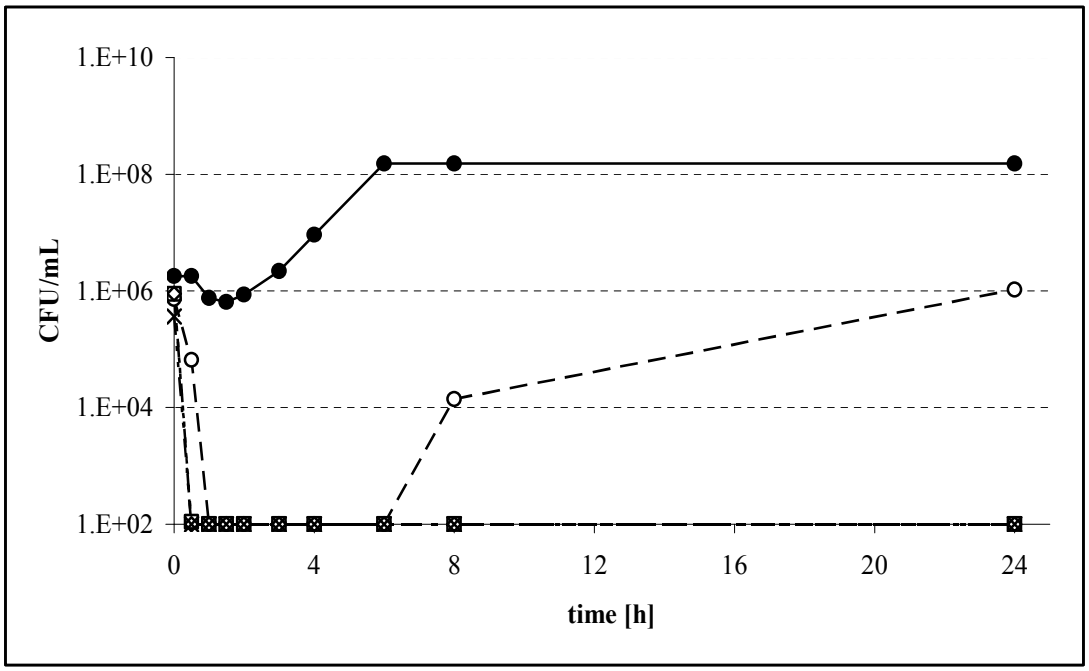

Figure 3.13 Time-kill analysis of *P. aeruginosa* ATCC 27853 with protegrin-1 (**11**); (●): control; (○): 0.5×MIC; (□): 1×MIC; (◊): 4×MIC; (×): 8×MIC.

3.3.4.1 Experimental considerations

To ensure maximum reproducibility, time-kill experiments were performed during the exponential growth-phase of *P. aeruginosa* PAO1; this strain was chosen because of the availability of its fully sequenced genome. For comparison with later experiments, such as those concerned with the incorporation of radioactively labelled precursor molecules into PAO1 cells, the assay was modified to accommodate a higher cell-density of about 1×10^8 CFU/mL, at the time of adding test peptide. A representative growth curve obtained for *P. aeruginosa* PAO1 is shown in **Figure 3.14**. It can be seen from this curve that the bacteria grow exponentially between about 60 and 180 minutes, when incubated at 200 rpm and 37 °C in an orbital shaker.

For all experiments, pre-warmed (37 °C) MH-broth was inoculated ~1:100 with an overnight culture of PAO1 cells grown under identical incubation conditions, to give a starting OD_{600nm} of ~0.05. Typically, under these conditions, an OD_{600nm} of 0.2 is reached 90 minutes after inoculation, which corresponds to the desired $\sim1\times10^8$ CFU/mL. Unless otherwise indicated, all further experiments were conducted with bacteria in the two hour time frame of exponential growth.

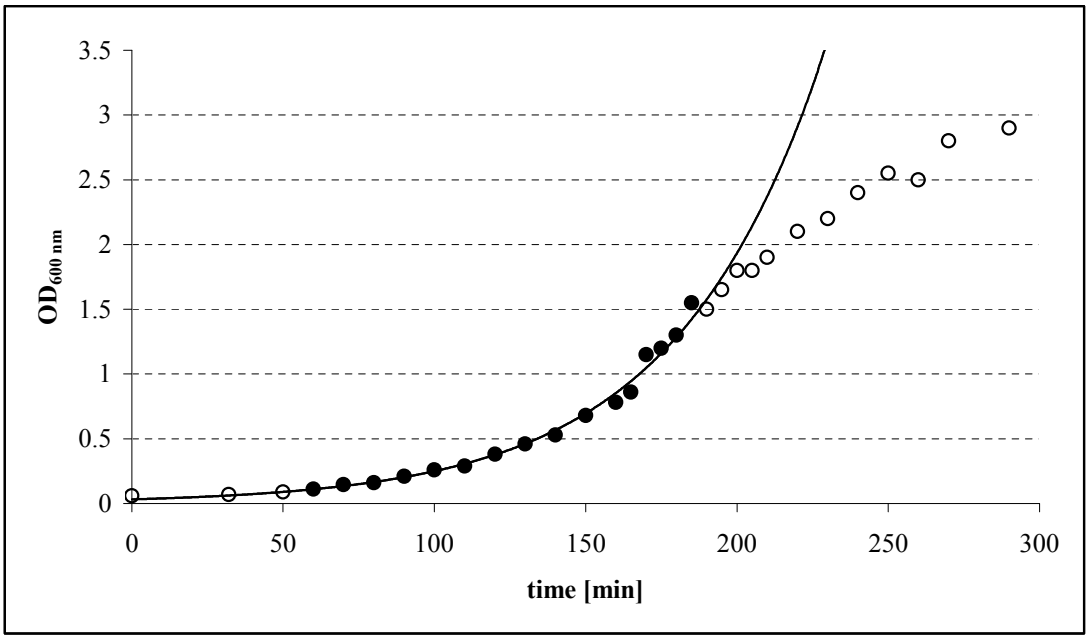

Figure 3.14 Growth curve of *P. aeruginosa* PAO1 incubated at 200 rpm and 37° C in MH-broth, and inoculated to a starting OD_{600nm} of 0.05; the generation time is estimated to be ~28 minutes.

Since it has been described that the amount of the inoculum can have profound effects on the obtained MIC values for certain antibiotics, such as macrolide

antibiotics and β-lactams,[345, 346] and even more so for AMPs and other peptide antibiotics,[347, 348] the MICs for the AMPM were re-determined for a higher inoculum of 1×10^8 CFU/mL. It was found that the size of the inoculum also had a significant effect on the AMPMs, as can be seen from **Table 3.6**, which compares the MIC values for *P. aeruginosa* PAO1 obtained according to the standard protocol (5×10^5 CFU/mL) with those obtained for the higher inoculum. Influences of the inoculum size are less pronounced for other classes of antibiotics, such as quinolones and fluoroquinolones,[349] and such behaviour was indeed found for ciprofloxacin (**7**) and tobramycin (**25**), which are included in **Table 3.6**.

Table 3.6 Comparison of the MIC values obtained with different sizes of inoculum for AMPMs and some control antibiotics against *P. aeruginosa* PAO1.

substance	MIC[a] [μg/mL]		MIC ratio
	standard inoculum[b]	high inoculum[c]	high/standard
mimetic-**16**	2	8	4
mimetic-**17**	1	4	4
mimetic-**18**	0.03	0.25	8
polymyxin B (**1**)	0.125	1	8
ciprofloxacin (**7**)	0.06	0.06	1
protegrin-1 (**11**)	0.5	16	32
tobramycin (**25**)	0.5	0.5	1

[a] minimal inhibitory concentration; [b] 5×10^5 CFU/mL; [c] 1×10^8 CFU/mL.

The MIC values for the peptide antimicrobial agents typically increased 4- to 8-fold when the higher inoculum was used. An exception is the 32-fold increase of the MIC value for protegrin-1 (**11**) and this might originate either in a mechanistic requirement for a certain threshold concentration of the AMP (e.g. in a carpet model), or it could reflect a higher instability towards proteolytic degradation; **11** is the only peptide from **Table 3.6**, which is not backbone-cyclic. Unless otherwise indicated, the MIC values used for all following experiments are those determined with the high inoculum.

3.3.4.2 Experiments with mimetics 17 and 18

To study the kinetics of killing of *P. aeruginosa* PAO1, time kill analyses were carried out with mimetics **17** and **18**. A representative experiment with mimetic-**18** at 1×MIC and 5×MIC is depicted in **Figure 3.15**.

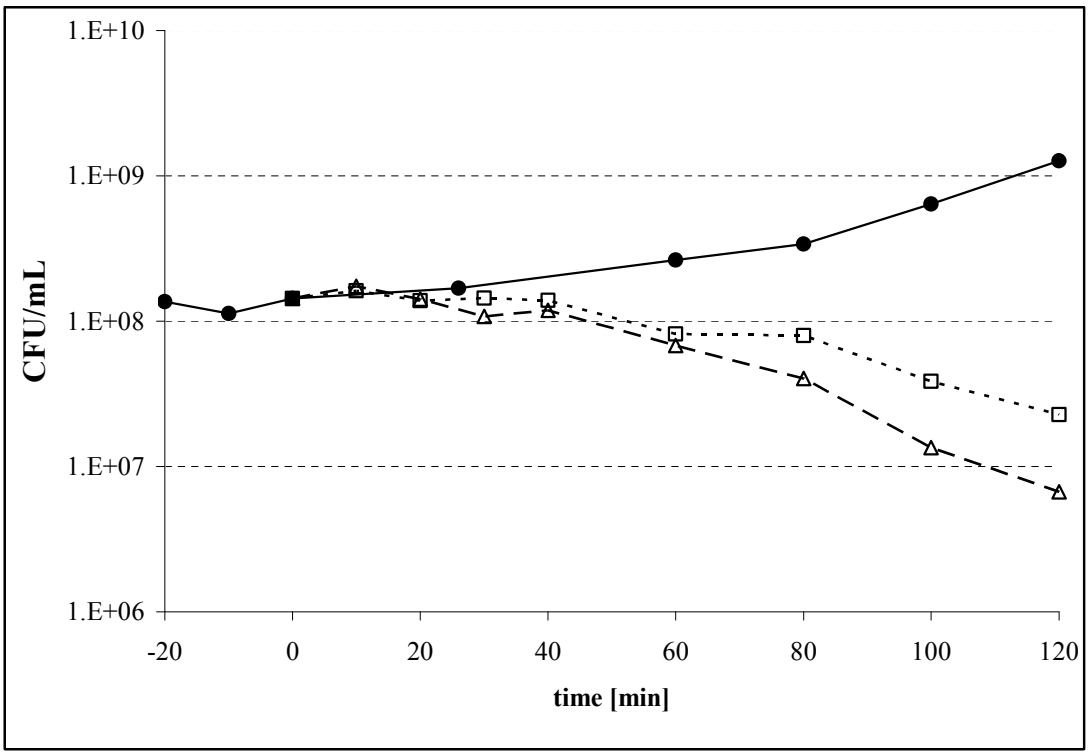

Figure 3.15 Time-kill analysis of mimetic **18** with *P. aeruginosa* PAO1; (●): control; (□): 2×MIC; (◊): 10×MIC.

As can be seen from **Figure 3.15**, mimetic **18** displays an essentially bacteriostatic effect with respect to the PAO1 cells during the first two hours after induction. The observed decrease in the viable cell count does not fulfil the $3\log_{10}$ criterion of bactericidal action for either concentration. On the contrary, the number of viable cells stays on a level comparable to the amount present in the inoculum for up to 40 minutes after induction with **18**. After this time period, the viable cell count decreases slowly for both concentrations, the effect for the higher concentration being somewhat larger. The time course of the viable cell count can be followed more clearly if the percentage of surviving (viable) cells relative to the viable cell count at the time point of addition of the test compounds is plotted against time, as demonstrated in **Figure 3.16**. Mimetic **17**, as well as protegrin-1 (**11**) and the aminoglycoside antibiotic tobramycin (**25**) are included therein for comparison. Under these conditions, mimetic-**17** displays a similar bacteriostatic effect at 1×MIC.

Interestingly, at 5×MIC of **17**, there was a more rapid drop in the viable cell count during the first hour following induction, after which time the viable cell count remained on a comparable level throughout the rest of the experiment.

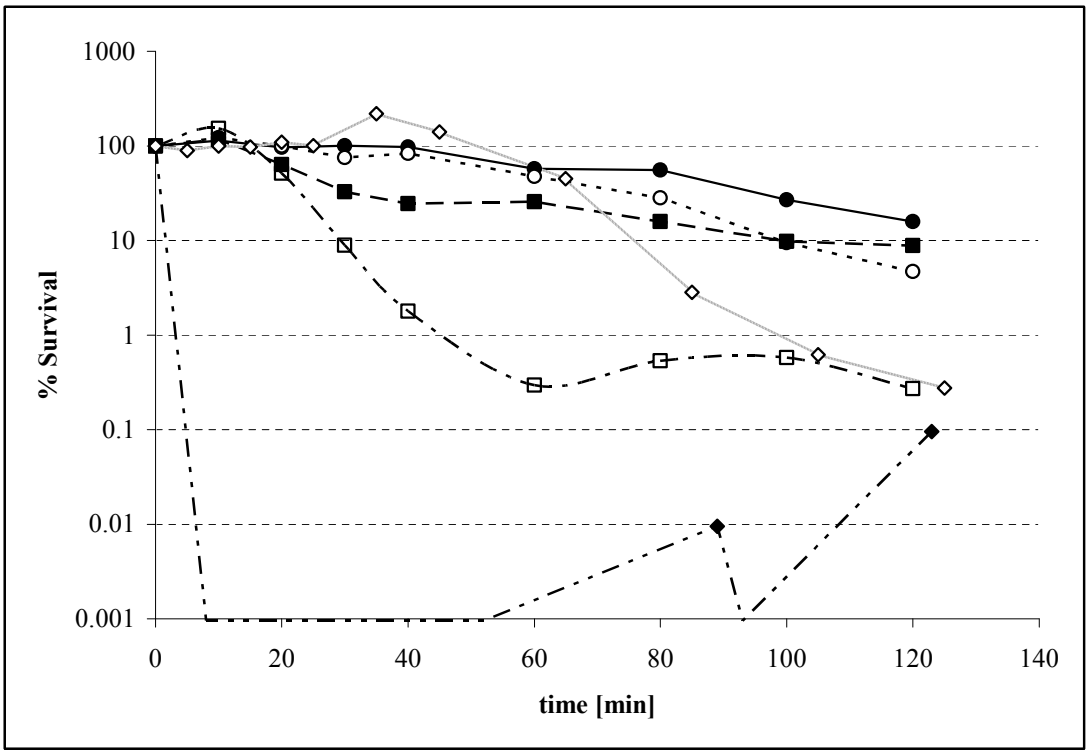

Figure 3.16 Survival of *P. aeruginosa* PAO1 after induction with (●): 1×MIC mimetic-**18**; (○): 5×MIC mimetic-**18**; (■): 1×MIC mimetic-**17**; (□): 5×MIC mimetic-**17**; (♦):2×MIC protegrin-1 (**11**); (◊): 1×MIC tobramycin (**25**).

It could be possible that this behaviour is a manifestation of the above mentioned putative residual membrane-lytic activity of the AMPMs. For example, 5×MIC of mimetic **17,** under high inoculum conditions, correspond to a concentration of 20 μg/mL, a value well within the MIC range of **17** displayed against *E. coli* and *S. aureus* ATCC 25923 (albeit determined for a lower inoculum). The aminoglycoside antibiotic tobramycin (**25**) shows a slower onset of its bactericidal action as compared to protegrin-1 (**11**), which exhibits a minimum decrease of $5\log_{10}$ in the viable cell count 10 minutes after induction. Such rapid bactericidal action is expected for an AMP that acts by a membrane-lytic mode of action. Identical results have been described for protegrin-1,[312] and other AMPs that are thought to operate by membrane-active mechanisms, in the literature.[350, 351] Additional time-kill analyses were performed with mimetic **18** at higher concentrations, *inter alia* to determine concentrations for which the onset of the putative residual lytic activity might occur.

From **Figure 3.17** it can be seen that **18** displays a concentration-dependent bactericidal action during the 2 hours incubation period of the experiment, i.e. increasing concentrations of the mimetic lead to an increased drop in the viable cell count.

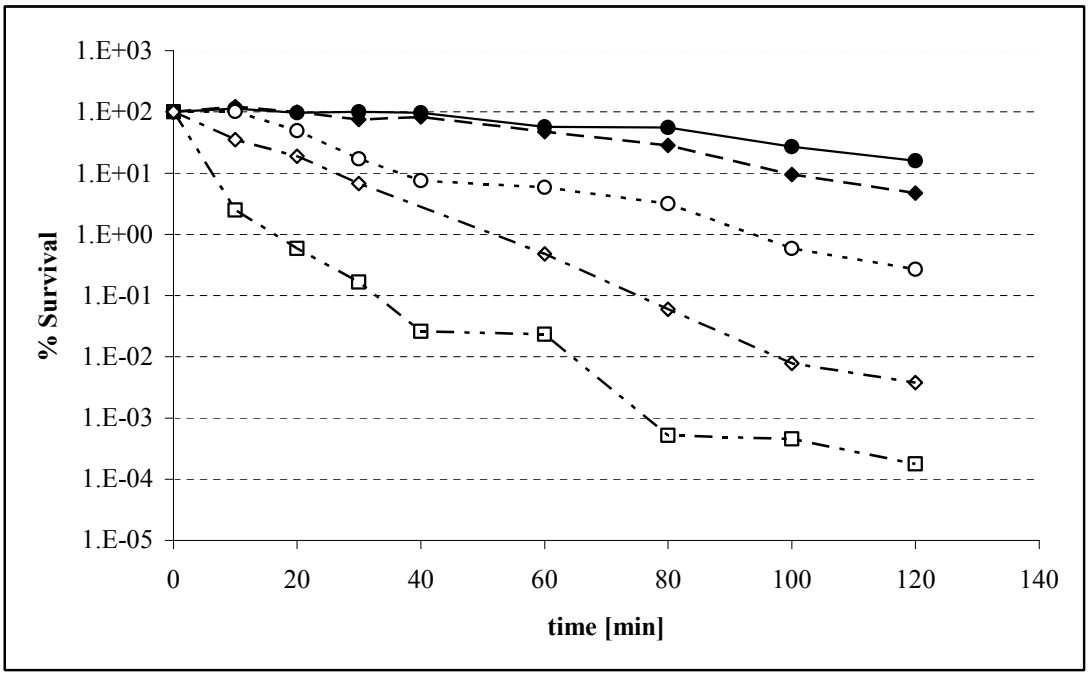

Figure 3.17 Concentration-dependent bactericidal action of mimetic **18** against *P. aeruginosa* PAO1; (●): 2×MIC; (♦): 10×MIC; (○): 128×MIC; (◊): 256×MIC; (□): 512×MIC.

It is remarkable, however, that the bactericidal action is not pronouncedly rapid even at the highest concentration of **18**, corresponding to 128 µg/mL. At this concentration the $3\log_{10}$ threshold is reached only 40 minutes after induction, suggesting that even for such a high concentration, a typically membrane-lytic mode of action is not in operation for mimetic **18**, at least not with respect to *P. aeruginosa* PAO1.

3.3.4.3 Post-antibiotic effect of mimetic 18

The post antibiotic effect (PAE) describes a delay of re-growth of bacteria after short exposure to a test antibiotic, and is described by the formula PAE = T – C where T is the time in hours required for the culture induced with the test substance to increase its viable cell count by about $1\times\log_{10}$ after removal of the drug, as compared to the control, as denoted by C. The degree of an observed PAE can be related to the amount and degree of damage inflicted upon the bacterial culture. The PAE effect of

18 on *P. aeruginosa* PAO1 was studied by a drug-removal procedure involving centrifugation and washing steps. Briefly, bacterial suspensions were grown and induced with **18** according to the standard protocol (vide supra) and after two hours of incubation, one sample was washed and centrifuged twice with pre-warmed fresh MH-broth while the control samples were handled identically, but without replacement of the medium. Experiments were carried out at 5×MIC of **18** and a representative example is shown in **Figure 3.18**.

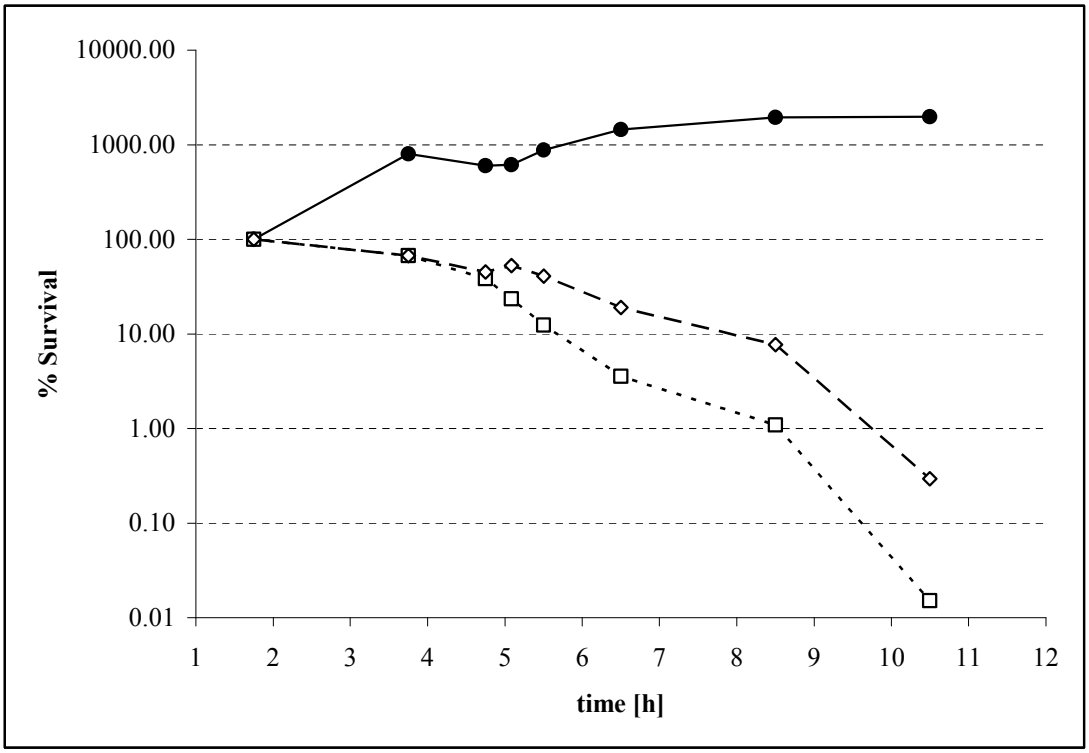

Figure 3.18 Effect of removing mimetic-**18** from the incubation medium (PAE) on the survival of *P. aeruginosa* PAO1; (●): control without added **18**; (◊): control with 5×MIC **18**; (□):5×MIC **18**.

Interestingly, **18** exerts a remarkable PAE; in fact the decrease in the viable cell count is even higher for the sample that has been washed than for the control sample which contains an identical amount of **18**. Post-antibiotic effects are common for many antibiotics such as ciprofloxacin (**7**)[352] or tobramycin (**25**).[353] It is especially noteworthy that two synthetic magainin derivatives, as well as the AMP lactoferricin B, all of which are thought to act by a lytic mode of action, showed no PAE.[347, 354]

3.4 Enantiomers of AMP(M)s

An versatile approach for studying modes and mechanisms of action of an AMP(M) consists of the synthesis of both its enantiomers and the evaluation of their biological and/or antimicrobial activities. The attractiveness of this methodology has several origins, for example the ease of preparation of both enantiomeric forms, given the fact that most AMPs are relatively small polypeptides easily accessible via SPPS. Due to the wide availability of L- and D-amino acid building blocks for SPPS employing either Boc- or Fmoc-based chemistry, the synthesis and purification of the enantiomer of an AMP(M) is not more difficult or time-consuming than the synthesis of its parent compound; the synthetic protocols necessarily have to be identical. Additionally, as will be described in this section, a considerable amount of data has already been collected, with which newly obtained results can be compared. Most importantly, however, the biological activities of enantiomers of AMP(M) can give invaluable clues as to possible mechanisms of action for this class of compounds.

Biological membranes are chiral entities not only by virtue of imbedded or attached chiral macromolecules, but also due to the phospholipid bilayer which is composed of optically active phospholipids, along with other chiral lipids such as steroids. The same holds true for additional components of fungal or bacterial cell walls such as chitin, peptidoglycan, teichoic acids, or lipopolysaccharides (LPS). Despite this inherent chirality of microbial cell walls it has been hypothesised that peptides that can alter properties of the phospholipid surface, for example toxins and venoms, might exert their action without involvement of specific receptors.[355] This hypothesis was extended to include AMPs by Merrifield and co-workers, based on biophysical experiments and the activity patterns of compounds such as magainin, cecropin, and melittin.[356] As exemplified by melittin, the distinction between AMPs and venoms is not always clear. Generally, the toxicity towards erythrocytes is used as a parameter, although the classification of a certain peptide into either class might vary from author to author.

The aforementioned hypotheses are in stark contrast to the situation encountered with peptide hormones such as oxytocin,[357] bradykinin,[358] and gastrin,[359] whose enantiomers are devoid of the biological activity of the naturally occurring all-L forms. It is generally assumed that the interaction of a ligand with its receptor, or more precisely, with its recognition site (which is part of the receptor),

depends on the involvement of complementary surfaces and thus on the topology of the ligand. In this context it seems appropriate to state the definition of a receptor molecule as given by the NC-IUPHAR (The International Committee of Pharmacology Committee on Receptor Nomenclature):[360]

"A cellular macromolecule, or an assembly of macromolecules, that is concerned directly and specifically in chemical signaling between and within cells. Combination of a hormone, neurotransmitter, drug, or intracellular messenger with its receptor(s) initiates a change in cell function."

The complementary interaction of ligand and receptor as epitomised by Fischer's lock-and-key hypothesis[361] is well established, and examples such as the different odours produced by enantiomeric terpenes have become commonplace in chemical education.

3.4.1 Enantiomers of AMPs described in the literature

To test the hypothesis of antimicrobial action independent from chiral recognition for AMPs, Merrifield and colleagues[362] as well as Bessalle et al.[363] independently synthesised the first enantiomers of naturally occurring AMPs in 1990. The biological activities recorded for these compounds, all belonging to the α-helical subclass of AMPs (respectively venoms), were comparable to those of the naturally occurring all-L forms, thus supporting the original hypothesis and corroborating mechanistic frameworks in favour of a membrane-lytic action of AMPs. On the other hand, in 1994, Casteels et al. reported for the first time an AMP whose all-D form was significantly less active than its naturally occurring optical antipode, apidaecin[235].

It is noteworthy, not only from a historical point of view, that in 1967, Shemyakin et al. already described the first example of a peptidic compound that showed equivalent antimicrobial activity for both its enantiomers towards a variety of micro-organisms.[364] This at the time exceptionally unusual behaviour of enniatin-B, a cyclic non-ribosomally synthesised depsipeptide, was explained by the authors via a topological similarity of both enantiomers, sufficient to account for identical interaction with a receptor molecule.[365] From today's point of view, however, it seems likely that the activity of both enantiomers can be explained by the identical ability to transport potassium ions through bacterial target membranes. Indeed, Shemyakin et al. noted that enniatins preferably bound potassium ions, and that this

binding only occurred when the peptides were in contact with membranes. Notably, such crown-ether like binding of potassium ions would be expected to be identical for both enantiomers.

Since these first syntheses of enantiomeric pairs of AMPs, around 50 of them have been prepared and studied with respect to their biological activity towards various micro-organisms including fungi and protozoa. The D/L activity ratios of enantiomeric pairs of AMPs of various origins are summarised in **Table 3.7**. In this table, the differential activity of the enantiomers is quantified by the ratio of the antimicrobial activity of the naturally occurring or synthetically derived all-L form over the activity of its corresponding enantiomer. Therefore, D/L activity ratios larger than unity indicate a higher antimicrobial activity of the all-L[§] compound, indicating the involvement of a stereospecific interaction in its mechanism of action with respect to the tested micro-organism.

There are some additional reports on enantiomeric pairs of AMPs, which could not be fitted into **Table 3.7**, for instance because of the methods used for the determination, or quantification of the antimicrobial activity. Pelligrini et al. described that the all-D form of a modified 9 residue fragment of chicken egg white lysozyme showed significantly less bactericidal activity towards several *Staphylococcus* strains as well as towards *Serratia marcescens* and *Micrococcus luteus* in an assay based on determination of viable counts after a 2 hour incubation period than its all-L counterpart.[366] Another interesting report is concerned with leucocin A, a type IIa bacteriocin from lactic acid bacteria that contains an α-helical as well as a β-sheet element, and whose enantiomer was reported to show no antibacterial activity against several species of the genera *Carnobacterium*, *Leuconostoc*, and *Listeria*.[328]

[§] The term all-L form also includes compounds that contain a minor amount of D-amino acids and vice versa.

Table 3.7 D/L Activity ratios for enantiomeric pairs of AMPs reported in the literature (polymyxin B nonapeptide is included for comparison). The activity ratios are calculated as described in the text. Ratios that arise from a difference of 8 fold or higher in the biological activities between the all-L and all-D form are highlighted in boldface. Numbers in parentheses indicate the number of different species tested; names of species are given for those with unusual large differences

substance	sequence[a]	class	range of activity ratios (number of tested species)	activity criterion[b]	reference
androctonin	H-RSVC_1RQIKIC_2RRRGGC_2YYKC_1TNRPY-OH	β-sheet	0.3 to 2 (3)	MIC	[183]
CG117-136	H-RPGTLCTVAGWGRVSMRRGT-OH	β-sheet	0.9 and 1 (2)	ED_{90}	[367]
IB-625	H-RGGLC_1YC_2RGRFC_2VC_1VGR-NH_2	β-hairpin	2 and 4 (2)	MIC	[115]
IB-739	H-OGGOLC_1YC_2OOOFC_2VC_1VGO-NH_2	β-hairpin	0.1 and 1.8 (2)	MIC	[115]
IB-513	H-WLC_1YC_2OOOFC_2VC_1V-NH_2	β-hairpin	0.5 and 0.7 (2)	MIC	[115]
Ib-AMP1	H-EWGRRC_1C_2GWGPGRRYC_1VRWC_2-OH	β-turn	0.1 and 1.6 (2)	IC_{50}	[368]
Ib-AMP4	H-EWGRRC_1C_2GWGPGRRYC_1RRWC_2-OH	β-turn	0.2 and 1.3 (2)	IC_{50}	[368]
Lfcin B(17-31)	H-FKC_1RRWQWRMKKLGAPSITC$_1$VRRAF-OH	β-sheet	0.4 and 0.5 (2)	MIC	[369]
polymyxin B nona-peptide	H-T(Dab)(Dab)(Dab)fL(Dab)(Dab)T └CH_2─CH_2─NH─CO┘	β-turn and/or γ-turn	1 and 1 (2) **> 128 (*P. aeruginosa*)**	MIC	[370]
protegrin-1	H-RGGRLC_1YC_2YRRRFC_2VC_1VGR-NH_2	β-hairpin	0.7 and 0.9 (2)	MIC/IC_{50}	[66, 371]
thanatin	H-GSKKPVPIIYC_1NRRTGKC_1QRM-OH	β-hairpin	0.2 to 4 (17) **8 (*B. subtilis*)** **> 67 (*E. coli*)** **> 33 (*K. pneumoniae*)** **> 33 (S. *typhimurium*)**	MIC	[93]
$((RLA)_2R)_2$	H-RLARLARRLARLAR-OH	α-helical	<0.3 (1)	MIC	[372]
CA-(1-13)-M-(1-13)-COOH	H-KWKLFKKIEKVGQGIGAVLKVLTTGL-COOH	α-helical	0.2 to 1.1 (5)	LC	[373]
CA-(1-13)-M-(1-13)-NH_2	H-KWKLFKKIEKVGQGIGAVLKVLTTGL-NH_2	α-helical	0.4 to 4 (5)	LC	[362, 373, 374]
CA-(1-7)-M-(1-18)-NH_2	H-KWKLFKKGIGAVLKV-NH_2	α-helical	0.5 to 5.7 (5)	LC	[375]
CA(1-7)M(2-9)-COOH	H-KWKLFKKIGAVLKVL-COOH	α-helical	0.2 to 1.5 (4) **0.07 (*P. aeruginosa*)**	LC	[373]
CA-(1-7)-M-(2-9)-NH_2	H-KWKLFKKIGAVLKVL-NH_2	α-helical	0.2 to 0.8 (5)	LC	[374, 375]
CA-(1-7)-M-(3-10)-NH_2	H-KWKLFKKGAVLKVLT-NH_2	α-helical	0.3 to 2.3 (4)	LC	[375]
CA(1-7)M(4-11)NH_2	H-KWKLFKKAVLKVLTT-NH_2	α-helical	0.5 to 1.7 (5)	LC	[375]
CA(1-7)M(5-12)NH_2	H-KWKLFKKVLKVLTTG-NH_2	α-helical	0.5 to 2 (5)	LC	[375]

Table 3.7 (continued)

CA-(1-7)-M-(6-13)-NH_2	H-KWKLFKKLKVLTTGL-NH_2	α-helical	0.8 to 2 (5)	LC	[375]
CA-(1-8)-M-(1-18)-NH_2	H-KWKLFKKIGIGAVLKVLTTGLPALIS-NH_2	α-helical	0.5 to 1 (5)	LC	[362]
CA-(1-8)-M-(1-18)-NH_2	H-KWKLFKKIGIGAVLKVLTTGLPALIS-NH_2	α-helical	0.3 (1)	LD_{50}	[376]
cecropin A	H-KWKLFKKIEKVGQNIRDGIIKAGPAVAVVG QATQIAK-NH_2	α-helical	0.8-2 (5)	LC	[362]
cecropin B	H-KWKVFKKIEKMGRNIRNGIVKAGPAIAV LGEAKAL-NH_2	α-helical	2 (E. coli) 0.8 (P. aeruginosa)	LC	[377]
cecropin-P1	H-SWLSKTAKKLENSAKKRISEGIAIAIQGGPR-OH	α-helical	0.4 to 4 (2) **> 23 (*P. aeruginosa*)** **< 0.1 (*S. aureus*)** **0.07 (*S. pyogenes*)**	LC	[244]
KL peptide	H-KLKLLLLLKLK-NH_2	α-helical	0.5 (1)	MIC	[378]
KSLK	H-KKVVFKVKFKK-NH_2	α-helical	1 (5)	MIC	[379]
maculatin 1.1	H-GLFVGLAKVAAHVVPAIAEHF-NH2	α-helical	0.5 to 2 (10)	MIC	[380]
magainin-2	H-GIGKFLHSAKKFGKAFVGEIMNS-OH	α-helical	0.5 to 2 (5)	MIC	[363]
magainin-2 amide	H-GIGKFLHSAKKFGKAFVGEIMNS-NH_2	α-helical	0.3 to 1 (5)	LC	[362]
mastoparan-M	H-INLKAIAALAKKLL-NH_2	α-helical	0.5 (3)	MIC	[381]
melittin	H-GIGAVLKVLTTGLPALISWIKRKRQQ-NH_2	α-helical	0.5 to 2 (5)	LC	[362]
P113	H-AKRHHGYKRKFH-NH_2	α-helical	0.5 to 1 (2)	MIC/LD_{50}	[231, 232]
PBP10	RhB-QRLFQVKGRR-OH	α-helical	1 (1)	LC	[382]
plantaricin A	H-KSSAYSLQMGATAIKQVKKLFKKWGW-OH	α-helical	0.8 to 1.7 (2)	MIC	[383]
PlnA22	H-YSLQMGATAIKQVKKLFKKWGW-OH	α-helical	1 to 2 (3)	MIC	[384]
TAL L512	H-FLPLLGRVLSGLL-NH_2	α-helical	0.7 (1)	MIC	[385]
temporin A	H-FLPLIGRVLSGIL-NH_2	α-helical	0.5 to 1.2 (3)	MIC	[386]
V13A	Ac-KWKSFLKTFKSAAKTVLHTALKAISS-NH_2	α-helical	0.3 to 2 (6)	MIC	[387]
V13K	Ac-KWKSFLKTFKSAKKTVLHTALKAISS-NH_2	α-helical	0.3 to 2 (6)	MIC	[387]
V_{681}	Ac-KWKSFLKTFKSAVKTVLHTALKAISS-NH_2	α-helical	0.3 to 2 (6)	MIC	[387]
apidaecin	H-GNNRPVYIPQPRPPHPRL-OH	Pro/Arg-rich	**up to >1600 (*E. coli*)**	MIC	[235]
drosocin	H-GKPRPYSPRPTHSPRPIRV-OH	Pro/Arg-rich	**51-143 (*E. coli*)** **50 (*M. luteus*)**	MIC	[87]

Table 3.7 (*continued*)

PR-39	H-RRRPRPPYLPRPRPPPFFPPRLPPRIPPGFPP RFPPRFP-NH_2	Pro/Arg-rich	1 to 2 (3) **0.02 (*P. aeruginosa*)** **< 0.001 (*S. aureus*)**	LC	[244]
pyrrhocoricin	H-VDKGSYLPRPTPPRPIYNRN-OH	Pro/Arg–rich	4 (1) **> 1067 (*A. tumefaciens*)** **> 16 (*B. subtilis*)** **> 1067 (*E. coli*)** **> 133 (*S. typhimurium*)**	IC_{50}	[236]
IIGGR	H-IIGGR-OH	n.d.[c]	1 (2)	LD_{90}	[388]
p-EM2	H-KKWRWWLKALAKK-OH	n.d.	1 (2)	MMC	[389]
Lfcin (4-12)-NH_2	H-RRWQWRMKK-NH_2	n.d.	0.2 to 1 (5)	MIC	[390]
Lfcin acyl-10-(4-12)-NH_2	decanoyl-RRWQWRMKK-NH_2	n.d.	0.5 to 1 (5)	MIC	[390]

[a] the pattern of the disulfide bonds are indicated by subscripts, Dab = *L*-1,4-diaminobutyric acid; Rhb = rhodamine B; [b] MIC = minimal inhibitory concentration; ED_{90} = concentration of the test compound required to reduce the number of viable cells by $1\times\log_{10}$; IC_{50} = peptide concentration required to inhibit 50 % of microbial growth; LC = lethal concentration; LD_x = lethal dose leading to killing of x % of the micro-organisms; MMC = minimum microbicidal concentration; [c] n.d. = not determined.

In addition to the determination of their *in vitro* activities, some enantiomeric pairs of AMPs have also been studied *in vivo*. For example, Darveau et al. showed that C18X, the enantiomer of a 13 residue peptide corresponding to the C-terminal end of human platelet factor IV, possessed comparable antimicrobial activity in a neutropenic murine model of infection[391]. They also reported on similar activities of both enantiomers *in vitro*, although no quantitative data was given. Similar results were found in another murine model of infection for a synthetic, α-helical undecapeptide, although the authors proposed that this chemotherapeutic *in vivo* effect was mediated by the activation of neutrophils rather than by direct interaction of the peptides with the bacterial cells.[392]

The D/L activity ratios of the enantiomeric pairs from **Table 3.7** are summarised in **Table 3.8** together with their classification into secondary structures and according to differences in these ratios. It can be seen that the majority of AMPs that have been studied show behaviour that is to be expected for substances acting by a membrane-active mechanism, i.e. they possess a D/L activity ratio of around unity. However, there are several examples of AMPs with ratios significantly deviating from unity, and these examples typically belong to the Pro/Arg-rich class of AMPs. Only few examples exist of a D/L activity ratio corresponding to a difference of more than 2 orders of magnitude in favour of the naturally occurring all-L form, the most prominent being the insect peptide apidaecin, again a representative of the Pro/Arg-rich class of AMPs. Other naturally occurring AMPs belonging to different classes of secondary structure, and with activity ratios significantly exceeding unity are thanatin,[93] a 21 residue AMP from insects which adopts a β-hairpin conformation, and cecropin-P1,[244] an α-helical AMP originally isolated from pig small intestine but subsequently found to originate from the nematode *Ascaris suum*.[393] To conclude, it is noteworthy that cecropin-P1 and most notably PR-39, yet another Pro/Arg-rich AMP, show activity ratios significantly lower than unity towards some microbial species. For PR-39, the all-D form is about three orders of magnitude more active than the naturally occurring isomer, and the unusually low activity ratio has been proposed to arise from increased proteolytic stability of the all-D form.[244] It should be noted, however, that an increase in the activity of all-D peptides, if observed, is generally around a factor of two (cf. **Table 3.7**).

Table 3.8 Summary of activity ratios of enantiomeric pairs of AMPs described in the literature and correlation with their secondary structural elements.

secondary structure	D/L activity ratios from **Table 3.7**					total from **Table** 3.7
		higher activity for the all-L form		higher activity for the all-D form		
	> 0.13 and < 8	≥ 8 and < 1000	≥ 1000	≤ 0.13 and > 0.001	≤ 0.001	
β-sheet or β-turn	**9**	**1**	**-**	**-**	**-**	**10**
α-helical	**29**	**1**	**-**	**1**	**-**	**31**
Pro/Arg-rich	**-**	**1**	**2**	**-**	**1**	**4**
not determined	**4**	**-**	**-**	**-**	**-**	**4**
total from **Table 3.7**	**42**	**3**	**2**	**1**	**1**	**49**

3.4.2 Enantiomers of related compounds

In addition to AMPs, enantiomeric pairs of related peptidic compounds have been synthesised. For example, Raguse et al. reported that both enantiomers of a 9 residue β-peptide showed identical antimicrobial activity against *E. coli*, *S. aureus*, *E. faecium*, and *B. subtilis*.[394] Furthermore, a variety of cell penetrating peptides (CPP), which are of interest because of their potential as drug-delivery systems, were studied in more detail. Notably, most CPPs bear an overall positive charge, usually due to arginine side-chains, emphasising the similarity between CPPs and AMPs. The ability of several enantiomeric pairs of these compounds to translocate across cell membranes has been assessed by confocal fluorescence microscopy with fluorescin-labelled derivatives, and, for example, no differences in the uptake of pVEC, an 18 residue peptide derived from murine endothelial cadherin,[395] or of a 16 residue hydrophobic peptide derived from a human fibroblast growth factor,[396] into eukaryotic cell lines were detected. Similarly, Derossi et al. reported that both enantiomers of a 16 residue helical peptide derived from a DNA binding domain are translocated with equal efficiency into cell cultures.[397] The same holds true for KLA peptide, a *de novo* designed amphipathic α-helical model compound, with respect to the ability of both enantiomers to translocate across the plasma membrane of rat peritoneal mast cells.[398]

3.4.3 Other activities of AMPs

In addition to their antimicrobial activity, other more discrete biological activities of AMPs have been examined for the involvement of stereospecific interactions. For instance, another motivation for the synthesis of all-D peptides lies in their predicted proteolytic stability (vide supra). It is generally assumed that peptides containing D-amino acids are more stable towards enzymatic degradation than their natural counterparts, and indeed several of the above mentioned enantiomeric pairs have been used to demonstrate this fact; for an illustrative example see the work of Besalle et al.[363] This proteolytic stability has been suggested to allow for the use of these compounds as therapeutics with potentially increased bioavailability.

In addition to its antimicrobial activity ratio of around unity (cf. **Table 3.7**), magainin-2, a broad-spectrum membrane-lytic AMP, showed no differences in the toxicity of both enantiomers towards several tumour cell lines, as studied by flow cytometry.[399] Also, the promotion of cell adhesion and tumour growth by two short peptides derived from type IV collagen and from laminin was studied, once again showing no involvement of stereospecific components.[400-402] Furthermore, the interaction of both enantiomers of polymyxin B nonapeptide,[370] as well as of pEM2,[389] a short peptide derived from myotoxin II, with bacterial LPS, have been studied. It was found that there was no difference in LPS binding for both enantiomers of polymyxin B nonapeptide, as judged by a polymyxin displacement assay, whereas a slightly higher LPS neutralising property was found for all-L pEM2.

An interesting case is the α-helical plant pheromone plantaricin A which, in addition to its antimicrobial activity that is independent of its stereochemistry, also displays activity as a pheromone, but only the all-L form is capable of inducing the production of bacteriocins.[384] It has been suggested that non-specific interaction of plantaricin A with the membrane - presumably connected to the intrinsic antibacterial properties of this molecule - induces secondary structure which is involved in the stereospecific pheromone activity[383].

3.4.4 Synthesis of enantiomeric AMPMs

To gain insights into the antimicrobial mechanism(s) of our AMPMs, the enantiomers of mimetics **16**, **17**, and **18** were prepared. The synthesis of these

compounds was carried out analogously to that of the parent compounds (as described in **Section 3.1)**, and as was to be expected, no differences or difficulties other than those mentioned earlier were encountered. The only difference in the synthesis of ent-**17** was the use of a trityl protecting group for D-Gln in place of methyltrityl, which was routinely used as protecting group for L-Gln, and this minor modification had no apparent effect on the synthesis of the protected precursor molecule. A comparison of the HPLC chromatograms of the enantiomeric pairs of our AMPMs is given in **Figures 3.19-3.21**.

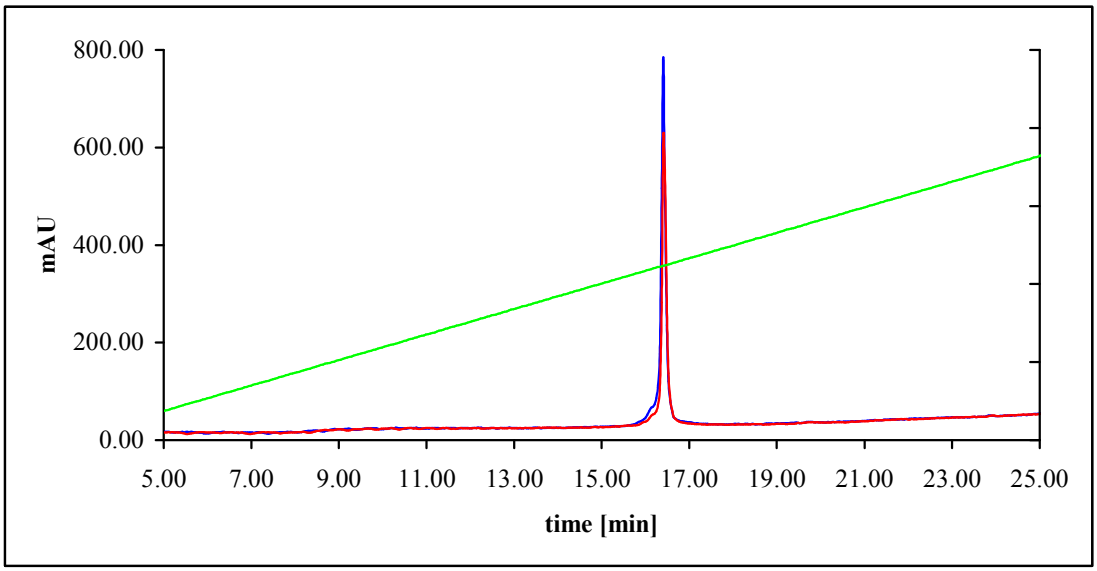

Figure 3.19 HPLC chromatograms of **16** (blue) and ent-**16** (red). Vydac218TP54 C18 analytical column; 5 to 100% acetonitrile in water (+0.1% TFA) in 7 column volumes; flow 1 ml/min.

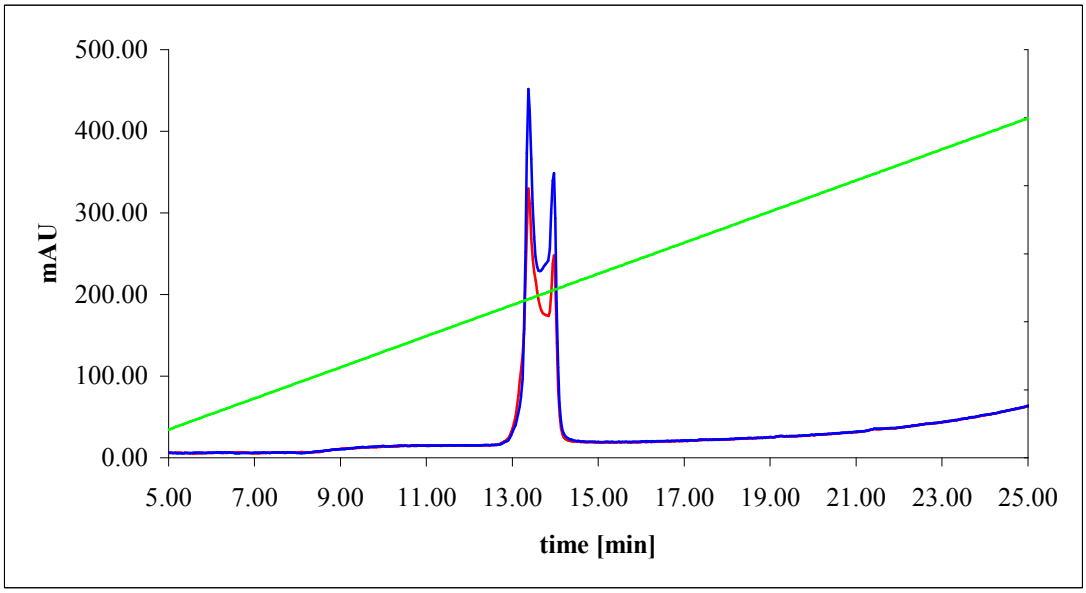

Figure 3.20 HPLC chromatograms of **17** (blue) and ent-**17** (red). Vydac218TP54 C18 analytical column; 5 to 100% acetonitrile in water (+0.1% TFA) in 7 column volumes; flow 1 ml/min.

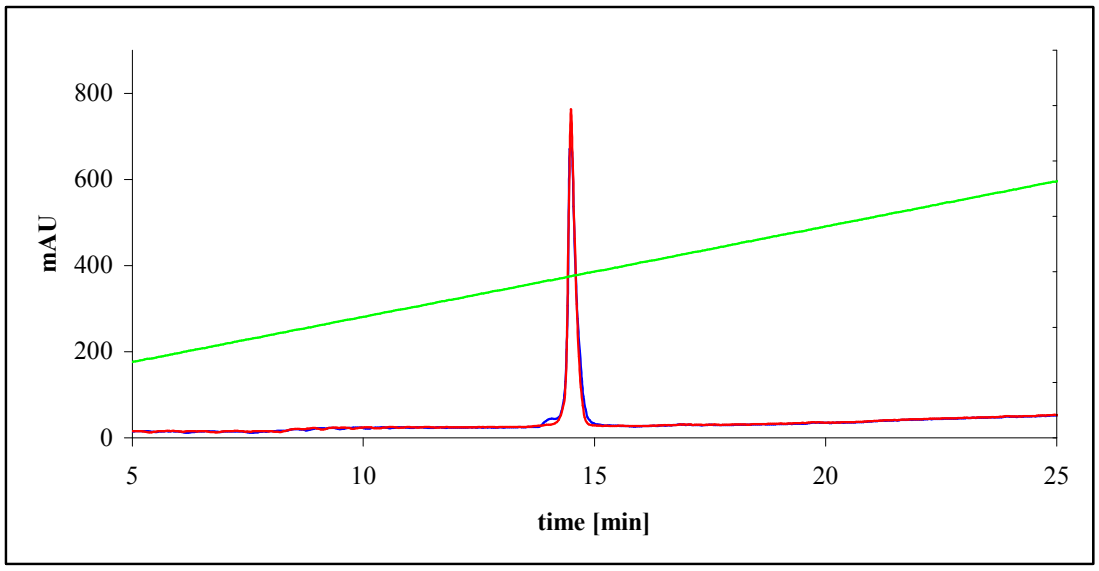

Figure 3.21 HPLC chromatograms of **18** (blue) and ent-**18** (red). Vydac218TP54 C18 analytical column; 5 to 100% acetonitrile in water (+0.1% TFA) in 7 column volumes; flow 1 ml/min.

3.4.5 D/L activity ratios of the AMPMs

The MIC values of the enantiomeric pairs of our AMPMs were determined against the standard panel of micro-organisms, and according to our routine protocol (cf. **Section 3.3.1**), employing a standard inoculum of ~5×10^5 CFU/mL. The results are summarised in **Table 3.9** together with the resulting D/L activity ratios for each tested species, respectively strain.

Table 3.9 MIC values and corresponding D/L activity ratios for the enantiomeric pairs of AMPMs derived from protegrin-1; results from at least three experiments were averaged.

peptide	MIC[a] [μg/mL]				
	E. coli ATCC 25922	*S. aureus* ATCC 25923	*S. aureus* ATCC 29213	*P. aeruginosa* ATCC 27853	*P. aeruginosa* PAO1
16	6.0	6.2	17	2.3	2.0
ent-**16**	2.0	4.3	12	0.75	1.5
D/L ratio	0.33	0.69	0.71	0.33	0.75
17	14	21	> 64	0.29	2.4
ent-**17**	16	32	> 64	43	> 64
D/L ratio	1.1	1.5	n.a.[b]	150	> 27
18	32	41	> 64	0.02	0.03
ent-**18**	16	49	> 64	28	20
D/L ratio	0.5	1.2	n.a.	1400	670

[a] minimal inhibitory concentration; [b] not applicable

As can be seen from **Table 3.9**, the enantiomer of mimetic **16** is more active against all tested micro-organisms than the parent compound. The activity ratio for **16** is between 0.33 and 0.75, thus indicating that ent-**16** is about twice as potent as **16**. Such an activity ratio is in accordance with a membrane-active mechanism, as is also reflected by many compounds from **Table 3.8** that are believed to follow such mechanisms. In contrast, **17** shows an activity ratio favouring the all-L form by about one order of magnitude for *P. aeruginosa*. This trend is even more pronounced for **18**, which achieves an activity ratio of up to 1400 for *P. aeruginosa* ATCC 27853. Notably, both mimetics display ratios between 0.5 and 2 for the other bacterial species; an activity ratio could not be calculated for *S. aureus* ATCC 29213 because both mimetics were inactive against this strain up to the highest assay concentration.

3.4.6 Remarks and Conclusions

As outlined in **Chapter 2**, the presence or absence of a stereospecific component in the killing or the bacteriostatic action of an AMP as described by the D/L activity ratio is a very powerful indicator for the possible involvement of alternative mechanisms of action. Aspects that are related to the attractiveness of this parameter are the simplicity and reliability of its determination. The simplicity is not only manifested in the accessible synthesis of the enantiomeric compounds, but also in the various protocols employed for the quantification of antimicrobial action. Moreover, since the effects of the test compounds are studied on whole organisms rather than on isolated biochemical systems, an irrevocable result can be obtained.

Unfortunately, this global nature of the D/L activity ratio is accompanied by the loss of any information that could be obtained about the mechanism itself. Activity ratios around unity or smaller strongly suggest a mechanism that is primarily dependent on the interaction of the AMP(M) with membranous systems, but no more can be learned about the exact nature of this interaction; the same limitations obviously apply to the case of unusually high activity ratios. However, the synthesised enantiomers can also serve as invaluable control compounds in any experiment that is concerned with an isolated biochemical system.

Although the association of activity ratios around unity with a membrane-active mechanism is generally accepted, there could be exceptions. For example, whereas a slightly higher activity of the unnatural all-D enantiomer is easily explicable

by an increased proteolytic stability, the unusually low activity ratio, observed for example for PR-39 towards some micro-organisms, poses a conceptual problem. If an unusually low activity ratio, of less than 0.001 (c.f. **Table 3.7**), indeed originates from an increased stability of the all-D form, than it is justified to ask whether such an effect exists for other AMPs as well (especially since PR-39 is a linear peptide consisting of only natural amino acids). Hence, it would be conceivable that stereospecific preferences for antimicrobial killing exerted by all-L forms are not detected, because their increased activity could be masked by an increased rate of proteolysis. Along these lines, it would then also be possible that observed D/L activity ratios underestimate the value that would be obtained in the absence of enzymatic degradation.

Of course, with respect to unusually low activity ratios, it is also imaginable that some peptides are much more prone to enzymatic degradation than others, for example by virtue of their structure, or if the micro-organism possesses enzymes that are especially well suited for the degradation of a given AMP. Additionally, it can also not be excluded that an unnatural all-D form might interact specifically with a target.

Shai and co-workers reported on the specific association of an all-D glycophorin A (GPA) trans-membrane helical domain with its enantiomeric trans-membrane helical domain,[403] as well as on the inhibition of dimerisation of a trans-membrane domain of an *E. coli* aspartate receptor involved in chemotaxis, by both enantiomers of a peptide derived from the corresponding trans-membrane helix of the receptor.[404] Based on these findings, the authors suggest that helix-helix recognition in a membranous environment - at least in these two cases - does not depend on the chirality of the helices involved and is governed mainly by side-chain interactions of the enantiomeric peptides rather than by a geometrical fit of their respective conformations. With respect to the interpretation of enantiomeric activity ratios, this would imply that an activity ratio of unity does not necessarily preclude the involvement of a specific target in the antibacterial mechanism.

On the other hand, Suchyna et al. reported on the inhibition of stretch-activated cation-channels (SAC) by GsMTx4, a peptide isolated from tarantula venom.[405] It was found that both enantiomers of GsMTx4 inhibit SACs, and this was demonstrated to originate from altered bilayer properties in the local environment of the ion-channel. SACs belong to the so-called mechanosensitive channels, a class

of proteins that responds to mechanical stress; other examples of this class comprise phospholipase A and G proteins.[406, 407] The authors suggested that mechanosensitive proteins, especially those sensitive towards the bilayer tension, could be regarded as receptors for amphipathic messenger compounds. In view of this suggestion, an activity ratio of around unity is once again placed firmly into the domain of membrane-activity as defined in **Section 2.1.1**.

Finally, it has to be emphasised, that the absence of a chirality-dependent component in antimicrobial action does not imply that the AMP under consideration is completely devoid of such a component. Naturally, conclusions can only be drawn for the panel of tested micro-organisms. This is evident from several cases shown in **Table 3.7**. Moreover, mimetic-**18** is a prime example of this behaviour, showing a very high D/L activity ratio concomitant with a high selectivity towards *P. aeruginosa* strains but not towards *E. coli* or *S. aureus*.

3.5 Dye-leakage experiments

Dye leakage experiments are frequently used as a means of investigating the ability of AMPs to induce permeabilisation of membrane structures. Typically, liposome vesicles are used as model membranes, although studies involving more complex systems are known. For example, Edgerton et al. studied calcein release from intact *C. albicans* cells treated with the Pro/Arg-rich AMP histatin-5 (c.f. **Section 2.2**).[211]

Vesicles of various compositions are used to emulate the differential makeup of microbial versus mammalian membranes. Frequently, binary systems employing zwitterionic and negatively charged phospholipids are used, and amongst these the most common system is composed of varying ratios of 1-palmitoyl-2-oleoyl-*sn*-glycero-3-phosphocholine (POPC, **26**) and 1-palmitoyl-2-oleoyl-*sn*-glycero-3-[phospho-*rac*-(1-glycerol)] (POPG, **27**) (**Figure 3.22**).

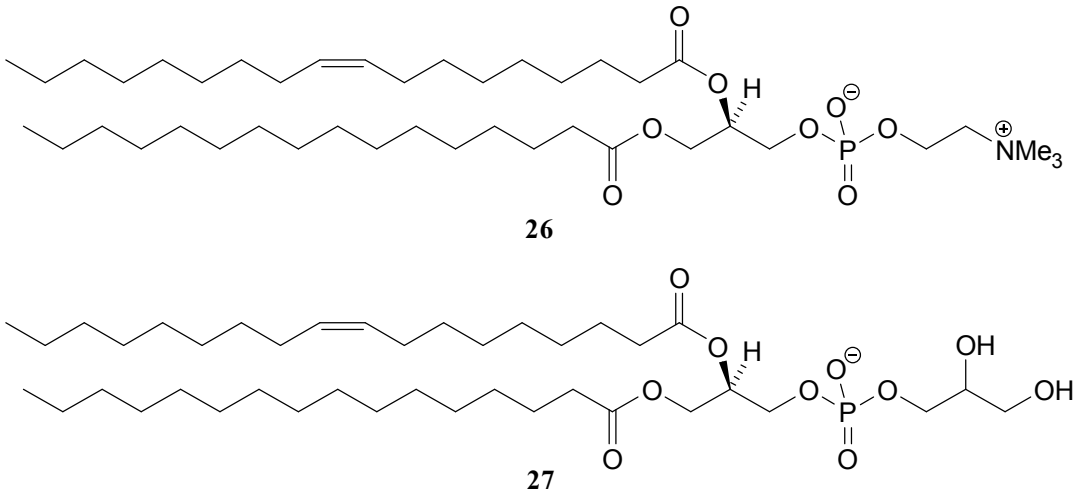

Figure 3.22 Zwitterionic POPC (18) and negatively charged POPG (19), two phospholipids frequently used in dye-leakage experiments.

In such binary systems, liposomes prepared only of zwitterionic phospholipids are taken to represent eukaryotic membranes, which in contrast to their bacterial counterparts carry less negatively charged phospholipids on their surface. The relationship between dye-leakage from POPC vesicles and the haemolytic activity of several AMPs, or peptide venoms, has been studied and found to be well

correlated.[105] Analogously, vesicles composed of increasing amounts of negatively charged POPG lipids are used to mimic prokaryotic membranes.[408]

POPC/POPG systems containing varying ratios of these two phospholipids have been used inter alia in dye-leakage experiments with the AMPs polyphemusin-1,[111] indolicidin,[111] KLAL peptides,[118] tritrpticin,[409] cathelicidins,[410] tachyplesin-1,[106] P-Der,[245] magainin-2,[411] or the peptide antibiotic gramicidin S.[111] Other phospholipid systems such as POPE/POPG or POPS/POPC were used to study androctonin[183] and dermaseptin.[182] Finally, DOPC/DOPG systems containing a dioleoyl moiety have been described for the AMPs pleurocidin,[412] and several magainins.[413]

Naturally, binary systems can only be a simplified model of a real membrane environment and accordingly, more complex systems have been described. For instance, systems including additional lipid compounds such as cholesterol are occasionally taken to mimic mammalian membranes,[414] and vesicles containing lipid A analogues have been used to mimic the outer membrane of Gram-negative organisms,.[238] Another more complex system consisting of egg-PE/egg-PG/LPS/cardiolipin, chosen to resemble Gram-negative membranes, was used by Waring et al. to study the behaviour of protegrin-1 (**11**) in model membranes.[415]

3.5.1 Principle of the Assay

The principle of the dye leakage assay is based on the observation that certain fluorophores like calcein (**28**) and carboxyfluorescein (**29**) quench their own fluorescence at higher concentrations (**Figure 3.23**).[416] Both **20** and **21** have been used for experiments with AMPs, although calcein is employed much more frequently.

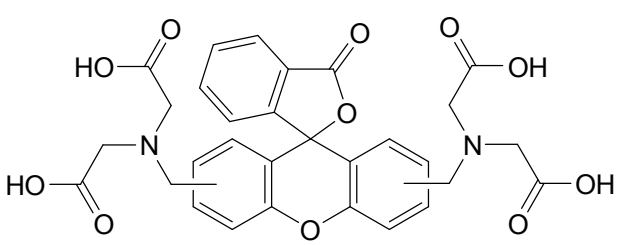

28

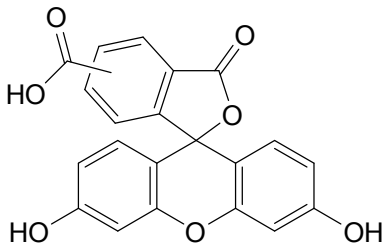

29

Figure 3.23 Calcein (**28**) and carboxyfluorescein (**29**), two self-quenching fluorescent dyes employed in dye-leakage experiments.

Therefore, the use of calcein in dye-leakage experiments will be implied unless noted otherwise; for an example with carboxyfluorescein as self-quenching dye, c.f. reference [417]. Concentrated solutions of a self-quenching fluorophore experience a strong increase in fluorescence intensity upon dilution (**Figure 3.24**). The fluorescence intensity of calcein is found to be approximately linear in a concentration range between 30 and 3 μM, thus allowing for quantification of the results (**Figure 3.24B**).

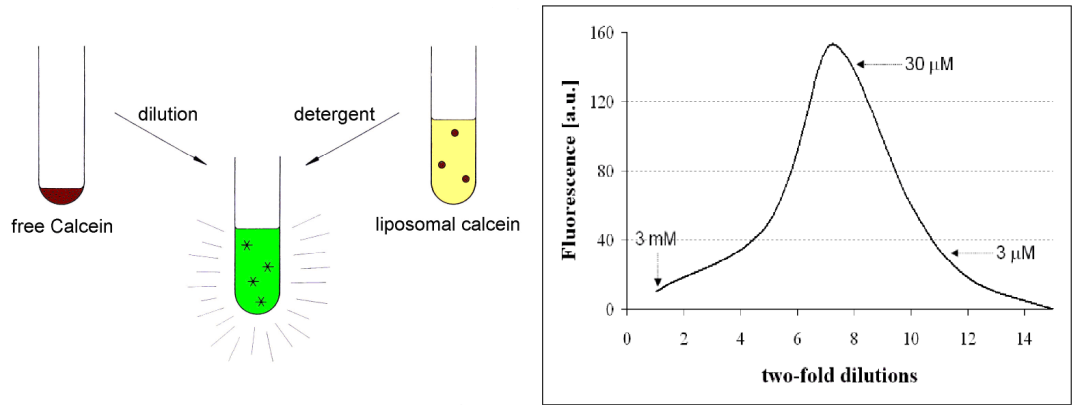

Figure 3.24 (A) Increase in fluorescence intensity of a self-quenching dye upon dilution; adapted from ref [418]. (B) Concentration dependence of fluorescence intensity (arbitrary units) for calcein.

In practice, higher concentrations of the self-quenching dye (30 to 70 mM) are encapsulated into liposomes of the desired phospholipid composition. Addition of membrane permeabilising compounds, or detergents, then leads to dilution of the fluorophore into the surrounding medium, with a concomitant strong increase in fluorescence intensity (c.f. **Figure 3.24B**). The calcein fluorescence is measured with an excitation wavelength between 430 and 470 nm, chosen to achieve a maximal dynamic range for the fluorescence signal, and an emission wavelength of 520 nm.[419]

Appropriate amounts of the permeabilising compound are added, and the increase in fluorescence intensity is monitored over time. At the end of each experiment a detergent such as a 10 % (w/v) solution of Triton X-100™ is added, in order to determine the maximal fluorescence signal, i.e. the value corresponding to the total disruption of the calcein-entrapped vesicles (**Figure 3.25**).

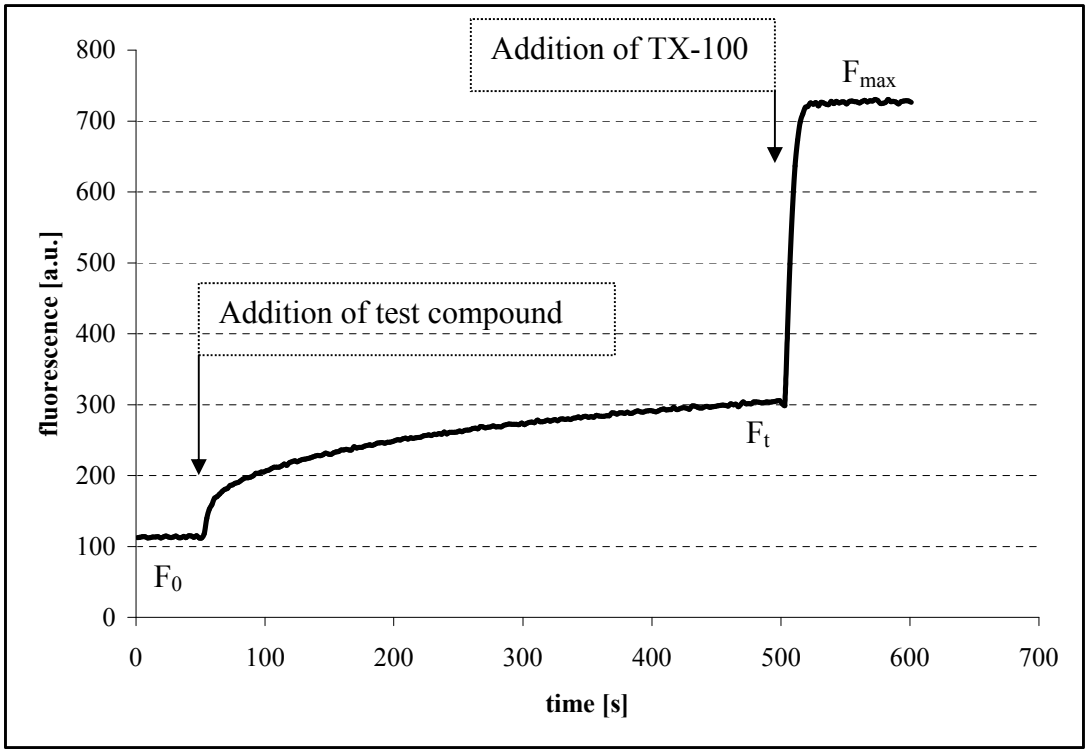

Figure 3.25 Time course of fluorescence intensity in a dye-leakage experiment carried out with 20 μM of mimetic **16** as permeabilising compound and 30 μM of POPC/POPG (80:20) LUVs.

The dye-leakage data can be plotted in a dose-dependent fashion according to **equation 3.1**, which describes the fraction of calcein released into the surrounding medium. Calcein release is calculated from F_t, the fluorescence at a specified time t (e.g. 5 minutes), F_0, the background fluorescence before addition of the permeabilising compound, and F_{max}, the maximal fluorescence after addition of the detergent, taken to represent complete lysis of the liposomes.

$$calcein\ \ release = \frac{(F_t - F_0)}{(F_{\max} - F_0)} \qquad \text{[equation 3.1]}$$

3.5.2 Preparation of liposomes

The vesicles used in the dye-leakage experiments were prepared according to a liposome extrusion method.[418] Briefly, POPC and POPG phospholipids in the appropriate ratios were dissolved in an organic solvent or solvent mixture such as chloroform or methanol/DCM in a round-bottom flask. The solvent was evaporated to dryness on a rotary evaporator to afford an evenly distributed lipid film on the wall

of the vessel. Lipid vesicles are formed when such a lipid film is hydrated with an aqueous solution. During this process, hydrated lipid sheets become detached from the lipid film and form large, multi-lamellar vesicles (MLVs) which possess an onion-like makeup of multiple phospholipid bilayers. In the case of the preparation of calcein entrapped vesicles, the hydration solution contained the appropriate amount of the fluorophore, i.e. a concentration in the self-quenching range. Typically, a 10 mM Tris-buffer containing 50 mM calcein, 10 mM NaCl and 0.1 mM EDTA, pH 7.4 was used. Once MLVs have been formed, energy input is required to reduce their size and to break up their multi-lamellar structures. This energy is generally provided either by sonication or in mechanical form, via extrusion.

The extrusion technique employed in the preparation of the calcein entrapped vesicles is based on forcing the MLV suspension repeatedly through polycarbonate membranes of defined pore size, resulting in the formation of large unilamellar vesicles (LUVs) with a mean particle size in the range of the membrane pore diameter. Prior to the extrusion process, calcein encapsulated MLVs were subjected to six freeze-thaw cycles with liquid nitrogen, which is thought to improve the homogeneity of the resultant LUVs. For the preparation of LUVs, thirteen extractions through 100 nm membranes were carried out, and the size distribution and homogeneity of the liposome preparations was confirmed by dynamic light scattering. Due to the phase transition temperatures of POPC and POPG, which both have a value of T_C = -2°C, all manipulations were carried out at room temperature, and the prepared liposomes could conveniently be stored at 4°C.

Subsequent to the preparation of calcein entrapped vesicles, unencapsulated dye had to be removed from the preparations. Therefore, the obtained liposomes were subjected to gel filtration through a Sephadex G-25 column (1 × 25 cm) with standard buffer (10 mM Tris, 100 mM NaCl, 0.1 mM EDTA, pH 7.4) as eluent. Care has to be taken that the calcein-entrapped vesicles are treated with a buffer system that has a comparable osmolarity to the buffer used to hydrate the liposomes, in order to avoid efflux of dye due to an osmotic gradient.[420] The phospholipid concentration of the liposome preparations was then determined using a colorimetric phosphorous assay (Bartlett assay),[421] with minor modifications.[422]

3.5.3 Dye-leakage experiments with AMP(M)s

To study the membrane permeabilising properties of the antimicrobial peptide mimetics **16** and **17**, as well as of the positive control AMP, protegrin-1 (**11**), dye leakage experiments were carried out with the POPC/POPG liposomal system at four different phospholipid ratios. A summary of the results of these experiments, employing a total liposome concentration of 30 μM in each experiment is given in **Figures 3.26-3.28**.

It can be seen from the results that protegrin-1 (**11**) causes substantial leakage of calcein from POPC/POPG vesicles at all tested ratios. In contrast, the AMPMs **16** and **17** only showed a significant ability to induce dye-leakage from the highly negatively charged vesicles composed solely of POPG phospholipids, and a comparison of the induced dye-leakage from pure POPG vesicles by all three compounds is shown in **Figure 3.29**. It is evident from this figure that there are no fundamental differences between the three peptides. The ability of protegrin-1 (**11)** to disrupt the purely zwitterionic POPC vesicles is in agreement with its pronounced haemolytic activity (c.f. **Section 1.5**) and with the notion that liposomes composed of POPC can act as models of erythrocytic membranes.[105]

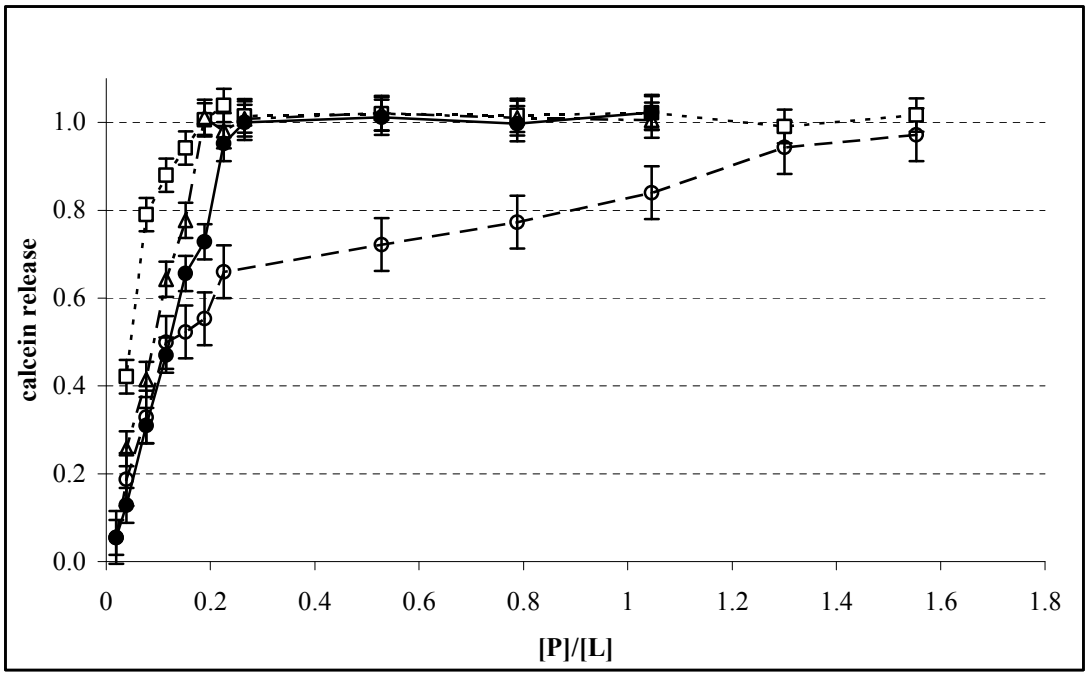

Figure 3.26 Calcein release from POPC (○), POPC/POPG 80:20 (□), POPC/POPG 70:30 (◊) and POPG (●) LUVs induced by protegrin-1 (**11**). [L] = 30 μM.

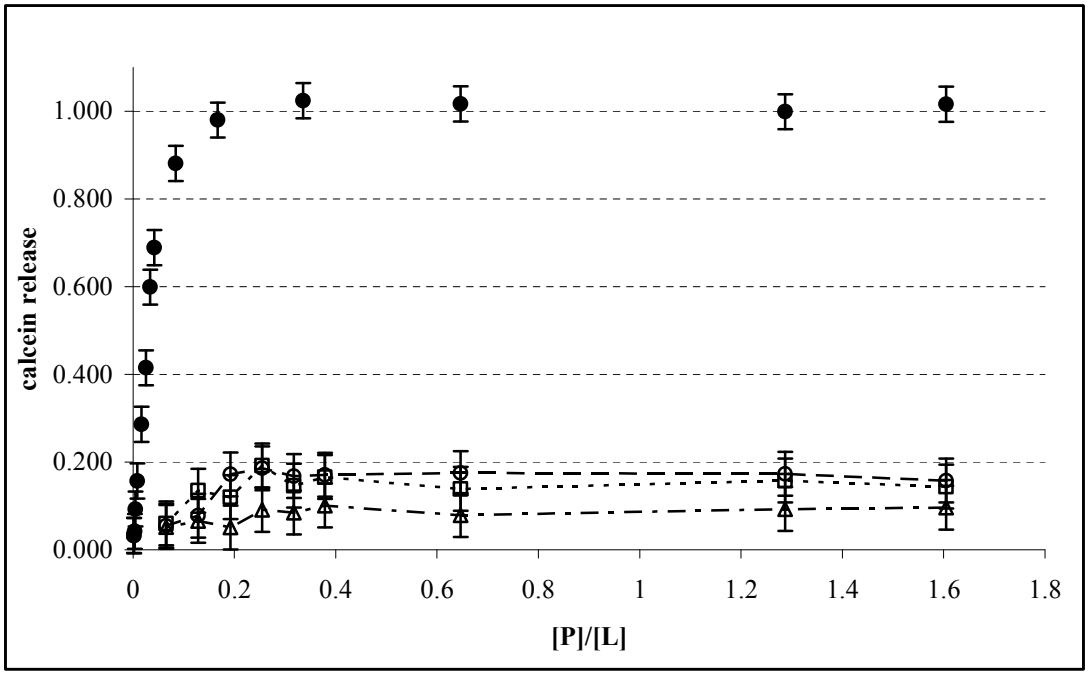

Figure 3.27 Calcein release from POPC (○), POPC/POPG 80:20 (□), POPC/POPG 70:30 (◊) and POPG (●) LUVs induced by mimetic **16**. [L] = 30 μM.

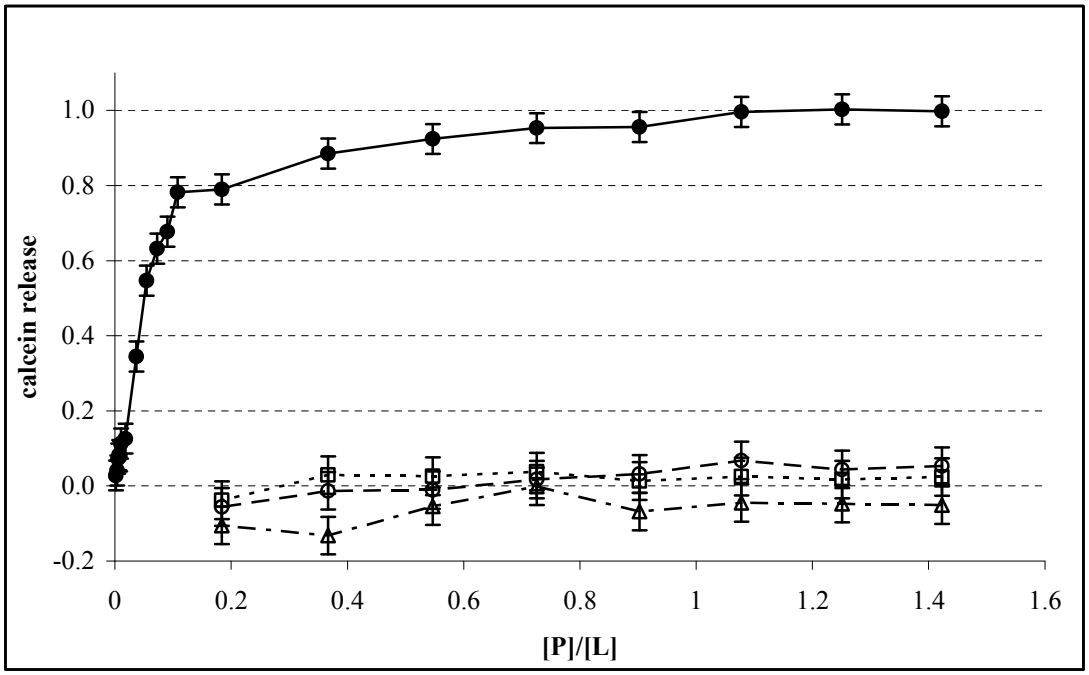

Figure 3.28 Calcein release from POPC (○), POPC/POPG 80:20 (□), POPC/POPG 70:30 (◊) and POPG (●) LUVs induced by mimetic **17**. [L] = 30 μM.

Dye-leakage experiments with **11** and derivatives, employing LUVs composed of either egg-PC,[133] POPC/POPG (70:30),[423] or more complex phospholipid mixtures,[415] have been described. In agreement with our experiments, these studies

attributed a pronounced lytic behaviour to protegrin-1 (**11**) and a derivative in which the phenylalanine residue has been replaced with tryptophan to render the molecule amenable to fluorescence spectroscopy. It has to be mentioned, however, that the reported dye-leakage ability of **11** is generally slightly higher than observed in our experiments. For instance, Waring et al. observed an R_f value of around 0.3 for a peptide to lipid ratio of 0.01, compared to $R_f \approx 0.05$ at a lipid to peptide ratio of 0.02 for the various phospholipid compositions used in our experiments. It was also found that derivatives of **11** with reduced disulfide bonds, or with cysteine residues mutated to alanine, were significantly less prone to induce dye-leakage from the corresponding liposome systems, thus highlighting the importance of secondary structural elements in the peptide/lipid interactions of the compound. It is also of interest to consider β-hairpin AMPs other than **11**, for which dye-leakage experiments have been described. Both tachyplesin-1[106] and polyphemusin-1[111] show a comparable tendency to induce dye-leakage from at least partially negatively charged model systems.

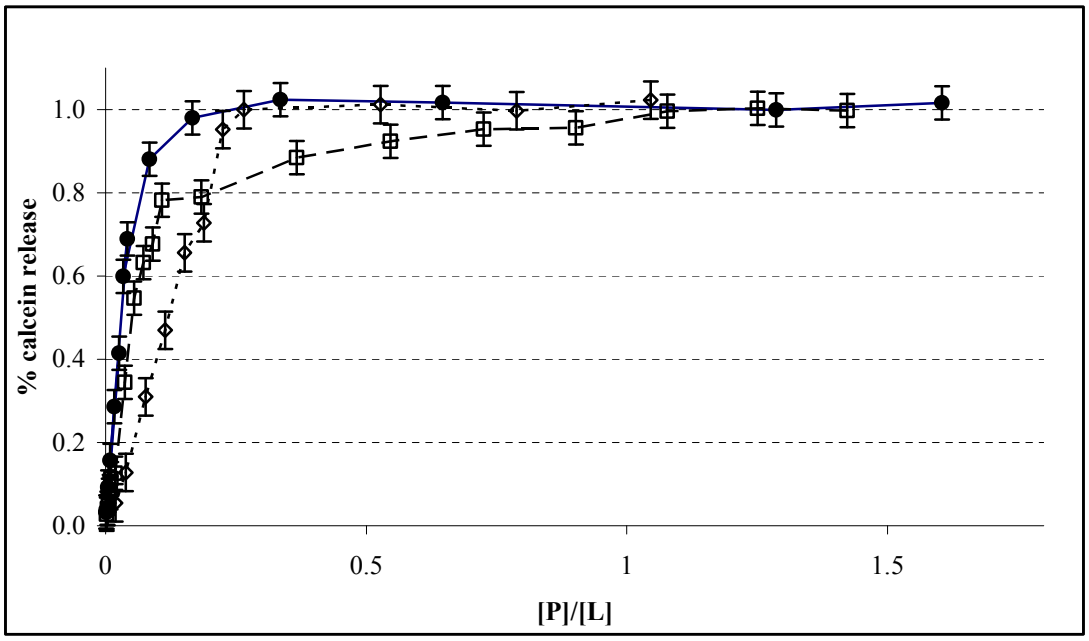

Figure 3.29 Comparison of the calcein release (R_f) from POPG LUVs induced by mimetic-**16** (●), mimetic-**17** (□), and protegrin-1 (**11,** ◊). [L] = 30 μM.

Unlike the dye-leakage induced by **11**, which was largely independent of the phospholipid composition of the vesicles, both **16** and **17** only caused a background level of fluorescence intensity for the mixed POPC/POPG and the pure POPC systems, which was slightly larger for mimetic **16** than for mimetic **17**. The influence of introducing zwitterionic phospholipids into the model systems has been

documented in several studies. For instance, it has been reported that defensins display a reduced ability to fuse membranes composed largely of zwitterionic phospholipids,[424] and that dye-leakage caused by defensins is diminished upon introduction of zwitterionic phospholipids into POPG LUVs.[425] Comparable behaviour has been demonstrated for the cathelicidin PMAP-23,[410] and for magainin-1.[426]

3.5.4 Conclusions of the dye-leakage experiments

It has been shown that neither mimetic **16** nor mimetic **17** were able to induce significant dye-leakage except from the most negatively charged model system, composed of POPG alone. Nevertheless, both AMPMs were able to interact with and to permeabilise this model system to an extent that allowed the efflux of the fluorescent probe molecule. Thus, it has to be concluded that both compounds possess, in principle, membrane-active properties. Additionally, with respect to the POPG system, these properties are manifested at peptide to lipid ratios that are in good agreement with the ratios reported in the literature for other AMPs such as tachyplesins,[106] polyphemusins,[111] or indolicidin.[111]

With respect to the question of antimicrobial mechanisms of action, however, it has to be emphasised that in the test liposomal systems more reminiscent of bacterial membranes, there were pronounced differences in the peptide to lipid ratios necessary to effect significant dye efflux, as compared to other AMPs such as protegrin-1 (**11**). On the basis that peptide to lipid ratios sufficient to induce dye-leakage can become quite high for some AMPs, it has been argued that these ratios are too high to render most AMPs unusually membrane-active compounds.[111] However, it must be mentioned that peptide to lipid ratios usually encountered at the onset of dye-leakage are found to be between 0.005 and 0.01, i.e. well within the span of one order of magnitude. Moreover, such ratios are found for notorious examples of membrane-lytic or pore-forming compounds such as the peptide venom melittin,[427] or the peptide antibiotic gramicidin S.[414] The authors of the aforementioned study do not clearly define at which point a peptide to lipid ratio should be considered too high to point to a membrane-active mechanism. However, in the case of **16** and **17**, there is no appreciable dye efflux in liposomes containing zwitterionic phospholipids up to ratios larger than unity, and this can safely be equated with an absence of membrane

permeabilisation, at least with respect to a pore size and/or lifetime of the pores that would allow for efflux of the fluorescent probe molecule. For example, the absence of dye leakage at concentrations where lipid flip-flop occurs was correlated with the transient character of the putative pores according to a toroidal pore mechanism, and with the variable size that these pores have in the said model.[111]

Therefore, if we accept, for the time being, the mixed liposomal systems as an adequate first order approximation to bacterial membranes, the results obtained with **16** and **17** are only very difficult to account for with a classical carpet model that postulates complete lysis of the bacterial membrane, and which would require a complete efflux of the fluorescent marker at concentrations comparable to the MIC. This incompatibility becomes more drastic for the behaviour of mimetic-**17** towards *P. aeruginosa* because of the decrease in the corresponding MIC value, and it might be anticipated that this could be even more the case for the later AMPMs **18** and **19**.

However, since the possibility, in principle, of membrane activity with **16** and **17** has been proved, it is possible that the AMPMs either directly kill microbial organisms according to the definitions of membrane-active mechanisms, or according to a SMH model (c.f. **Section 2.1.2**), with involvement of intracellular targets. Finally, the absence of dye-leakage in POPC systems is in good agreement with the low haemolytic properties of **16** and **17**.

3.6 Macromolecular biosynthesis

A powerful approach towards elucidating possible modes of action of an antibacterial substance consists of studying the incorporation kinetics of radio-labelled precursor molecules for the biosynthesis of bacterial macromolecules such as protein, DNA, RNA, and peptidoglycan. A classical example of this methodology is given by the studies directed towards chloramphenicol, a broad-spectrum antibiotic first isolated from *Streptomyces venezuelae* in 1947.[428-430] Gale and Folks as well as Wisseman et al. observed inhibition of protein synthesis by chloramphenicol in *S. aureus* and in *E. coli*, respectively during the course of studying the incorporation of radioactively labelled amino acids into the trichloroacetic acid (TCA) insoluble fractions of these bacterial species.[429, 431]

Changes in the efficiency of incorporating labelled precursor molecules into bacterial macromolecules can thus allow for the identification of, or give hints towards the primary site of action of the substance under consideration. This is especially the case if on the one hand the effect is selective towards the incorporation of a particular precursor, and on the other hand, it occurs rapidly after addition of the antimicrobial compound. These limitations arise *inter alia* because of the close interconnection between protein and nucleic acid biosynthesis in cells. For instance, DNA biosynthesis requires protein biosynthesis for the initiation of new rounds of replication, furthermore, an inhibition of RNA synthesis eventually leads to a halt in protein synthesis, inasmuch as the supply of mRNA diminishes. Such indirect effects are usually characterised by a later onset than the direct inhibition that is observed for the case of inhibition of protein biosynthesis by chloramphenicol.[432] With respect to the selectivity of the inhibitory action, it should be mentioned that antimicrobial modes of action that interfere with the cellular membrane integrity, or with processes involved in energy generation and/or utilization, can also show rapid kinetics of inhibition, but these are typically characterised by the simultaneous cessation of all macromolecular synthetic activity. Examples of this pattern pertain especially to the field of AMPs, and will be discussed in the following sub-sections.

Since all experiments conducted with mimeticsv**17** and **18** described in the previous sections corroborated the notion of an alternative antibacterial mechanism of action, their influence on the incorporation of radioactively labelled precursors of macromolecular biosynthesis into *P. aeruginosa* PAO1 has been studied.

3.6.1 Incorporation experiments with AMPMs

The radioactively labelled precursors that have been used for these experiments are summarized in **Figure 3.30**, they were: L-[4,5-^{3}H]-leucine (**30**) for protein biosynthesis, [5,6-^{3}H]-uridine (**31**) for RNA biosynthesis, [methyl-^{3}H]-thymidine (**32**) and [8-^{3}H]-adenine (**33**) for DNA biosynthesis, and *N*-acetyl-D-[1-^{3}H]-glucosamine (**34**) for peptidoglycan biosynthesis.

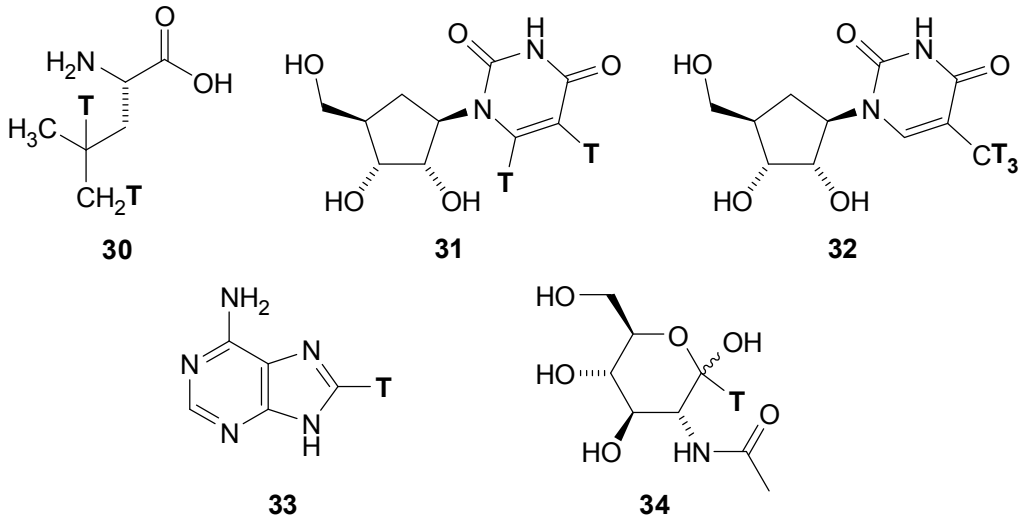

Figure 3.30 Tritiated precursors of macromolecular biosynthesis employed in the incorporation studies directed towards possible modes of action for AMPMs derived from protegrin-1 (**11**).

As mentioned, experiments studying the incorporation of a labelled nutrient into a bacterial macromolecular fraction should not be interpreted in isolation from the biosynthesis of other classes of macromolecules, or from other bacteriological data such as the kinetics of bacterial killing. Another indispensable aid in the interpretation of the results obtained consists of the use of positive control antibiotics, which exert their antibacterial action by an already known mechanism, and against which the experimental data can be compared. These positive controls also allow for the validation of the applicability of the chosen experimental setup to the presented problem. The control antibiotics employed for this purpose are shown in **Figure 3.31**, and they were chosen based on their known mode of action, in combination with their reported activities against *Pseudomonas* strains.[1] As positive control for the inhibition of protein biosynthesis, tobramycin (**25**), a semi-synthetic aminoglycoside, has been chosen. It acts by binding to the A-site decoding region of the bacterial 16S rRNA subunit.[433] Tobramycin shows good activity in the micromolar range against several *P. aeruginosa* strains that are resistant towards other aminoglycosides, such as

gentamicin.[434] Ciprofloxacin (**7**), a synthetic fluoroquinolone, inhibits DNA synthesis by binding to bacterial DNA gyrase[435] and is one of the most effective fluoroquinolones acting on *P. aeruginosa*.[436]

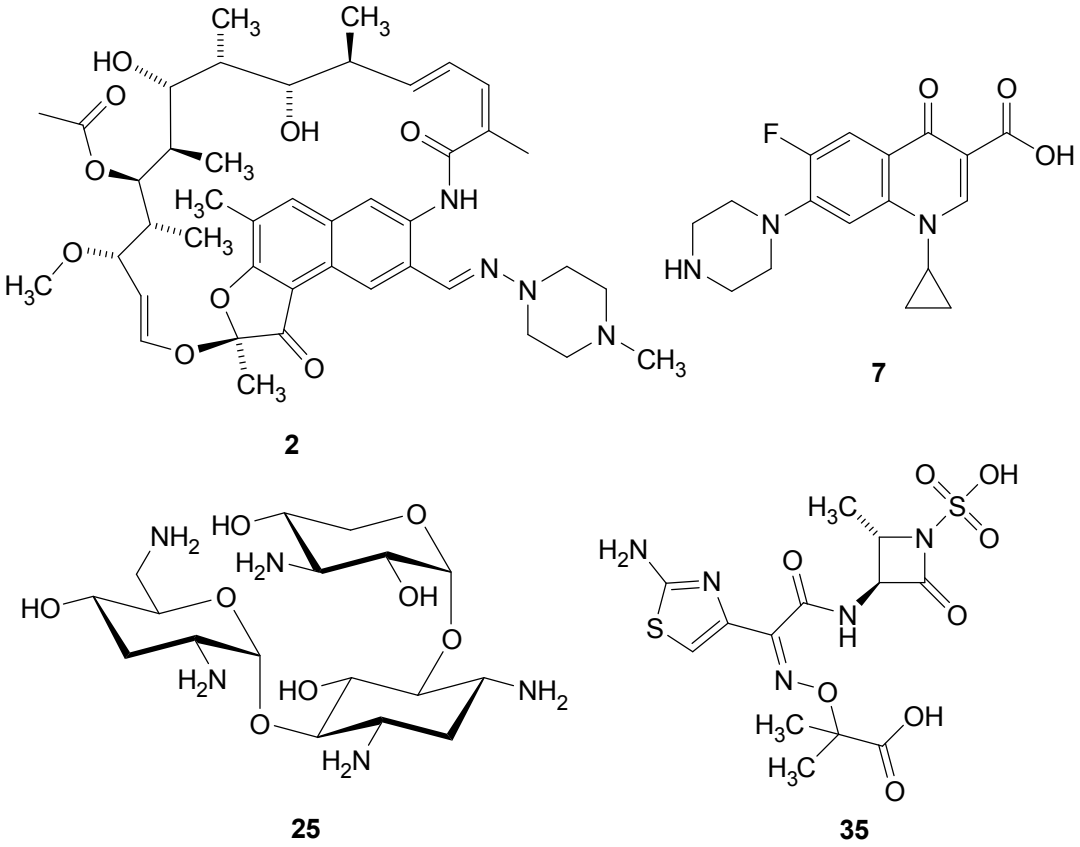

Figure 3.31 Clinically used antibiotics employed as controls in the incorporation of radioactively labelled precursor uptake experiments.

As control inhibitor of RNA biosynthesis, a semi-synthetic rifamycin, rifampicin (**2**) was used. It has been shown to act by inhibiting DNA-dependent RNA polymerase[437] and although intrinsically inactive against *P. aeruginosa*,[438] the *in vitro* activity was sufficient for its use as a positive control (vide infra). Finally, as a positive control for the inhibition of peptidoglycan biosynthesis, aztreonam (**35**), a monobactam from *Chromobacterium violaceum* was chosen. **35** acts by inhibiting peptidoglycan cross-linking via binding to PBP-3 (penicillin binding protein-3), and shows good activity against *P. aeruginosa*.[439, 440]

3.6.2 Experimental considerations

In principle, two different approaches exist for studying the uptake of radioactively labelled precursors into bacterial cells. In the continuous labelling approach, bacteria are first grown in the presence of the labelled nutrient, but without test compound. After addition of the test compound to the labelled medium, samples are taken at regular time intervals and processed as described below. In the second approach, bacterial cultures are pulse-labelled (pulsed) with the radioactive building block, i.e. samples of a bacterial suspension grown under standard conditions are taken at regular time intervals and treated with the labelled compound for a short period of time, typically two to ten minutes. For the incorporation experiments with AMPMs, both of these methods have been used, although it was not possible to use both methods for all classes of macromolecules.

It is instructive at this point to consider briefly the general experimental setup of both approaches, in order to aid in the interpretation of the reported results. Firstly, the assessment of the incorporation of labelled precursors relies on enumerating the radioactivity retained in macromolecular components of the bacterial cell, and this was achieved by a precipitation step with ice-cold 10% trichloroacetic acid (TCA), which is commonly employed to precipitate protein, RNA, and DNA for analytical purposes.[441] The acid-insoluble material is collected on glass-fibre filters and washed extensively to remove unincorporated, radioactively labelled building blocks as well as other non-macromolecular radioactive contaminants that might have arisen during metabolism of the label. After drying, radioactivity is quantified in a liquid scintillation counter, with a scintillation cocktail designed for organic samples that does not dissolve the precipitate.[442, 443] That this was indeed the case has been verified by repeating the scintillation measurements on consecutive days, which always led to identical count rates.

For both the continuous labelling, as well as pulse-labelling approach, *P. aeruginosa* PAO1 cultures were grown to an optical density ($OD_{600\ nm}$) of 0.2, which corresponded to ~$1x10^8$ CFU/mL as determined by viable cell counts, to ensure exponential growth throughout the experiments (c.f. **Section 3.3**). In continuous labelling experiments, radioactive label was added to give a final activity of 37 kBq/mL (1 μCi/mL) and the bacterial suspension was grown for a further 15 to 20 minutes before being split into aliquots to which the test compounds were added; this

was done to ensure bacterial cultures with identical activity. At regular time intervals, samples were withdrawn, precipitated and quantified as described above. For pulse-labelling experiments, the starting culture was split into cultures to which test compounds were added, and from these cultures samples were taken at regular time intervals and added to medium containing 37 kBq/mL (1 μCi/mL) of the radio-labelled precursor. Additionally, this medium contained an appropriate concentration of the test compound. After incubation at standard conditions for four to ten minutes, the samples were processed as described above.

Experiments were carried out at and above the MIC of the test compounds, and the MICs were those determined for the higher inoculum (c.f. **Section 2.5**). The use of a higher inoculum in the incorporation experiments was required to achieve reasonable count rates, especially for the experiments directed towards protein biosynthesis. Due to the experimental error in determining the exact MIC value, most experiments were carried out above the MIC, typically at 5×MIC. This value was chosen to minimise potential membrane-lytic activities of the AMPMs that might occur at higher concentrations (vide supra).

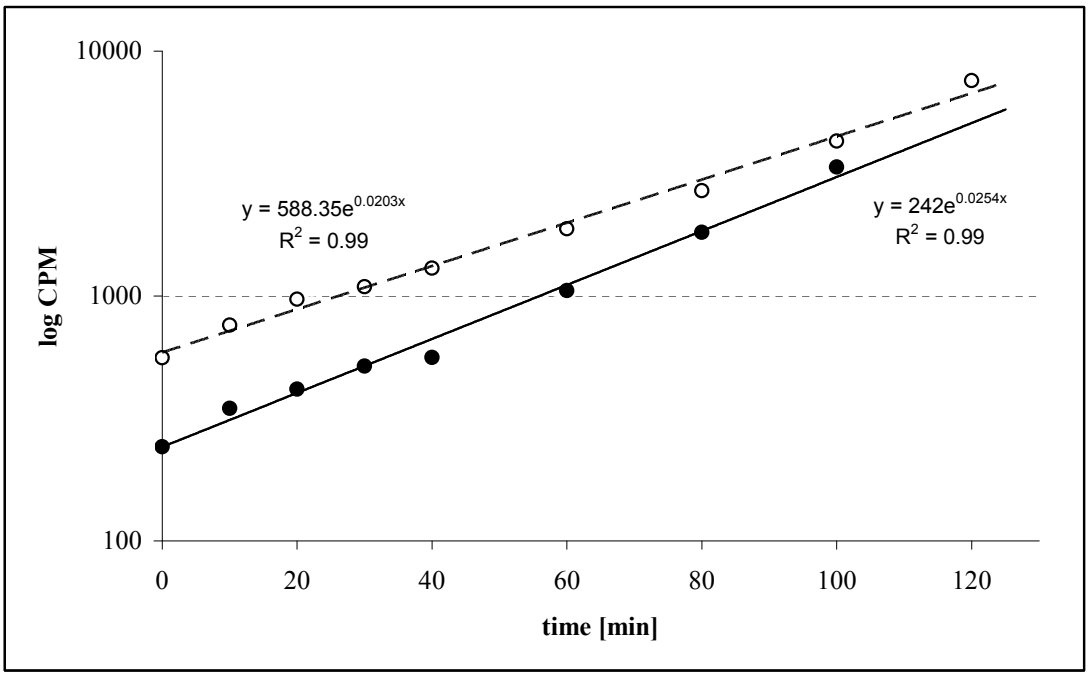

Figure 3.32 Exponential growth of *P. aeruginosa* PAO1 in the time interval during which incorporation experiments were carried out. (●): Incorporation of L-[4,5-^{3}H]-leucine (**30**) via continuous labelling; (○): incorporation of [5,6-^{3}H]-uridine (**31**) via pulse-labelling.

For comparison with other experiments, such as the killing kinetics of our AMPM, it was important to ensure that the bacterial cultures were in an exponential growth phase (vide supra). An example of the exponential growth under the experimental conditions of the incorporation experiments and representative examples of both continuous and pulse-labelling are shown in **Figure 3.32**. From these examples, the calculated generation time is about 30 minutes ± 3 minutes, which is in good agreement with the value obtained by other methods such as turbidimetry (30 minutes).

3.6.3 Protein Biosynthesis

Protein biosynthesis in *P. aeruginosa* PAO1 was studied with *L*-[4,5-^{3}H]-leucine (**30**) by the continuous labelling approach. **30** is often chosen for studying protein biosynthesis, because it does not serve as a precursor for the synthesis of other macromolecular building blocks such as aspartic acid. Pulse-labelling with **30** could not be carried out, since under the experimental conditions, the achievable count rate was too low to give meaningful results. An experiment on the effect of mimetic-**17** on protein biosynthesis is reproduced in **Figure 3.33**. As can be seen, the incorporation of **30** into the acid-insoluble fraction of *P. aeruginosa* PAO1 stopped markedly slower than for the positive control tobramycin (**25**).

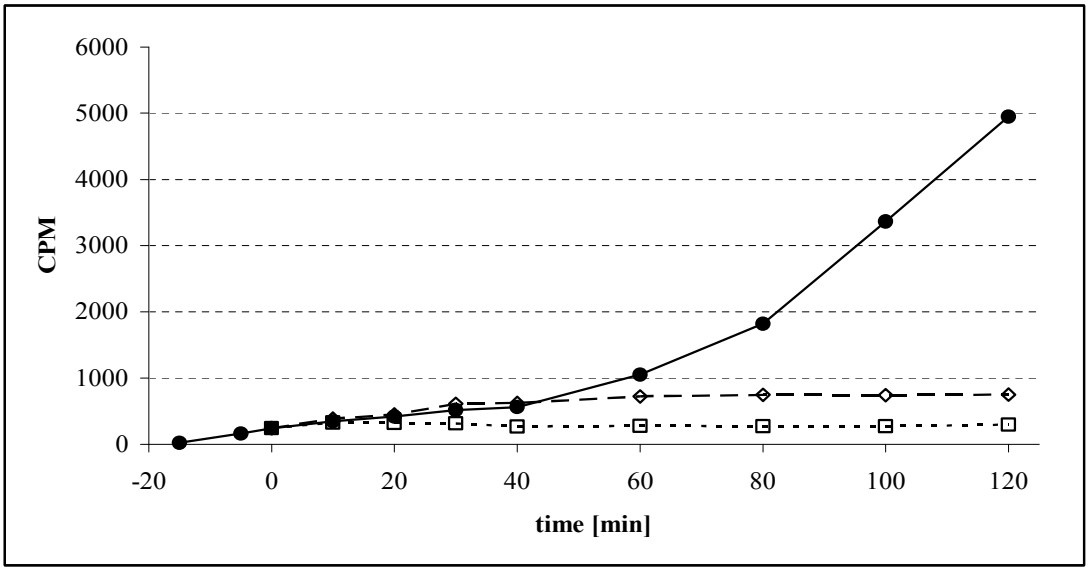

Figure 3.33 Incorporation of L-[4,5-^{3}H]-leucine (**26**) into the acid-insoluble fraction of *P. aeruginosa* PAO1; (●): control, (◊): 5×MIC mimetic **17**, (□): 5×MIC tobramycin (**25**)

Inhibition of incorporation of **30** by tobramycin set in immediately, whereas a comparable effect for mimetic-**17** is visible only about 40 minutes after its addition. This time delay corresponds roughly to a typical generation time of *P. aeruginosa* PAO1 under the experimental conditions of the incorporation assay (vide supra). As shown in **Figure 3.34**, an analogous result was obtained for mimetic **18**. Analogously, the reduction of incorporated radioactivity only set in significantly about 40 minutes after induction with **18**. The results of several experiments on protein biosynthesis are summarized in **Figure 3.35**, in which CPM obtained relative to the control, i.e. the labelled bacterial suspension without added antimicrobial compound, are plotted against time, to allow comparison of the data from different experiments.

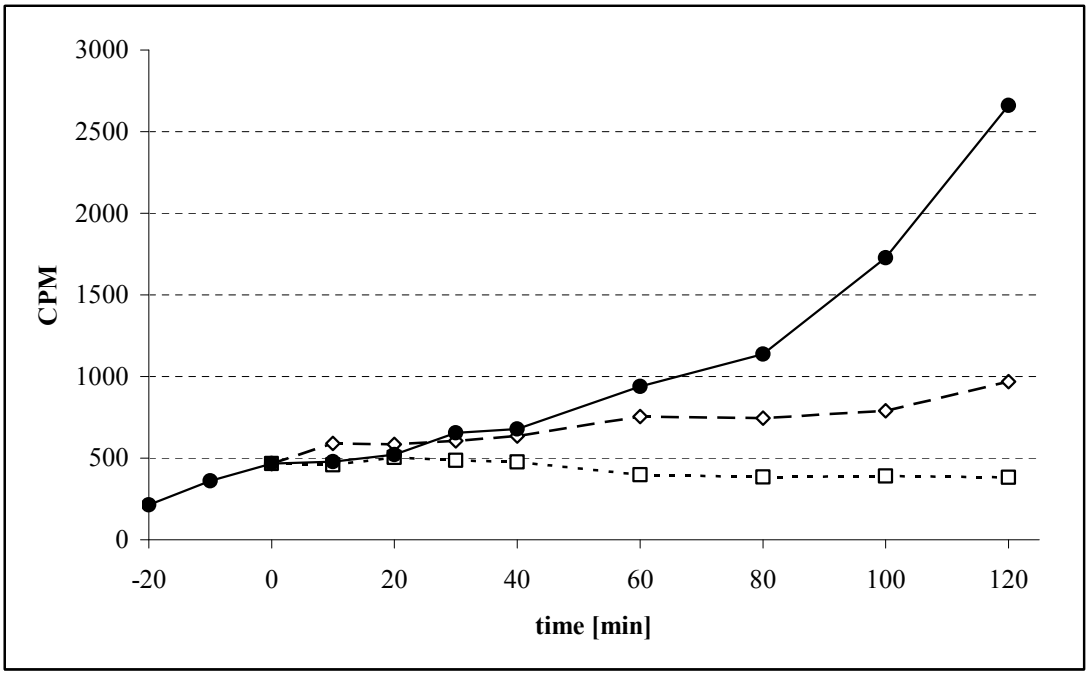

Figure 3.34 Incorporation of *L*-[4,5-^{3}H]leucine into the acid-insoluble fraction of *P. aeruginosa* PAO1; (●): control, no added compound; (◊): 5×MIC mimetic **18**; (□):5×MIC tobramycin (**25**)

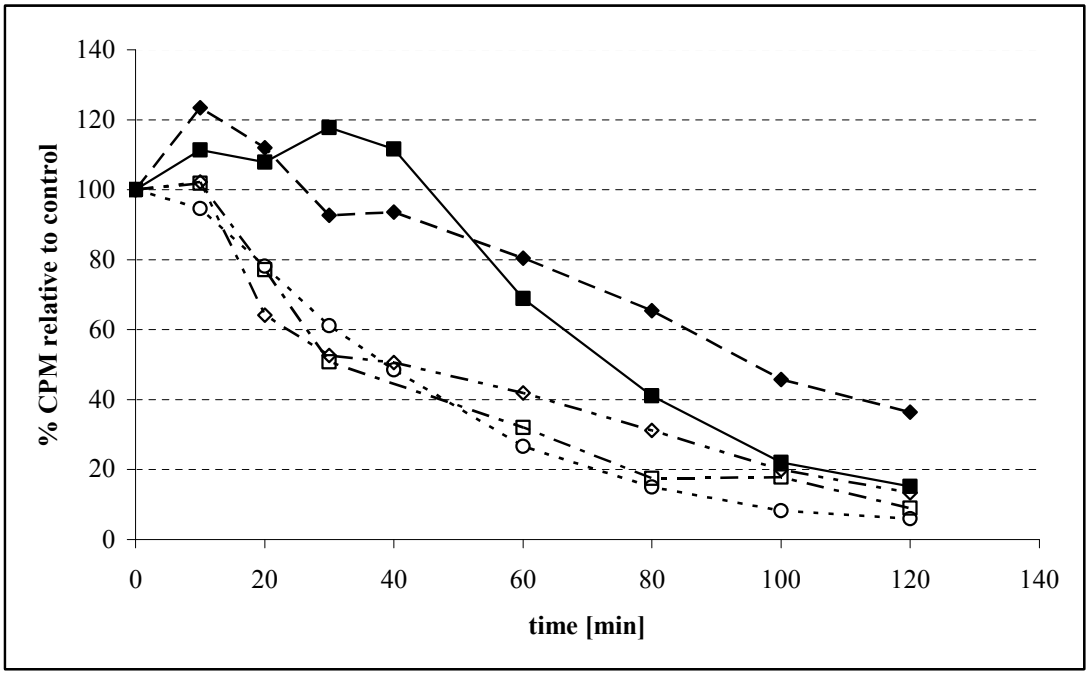

Figure 3.35 Summary of the Incorporation of *L*-[4,5-^{3}H]-leucine into the acid-insoluble fraction of *P. aeruginosa* PAO1 induced with various antimicrobial agents; (○): 5×MIC tobramycin; (◊): 5×MIC protegrin-1 (**11**); (□): 5×MIC mimetic-**16**; (♦): 5×MIC mimetic **18**; (■): 5×MIC mimetic **17**.

Clearly, fundamental differences are visible from examination of **Figure 3.35**, and the test compounds can be divided into two different classes. Protegrin-1 (**11**) and tobramycin (**25**), as well as mimetic **16,** show a faster onset of their inhibitory action on the incorporation of the radio-labelled leucine compared to both mimetics **17** and **18**. The time difference between these two couples, i.e. where the CPM relative to the control drop markedly below the 100 % level, is found to be about 30 minutes, which correlates well with the observed generation time under the experimental setup. It is noteworthy that **16** shows behaviour analogous to **11** and **25**. The fast inhibition of protein biosynthesis by tobramycin (**25**) is explicable by its mode of action, and attests its utility as a positive control for studying protein biosynthesis. Accordingly, the fast inhibition of incorporation of radio-labelled **30** by the AMP protegrin-1 (**11**) is also explicable by its mode of action. This agent has been repeatedly shown to rapidly kill susceptible organisms by a membrane-lytic mechanism, which implies immediate cessation of macromolecular biosynthesis. In view of these considerations, the results for mimetics-**17** and -**18** do not point towards a mode of action primarily affecting protein biosynthesis.

3.6.4 RNA biosynthesis

The effects of mimetic-**18** on RNA biosynthesis were studied using both continuous labelling and pulse-labelling approaches with [5,6-^{3}H]-uridine (**31**) as the labelled precursor molecule. Because of its unique occurrence in RNA, **31** is the precursor of choice for the study of RNA biosynthesis. The results of an experiment employing **18** and several control antibiotics are shown in **Figure 3.36**. As can be seen, the incorporation of the labelled precursor stops immediately after addition of the positive test antibiotic, rifampicin (**2**). In contrast, no inhibitory effect is seen upon addition of **18**, indeed there was even an apparent increase in the incorporation of the radioactive label. As was to be expected, the two other control antibiotics included in **Figure 3.36** showed a significantly later effect on the incorporation of **31** as compared to rifampicin (**2**). That is, a significant reduction in the incorporation of radioactivity becomes apparent only about one hour after the addition of these antibiotics. Such behaviour is not surprising, since after two generation times a substantial reduction of the viable cell count, compared to the control sample, is to be expected, thus leading to a concomitant decrease in incorporated radioactivity.

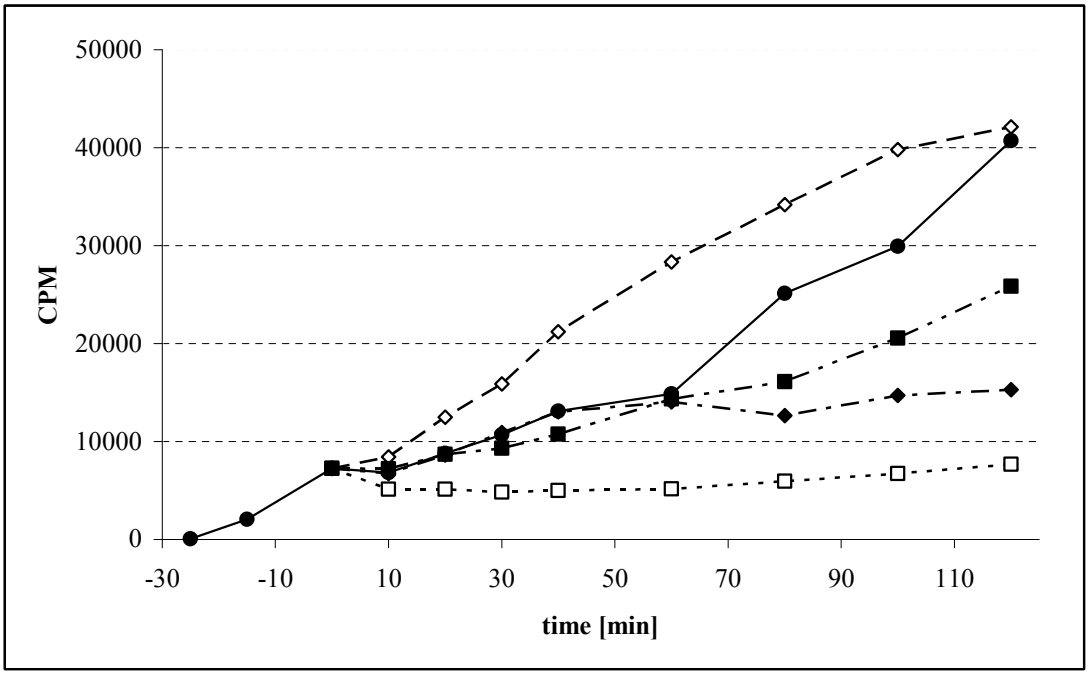

Figure 3.36 Incorporation of [5,6-^{3}H]-uridine into the acid-insoluble fraction of *P. aeruginosa* PAO1; (●): control; (◊): 5×MIC mimetic **18**; (□): 5×MIC rifampicin (**2**); (■):5×MIC ciprofloxacin (**7**); (♦):5×MIC tobramycin (**25**).

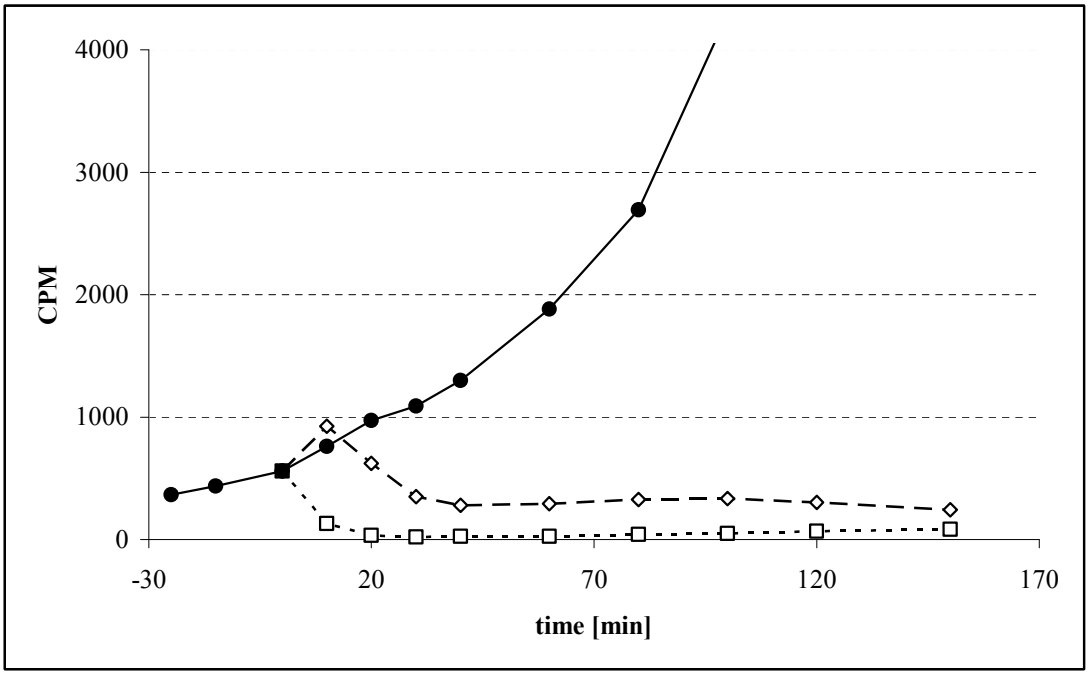

Figure 3.37 Pulse-labelling of *P. aeruginosa* PAO1 with [5,6-^{3}H]-uridine; (●): control; (◊): 5×MIC mimetic-**18**; (□): 5×MIC rifampicin (**2**).

The results of a pulse-labelling experiment with mimetic-**18** at 5×MIC and rifampicin (**2**) are shown in **Figure 3.37**. As can be seen, the incorporation of the labelled precursor is halted immediately by **2** as to be expected from its mode of action. In contrast, inhibition by **18** is slower, and the reduction in radioactive counts does not approach background level, as was the case for rifampicin (**2**). For mimetic **18**, the amount of incorporated radioactivity decreases to about half its original value within 30 minutes after addition of the AMPM and stays at about this level throughout the rest of the experiment. This reduction in labelling parallels the reduction in the viable cell count, and indicates that RNA biosynthesis continues without significant inhibition in the fraction of viable bacterial cells. Therefore, inhibition of RNA biosynthesis in *P. aeruginosa* PAO1 is unlikely to be the cause of the activity of our AMPMs.

3.6.5 DNA biosynthesis

The first approach towards studying DNA biosynthesis in *P. aeruginosa* PAO1 induced with AMPMs consisted of incorporation experiments with [methyl-^{3}H]-thymidine (**32**) as the radioactive precursor by continuous labelling. In fact, **32** is commonly used in incorporation experiments directed towards DNA synthesis

because of the absence of thymidine from RNA. Although there is literature precedence for the use of a radio-labelled thymidine in studying the synthesis of DNA in a *Pseudomonas* species, experiments employing **32** as labelled precursor were unsuccessful. In such experiments, only very low count rates, below 100 CPM, with no discernible patterns were observed.

This inability to follow incorporation of **32** into the acid-insoluble fraction of *P. aeruginosa* might be explicable in the light of the study by Gottfreddson et al, who reported on the inability of *P. aeruginosa* to incorporate labelled thymidine.[444] The reason for this was argued to stem from the absence of a salvation pathway in *P. aeruginosa* for the synthesis of TTP. Therefore, DNA biosynthesis was studied by the incorporation of [8-^{3}H]-adenine (**33**) into the acid-insoluble fraction. Because of the occurrence of adenine in both RNA and DNA, the general protocol had to be modified. A digestion step was introduced before the TCA precipitation, in which the sample is treated overnight with 0.3M NaOH and 0.1% EDTA.[444] Continuous labelling of bacterial DNA was not possible since the uptake of the labelled precursor was too efficient under the experimental setup. Typically, all of the radiolabel had already been incorporated before the addition of the test compound(s), and no further increase in CPM after this 15 to 20 minutes period was observed.

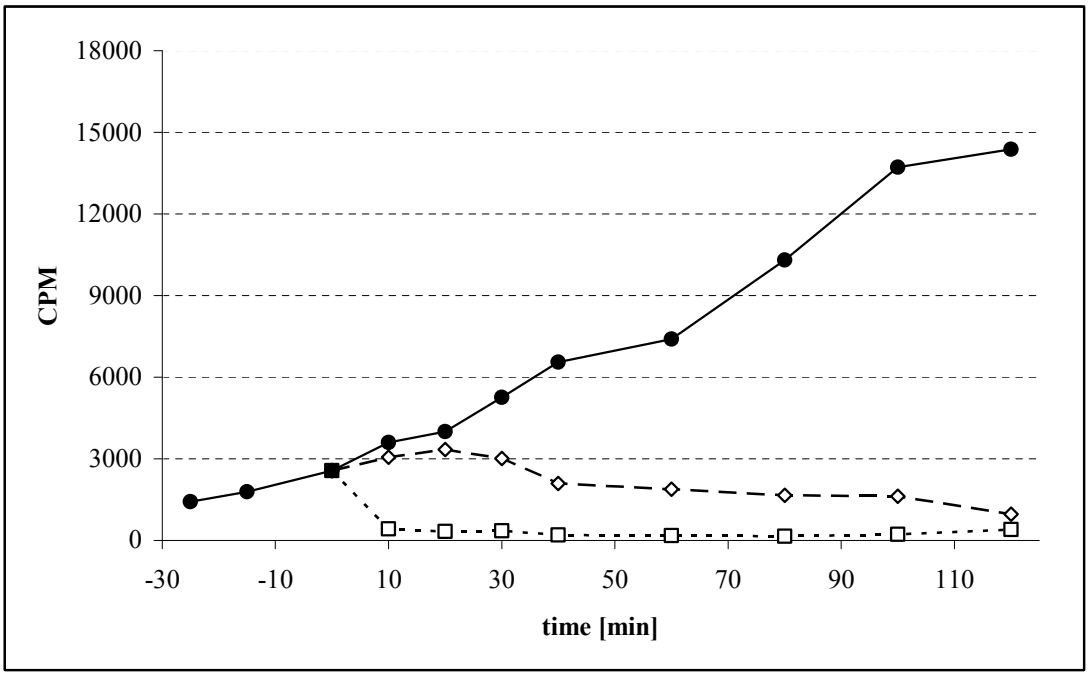

Figure 3.38 Pulse-labelling of *P. aeruginosa* PAO1 with [8-^{3}H]-adenine; (●): control; (◊): 5×MIC mimetic **18**; (□): 5×MIC ciprofloxacin (**7**).

Therefore, the biosynthesis of DNA in *P. aeruginosa* PAO1 was studied by the pulse-labelling approach. An example of a pulse-labelling experiment with mimetic **18** and the control antibiotic ciprofloxacin (**7**) is shown in **Figure 3.38**. As to be expected from its mode of action, ciprofloxacin (**7**) immediately stopped the incorporation of the labelled precursor into the acid-insoluble fraction of *P. aeruginosa*. Already at the first time point, the detectable amount of radioactivity was reduced to less than 500 CPM, at which value it remained throughout the experiment. In contrast, the incorporation of the label following addition of mimetic-**18** increased slightly from the level observed at the addition of **18**. The incorporation of radioactive marker starts to decrease slowly around 40 minutes after addition of **18** and stays above the level observed for the positive control throughout the experiment. Again, the pattern of the slow decrease in measured radioactivity incorporated into the acid-insoluble fraction is explicable by the bacteriostatic effect of **18** alone, and does not point towards a direct influence of **18** on pseudomonal DNA synthesis. That this statement is justified can be seen from **Figure 3.39** which illustrates an experiment conducted with tobramycin (**25**) and protegrin-1 (**11**). Analogously to **18**, the reduction of incorporated radioactivity by tobramycin (**25**) shows a slow onset, as to be expected from its primary action on protein biosynthesis. The stronger inhibition after 40 minutes is also in agreement with the beginning of dose-dependent bactericidal behaviour, which is often encountered for aminoglycosides.[445]

The immediate effect of protegrin-1 (**11**) on DNA synthesis is apparent from **Figure 3.39** and is once again another manifestation of its membrane-lytic behaviour. A comparison of several pulse-labelling experiments is shown in **Figure 3.40** wherein the obtained CPMs relative to the untreated control of each experiment are plotted against time.

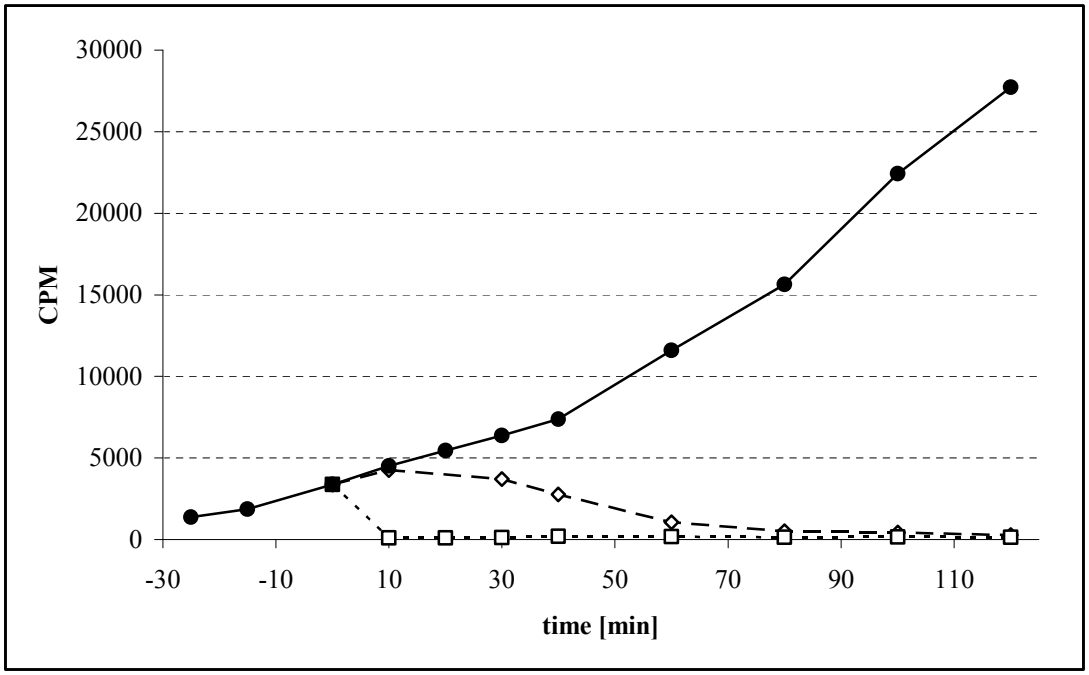

Figure 3.39 Pulse-labelling of *P. aeruginosa* PAO1 with [8-^{3}H]-adenine; (●): control; (◊): 5×MIC tobramycin (**25**); (□): 5×MIC protegrin-1 (**11**).

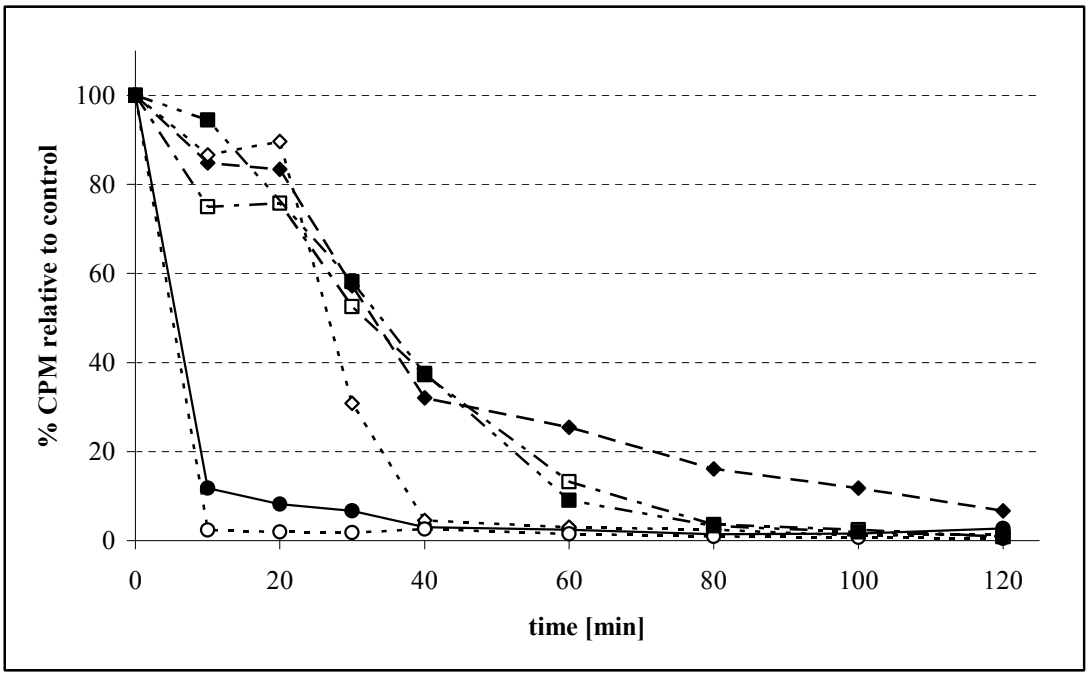

Figure 3.40 Comparison of various pulse-labelling experiments with [8-^{3}H]-adenine on *P. aeruginosa* PAO1; (●): 5×MIC ciprofloxacin (**7**); (○): 5×MIC protegrin-1 (**11**); (■):5×MIC tobramycin (**25**); (□): 5×MIC rifampicin (**2**); (♦): 5×MIC mimetic **18**; (◊): 5×MIC mimetic **17**.

Apparently, the tested compounds can be grouped into two different classes. The first class is formed by the positive control (**7**) and the membrane-lytic protegrin-1 (**11**), whereas the second class is made up of control antibiotics, which possess

modes of action that do not directly inhibit DNA biosynthesis (**2** and **25**), and the two AMPMs **17** and **18**. It is instructive to compare the effects of **17** and **18** directly. The reduction in the observed CPM after 40 minutes is more pronounced for **17** (c.f. **Figure 3.40**), but that this is in agreement with the reduction of viable cells still capable of DNA synthesis can be seen from the correlation of the trends in the kinetics of bacterial killing with the incorporation of radioactive label, as shown in **Figure 3.41**.

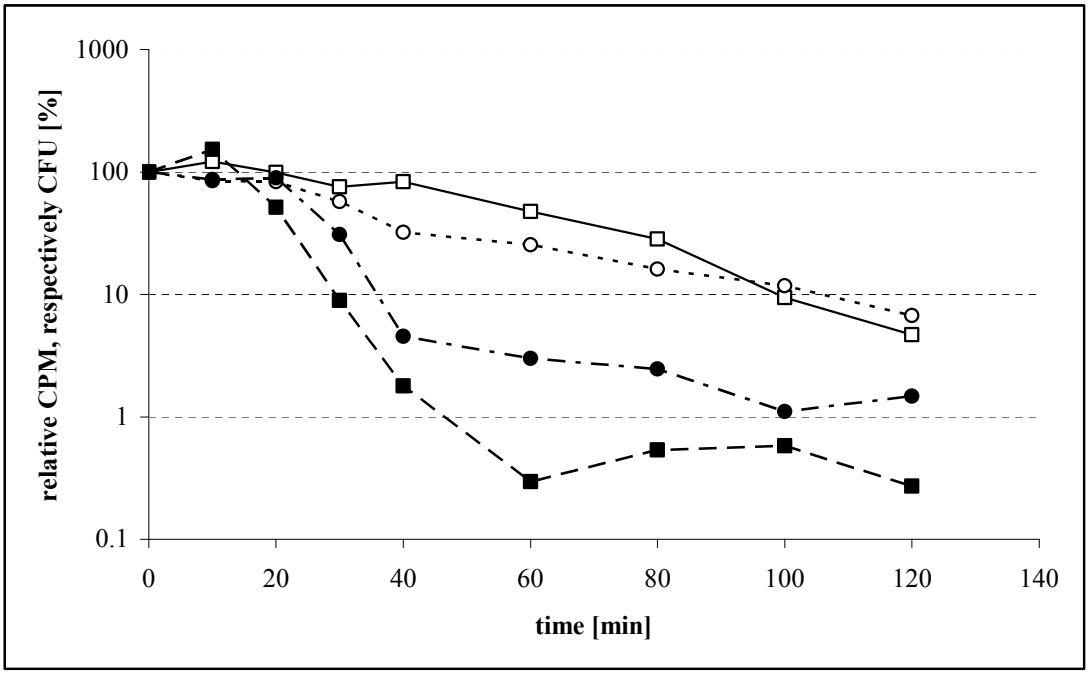

Figure 3.41 Comparison of the decrease in CPM and the decrease in viable cell count [CFU/mL] relative to the control for **17** and **18**; (●): 5×MIC mimetic-**17**, CPM; (■): 5×MIC mimetic-**17**, CFU; (○): 5×MIC mimetic-**18**, CPM; (□): 5×MIC mimetic **18**, CFU.

3.6.6 Peptidoglycan Biosynthesis

Attempts were made to study the biosynthesis of pseudomonal peptidoglycan with acetyl-*D*-[1-^{3}H]-glucosamine (**34**) as radioactively labelled precursor and aztreonam (**35**) as positive control antibiotic. Although comparable approaches have been used, for example, in studying peptidoglycan synthesis in *B. licheniformis*,[446] or the mode of action of pesticin, a bacteriocin produce by *Y. pestis*, in *E. coli*,[447] preliminary incorporation experiments were unsuccessful. Incorporation of radioactivity was unaffected by either mimetic **18** or the positive control antibiotic **35**. Additionally, low count rates were observed, which might have been caused by

metabolism of the labelled nutrient. Since experiments in media with added alternative carbon sources such as glycerol and D-glucose were also unsuccessful, the experiments on peptidoglycan biosynthesis were discontinued.

3.6.7 Conclusions

Summarizing the experimental data, it can be concluded that neither mimetic **17** nor mimetic **18** primarily interfere with protein, RNA, or DNA biosynthesis in *P. aeruginosa* PAO1. Clear differences between the behaviour of these AMPMs and the positive control antibiotics employed were always observed. An inhibitory effect for the AMPMs only became pronounced after about 40 minutes subsequent to their addition, thus correlating with their bacteriostatic effects on *P. aeruginosa* during the experiments. The incorporation experiments further support the notion of a mode of action for this class of AMPMs that is not membrane-lytic, and that does not depend on impairment of membrane functions necessary for macromolecular biosynthesis. This becomes evident if one considers that the expected outcome of such mechanisms is the immediate and simultaneous cessation of macromolecular biosynthesis, of which examples can be found in the literature. AMPs for which such behaviour has been demonstrated include bactenecins,[448] HNP-1,[145] and PR-39[243] (in my opinion, c.f. **Section 2.2**). This also parallels the behaviour of membrane-lytic lantibiotics, such as pep-5[449] and aureocin A53.[450]

3.7 Interaction of AMPMs with lipopolysaccharides

The interactions of several AMPs with bacterial lipopolysaccharides (LPS) have been studied regarding their effect on the direct antimicrobial activity and on the immuno-modulatory functions of this class of compounds.[451] With respect to the direct antimicrobial activity of AMP(M)s, lipopolysaccharides are mostly thought to be involved in selectivity issues (differentiation between mammalian and bacterial organisms as well as between different bacterial organisms/species), and to confer bacterial resistance against AMPs via alteration in their structures. Both of these aspects are linked to the major function of LPS as a permeability barrier in Gram-negative bacteria. The role of LPS in the immuno-modulatory properties of AMPs, on the other hand, is related to the recognition of LPS by the host innate immune system; a process which could be impaired by AMP(M)s via their direct binding to LPS, by their competition with LPS for its innate immune system receptor(-complex), or by their affecting the aggregation state of LPS oligomers.[451] Irrespective of which mode of action dominates in a given case (i.e. either direct antimicrobial or immuno-modulatory), or even if they both operate simultaneously, the interaction of AMP(M)s with bacterial LPS is an important aspect of their antimicrobial activity towards Gram-negative organisms.

Therefore, this peptide-LPS interaction was studied for our AMPMs, employing a dansyl-polymyxin B displacement assay developed by Hancock et al.[452] Additionally, three hairpin mimetics derived from a naturally occurring LPS binding motif, and based on the D-Pro-L-Pro template, were synthesised and tested for their ability to bind to LPS. With respect to our AMPMs it was also of special interest to determine whether the remarkable selectivity towards *P. aeruginosa* could be correlated with their interaction with LPS.

3.7.1 Structure and function of bacterial lipopolysaccharides

Lipopolysaccharides are an essential component of the outer membrane of virtually all Gram-negative bacterial organisms.[453] As depicted in **Figure 3.42**, LPS is generally thought to be localized asymmetrically to the outer membrane's outer leaflet,[454] and this renders LPS the major surface component of Gram-negative bacterial cell envelopes. It should be noted, however, that at least for *Vibrio cholerae,*

phospholipids have been shown to be present in the outer leaflet, and this has been associated with the increased sensitivity of this organism towards hydrophobic compounds. [455] Lipopolysaccharides are amphipathic molecules that are evolutionarily conserved components of Gram-negative organisms, but nevertheless different bacterial genera, species, and even strains can display large variations in their structure. The general architecture of LPS comprises three distinct subunits: the hydrophobic lipid A domain, a core oligosaccharide, and an O-antigen polysaccharide repeat region (**Figure 3.37**).

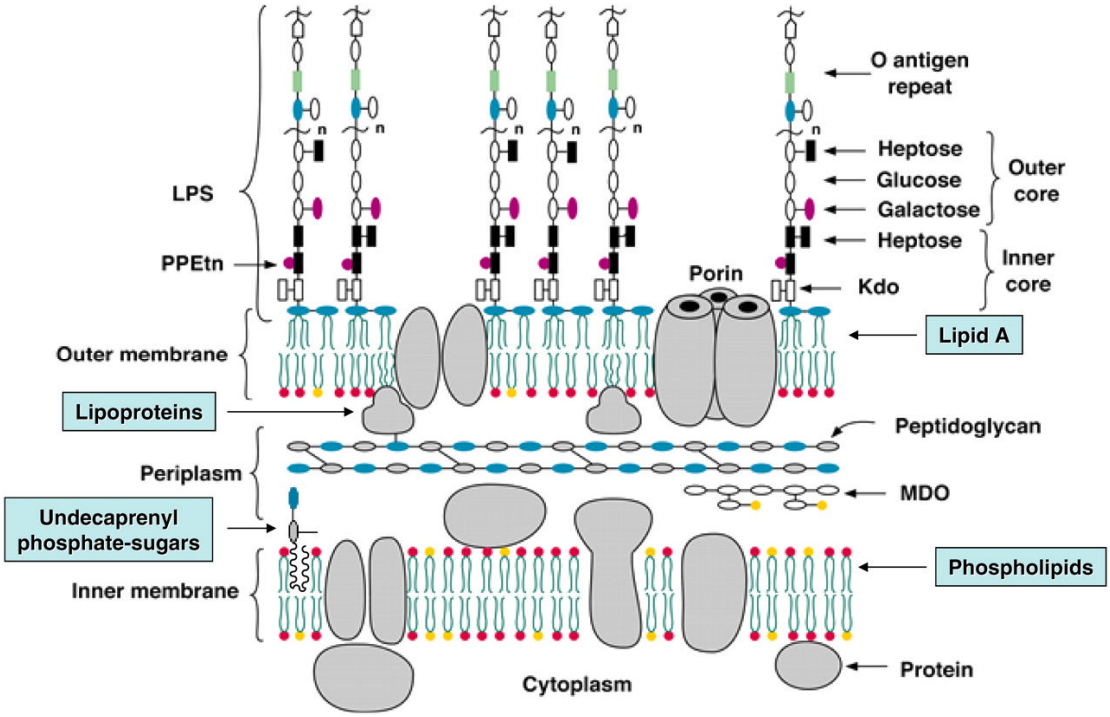

Figure 3.42 Schematic representation of the Gram-negative cell wall of *E. coli* K-12. Kdo = (3-deoxy-D-*manno*-oct-2-ulosonic acid); PPEtN = pyrophosphorylethanolamine; MDO = membrane-derived oligosaccharides. Note that in this case the outer leaflet on the bacterial surface is solely composed of LPS.

Lipid A (endotoxin) consists of a phosphorylated *N*-acetylglucosamine (NAG) dimer to which saturated fatty acids are attached (**Figure 3.43**), and functions as a lipophilic anchor for attachment of LPS to the bacterial surface. The innate immune system's response towards a bacterial infection depends upon the recognition of evolutionarily conserved patterns that are unique to the certain classes of pathogens,[456] and lipid A functions as such a pattern, which is recognised by the TLR-4 receptor (toll like receptor) during infection in higher organisms. Therefore,

lipopolysaccharides are powerful modulators of the immune system in an infected host; uncontrolled or prolonged exposure to LPS can lead to the severe pathological condition of endotoxic (septic) shock, which is associated with a high mortality rate. Despite the role of lipid A as a conserved recognition pattern of the innate immune defence, large structural variations exist between different organisms in the amount, length, and structure of attached fatty acid chains (**Figure 3.43**), and this can have a profound influence on the recognition of these molecules by the TLR-4 receptor complex.[457]

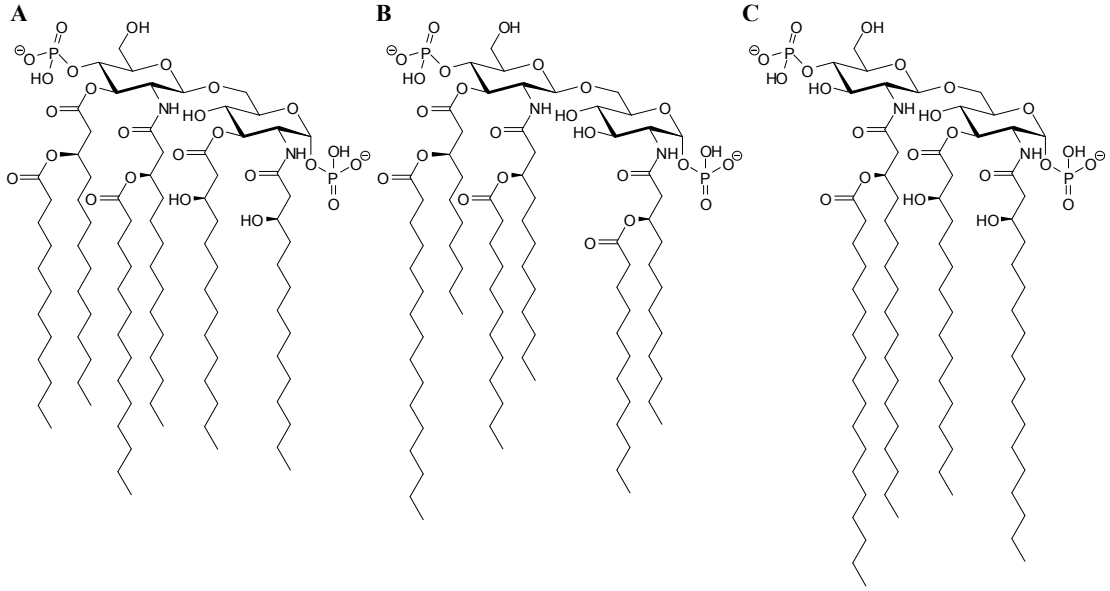

Figure 3.43 Structural diversity of lipid A from three different Gram-negative organisms. (**A**) *E. coli*; (**B**) *P. aeruginosa*; (**C**) *H. pylori*.

The core polysaccharide (also called core antigen) contains a short chain of hexose and heptose sugars (**Figure 3.44**). There are only minor variations of the core polysaccharide within a genus, but different species can show pronounced differences.[453] The core oligosaccharides are generally divided into an inner core region (close to lipid A) and an outer core region (close to the O-antigen) (c.f. **Figure 3.42**). A particular feature of the inner core region is the presence of L-glycero-D-mannoheptose (2-keto-3-deoxyoctonic acid; KDO) residues which are extended by heptose residues, the latter of which can be either phosphorylated, or modified with phosphoethanolamine or pyrophosphoethanolamine (PPEtn) substituents.

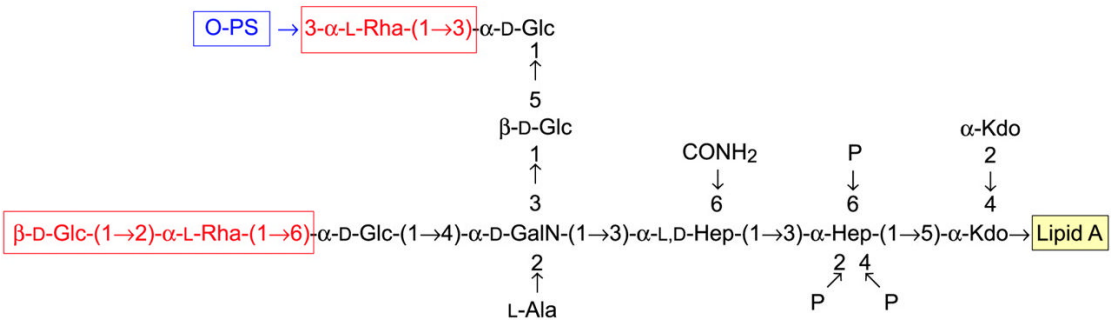

Figure 3.44 Structure of the core oligosaccharide of *P. aeruginosa* O5. The attachment points of lipid A and the O-polysaccharide are indicated. Rha = rhamnose; Hep = glycero-mannoheptose. The sugar moieties marked in red and the O-polysaccharide chain are missing in R-type LPS.

Finally, the O-polysaccharide (also called O-antigen) consists of repeating oligosaccharide (3 to 5 sugars) subunits. An individual chain can consist of up to 40 repeat units and these chains are the dominant surface antigens of LPS.[453] Because of the large amount of available monomeric units (over 60 different sugar moieties and more than 30 different non-sugar building blocks), this structure shows remarkable diversity and determines the serological specificity in an organism.[458]

3.7.2 LPS-binding mimetics

Mimetics that are able to bind to bacterial LPS are attractive from at least two different points of view. Firstly, binding to LPS might protect from severe complications related to Gram-negative bacterial infections, such as endotoxic shock (vide supra) and secondly, such mimetics could be useful antimicrobial compounds in their own right, especially against Gram-negative organisms.

Several proteins are known to interact with LPS, and amongst these the most well characterised are the lipopolysaccharide binding protein (LBP),[459] the bactericidal/permeability increasing protein (BPI),[460] and the *Limulus* anti-LPS factor (LALF).[461] Binding of these macromolecules to LPS can have different outcomes, that is, BPI and LALF exert a detoxifying effect on LPS, whereas LBP, which is a lipid transfer protein, can enhance LPS activity by facilitating binding of LPS to CD14 in the TLR-4 receptor complex.[462] Additionally, AMPs such as CAP-18,[463] LL-37,[464] buforin-2,[465] and indolicidin,[465] have been documented to bind to LPS

and to neutralise its biological effects. Therefore, AMP(M)s have been proposed to represent a promising starting point for the development of anti-LPS agents.[327]

Originating from experiments with domain exchanged hybrid proteins, it has been proposed that despite their partially different activities, LBP, BPI, and LALF share a similar LPS binding motif, in the form of a solvent-exposed loop structure.[466] Constrained peptides of this binding motif have been described as LPS-neutralising compounds,[467-470] and as Gram-negative selective AMPs.[327]

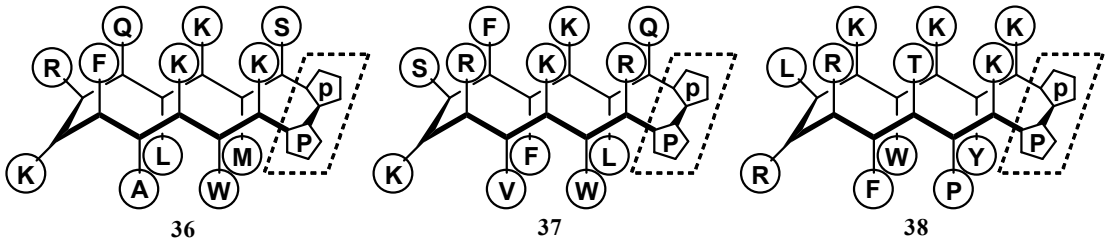

36 37 38

Figure 3.45 Schematic representation of LPS-binding hairpin mimetics of BPI (**36**), LBP (**37**), and LALF (**38**). The D-Pro-L-Pro template is indicated.

Based on the structure of the putative LPS binding loop of BPI/LBP/LALF,[461] three hairpin mimetics, incorporating the D-Pro-L-Pro structural template (**10**), were prepared in order to test the applicability of the peptidomimetic approach for the development of LPS-binding mimetics. The three mimetics, whose structures are depicted schematically in **Figure 3.45**, were synthesised according to our standard mixed solid phase/solution phase protocol (c.f. **Section 3.1**). All three mimetics proved to be inactive against our panel of microbial test organisms (c.f. **Section 3.3**) up to concentrations of 64 μg/mL.

3.7.2 Principle of the dansyl-polymyxin B displacement assay

The dansyl polymyxin displacement assay is based on the fact that the peptide antibiotic polymyxin B (**1**) and its mono-dansylated derivatives, bind to LPS.[471] Dansylated-polymyxin B fluoresces only weakly when excited at a wavelength of λ_{ex}=335 nm in aqueous solution. Upon binding to LPS, the fluorescence of dansyl-polymyxin is greatly enhanced,[471] and the emission maximum is shifted from λ_{em}(max)=520 nm to λ_{em}(max)=485 nm (**Figure 3.46**). The relative LPS-binding

affinity of a given test compound can then be evaluated on the basis of its ability to competitively displace dansyl polymyxin B from LPS.

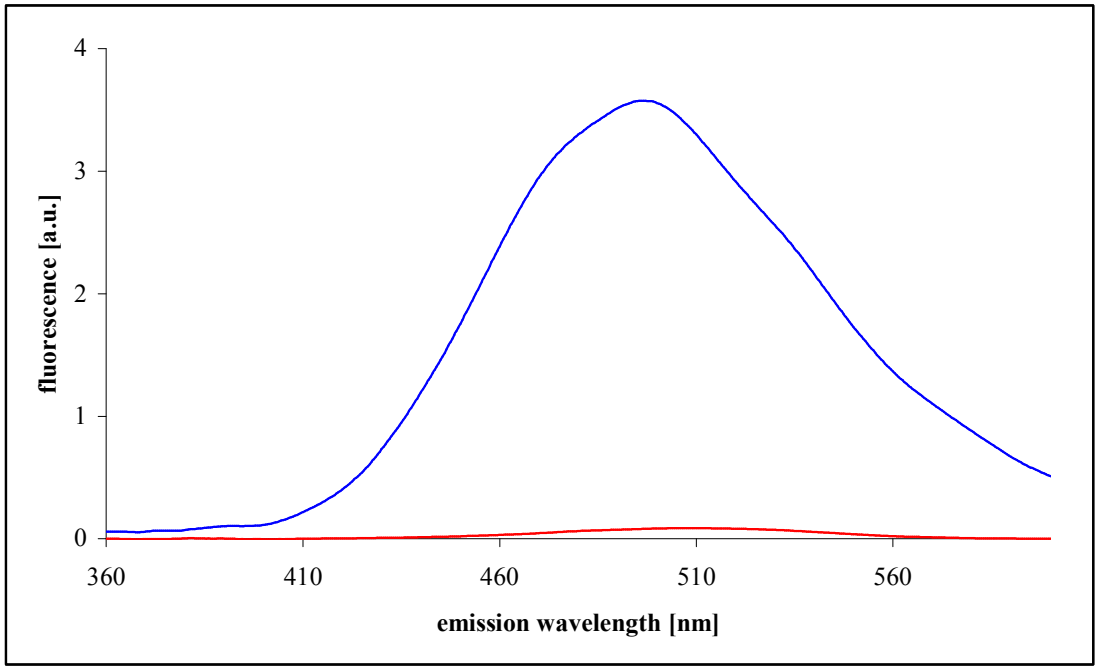

Figure 3.46 Enhancement of the fluorescence intensity of dansyl-polymyxin B upon binding to LPS. *Red curve*: 0.2 µg/mL dansyl-polymyxin B in 5 mM HEPES buffer, pH 7.2; λ_{ex}=335 nm. *Blue curve*: 0.2 µg/mL dansyl-polymyxin B together with 0.6 µg/mL of *E. coli* LPS in 5 mM HEPES buffer, pH 7.2; λ_{ex}=335 nm.

For the preparation of dansylated polymyxin B, polymyxin B sulfate was reacted with dansyl chloride, according to a published procedure.[472] As was to be expected, a mixture of mono-dansylated polymyxins, together with minor amounts of multiply substituted compounds was obtained. The crude mixture of dansylated regioisomers was purified by HPLC chromatography, but no attempts were made to isolate individual monosubstituted compounds. Therefore, the term dansyl-polymyxin B will be used to denote the mixture of monosubstituted polymyxins, and all experiments were carried out with dansyl-polymyxin B obtained from a single dansylation reaction. The concentration of dansyl-polymyxin B stock solutions was determined by a dinitrophenylation assay, as described in the literature.[473]

The dansyl-polymyxin B displacement assay was chosen because of its robust experimental setup, the availability of data on antimicrobial agents studied with this method,[160, 471, 474-476] and its potential for being implemented as a high throughput assay. Other methods for the study of LPS-binding interactions include the

chromogenic *Limulus* amoebocyte lysate (LAL) assay,[477] and the rabbit pyrogen test,[477] or surface plasmon resonance spectroscopy.[478]

3.7.3 Displacement assays with AMPMs and LPS-binding mimetics

To assess the LPS binding affinities of the three LPS-binding mimetics (**36-38**) as well as of the AMPMs **16**, **17**, **18**, **39** and **40**, dansyl-polymyxin B displacement assays were carried out with LPS from *E. coli* O111:B4 (**Table 3.10**) and *P. aeruginosa* Serotype 10 (**Table 3.11**).

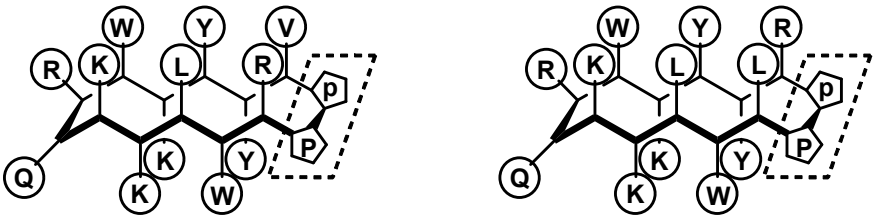

39 **40**

Figure 3.47 Mimetics **39** and **40**, derived from **17** by replacement of Arg-12 with Val-12 in **39**, and by replacement of Arg-1 with Leu-1 in **40**.

As controls, the AMP protegrin-1 (**11**), and the commercially available antibiotics polymyxin B (**1**) and gentamicin (**9**) were used (**Figure 3.48**). Additionally, Mg^{2+} ions were tested for their ability to displace the fluorescently labelled polymyxin from LPS, since cationic compounds have been suggested to permeabilise the outer membrane via displacement of these cations from LPS.[479]

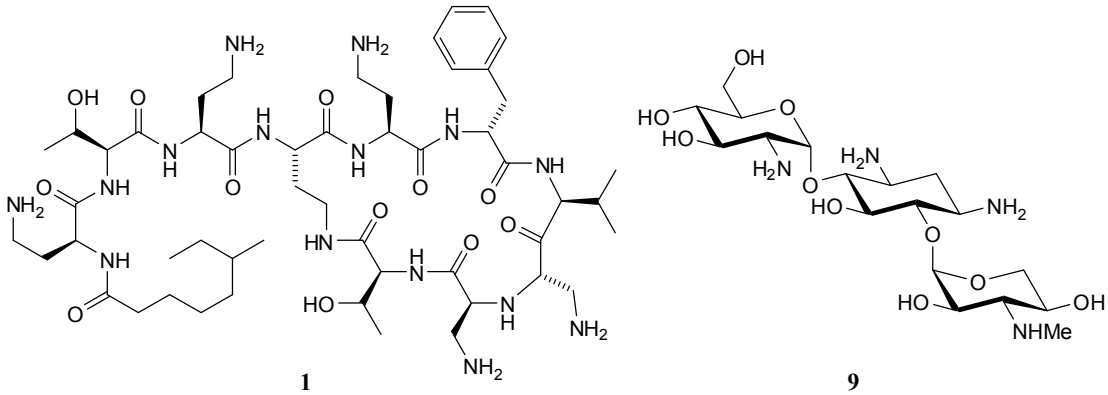

1 **9**

Figure 3.48 Polymyxin B (**1**) and gentamicin (**9**), two clinically used antibiotics employed as control compounds in the polymyxin B displacement assays. Note that both compounds are positively charged at physiological pH.

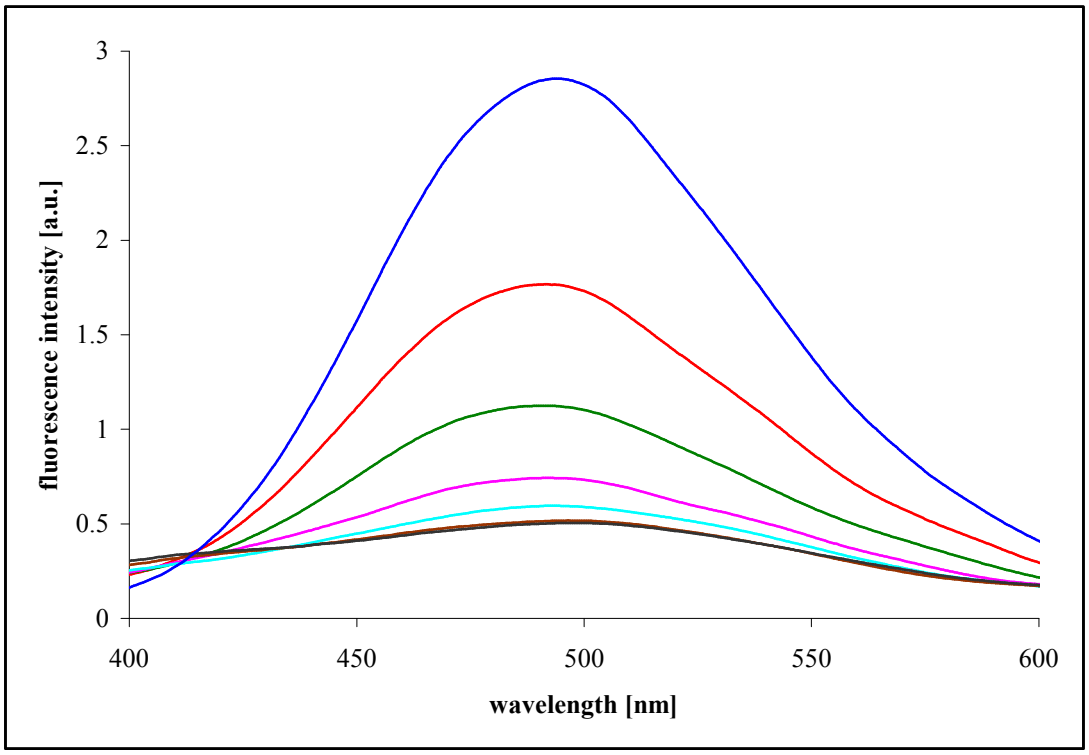

Figure 3.49 Representative example of a dansyl-polymyxin displacement experiment with 3 µg/mL of E. coli 055:B5 LPS and 2 µM dansyl polymyxin B in 5 mM HEPES buffer, pH 7.2; λ_{ex}=335 nm. For this experiment, increasing amounts of polymyxin B (**9**) were titrated to give concentrations of 0, 1, 3.5, 8.4, 15.7, 25.4, 39.8, 58.9, and 82.7 µM.

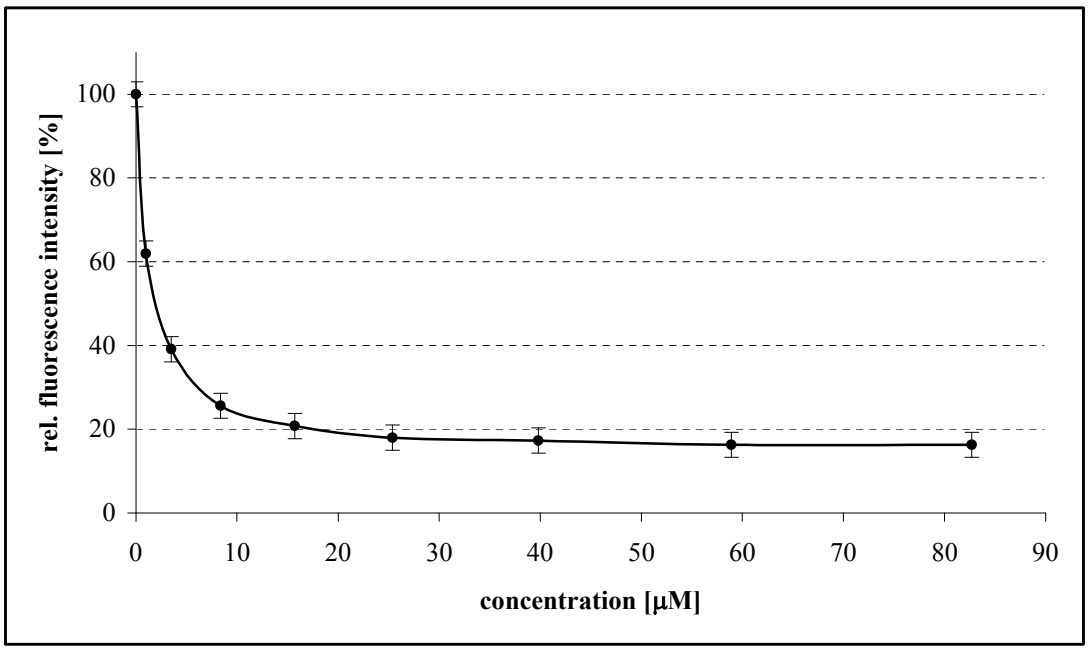

Figure 3.50 Decrease in the relative fluorescence intensity of dansylated polymyxin B for the experiment from **Figure 3.48**.

For the quantification of the LPS-binding affinities, the test compounds were titrated into cuvettes containing 3 μg/mL LPS and 2μM of dansyl polymyxin B (**Figures 3.49** and **3.50**). The maximum displacement (I_{max}) of dansylated polymyxin by a given test compound is calculated from the extrapolated ordinate intercept of a plot of the reciprocal of % inhibition as a function of the reciprocal of the inhibitor concentration (**Figure 3.51**). The I_{50} value (i.e. 50% displacement of labelled polymyxin at the LPS and dansyl-polymyxin concentrations used) is obtained from the extrapolated intercept of the double reciprocal plot with the abscissa, which furnishes the value for $-1/I_{50}$.

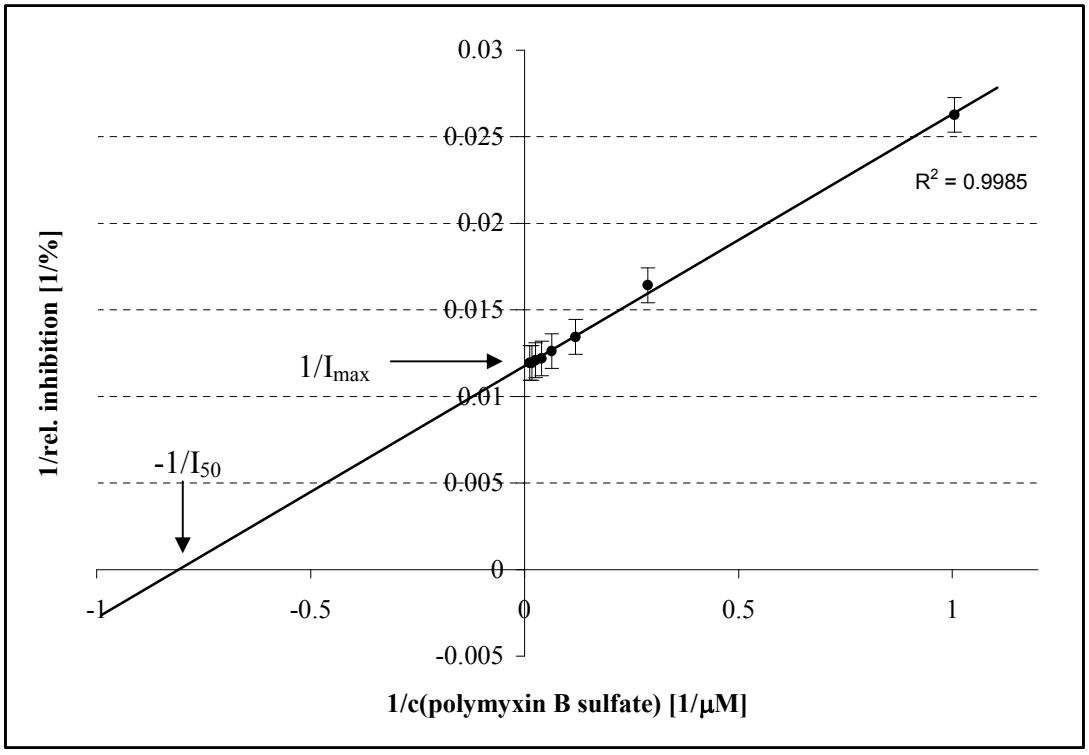

Figure 3.51 Double reciprocal plot of the inverse of relative inhibition vs. the inverse of concentration for the displacement experiment from **Figure 3.48**. The intercept of the extrapolated plot with the abscissa gives the value for $-1/I_{50}$.

As can be seen from **Table 3.10**, the tested compounds can be broadly categorized into two groups. Firstly, the controls gentamicin and magnesium show high IC_{50} values, concomitant with only about 50% of maximal displacement. The second group, which contains the synthesised LPS-binding mimetics as well as the AMP(M)s and polymyxin B all possess comparable I_{50} values in the low micromolar range, albeit with variations in their maximal displacement values. It can also be

observed that for the peptidic compounds, the I_{50} values correlate well with the overall positive charge of these molecules (estimated at physiological pH). Compounds with a charge of +5, for instance, display I_{50} values between 1.2 and 7.1 μM. The value of 1.2 μM for polymyxin B sulphate (**9**) is somewhat lower than for the peptidomimetics, but it has to be borne in mind that this compound is structurally different from the mimetics in that it carries a hydrophobic lipid moiety. Indeed, it has been found that polymyxin B nonapeptide possesses a lower ability to displace dansyl-polymyxin B than its parent compound.[471, 476] More precisely, Tsubery et al. determined I_{50} values of 2.5-3.0 μM for polymyxin B nonapeptide as compared to 0.5 μM for the parent compound. It is noteworthy that the I_{50} values reported in the literature for **1** of 0.5 μM,[476] and 2.2 μM,[471] are in good agreement with our obtained I_{50} values of 1.2 μM (*E. coli* LPS) and 1.8 μM (*P. aeruginosa* LPS).

Table 3.11 I_{50} and I_{max} values for LPS from *E. coli* 055:B5 obtained for $MgCl_2$, control antibiotics (**1** and **9**), LPS-binding mimetics (**36**-**38**), and AMP(M)s (**11**, **16**, **17**, **39**, and **41**).

Substance	I_{50} [μM]	I_{max} [%]	Charge[a]
$MgCl_2$	660	50	+2
9	240	49	+4
1	1.2	85	+5
36	7.1	91	+5
37	3.8	54	+5
39	3.8	54	+5
40	3.7	69	+5
ent-**17**	2.6	60	+6
17	2.4	81	+6
38	2.0	47	+6
16	0.5	74	+7
11	0.3	85	+7

[a] estimated for physiological pH

Table 3.11 I_{50} and I_{max} values for LPS from *P. aeruginosa* 10 obtained for AMP(M)s and for **1**.

Substance	I_{50} [μM]	I_{max} [%]
1	1.8	93
17	2.2	56
ent-**17**	2.5	68
18	1.1	75

From **Table 3.11** it can be seen that there were only marginal changes in the obtained I_{50} values for mimetics **17**, **18** and ent-**17**, as well as for polymyxin B (**1**), when testing LPS from *P. aeruginosa*. Most importantly, there was no significant difference in the displacement of labelled polymyxin by either mimetic **17** or its (antimicrobially) inactive enantiomer ent-**17**. AMPM **18** displayed the lowest I_{50} value of all compounds tested with pseudomonal LPS and again, this could be easily explicable by its increased charge of +7.

3.7.4 Conclusions

It has been argued that the interaction of AMPs with bacterial LPS is an important aspect of their selectivity towards these organisms.[451] On the other hand, the majority of AMPs are also active against Gram-positive bacteria (broad-spectrum activity), and from this point of view it seems likely that AMP-LPS interactions are not a particularly fundamental feature of AMP action. Gram-positive organisms display teichoic acids in their cell wall which, analogously to LPS, are recognised by the innate immune system. Of course, such molecules could play a role comparable to that of LPS in conferring selectivity of AMPs towards bacterial micro-organisms, but the question of how specific these interactions are on the molecular level is then immediately raised. That is, if interaction with negatively charged molecules on the surface of micro-organisms is conferring selectivity to the AMP action, then for broad-spectrum AMPs these interactions would have to involve structurally quite diverse molecules. Therefore, this rather points to an unspecific interaction that could for example be driven by electrostatic interactions between cationic AMPs and LPS, or teichoic acids, which could also be assisted by the eventual amphipathic properties of the AMPs. It has been mentioned already that the membranes of higher organisms also display a multitude of negatively charged molecules on their surface (c.f. **Section 1.4.2**), another aspect that disfavours LPS as the sole cause for AMP selectivity.

Along these lines, it has been found, for both our LPS-binding mimetics and our AMPMs, as well as for all tested compounds in general, that their ability to displace labelled polymyxin B from LPS is correlated well with the amount of positive charge that these molecules carry at physiological pH. The antimicrobial activity of protegrin-1 (**11**) has been suggested to be correlated with its ability to bind to the lipid A moiety of LPS.[480] It can be seen from our experiments, that although

11 possesses a low I_{50} value, this value is not unusually low as compared to the peptidomimetics, since **11** carries seven positive charges at physiological pH.

Of special importance is the affinity of **17** and ent-**17** towards pseudomonal LPS, since it has been found that this mimetic (and its later generation congeners) is especially active against a variety of pseudomonal species (c.f. **Section 3.3**). Therefore, it seems highly unlikely that interaction with LPS is a cause for the remarkable selectivity towards this organism. This notion is further corroborated by the findings that there are no significant differences in the affinities of mimetic-**17** towards both types of LPS, despite its antimicrobial selectivity towards *P. aeruginosa*. Interestingly, both polymyxin B nonapeptide and its enantiomer were reported to show identical I_{50} values in their interaction with LPS and, as with our AMPMs, these compounds showed a high D/L activity ratio for *P. aeruginosa*.[370]

3.8 Fluorescently labelled AMPMs

Fluorescent labelling of proteins is an important methodology in modern biochemical and biophysical studies. In particular, fluorescent labelling of proteins allows for their visualisation, tracking, or quantification in living cellular systems.[481] Additionally, fluorescently labelled proteins can be used to obtain direct physical information about the structure of a ligand-binding site, about protein-membrane interactions, or about the folding of proteins into their native state.[482] Analogously, fluorescently labelled peptides are versatile tools, which allow probing of their structure and biological function. Instead of labelling peptides with a (synthetic) fluorophore, the intrinsic fluorescent properties originating from aromatic amino acids, most notably from tryptophan, are frequently employed in bio-physical studies.[483]

3.8.1 Fluorescence spectra of mimetics 16 and 17

Tryptophan is an environmentally sensitive probe,[483] which means that both its fluorescence maximum and its fluorescence intensity depend on the molecular environment of the fluorophore. Typically, a blue-shift (i.e. towards lower wavelengths) of the emission maximum, as well as an increase in the fluorescence intensity upon change from an aqueous to a more apolar environment is observed for environmentally sensitive fluorophores. The dependence of the spectroscopic characteristics of such fluorophores on the polarity of their molecular environment apparently renders them suitable for studying peptide-membrane interactions.[484]

To provide an illustrative example, the fluorescence spectra of 2 μM solutions of the AMPMs **16** and **17** were recorded in the presence or absence of 25 mM SDS and are depicted in **Figures 3.52** and **3.53**. In such experiments, the micellar structures formed by the anionic detergent SDS are commonly employed as a membrane-mimicking environment. Interestingly, although the fluorescence spectrum of mimetic-**17** shows the expected blue shift in the presence of SDS micelles, the fluorescence intensity decreases.

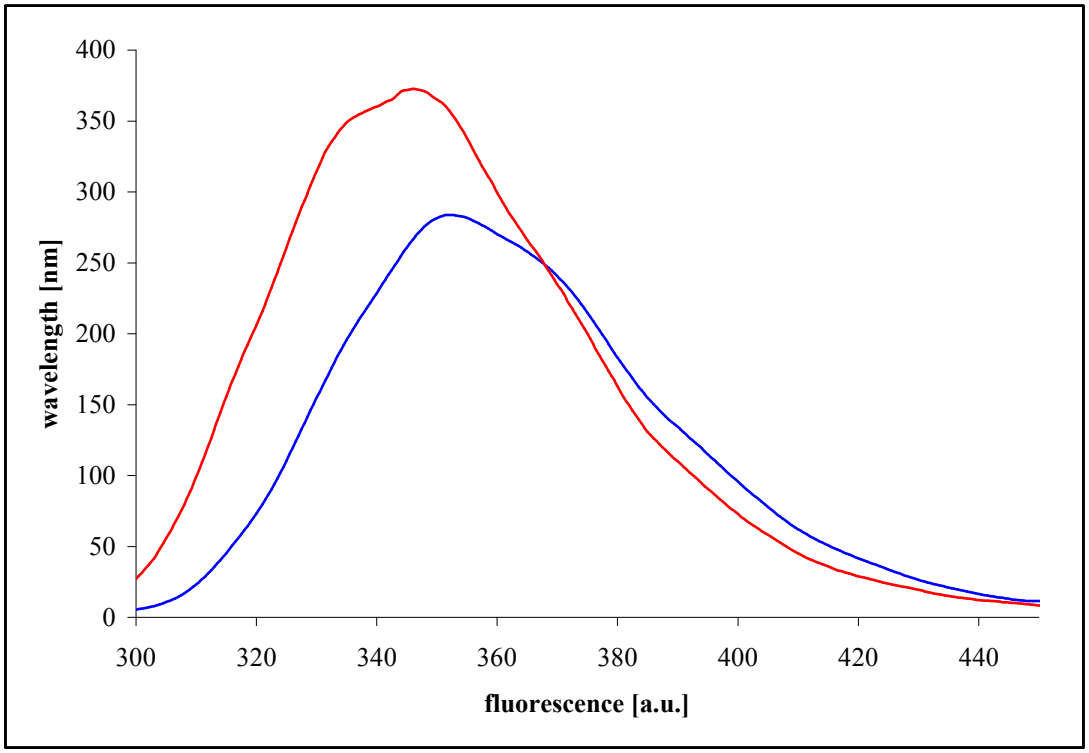

Figure 3.52 Intrinsic tryptophan fluorescence of 2 μM mimetic **16** in the presence (red) and absence (blue) of 25 mM SDS (10 mM Tris, 10 mM NaCl, pH 7, λ_{ex}=280 nm).

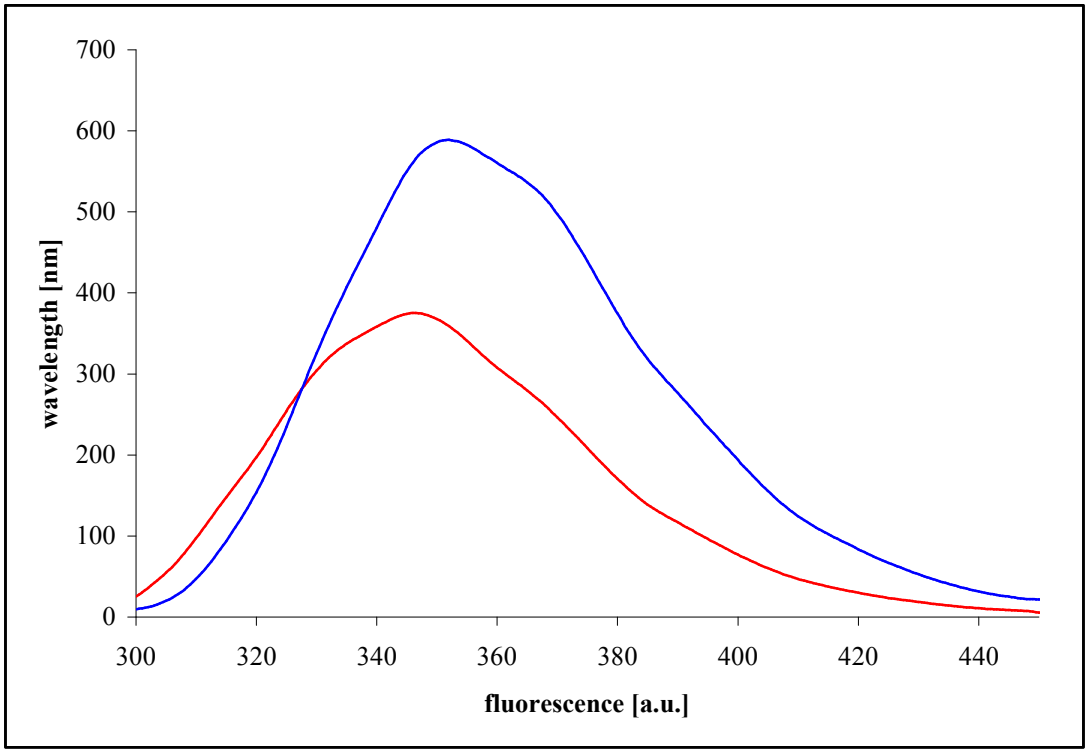

Figure 3.53 Intrinsic tryptophan fluorescence of 2 μM mimetic **17** in the presence (red) and absence (blue) of 25 mM SDS (10 mM Tris, 10 mM NaCl, pH 7, λ_{ex}=280 nm).

Although the use of intrinsic tryptophan fluorescence in biophysical studies is straightforward, there are several problems associated with it. The most severe limitations restricting its broader applicability are the ubiquitous abundance of tryptophan residues in proteins and the generally unfavourable spectroscopic characteristics of tryptophan (i.e. low excitation and emission wavelengths in the UV region).

One way to overcome the inherent problems of tryptophan fluorescence consists of labelling peptides with fluorophores that possess superior spectroscopic characteristics. The use of longer excitation and emission wavelengths, for example, avoids interference from the ubiquitous tryptophan residues of peptides and proteins, and opens up the possibility of studying labelled compounds in complex systems. In particular, it allows for the use of methods such as fluorescence spectroscopy in live cellular systems, which would otherwise not be possible due to auto-fluorescent interference of the studied cells.

Apart from being a necessary prerequisite for studies on peptide interactions with complex systems, fluorescent labelling also offers additional advantages for the study of smaller model systems. For instance, the interaction of peptides with model membrane systems is often investigated by fluorescent methodologies, and although such studies often use tryptophan as the fluorescent probe, the advantage of fluorophores with longer excitation and emission wavelengths in applications with model membrane systems lies in an reduced amount of scattering brought about by liposomes or micelles, since this phenomenon decreases with increasing wavelength.[483]

Additionally, even for the relatively small cyclic peptides in which we are interested, the presence of multiple tryptophan and tyrosine residues can become a complicating factor. For example, these multiple fluorescent residues may experience different molecular environments even within the same molecule, and this can render it impossible to specifically probe a distinct position in the molecule under investigation.

3.8.2 Fluorescence labelling

There exist two conceptually different approaches to the incorporation of fluorophores into (proteinaceous) target molecules. Firstly, the fluorophore(s) can be introduced either during the (bio-)synthetic elaboration of the target molecule, or secondly it (they) can be introduced after the target molecule has been synthesised.

Traditionally, the most frequently used approach to the fluorescent labelling of proteins consists of derivatisation with a reactive fluorophore, following synthesis and/or purification. This is commonly achieved at the free N-terminus or at nucleophilic amino and thiol side-chain functionalities. Naturally, the simultaneous presence of several reactive sites in the vast majority of protein/peptide substrates precludes a global procedure for site-specific labelling of these molecules.

Due to the aforementioned, and still growing, importance of fluorescent methodologies, a variety of novel approaches have been developed to achieve more specific labelling of target proteins with a variety of fluorophores (or other functionalities such as photo-labels, biotin, etc.). Frequently, genetically encoded fluorescent labels such as GFP can be fused to a target protein, which also allows the labelling of proteins in live cellular systems.[485] Another genetic approach consists of fusing the target protein with either a receptor domain or a peptide sequence that can be selectively modified by a fluorescent labelling reagent. For example, the biarsenical compound 4',5'-bis(1,3,2-dithioarsolan-2-yl)fluorescein (FlAsH) can be used to covalently label a tetra-cysteine motif,[486] and biotin ligase (BirA) permits the attachment of biotin to a 15-amino acid consensus sequence.[487]

Another way of incorporating novel functionality into target macromolecules is represented by the bio-orthogonal chemical reporter strategy. Therein chemical reporters, which can later be reacted with the fluorescent probe molecules of appropriate functionality, are incorporated into the proteins by the biosynthetic machinery of the target cell. Bio-orthogonal amino acids, containing azide or alkyne functionalities, for example, can be incorporated site-specifically into proteins by using the nonsense suppression technique.[488] Examples of the highly selective reactions used in bio-orthogonal approaches to attach the probe molecules comprise Staudinger ligation, [3+2] cycloadditions with azides and alkynes, or strain-promoted cycloadditions.[489]

An important requirement for the applicability of labelled molecules is that the structural change due to the incorporation of the fluorophore should be kept as small as possible. This structural confinement can be of paramount importance for maintaining the biological activity of the labelled compound, and thus for its usefulness as a tool for studying the physico-chemical properties of the parent compound. Not surprisingly, perturbation of structure and/or function can be a severe problem for proteins labelled via genetic fusion to GFP and similar fluorophores. In comparison, one of the advantages of labelling with bio-orthogonal amino acids is that the structural perturbations can be kept to a minimum.

Due to their smaller molecular mass, such factors naturally affect peptides to a greater extent than proteins. In comparison to peptides, fluorescence labelling of proteins usually poses less stringent criteria for the introduction of the fluorophore due to their larger size and domain architecture. Frequently, a variety of residues are available on the surface of the protein that are not directly involved in the activity/function of the protein, and lend themselves to modification by a fluorophore.

With respect to AMPs, the incorporation of larger sequences is obviously not desirable; additionally the modification of the abundant positively charged lysine residues could lead to undesirable changes in physico-chemical parameters such as amphipathicity, hydrophobicity and charge that might adversely affect their biological activity.

3.8.3 Labelling with fluorescent amino acids

The second approach, which was employed here to fluorescently label AMPMs, consists of incorporating a fluorescent amino acid during the synthesis of the target molecule. An apparent advantage lies in the fact that the incorporation of the fluorophore can be achieved selectively in the desired position during the SPPS of the peptide chain. Alternatively, fluorescent amino acids can be introduced biosynthetically using nonsense suppression.[490]

Compared to the more traditional approach of labelling proteins with fluorophores containing reactive moieties, another advantage of the direct incorporation of the fluorophore lies in the fact that it is not restricted to the labelling of positions in the primary sequence that carry particular functional groups, that is, any chosen residue can be replaced by the fluorophore.

Several fluorescent amino acids have been reported in the literature, and a selection of amino acids with different fluorophores that have been used in SPPS is given in **Figure 3.54**. Fluorophores that have been incorporated into amino acids include the DANA system (**41**),[490, 491] coumarin-based dyes (**42**),[492] the 8-hydroxyquinoline system (**43**),[493] fluorescein derivatives (**44**),[494] the anthraniloyl group (**45**),[495] and the NBD system (**46**).[496]

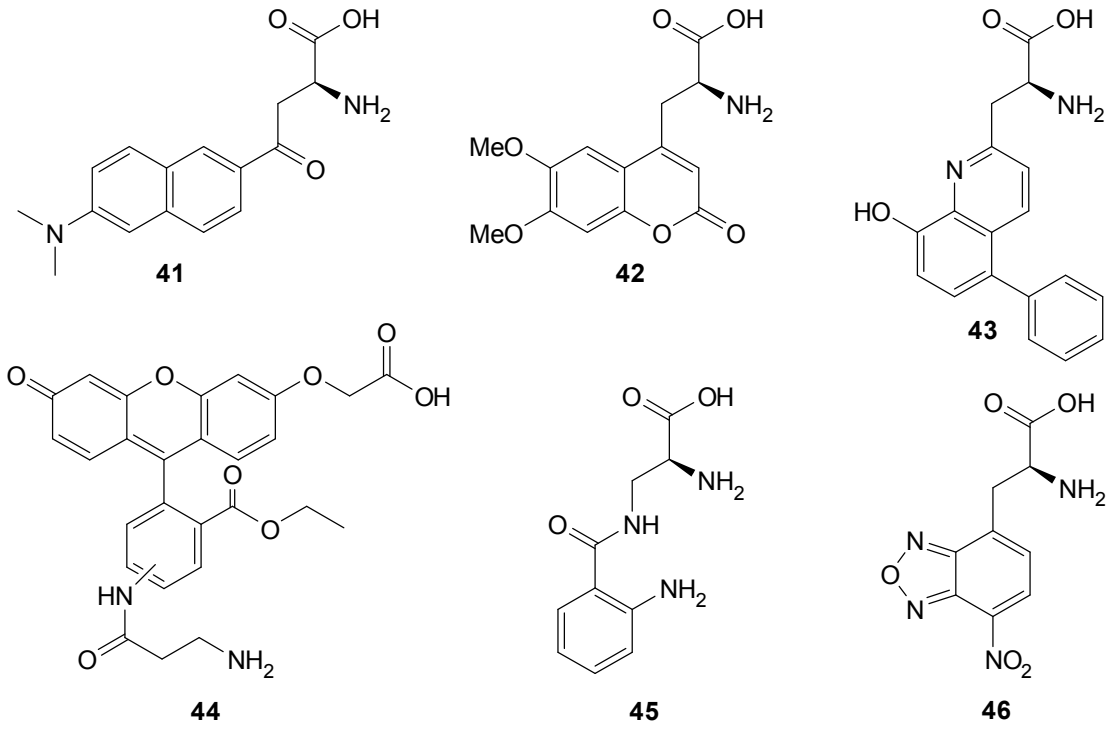

Figure 3.54 A selection of synthetic fluorescent amino acids that have been used in SPPS for labelling peptides and proteins.

For the synthesis of fluorescently labelled AMPMs, we chose the so-called DANA (6-(2-dimethylaminonaphthoyl)alanine; Aladan; **41**) system, developed independently by Imperiali and Cohen.[490, 491] The fluorescent amino acid **41** is derived from the well-studied PRODAN fluorophore, pioneered by Weber, that has been extensively used for bio-physical studies of peptides and proteins.[497]

Like PRODAN, DANA (**41**) is an environmentally sensitive fluorophore that can be used to study peptide-membrane interactions, and it has been used to probe protein electrostatics. However, no applications of **41** for studying peptide-membrane interactions, especially in the field of antimicrobial peptides, have been reported so

far. Fmoc-protected DANA (**52**) is fully compatible with standard SPPS protocols, and could be used in the syntheses of various fluorescently labelled peptide mimetics, according to the general mixed solid-phase/solution chemistry strategy used in our laboratory (c.f. **Section 3.1**).

3.8.3.1 Synthesis of the fluorophore

Our synthetic approach to Fmoc-DANA essentially follows that developed independently by Imperiali and by Cohen,[490, 491] and is outlined in **Scheme 2**. Briefly, commercially available 2-acetyl-6-methoxynaphthalene (**47**) was reacted with lithium dimethylamide in HMPA to give acedan (**48**) in 70 % yield after recrystallisation from ethanol. Compound **48** was deprotonated using lithium bis-hexamethyldisilazide as a sterically hindered, non-nucleophilic base, in THF at –78 °C, followed by iodination in THF to afford crude iodo-acedan (**49**) as an orange solid in 95 % yield. NMR analysis of the crude reaction product showed complete consumption of the starting material, and formation of a small amount of bis-iodinated side-product. Compound **49** has been found to be prone to rapid degradation at room temperature and under light, especially in chlorinated solvents. Nevertheless, pure **49**, as well as its bis-iodinated side product could be isolated by column chromatography using ethyl acetate as eluent. However, the crude reaction product of the iodination reaction was used without further purification in the following reaction.

The key step in the synthesis of **52** consists of an asymmetric electrophilic alkylation of *N*-(diphenylmethylene)glycine *tert*-butylester[498] with **49**. The alkylation reaction was carried out using 20 mol% of *O*-(9)allyl-*N*-(9-anthracenylmethyl)cinchonidinium bromide (**50**) as a phase transfer catalyst and afforded the crude Schiff base **51** in 85% yield, which was used without further purification. The enantiomeric excess of 90% ee of **51** was determined by derivatisation with N_{α}-(2,4-dinitro-5-fluorophenyl)-L-valinamide (modified Marfey's reagent) and subsequent HPLC analysis.[499] Deprotection of the Schiff base in TFA containing ethanedithiol as a scavenger, yielded DANA (**41**), which was Fmoc-protected using Fmoc-OSu in water/acetone at pH 8, to furnish Fmoc-DANA-OH (**52**) in 96% yield.

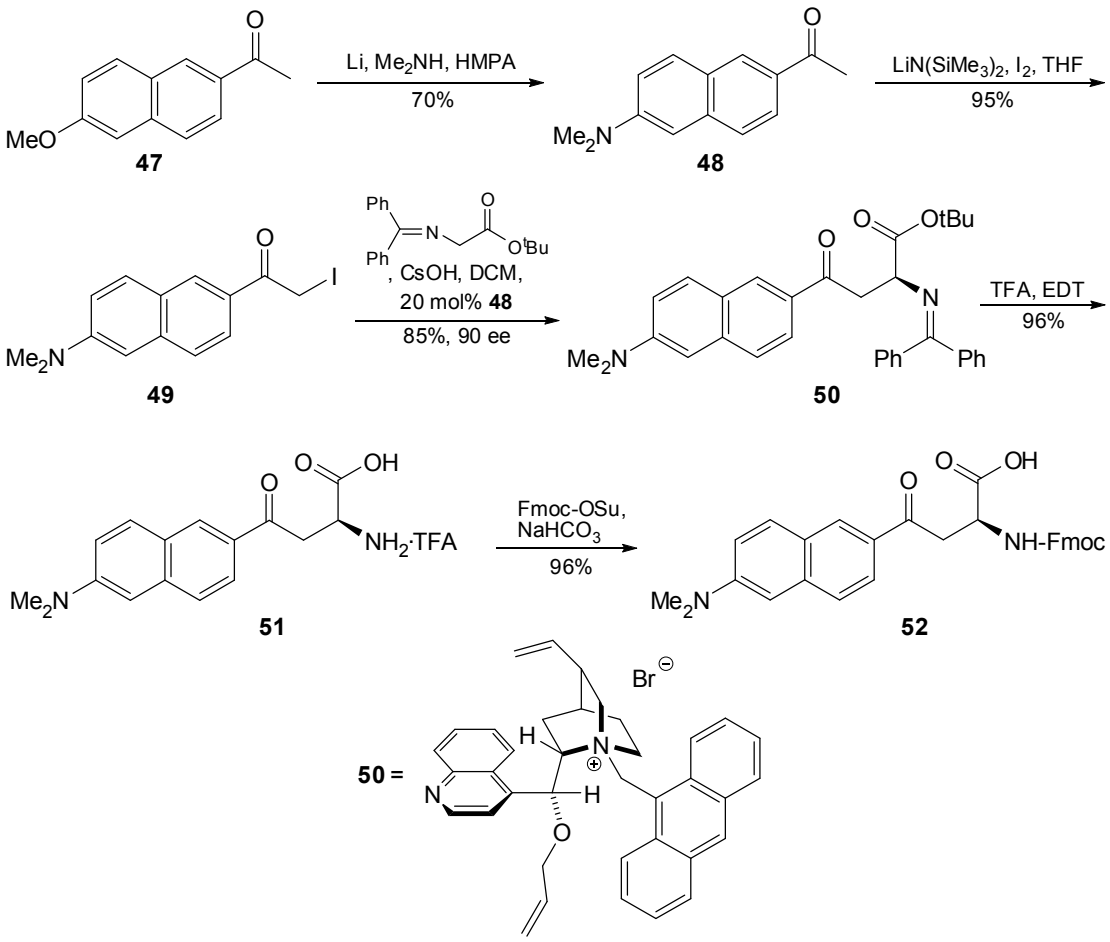

Scheme 2 Synthetic approach to the synthesis of Fmoc-DANA-OH (**52**).

3.8.3.2 Synthesis of fluorescently labelled AMPMs

Fluorescently labelled peptide analogues of mimetic **16** and mimetic-**17** were prepared recently by a co-worker in our group, permuting the DANA fluorophore through all positions in the peptide with the exception of the D-Pro-L-Pro template.[500] In this work, **72** and **77**, in which Trp-8 of the scaffolds of mimetics **17** and **19**, respectively is replaced with the fluorophore, were synthesised. The synthesis of fluorescently labelled analogues was carried out according to the standard protocol for the synthesis of AMPMs outlined in **Section 3.1** and described in detail in **Section 5.2**. The fluorescent amino acid was incorporated into the peptide chain by manually coupling 1.5 equivalents of **52** using 1.45 equivalents of HATU as activating reagent and 3.0 equivalents of DIEA. Crude peptides were purified by RP-HPLC and determined to be of at least 98% purity by analytical HPLC. ESI mass spectrometric and analytical HPLC data are summarised in **Appendix 2**.

Table 3.12 Antimicrobial activities for the fluorescently labelled analogues of mimetics **16** .and **17**, as well as for a fluorescently labelled analogue of mimetic **19**. The position of the incorporated DANA fluorophore is underlined and highlighted in green, and the numbering of amino acid residues is given for the parent compounds. The fluorescently labelled analogues that retain the characteristic activity pattern are highlighted.

ID[a]	sequence[b]	MIC[c] [µg/mL]				
		E. coli	*P. aeruginosa*		*S. aureus*	
		25922[d]	27853[d]	PAO1[d]	25923[d]	29213[d]
16	^{1}L^{2}R^{3}L^{4}K^{5}K^{6}R^{7}R^{8}W^{9}K^{10}Y^{11}R^{12}VpP	4	2	2	16	16
53	LRLKKRRWKYRVpP	4	2	4	16	8
54	LRLKKRRWKYRVpP	16	16	32	16	16
55	LRLKKRRWKYRVpP	16	8	8	8	8
56	LRLKKRRWKYRVpP	8	8	16	8	8
57	LRLKKRRWKYRVpP	8	16	16	8	8
58	LRLKKRRWKYRVpP	4	4	8	8	8
59	LRLKKRRWKYRVpP	8	4	8	16	8
60	LRLKKRRWKYRVpP	8	4	8	16	16
61	LRLKKRRWKYRVpP	8	8	8	8	4
62	LRLKKRRWKYRVpP	8	8	8	8	4
63	LRLKKRRWKYRVpP	16	16	32	16	16
64	LRLKKRRWKYRVpP	8	8	16	16	8
17	^{1}R^{2}W^{3}L^{4}K^{5}K^{6}Q^{7}R^{8}W^{9}K^{10}Y^{11}Y^{12}RpP	16	0.25	1	16	> 64
65	RWLKKQRWKYYRpP	8	64	64	32	16
66	RWLKKQRWKYYRpP	4	16	16	64	32
67	RWLKKQRWKYYRpP	8	64	64	16	16
68	RWLKKQRWKYYRpP	4	64	64	32	16
69	RWLKKQRWKYYRpP	4	32	32	32	16
70	RWLKKQRWKYYRpP	4	8	8	8	8
71	RWLKKQRWKYYRpP	8	32	32	32	16
72	RWLKKQRWKYYRpP	8	0.5	0.5	32	16
73	RWLKKQRWKYYRpP	16	32	32	16	16
74	RWLKKQRWKYYRpP	16	32	16	32	16
75	RWLKKQRWKYYRpP	8	16	16	16	8
76	RWLKKQRWKYYRpP	8	64	32	64	32
19	^{1}T^{2}W^{3}L^{4}K^{5}K^{6}R^{7}R^{8}W^{9}K^{10}K^{11}A^{12}KpP	64	0.008	0.015	> 64	> 64
77	TWLKKRRWKKAKpP	64	0.125	0.5	> 64	> 64

[a] Substance identifier; [b] p = D-Pro; [c] minimal inhibitory concentration; [d] strain or ATCC number.

3.8.3.3 Biological activities of the fluorescently labelled AMPMs

The biological activities of the synthesised AMPM analogues were evaluated against our panel of microbial test organisms and the results are summarized in **Table 3.12**. It can be seen that the series of compounds derived from mimetic-**16** was insensitive to the position into which the fluorescently labelled amino acid was incorporated. All compounds retained the broad spectrum activity of the parent mimetic, albeit with a slightly reduced potency. Only compound **53**, in which the Leu-1 was replaced by the fluorophore, fully retained the antimicrobial activity of mimetic **16**, whereas replacement of Arg-2 or Arg-12 in **54** and **63** lead to a larger decrease in activity than for the rest of the series.

For the series of analogues derived from mimetic-**17**, on the other hand, only substitution of Trp-8 by the DANA fluorophore in compound **72** resulted in retention of the selectivity towards *P. aeruginosa*, which is characteristic for the second to fourth generation AMPMs derived from protegrin-1. This might be explicable by the similar physico-chemical properties of the fluorescent label as compared to tryptophan, both being amino acids bearing aromatic side chain functionalities of comparable steric bulk. Analogously, the DANA fluorophore could also be incorporated into the Trp-8 position of mimetic **19** to yield an analogue with good activity against *P. aeruginosa*. Interestingly, the replacement of residues other than Trp-8 in the scaffold of **17** did not lead to a complete loss of antimicrobial activity. In fact, a slight improvement of activity against *E. coli* and *S. aureus* was observed, while on the other hand, the activity against *P. aeruginosa* was reduced to a level comparable to that observed for *E. coli* and *S. aureus*.

3.8.4 Fluorescent properties of the DANA fluorophore

As a first step in evaluating the fluorescence properties of the labelled model compounds, NAAA (*N*-acetyl-aladan amide, **78**), an amidated and *N*-acetylated derivative of DANA was prepared (**Figure 3.55**), and the dependence of the fluorescence spectroscopic characteristics of the fluorophore on the environment was examined by recording fluorescence emission spectra of **78** in various bulk solvents (**Figure 3.56**)

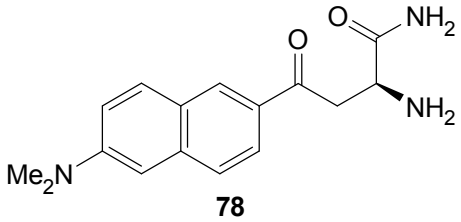

78

Figure 3.55 *N*-Acetyl-aladan amide (**78**); an amidated DANA derivative used for the evaluation of the spectroscopic properties of the fluorophore.

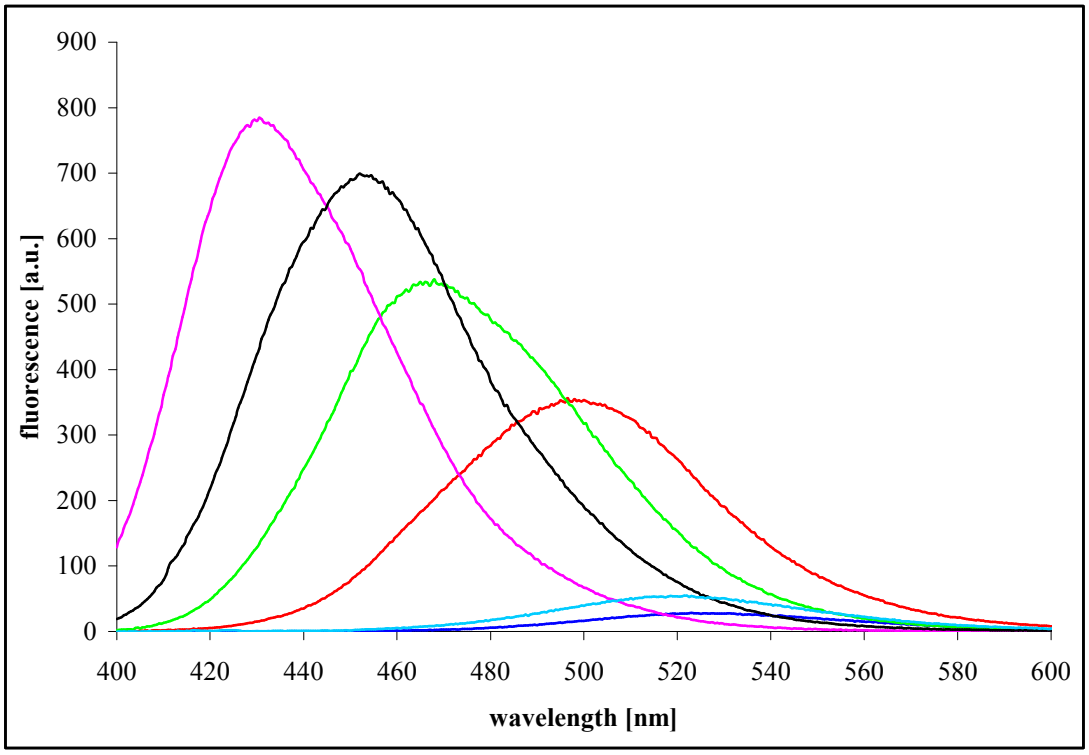

Figure 3.56 Fluorescence emission spectra of **78** in various bulk solvents. Water (blue), TFE (light blue), ethanol (red), DMF (green), Ethyl acetate (black), and diethyl ether (pink).

Apart from cyclohexane and carbon tetrachloride, in which **78** was not sufficiently soluble, all tested solvent systems caused a more or less pronounced

increase of fluorescence intensity, concomitant with the typical blue-shift of the emission maximum. The largest effects were found for ether solvents, whereas alcoholic solvents resulted in intermediate changes in the fluorescence spectra. The emission maxima and the relative fluorescence intensities of **78** in over 20 common solvents are given in **Table A5.1** (see **Appendix 5**).

Additionally, the fluorescence spectra of **78** in the presence or absence of SDS micelles, as a simple membrane mimicking environment, were recorded and are shown in **Figure 3.57**. It was found that **78** showed about a sevenfold enhancement in fluorescence intensity upon transition to the membrane-mimicking environment, thus rendering it potentially useful for studying peptide-membrane interactions.

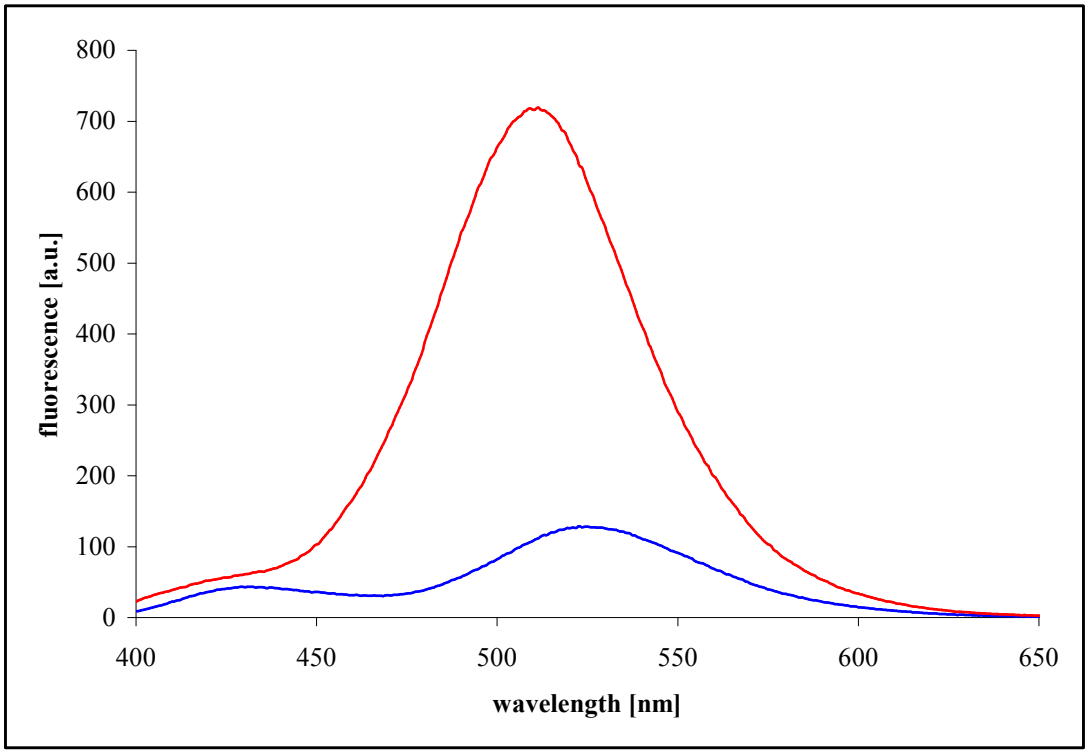

Figure 3.57 Fluorescence emission spectra of 2 μM **78** in the presence (red) and absence (blue) of 25 mM SDS (10 mM Tris; 10 mM NaCl; pH 7.0; λ_{ex} = 360 nm).

The increase in fluorescence intensity in the presence of SDS is comparable to the values obtained for **78** in alcoholic solvents (c.f. **Figure 3.56**). It is interesting to note in this respect, that TFE which is often used as a membrane-mimicking solvent in NMR studies, only leads to a very weak increase in DANA fluorescence as compared to an aqueous solution.

3.8.4 Applications of fluorescently labelled AMPMs

With a variety of fluorescently labelled analogues in hand, several experiments were carried out to demonstrate the usefulness of DANA-labelled mimetics as model compounds for studying mechanisms of action of AMPMs. For example, the interaction of fluorescently labelled analogues of mimetic-**16** with liposomal model membrane systems has been studied by a fluorescence spectroscopic method, and furthermore, the practicality of DANA-labelled AMPMs for (confocal) fluorescence microscopy studies has been investigated.

3.8.4.1 Peptide-bilayer interactions of the mimetic 16 scaffold

As discussed above, the properties of the DANA fluorophore can be used to study the interaction of labelled AMPMs with model membrane systems. Such interaction is best described as the partitioning of the peptides into the (model) membrane. Frequently, the partitioning of peptides into membranes is accompanied by the formation of secondary structure, and this has also been found to be the case for mimetic-**16** (c.f. **Section 3.2**). As a result, peptides bound to membranes often have a much higher structural content than they do in aqueous solution, and this is a widespread phenomenon encountered with antimicrobial peptides.[501]

The folded peptide must have a lower free energy in the membrane compared to the unfolded peptide. Because of the fluid nature of membranes, and since the hydrophobic and electrostatic components that are the major driving forces of most peptide-bilayer interactions arise from the collective properties of the lipids comprising the bilayer, the interactions of peptides with membranes should be considered as interactions with an assembly of lipids (bilayer), rather than as interaction with the individual lipid molecules of which it is comprised. Thus chemical equilibria such as $P + L \rightleftharpoons PL$ are inappropriate descriptions of peptide-bilayer interactions. Biologically relevant bilayers are in highly thermodynamically disordered states, and the association of peptides with bilayers should therefore be treated as partitioning between two immiscible fluid phases. The chemical potentials μ of a peptide in the aqueous and in the bilayer phase must be equal at equilibrium. Hence one can define a mole fraction partition coefficient K_x given by

$$K_x = \frac{[P]_{bilayer}/([L]+[P]_{bilayer})}{[P]_{water}/([W]+[P]_{water})} \qquad \text{[equation 3.2]}$$

where $[P]_{bilayer}$ and $[P]_{water}$ denote the bulk molar concentrations of peptide in the bilayer, respectively water, phase and [L] and [W] stand for the molar concentrations of lipid and water.[502]

3.8.4.2 Determination of membrane partitioning coefficients

Methods for the experimental determination of partition coefficients are based on either physical separation such as dialysis, or on titration methods such as fluorescence and CD spectroscopy.[502] In the case of spectroscopic titration methods, the fraction f_p of partitioned molecules is not immediately known. Instead, one measures a spectroscopic response, such as fluorescence intensity, that is assumed to be proportional to the f_p, and the proportionality constant must be defined by the maximum signal change at full binding. To be of use for binding measurements, spectroscopic parameters need to be linear-response functions. An example of a linear-response function is steady-state fluorescence intensity at a constant wavelength, as employed in our experiments.

Membrane partitioning coefficients for DANA labelled analogues of mimetic **16** were measured using a POPC/POPG liposomal model system. LUVs of appropriate phospholipid compositions and a diameter of 100 nm were prepared according to the extrusion method described in **Section 3.5**. To obtain the fraction of partitioned molecules, f_p, the increase in fluorescence intensity at 400 nm was measured and the data were fitted to the following equation:[503]

$$f_p = \frac{K_x[L]}{[W]+K_x[L]} \qquad \text{[equation 3.3]}$$

A representative fluorescence titration curve of **62** is shown in **Figure 3.58**, and the partitioning coefficients obtained for the series of analogues derived from mimetic-**16** with three different liposomal systems are summarized in **Table 3.13**.

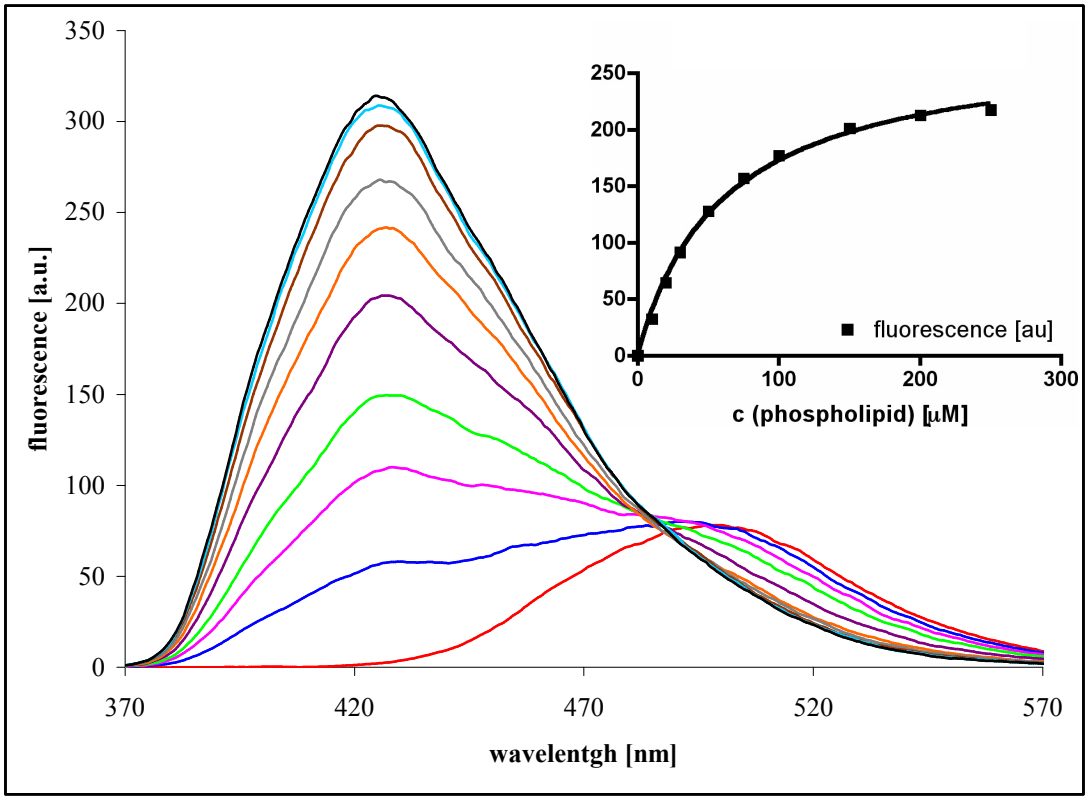

Figure 3.58 Fluorescence titration of **64** with increasing amounts of the POPC/POPG (80:20) liposomal system. The fitting of the fluorescence intensity at 400 nm to **equation 3.3** is shown in the inset.

It can be seen from **Table 3.13** that all tested compounds have the ability to partition into negatively charged model membranes, and that this ability generally increases with increased negative character of the liposome system. It is noteworthy that there was no observable change in the fluorescence intensity of DANA-labelled AMPMs when the purely zwitterionic POPC systems was used in the titration experiments, thus not allowing for the determination of a partitioning constant for this system.

Table 3.13 Membrane partitioning coefficients K_x obtained from fitting the experimental data to **equation 3.3** and free energies ΔG calculated as $\Delta G = -RT \ln(K_x)$[502] for the series of DANA labelled analogues derived from mimetic **16**. Measurements were carried out for three different POPC/POPG liposomal systems.

	POPC/POPG (80:20)		POPC/POPG (70:30)		POPG	
Substance	K_x [$\times 10^{-5}$]	ΔG [kJmol^{-1}]	K_x [$\times 10^{-5}$]	ΔG [kJmol^{-1}]	K_x [$\times 10^{-5}$]	ΔG [kJmol^{-1}]
53	4.8	-31.9	7.1	-32.8	155.4	-40.3
54	3.9	-31.3	9.5	-33.5	141.9	-40.1
55	1.8	-29.4	6.4	-32.6	257.0	-41.6
56	7.0	-32.8	16.3	-34.8	34.6	-36.7
57	7.8	-33.0	13.3	-34.4	236.8	-41.4
58	9.1	-33.4	n.d.[a]	n.d.	189.7	-40.8
59	3.4	-31.1	6.8	-32.7	35.9	-36.8
60	5.4	-32.2	4.9	-31.9	131.5	-39.9
61	3.0	-30.6	21.1	-35.5	253.5	-41.5
62	7.5	-33.0	10.4	-33.7	56.8	-37.9
63	7.5	-33.0	15.2	-34.7	113.3	-39.6
64	3.2	-30.9	5.7	-32.3	50.2	-37.6

[a] n.d. = not determined.

3.8.5 Fluorescence microscopy with DANA labelled AMPMs

To test whether DANA-labelled mimetics could be used as tools in fluorescence microscopic studies, experiments were carried out on the incorporation of the labelled mimetics **56** and **72** into HeLa cells via confocal fluorescence microscopy (**Figure 3.59**). Compound **56** was chosen as a representative of the series of analogues derived from **16**, and compound **72** was selected since at the time it was the only DANA-labelled compound that retained the selective activity pattern of mimetic **17**.

Briefly, HeLa cells at a concentration of 6×10^4 cells/mL were incubated in Lab-Tek 22×22 mm flat-bottomed chamber slides (*Nunc*, Roskilde, Denmark), and incubated overnight at 37 °C. The fluorescently labelled peptides **56** or **72** were then added to the cell cultures and incubated at 37 °C for 1 to 6 hours. The cells were subsequently washed three times with PBS, and fixed in methanol-acetone (1:1) at −20°C for 30 min.

Additionally, *P. aeruginosa* PAO1 cells were incubated with mimetic **19** analogue **77** under conditions identical to those employed in the proteomic experiments towards target identification (**Figure 3.60**, c.f. Section **4.1**). Briefly, *P. aeruginosa* PAO1 cells were grown to an OD of 0.2 and corresponding to approximately 1×10^8 CFU/mL. Bacterial cells were washed twice in Mueller-Hinton broth and incubated with 0.3 μg/mL of **77**.

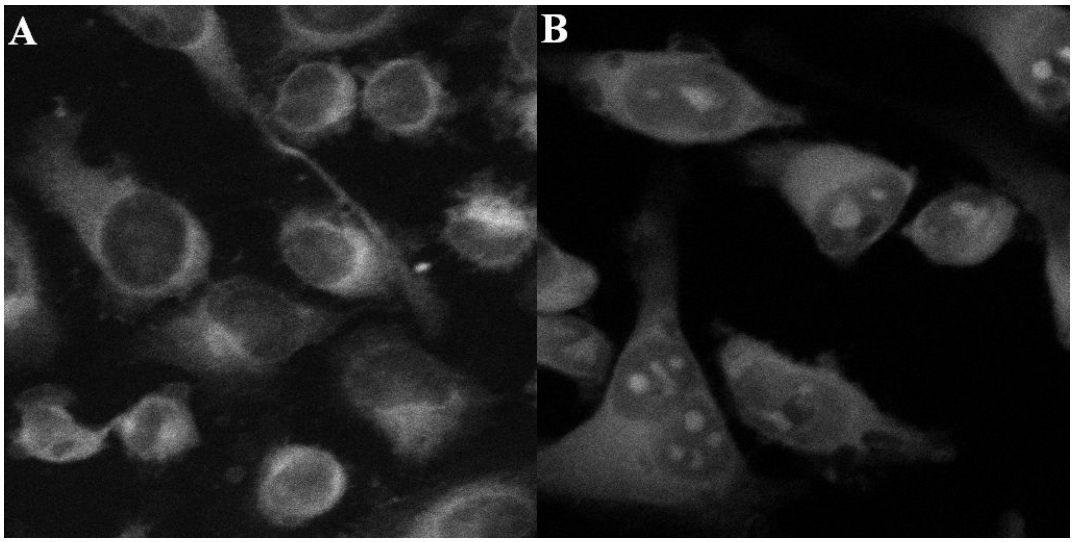

Figure 3.59 Uptake of fluorescently labelled analogues of AMPMs into HeLa cells. (A) 10 μM of **56**, 6h; (B) 1 μM of **72**, 6h.

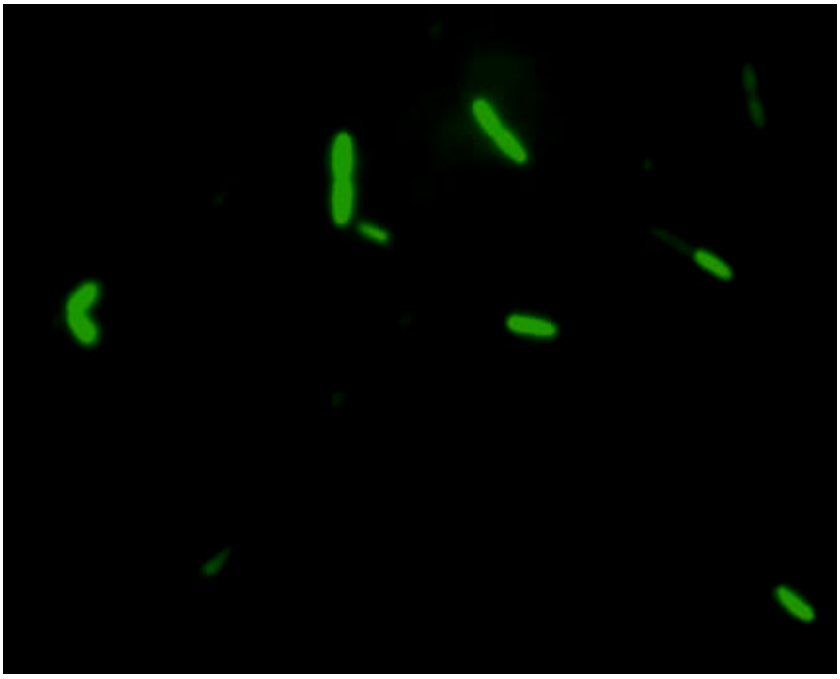

Figure 3.60 Fluorescence microscopy image of *P. aeruginosa* PAO1 cells treated with compound **77**. Cells were incubated with 0.3 μg/mL of **77** for 60 minutes.

As can been seen from **Figures 3.59** and **3.60**, DANA-labelled peptides could be used in fluorescent microscopy applications, thus validating the potential of site-specifically fluorescently labelled AMPMs for studying AMP action *in vivo*. Due to possible artefacts during the fixation procedure employed during experiments with HeLa cells, it is not advisable to make statements about uptake mechanisms into these cell cultures for our AMPMs. However, it can be clearly seen from **Figure 3.59** that there are significant differences in the obtained fluorescence pattern for both compounds. Compound **72**, on one hand, was incorporated more efficiently, since a tenfold higher concentration of **56** was required to achieve a similar level of fluorescence intensity under similar experimental conditions, and compound **72** was also able to translocate into the cell nucleus, as manifested by visualisation of nucleolic structures. Compound **56**, on the other hand, accumulated largely in a region around the cell nucleus which is typically occupied by the endoplasmatic reticulum (ER).

3.8.5 Conclusions

The synthesis of fluorescently labelled analogues of mimetics **16** and **17,** as well as of one compound derived from **19** showed that the DANA fluorophore could be conveniently incorporated site-specifically into the scaffold of AMPMs derived from protegrin-1 (**11**). It was found that in mimetic **17**, only the aromatic residue Trp-8 could be replaced by the DANA fluorophore with retention of the selective activity against *P. aeruginosa*. The loss of the anti-pseudomonal activity by the other analogues of **17** emphasises the need for methods capable of site-specific labelling in this system. Furthermore it corroborates the notion of a mechanism of antimicrobial action for mimetic **17** and the later generation AMPMs that depends on more than just the physico-chemical parameters of these molecules, such as hydrophobicity and amphipathicity.

However, the retention of antimicrobial activity for those analogues that lost the selectivity towards *P. aeruginosa,* as well as the insensitivity of mimetic **16** towards the incorporation of the fluorophore, indicates that for both AMPMs a more unselective, presumably membrane-active, mechanism of action is also operating. In the case of **16**, such a mechanism would account solely for the antimicrobial activity, whereas for mimetic **17** it can provide an explanation for the observed residual

antimicrobial activity against *E. coli* and *S. aureus*. In the case of **17** and congeners, this basic, or residual membrane-active mechanism is then supplemented by an alternative (and stereospecific, c.f. **Section 3.4**) mechanism of action, which does not necessarily have to be independent from the membrane-active mechanism. It is noteworthy that the MIC values obtained for the analogues of **17** are generally two- to fourfold higher than observed for the series derived from **16**, which might point towards a reduced potency of **17** for (stereo-)unspecific interaction with membrane systems or other cellular compounds.

The practicality of using DANA-labelled compounds for studying AMPMs by (confocal) fluorescence microscopy has been validated in this work. Also an assay has been established that allows for quantification of the interaction of labelled peptide mimetics with liposomal model membrane systems. In the latter experiments, which were carried out with analogues of mimetic **16**, it has been found that, paralleling their broad-spectrum antimicrobial activity, all tested analogues showed comparable energetics for the interaction with the model membranes. Moreover, it was found that increasing the negative charge of the model membrane system led to increased partitioning of the peptide mimetics into the bilayer. It is noteworthy that there was no appreciable partitioning into the purely zwitterionic model membrane system (i.e. into vesicles composed solely of POPC), which is in agreement with the results form the dye-leakage experiments of **16** (c.f. **Section 3.5**), and also with the low haemolytic activity of this compound. Although partitioning into the liposomal systems was most favourable for the purely anionic POPG system, substantial partitioning into the bilayer also occurred for the mixed liposomal systems. This is somewhat in contrast to the results of the dye-leakage experiments conducted with mimetics **16** and **17**, where it was found that appreciable leakage of encapsulated calcein only occurred with POPG liposomes. These findings could be interpreted as indicating that **16** and fluorescently labelled analogues of **16** are able to interact with (i.e. to partition into) mixed model membrane systems, but are unable to induce leakage of compounds the size of calcein or larger except from the most negatively charged model systems.

Finally, the fluorescently labelled compound **77**, which is derived from mimetic **19,** retained - analogously to compound **72** - the selective antimicrobial activity against *P. aeruginosa*. Due to the increased antimicrobial activity of **77**,

which also parallels the higher activity of **19** compared to **17**, this compound might prove a valuable tool for studying AMPMs via fluorescence methodologies.

4 Approaches towards target identification

With the experiments described in **Chapter 3** providing further corroborating evidence of the prevalence of an alternative mechanism of antimicrobial action for the AMPMs derived from protegrin-1 (**11**), several approaches have been employed towards the elucidation of putative molecular targets for this class of compounds in *P. aeruginosa* PAO1. As outlined in **Chapter 1**, there are two conceptually different approaches towards antibacterial drug discovery. Target based drug discovery starts from the identification of a viable (antibacterial) drug target, possibly via a bioinformatic approach that takes advantage of the increasing availability of genomic sequence data, and usually relies on high-throughput screening of large compound libraries with an assay system based on the putatively identified target. Several problems associated with this approach, such as the often unfavourable uptake characteristics of the identified drug candidates into bacterial cells were mentioned in **Section 1.1**.

The second and more classical approach, which is currently receiving renewed interest - not least because of the to date disillusioning results of target based drug discovery programmes - starts from a lead compound that is selected by virtue of its activity in an *in vivo* based assay system. That is to say that the identified lead compound(s) display(s) sufficient activity to elicit a desired phenotypic change in the assay system; in the case of antibacterial drug discovery the desired phenotypic change is represented by the inhibition of bacterial growth or by a direct bactericidal action. The advantage of this second approach with respect to the ultimately necessary *in vivo* activity is evident, but it suffers from the fact that the mode of action, and hence the molecular target(s) of the lead compound(s) emerging from activity based screens, are generally unknown.

However, identification of the molecular target(s) of potential therapeutic agents is important in several regards. First of all, an insight into drug-target interactions on the molecular level enables the design of target based assays, which in turn allow for more efficient SAR studies, and greatly aid in the efforts of medicinal chemistry towards modification of the lead structure. With respect to our AMPMs,

for instance, such knowledge might also allow us to extend the antibacterial spectrum towards other species. Secondly, knowledge of the lead compounds' mechanism of action should aid in the identification or anticipation of possible side-effects on human cells, and thus open the way to their minimisation. Moreover, once the mode of action of a potential drug candidate is established, target validation of structurally modified compounds derived from the lead compound becomes more straightforward. Finally, even though historically many antibiotics were successfully marketed and used long before their underlying mechanisms were elucidated, knowledge of an antimicrobial agent's mode of action is often regarded nowadays as mandatory for further development. The remainder of this chapter will thus be concerned with the problem of identifying putative targets subsequent to the establishment of a desired biological activity, whereby the discussion will be focused on biochemical/proteomic methodologies. For an overview on the use of genetic methods applied to the target identification problem, the reader is referred to the recent review article by Zheng et al.[504]

Again, there are two conceptually different approaches towards target identification for compounds resulting from phenotypic activity screening, such as our AMPMs. The first approach aims for the direct identification of molecular interactions of the lead compound with the target molecule, and employs methods such as affinity chromatography, photo-affinity labelling, (chemical) cross-linking, immune precipitation, display cloning, yeast two hybrid systems, or more recently protein micro-arrays.[505, 506] The second, complementary approach consists of the evaluation of mRNA, protein, or metabolite expression profiles obtained from organisms treated with the lead compound. The indirect nature of this approach renders the interpretation of its results dependent on the availability of expression profiles obtained with compounds of known mechanisms, against which the newly obtained data can be compared.

The process of target identification for a lead compound emerging from activity based phenotypic screening is often referred to as chemical genetics or forward chemical genetics, and the relation of this approach to the target identification problem posed by the AMPMs derived from protegrin-1 is evident. Therefore, in the following sections, experiments aimed at the identification of targets of the AMPMs are described, beginning with an indirect method, namely the recording of protein expression profiles of *P. aeruginosa* PAO1 in the presence and absence of mimetic

18. The chapter will then be concluded with the description of two direct biochemical approaches, based on affinity chromatography and photo-affinity labelling (PAL).

4.1 Proteomics approach

Since the completion of the first genome of a free-living organism, *Haemophilus influenzae* in 1995,[507] the number of fully sequenced genomes is growing at an ever increasing pace, not least due to the introduction of new sequencing technologies.[508] With an increasing amount of completely sequenced genomes at hand (460 as of November 2006**) - especially those of important model organisms - the elucidation of the functional roles of the newly available gene products has shifted into the focus of biological research. To emphasize the conceptual break between the acquisition of sequence data, and the experiments that are enabled by the availability of this data, the term post-genomic era is often used to encompass the new experimental methodologies that aim to extract structural and functional information out of the wealth of sequence information.

It is becoming increasingly clear that biological function is not mediated by a static genome, but rather by the cells' complement of proteins, which in turn is determined through a dynamic interplay of external stimuli, gene regulation and levels of expressed proteins.[509] The field of functional genomics focuses on such dynamic aspects as transcription, translation and protein/protein interactions by making use of large scale experiments (so-called -omics), enabled by the availability of the genomic sequence data and progress in bioinformatic methodologies. Transcriptomics, for instance, is concerned with the subset of transcribed genes in a given organism under specified conditions. This subset, which is also called the transcriptome, dynamically links the genome of an organism with its proteome and hence with the phenotype of the cell. Although transcriptomics offers immense potential for understanding complex biological systems on the molecular level, processes such as posttranslational modification of the translated proteins can influence their behaviour to a greater extent than their actual rate of synthesis. Additionally, mRNA profiling generally does not allow studies on the cellular localisation or on the sequestration of the protein products, for example by interaction with other macromolecules, or on other effects such as proteolysis.

Therefore, the expression patterns of proteins are expected to correlate more closely with cellular processes than the expression patterns of the corresponding genes, and the direct analysis of the cells' inventory of proteins is an important and

** http://www.genomesonline.org/gold.cgi

complementary approach to the analysis of the transcriptome. The field of proteomics is concerned with such an analysis of the expression, cellular localisation, structure, biochemical activity, and interaction with other cellular compounds of as many proteins as possible. Originally, the proteome was defined as the complete cellular complement of proteins expressed by a given genome.[510] More recently, since it has become clear that the complement of expressed proteins depends intricately on the cellular state of the organism, it was suggested that a definition of the proteome should include the state of the organism, as well as posttranslational modifications and protein isoforms which arise, for example, by alternative splicing.[509]

4.1.1 Proteomics and antibacterial target identification

The applicability of a proteomic approach to the identification of putative targets of antimicrobial agents is based on the general utility of the method in studying the adaptation of micro-organisms to environmental stimuli. That is, proteomics are widely used to analyse the proteomes of cells grown under specified growth conditions, and in this respect there are no conceptual differences between the study of the bacterial response to antibiotic action or to other stress factors, such as temperature shock or growth under limitation of certain nutrients.

In proteome mapping, 2D-PAGE gels are used to identify and locate as many proteins of the organism under investigation as possible, and to link this information with protein function. The latter can be achieved by computational methods and database searching, for example via identification of orthologous genes from different organisms with known function; such information is therefore ultimately dependent on classical biochemical experiments. There still exist limitations as to the amount of proteins that can be identified by 2D-PAGE analyses, but a variety of advanced protein maps for several prokaryotic organisms are available.[511-513] However, a major drawback of protein reference maps is that they do not represent an actual snapshot of the protein expression pattern of a given organism under specified experimental conditions, as would be obtained from a single experiment. The latter is rather referred to as a protein expression profile,[514] and the study of antibiotic action depends on obtaining such protein expression profiles. Accordingly, the term stimulon has been introduced to specify proteins whose expression profiles are affected by a stimulus such as antibiotic action on a phenotypic level.[515]

Furthermore, proteomic signatures are defined as subsets of proteins that show differential expression under specified experimental conditions, which can be related to functions or pathways specific to the stimulus. Proteins or sets of proteins that constitute a particular proteomic signature can be indicative of a particular physiological state of the organism under investigation. Since it is possible that more than one proteomic signature constitute the observable protein expression profile of a given stimulus, the determination of proteomic signatures has to depend on the analysis of expression profiles of various related and unrelated stimuli. While it may take considerable effort to determine reliable proteomic signatures, once available they can function as invaluable tools for the analysis of expression profiles obtained with a hitherto unstudied stimulus. It is important to emphasise at this point that proteomic signatures do not have to be identical for different organisms, even if the organisms are closely related.

Several proteomic studies have been undertaken with emphasis on the mode and/or mechanisms of action of antibacterial drugs, in which changes in the protein expression profiles of antibiotic challenged bacterial organisms were analysed. In an early set of experiments, van Bogelen et al. correlated the proteomic signatures for cold and heat shock in *E. coli* with the protein expression profiles obtained from cells treated with several antibiotics that impair protein biosynthesis, such as chloramphenicol, erythromycin, fusidic acid, aminoglycosides, or tetracycline.[516] Evers et al. examined the protein expression patterns of *H. influenza* cells treated with inhibitors of RNA and protein biosynthesis, and found that apart from the aminoglycosides employed in their experiments, all antibiotic compounds led to an increased expression rate of ribosomal proteins and of RNA polymerase subunits.[517] Another study with *H. influenza* was directed towards the two DNA gyrase inhibitors ciprofloxacin and novobiocin, where clear differences in the protein expression profiles induced by these two compounds, that act by different mechanisms, could be discerned.[518] Furthermore, Singh et al. described the protein expression profiles of *S. aureus* treated with several antibiotics that act on bacterial cell wall biosynthesis, and found that the patterns obtained were different from those displayed by antibiotics acting via different modes of action.[519] Additionally, inhibitors of peptide deformylase (PDF) have been studied, in which case the protein expression profiles were characterised by changes in the pI of the majority of proteins, caused by retention of the *N*-formyl-Met terminus.[520, 521] Other recent studies described in

more detail include the response of *P. putida* towards tetracycline,[522] and of *E. coli* towards silver nanoparticles.[523]

A logical extension to these experiments is the compilation of reference databases of protein expression profiles for a variety of different antibiotic compounds whose modes of action are secured, and which in an ideal case can permit the delineation of proteomic signatures for the antibiotic stimuli. One of the ultimate goals of such an approach is the prediction or delineation of the mode/mechanism of action for new antibacterial compounds by comparison with the protein expression profiles or proteomic signatures contained in the database.

Along these lines, Bandow et al. recently described a database containing the protein expression profiles of *B. subtilis* obtained with 30 antimicrobial agents, or generally cell-damaging compounds, via a dual-channel imaging protocol.[520] The authors could demonstrate the utility of the database approach by assigning the mechanism of action to nitrofurantoin as well as to a novel pyridiminone antibiotic, by comparison of the obtained protein expression profiles to the other profiles within the reference database. Additionally, they introduced marker proteins that were over-expressed at least two-fold and which comprised at least 0.05 % of the total protein synthesised after induction with the (antibiotic) stimulus, to allow for efficient, more reliable and less biased evaluation of the expression profile data sets. A natural requirement of the database approach in target identification is the availability of a sufficient number of proteomic signatures. However, compounds that display fundamentally new modes of action will not have corresponding proteomic signature entries in the database, and for such compounds, the analysis of mutants might aid in target validation and/or identification.

4.1.2 Experimental considerations

The most widely used experimental implementation of comparative proteome analysis to date is represented by two-dimensional polyacrylamide gel electrophoresis (2D-PAGE) combined with protein identification by mass spectrometric methods.[524] The experimental technique of 2D-PAGE, which allows for the analysis of complex protein mixtures based on separation according to the isoelectric point (pI, first dimension) and the molecular weight (second dimension) of the analytes, was developed in 1975 by O'Farrel[525] and by Klose.[526] Although this method was

already shortly thereafter applied to the study of protein expression profiles of organisms subjected to differential growth conditions[527] or to exogenous stress stimuli,[528] it was only after significant advances in the field of protein identification were made that the technique gained widespread popularity. The advances in the identification of proteins relied heavily both on progress in mass spectrometric methods and on the increased availability of DNA sequence data.

In principle, the mass spectrometric identification of protein spots obtained by 2D-PAGE can be achieved by two complementary methods. Firstly, in peptide mass fingerprinting (PMF), digestion of proteins with a sequence-specific endoprotease, typically trypsin, is followed by determination of the molecular masses of the generated protein fragments via MALDI-TOF, and the experimentally obtained molecular masses are compared with the theoretical molecular masses of protein fragments obtained from sequence databases. Additionally, and especially in such cases where PMF does not lead to unambiguous identification, tandem MS methods, which are used to obtain peptide fragments of the tryptic digests, can be used to identify the proteins via the obtained fragmentation patterns, again with the input of theoretically computed fragmentation patterns obtained from sequence databases. Since both mass spectrometric methods rely heavily on the availability of genomic sequence data to produce theoretical digestion fragments of proteins and/or theoretical fragmentation patterns, which can be compared to the experimentally obtained lists of peak intensities and m/z values, it is evident that the availability of genomic sequence data is indispensable for proteomic experiments.

Furthermore, technological advances concerning all aspects of gel-based proteomics, for example, the introduction of immobilised pH gradients (IPG) leading to improved reproducibility, the introduction of new staining methods, leading to increased sensitivity, the introduction of narrow pI IPG strips, leading to improved resolution, and advances in sample preparation and automation, have contributed to establish 2D-PAGE as the most versatile method for comparative proteomic analyses today. Last but not least, the introduction of and advances in image analysis software have greatly facilitated the quantification and analysis of protein spots obtained from large numbers of 2D gels. Today, 2D-PAGE is routinely applied for large-scale parallel quantitative profiling of complex protein mixtures, and can routinely separate 2000 individual protein spots or more, in favourable cases even over 5000. For a

recent comprehensive review on the experimental aspects of 2D-PAGE, the reader is referred to the review article by Görg et al.[524]

Nevertheless, there are several drawbacks to gel-based proteomics, such as difficulties in the analysis of proteins with extreme physicochemical properties. For example, large proteins or protein complexes might not enter the second dimension of the gel and may be lost from the protein expression profiles. Additionally, the isoelectric focussing of very acidic or very basic proteins often causes problems, and extremely hydrophobic proteins, such as membrane proteins, are often lost during sample preparation due to their lower solubility. Moreover, limitations in the resolution of 2D-PAGE still exist, and not all protein species of a given sample can be resolved. Another major problem of proteomic methods in general is the difficulty in detecting low-abundance proteins; typically such proteins have to be enriched in order to become detectable.

As alternatives to 2D-PAGE, several non-gel based methods have emerged recently that show promise in circumventing at least some of the above mentioned shortcomings. Generally, these methods are based on the combination of LC separation techniques with mass spectrometric analysis. For instance, in the MudPit approach, tryptic digests of complex protein samples are separated by cation exchange and reverse phase HPLC to reduce the sample complexity.[529] Additionally, heavy-isotope labelling is commonly used for the quantification of the results, and the labelling is achieved, for example, by stable isotope labelling with amino acids in cell culture (SILAC), or by the isotope-coded affinity tag technology (ICAT).[530] Although these alternative approaches seem to offer some advantages over gel based proteomics for the future, such as higher sensitivity, currently 2D-PAGE is without doubt the mainstay of comparative proteomics.[524] Finally, it should be mentioned that a major advantage of gel-based proteomics, as compared to LC-MS/MS proteomics, consists of the straightforward detection and quantification of post-translational modifications in the former method.

4.1.3 Expression profiles of *P. aeruginosa* PAO1 in the presence and absence of 18

For the determination of 2D protein expression profiles of *P. aeruginosa* PAO1 in the presence and absence of mimetic **18**, a protocol involving the prefractionation of the bacterial proteins, developed by Riedel et al, was employed.[531-533] The experiments were carried out under guidance of Dr. K. Riedel in the laboratory of Prof. Dr. L. Eberl at the University of Zurich. Prefractionation into intracellular, extracellular, and surface proteins serves several purposes. Firstly, it helps to reduce the complexity of the sample and can thus lead to a higher resolution in gels of the sub-cellular fractions. Secondly, fractionation can be an effective method for enriching particular types of proteins, such as hydrophobic membrane proteins in the membrane-, or surface-bound fractions, and thus often increases the sensitivity of the method towards the corresponding sub-proteome. Thirdly, pinning down identified protein spots to a certain sub-cellular location can provide a first clue as to their functional role. *P. aeruginosa* strain PAO1 was chosen for the proteomic experiments, since the genome of this organism has been fully sequenced, which is a pre-requisite for the identification of the protein spots via MALDI-TOF or other mass spectrometric methods (vide supra), and 5570 ORFs were annotated.[534]

Briefly, cultures of *P. aeruginosa* PAO1 were grown in the presence and absence of **18** at concentrations that inhibited, without completely suppressing, the growth of the bacteria. The general growth conditions were identical to those employed in the kinetic experiments (c.f. **Section 3.3**), apart from the use of larger culture volumes (1.2 or 2.4 L). To ensure maximal compatibility with the time-kill analyses as well as with the incorporation studies, **18** was added to bacterial cultures of an optical density of $OD_{600} = 0.2$. Due to the changes in culture volume and the need to work at sub-MIC concentrations, the necessary amount of **18** was determined in preliminary experiments that were identical in all experimental parameters to the later protein expression profiling experiments.

The effect of the change in culture volume on the required amount of mimetic **18** deserves special discussion. It was elaborated in **Section 3.3** that the positive charge inherent to the majority of AMP(M)s can lead to adsorption onto the surface of the culture vessel(s), with a concomitant increase in the apparent MIC, and that to

counteract this effect, 0.01% of BSA is added in the routine MIC protocol. However, no BSA was added for the recording of the protein expression profiles, the time-kill analyses and the incorporation studies, in order to exclude any potential side-effects of BSA on these experiments. Due to the larger culture volumes, 2L or 3L glass flasks were used for the incubation, and since it was found that the use of glass vessels in experiments conducted without added BSA leads to an even higher increase of the apparent MIC values than experienced with polypropylene or polyethylene surfaces, the optimal concentration of mimetic **18** for obtaining protein expression profiles was determined to be 0.3 μg/mL; a value that is considerably higher than would be expected from the routine determination of the MIC value of **18**.

As mentioned above, PAO1 cells were incubated at concentrations of **18** that did not completely inhibit the bacterial growth. However, it could be seen that the well-documented bacteriostatic effect of **18** set in about 30 minutes after addition (i.e. approximately one generation time under the experimental conditions), with no appreciable subsequent increase in the OD, which typically reached a final value of OD_{600} = 0.35. Cells were harvested after a maximum of 2 hours incubation to ensure that the control cultures were still in the exponential growth phase.

It is of interest to mention at this point, that the acquisition of sufficient quantities of surface-bound proteins from the mimetic **18** treated samples proved to be difficult, and could only be achieved by a large increase in the overall volume of cell culture used in the experiment. It is also interesting to note that the protocol for isolation of the surface-bound fraction involves re-suspending in 0.2M glycine buffer, and that this re-suspension proved to be difficult for mimetic **18** treated cells. Whereas the cell pellets of the control cultures were of a slightly pink colour and easily re-suspended, the mimetic **18** treated cells had a black appearance, displayed a slimy consistency, and were reluctant to re-suspend. While stirring of the control culture readily yielded a uniform bacterial suspension, the same procedure with the treated culture afforded a slightly grey suspension containing a large amount of unsuspended black flakes of cellular material.

2D gels were run with total protein concentrations of 350 μg, as determined by Bradford analysis.[535] For the isoelectric focussing of the intracellular protein fractions, IPG strips with an immobilised pH gradient 4-7 were used, whereas the other fractions were run with IPG strips with immobilised pH gradients of 3-10.

Scanned gel images of the different sub-cellular fractions challenged with **18** or the control cultures were overlaid for comparison, using the ProteomWeaver™ software package, to aid in the analysis of results by visual inspection. Protein spots whose expression was found to be differentially regulated by the addition of **18** were subjected to in-gel tryptic digestion followed by characterization by MALDI-TOF peptide mass fingerprinting and tandem MS/MS analysis at the Functional Genomics Center Zurich (FGCZ).

The excised protein spots are highlighted in **Figures 4.1-4.3**, and the results of the protein identification which was carried out employing the GPS-explorer™ software package with the included MASCOT search engine,[536] based on the obtained mass spectrometric data, are summarised in **Tables 4.1-4.3**. For the database searches, the non-redundant NCBI database and the updated *P. aeruginosa* genome sequences database of *P. aeruginosa* PAO1 from the *P. aeruginosa* Community Annotation Project were used.[537]

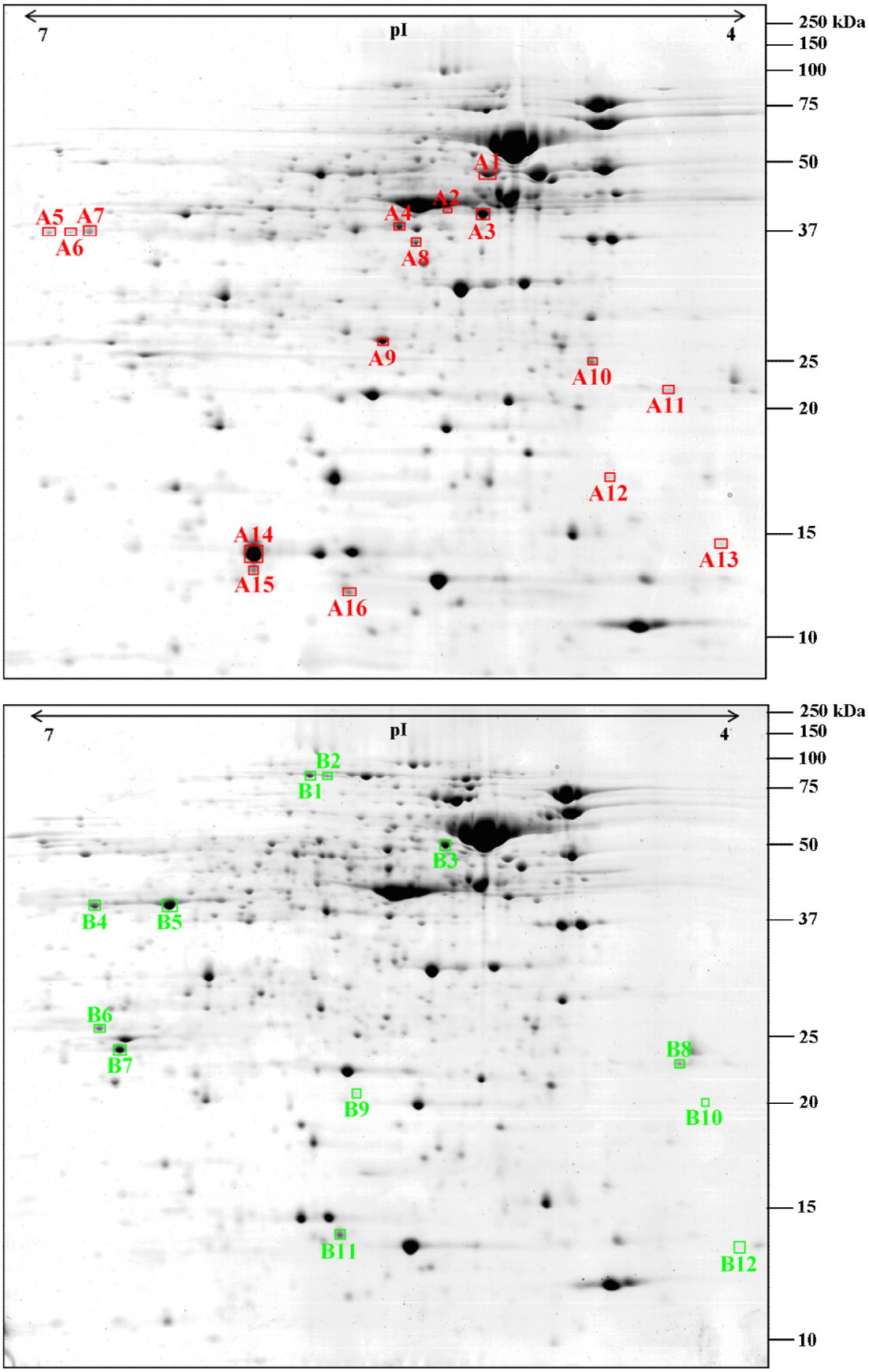

Figure 4.1 Differentially expressed proteins of the intracellular fraction of *P. aeruginosa* PAO1. Top: down-regulated; bottom: up-regulated after induction with mimetic **18**.

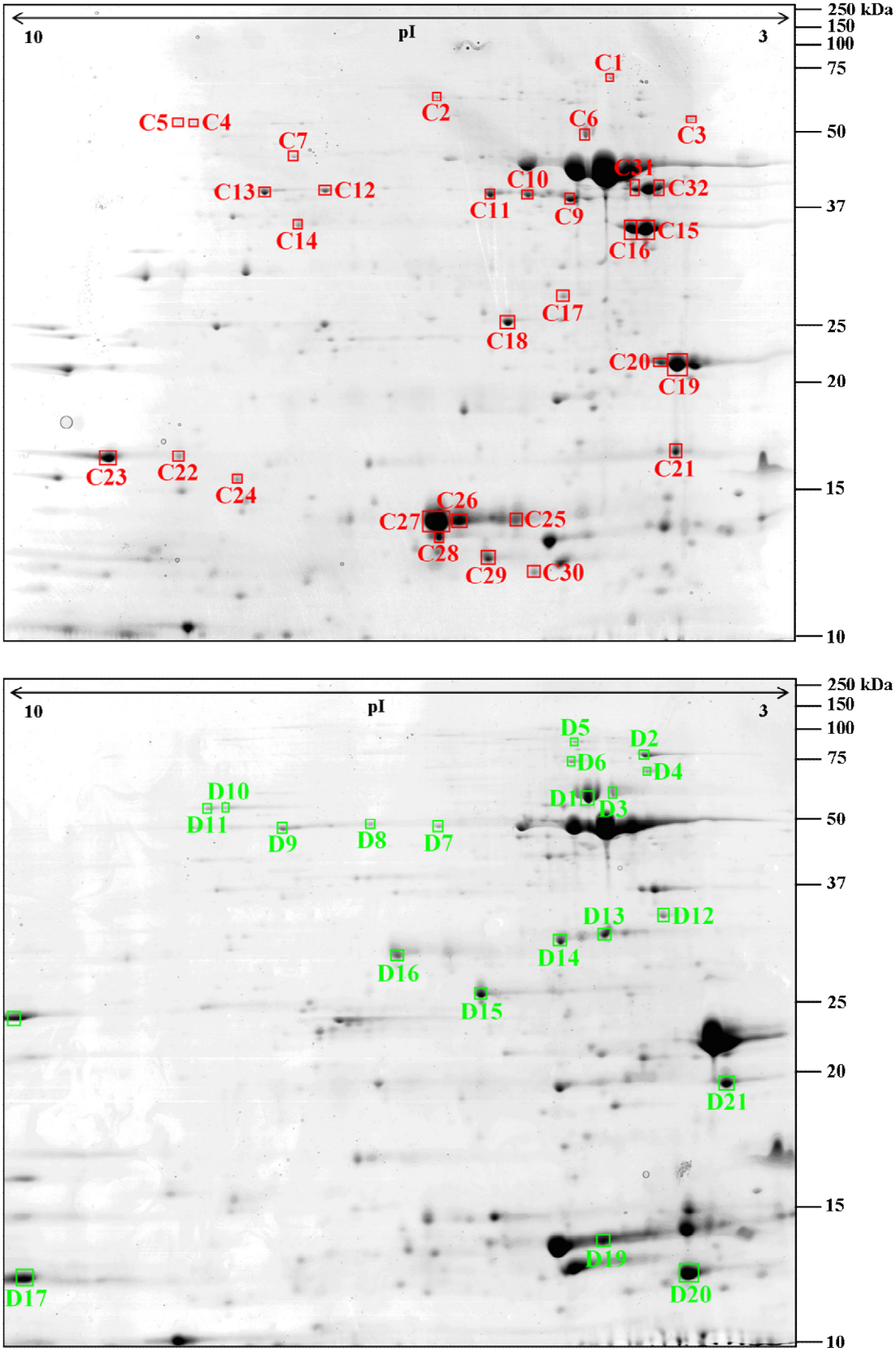

Figure 4.2 Differentially expressed proteins of the surface-bound fraction of *P. aeruginosa* PAO1. Top: down-regulated; bottom: up-regulated after induction with mimetic **18**.

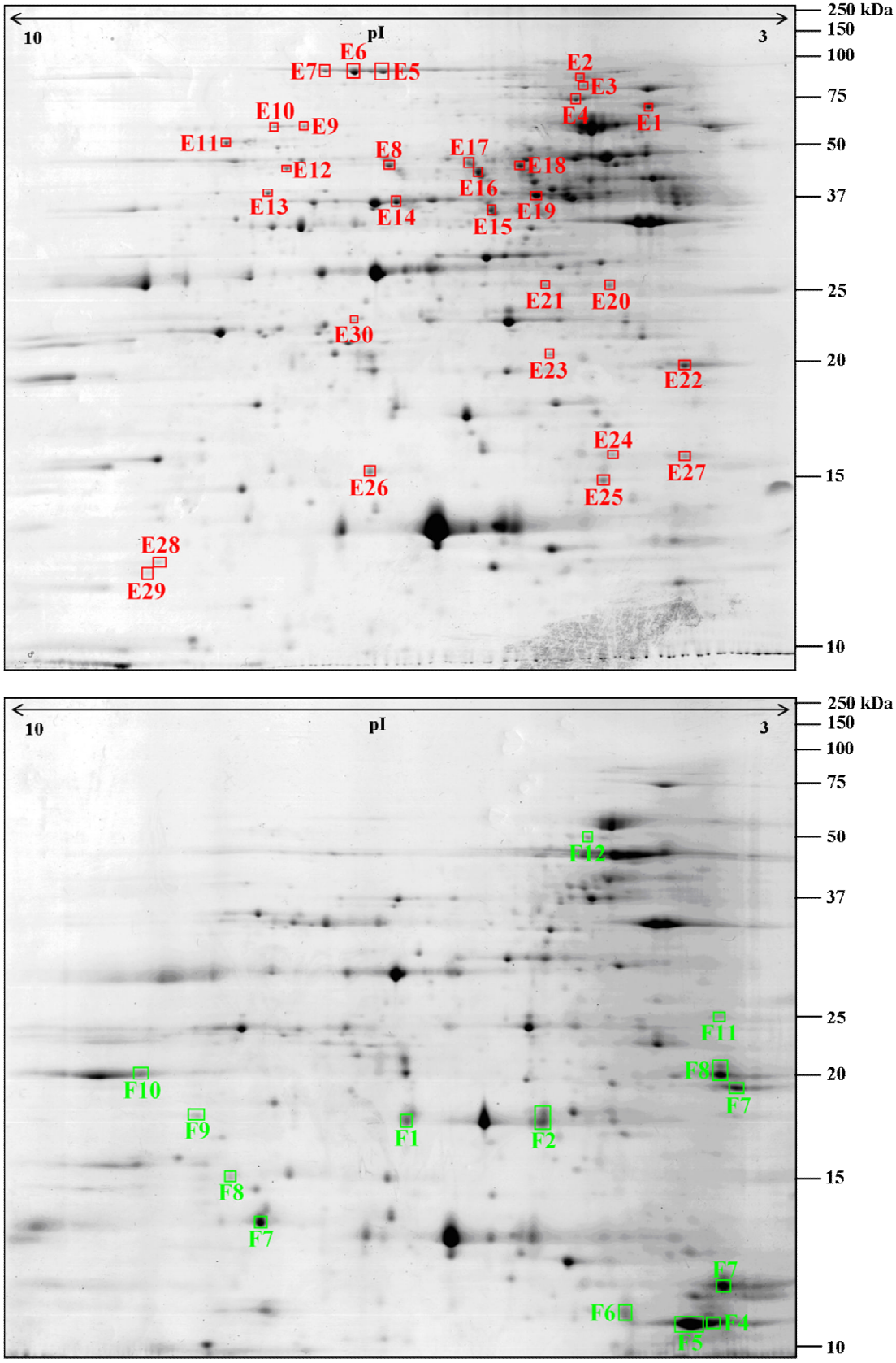

Figure 4.3 Differentially expressed proteins of the extracellular fraction of *P. aeruginosa* PAO1. Top: down-regulated; bottom: up-regulated after induction with mimetic **18**.

Table 4.1 Identification of mimetic **18** affected proteins in the intracellular fraction of *P. aeruginosa* PAO1. Spots A1-A16 were found to be down-regulated after induction with **18**, whereas spots B1-B12 where found up-regulated. Missing spot numbers correspond to unidentified proteins.

Spot no[a]	PA no[b]	Theoretical pI	Theoretical M_r	Protein score[c]	Sequence coverage [%][d]	Protein description
A1	PA1092	5.4	49.2	386	38	flagellin type B
A2	PA1074	5.6	39.9	187	47	branched-chain amino acid transport protein BraC
A3	PA1074	5.6	39.9	104	16	branched-chain amino acid transport protein BraC
A4	PA3190	5.7	45.3	271	32	probable binding protein component of ABC sugar transporter
A6	PA1493	7.8	36.5	228	58	sulfate-binding protein of ABC transporter
A7	PA0300	7	40.7	133	20	polyamine transport protein
A8	PA0301	5.5	40.2	182	31	polyamine transport protein
A9	PA0888	6.4	28.1	460	52	arginine/ornithine binding protein AotJ
A10	PA5153	5.1	27.7	137	26	probable periplasmic binding protein
A12	PA1657	4.8	18.2	78	29	hypothetical protein PA1657
A13	PA2966	4.1	8.7	88	12	acyl carrier protein
A14	PA4922	6.4	16.2	328	40	azurin precursor
A15	PA4067	4.9	25.2	137	21	outer membrane protein OprG precursor
A16	PA0388	6.6	15.4	203	41	hypothetical protein PA0388
B1	PA0482	5.5	78.8	273	35	malate synthase G
B2	PA0482	5.5	78.8	377	50	malate synthase G
B3	PA2300	5.2	53.1	128	18	chitinase
B4	PA2001	6	40.6	453	66	acetyl-CoA acetyltransferase
B5	PA1588	5.8	41.8	586	72	succinyl-CoA synthetase beta chain

Table 4.1 (continued)

B6	PA3686	6	23.2	367	63	adenylate kinase
B7	PA0139	5.9	20.6	419	57	alkyl hydroperoxide reductase subunit C
B8	PA1777	5	37.8	169	27	outer membrane protein OprF precursor
B10	PA0837	4.5	17	66	46	peptidyl-prolyl cis-trans isomerase Sly-D
B11	PA5178	5.5	15.5	249	64	hypothetical protein PA5178
B12	PA1777	5	37.8	173	11	outer membrane protein OprF precursor

[a] Spot numbers refer to **Figure 4.1**.

[b] Data generated from peptide mass maps were compared to the translated open reading frames (ORF) for P. aeruginosa PAO1 (http://v2.pseudomonas.com).

[c] Probability score of the MASCOT database search based on an implementation of the Mowse algorithm;[538] scores greater than 50 are considered significant ($p<0.05$).

[d] Sequence coverage denotes the percentage of the protein sequence for which matching peptide fragments have been identified.

Table 4.2 Identification of mimetic **18** affected proteins in the surface-bound fraction of *P. aeruginosa* PAO1. Spots C1-C32 were found to be down-regulated after induction with **18**, whereas spots D1-D22 where found up-regulated. Missing spot numbers correspond to unidentified proteins.

Spot no[a]	PA no[b]	theoretical pI	theoretical Mr	Protein score[c]	Sequence coverage [%]	Protein description
C8	PA0958	4.96	48.3	412	53	outer membrane porin protein OprD precursor
C9	PA2760	5.5	46.9	486	47	probable outer membrane protein
C10	PA1288	5.7	45.5	415	53	probable outer membrane protein
C11	PA1288	5.7	45.5	463	53	probable outer membrane protein
C12	PA0291	8.7	49.6	367	56	outer membrane porin OprE precursor
C13	PA0291	8.7	49.6	439	56	outer membrane porin OprE precursor
C14	PA0300	7	40.7	183	25	polyamine transport protein PotF2
C15	PA1777	5	37.8	500	63	outer membrane protein OprF precursor
C16	PA1777	5	37.8	472	70	outer membrane protein OprF precursor
C17	PA5472	5.5	29.3	248	60	hypothetical protein PA5472
C18	PA0888	6.4	28.1	629	78	arginine/ornithine binding protein AotJ
C19	PA4067	4.9	25.2	501	50	outer membrane protein OprG precursor
C20	PA4067	4.9	25.2	456	50	outer membrane protein OprG precursor
C21	PA4067	4.9	25.2	305	33	outer membrane protein OprG precursor
C22	PA1178	9	21.6	296	69	outer membrane protein H1 precursor
C23	PA1178	9	21.6	350	70	outer membrane protein H1 precursor
C24	PA3227	7.9	20.1	410	61	peptidyl-prolyl *cis-trans* isomerase A PpiA
C25	PA4922	6.4	16.2	202	26	azurin precursor
C26	PA4922	6.4	16.2	266	39	azurin precursor

Table 4.2 (continued)

C27	PA4922	6.4	16.2	334	40	azurin precursor
C28	PA4922	6.4	16.2	284	40	azurin precursor
C29	PA0388	6.6	15.3	318	74	hypothetical protein
C30	PA0409	5.4	13.3	315	83	twitching motility protein PilH
C31	PA0958	5	48.3	372	61	outer membrane porin protein OprD precursor
C32	PA0958	5	48.3	357	42	outer membrane porin protein OprD precursor
D1	PA4385	5	57.1	732	53	GroEL protein
D2	PA4761	4.8	68.5	689	69	DnaK protein
D3	PA4385	5	57.1	345	43	GroEL protein
D4	PA3162	4.8	62	166	38	30S ribosomal protein S1 RpsA
D5	PA4266	5.1	78.1	143	36	elongation factor G FusA1
D6	PA1596	5.1	71.6	363	51	heat shock protein HtpG
D7	PA1092	5.4	49.2	424	55	flagellin type B FliC
D8	PA1094	6.5	49.4	288	49	flagellar capping protein FliD
D9	PA0766	7	50.3	153	30	serine protease MucD precursor
D10	PA1587	6.5	50.4	325	46	lipoamide dehydrogenase-glc
D11	PA1587	6.5	50.4	302	42	lipoamide dehydrogenase-glc
D12	PA0946	4.9	36.8	278	40	hypothetical protein PA0946
D13	PA2951	5	31.4	477	74	electron transfer flavoprotein alpha-subunit EtfA
D15	PA4495	5.7	24.9	392	64	hypothetical protein PA4495
D16	PA1589	5.8	30.6	618	90	succinyl-CoA synthetase alpha chain SucD
D17	PA0329	9.3	11.8	439	76	hypothetical protein PA0329

Table 4.2 (continued)

D18	PA2952	9	26.4	561	76	electron transfer flavoprotein beta-subunit EtfB
D19	PA4386	5.2	10.3	268	65	GroES protein
D20	PA4271	4.7	12.5	191	79	50S ribosomal protein L7 / L12
D21	PA1777	5	37.8	332	36	outer membrane protein OprF precursor

[a] Spot numbers refer to **Figure 4.2**.

[b] Data generated from peptide mass maps were compared to the translated open reading frames (ORF) for P. aeruginosa PAO1 (http://v2.pseudomonas.com).

[c] Probability score of the MASCOT database search based on an implementation of the Mowse algorithm;[538] scores greater than 50 are considered significant ($p<0.05$).

[d] Sequence coverage denotes the percentage of the protein sequence for which matching peptide fragments have been identified.

Table 4.3 Identification of mimetic **18** affected proteins in the extracellular fraction of *P. aeruginosa* PAO1. Spots E1-E30 were found to be down-regulated after induction with **18**, whereas spots F1-F12 where found up-regulated. Missing spot numbers correspond to unidentified proteins.

Spot no[a]	PA no[b]	Theoretical pI	Theoretical M_r	Protein Score[c]	Sequence coverage [%]	Protein description
E1	PA3162	4.8	61.9	480	53	30S ribosomal protein S1
E2	PA4266	5.1	78.1	280	43	elongation factor G
E4	PA1596	5.1	71.6	347	53	heat shock protein HtpG
E7	PA0572	6.1	100.6	340	39	hypothetical protein PA0572
E8	PA1094	6.5	49.4	668	81	flagellar capping protein FliD
E9	PA5078	6.5	59.4	206	41	hypothetical protein PA5078
E10	PA4236	6.2	55.6	146	31	catalase
E11	PA1587	6.5	50.4	311	42	lipoamide dehydrogenase-glc
E12	PA4175	6.5	48.6	409	51	probable endoproteinase Arg-C precursor
E13	PA0291	8.7	49.6	272	45	outer membrane porin OprE precursor
E14	PA0852	6.4	42.3	324	61	chitin-binding protein CbpD precursor
E15	PA1094	6.5	49.4	628	70	flagellar capping protein FliD
E16	PA1094	6.5	49.4	752	81	flagellar capping protein FliD
E17	PA5171	5.5	46.8	248	58	arginine deiminase
E18	PA1094	6.5	49.4	686	79	flagellar capping protein FliD
E19	PA0622	5.3	41.4	538	81	probable bacteriophage protein
E20	PA5033	5.4	34.3	561	62	hypothetical protein PA5033
E22	PA4067	4.9	25.2	353	34	outer membrane protein OprG precursor
E23	PA5139	5.7	27.8	363	50	hypothetical protein PA5139

Table 4.3 (continued)

E24	PA0633	4.9	17.6	40	12	hypothetical protein PA0633
E25	PA0623	5.1	17.9	309	81	probable bacteriophage protein
E26	PA3309	5.5	16.5	340	75	hypothetical protein PA3309
E27	PA4067	4.9	25.2	89	34	outer membrane protein OprG precursor
E28	PA3021	7.6	14.5	318	68	hypothetical protein PA3021
E30	PA0807	5.9	28.7	461	70	hypothetical protein PA0807
F1	PA0423	6.1	20.8	444	80	hypothetical protein PA0423
F2	PA0423	6.1	20.8	610	82	hypothetical protein PA0423
F3	PA0320	4.7	12.6	359	66	hypothetical protein PA0320
F5	PA2659	4.9	11.2	145	44	hypothetical protein PA2659
F6	PA4578	5.9	17	174	33	hypothetical protein PA4578
F7	PA0315	6.6	15.5	109	71	hypothetical protein PA0315
F8	PA0833	8.9	24.8	140	40	hypothetical protein PA0833
F9	PA4495	5.8	24.9	226	41	hypothetical protein PA4495
F10	PA4453	9.1	23.7	374	70	hypothetical protein PA4453
F11	PA4273	9.6	24.2	43	31	50S ribosomal protein L1
F12	PA0766	7	50.3	49	7	serine protease MucD precursor

[a] Spot numbers refer to **Figure 4.3**.

[b] Data generated from peptide mass maps were compared to the translated open reading frames (ORF) for P. aeruginosa PAO1 (http://v2.pseudomonas.com).

[c] Probability score of the MASCOT database search based on an implementation of the Mowse algorithm;[538] scores greater than 50 are considered significant ($p<0.05$).

[d] Sequence coverage denotes the percentage of the protein sequence for which matching peptide fragments have been identified.

4.1.4 Results of the protein expression profiling

In total, 122 protein spots were excised from the 2D-PAGE gels and subjected to tryptic digestion and mass spectrometric analysis. Out of these, 104 could be identified by peptide mass fingerprinting (PMF) and MS/MS analyses, with a MASCOT probability score of at least 66. The probability score of the MASCOT database search is based on an implementation of the Mowse algorithm;[538] and scores greater than 50 are considered significant ($p<0.05$) for the used database(s). Additionally, the hypothetical protein PA0633, the 50S ribosomal protein L1 and the serine protease MucD precursor were identified in the extracellular protein fraction with probability scores of 40, 43 and 49, respectively.

It is noteworthy that several proteins were found to be differentially regulated in more than one location on the 2D-PAGE gels, thus resulting in the identification of a total of 66 unique proteins of *P. aeruginosa* PAO1, that were differentially regulated by induction with mimetic **18**.

To summarise, 14 out of 16 protein spots down-regulated in the intracellular fraction of *P. aeruginosa* PAO1 by induction with **18** could be identified, representing 13 unique protein species. Only BraC (PA1074), a branched-chain amino acid transport protein that binds to leucine, isoleucine, and valine was found in two different locations on the 2D gels, corresponding to slight variations in the observed pI values. Out of the 12 up-regulated protein spots in the intracellular fraction, 11 could be identified and were assigned to 9 unique proteins. In the surface-bound protein fraction of *P. aeruginosa* PAO1, 32 protein spots were found to be down-regulated, of which 25 could be identified, corresponding to 14 unique protein species, whereas from the 21 up-regulated protein spots, 20 protein species, comprising of 18 unique proteins, were identified. Finally, in the extracellular fraction, out of the 30 down-regulated protein spots, 25 could be identified, representing 21 unique proteins and from the total of 12 protein spots up-regulated after induction with **18**, 11 spots were identified, composed of 10 unique proteins. The identities of these 66 unique protein species are listed in **Table 4.4**, grouped according to the sub-cellular fractions from which they were identified.

Table 4.4 Differential regulation of the 66 unique protein species identified from mimetic-**18** challenged *P. aeruginosa* PAO1. The protein species are listed according to their functional classification in the COG database and the magnitude of the regulation is indicated by + (up-regulation in the presence of mimetic **18**) and – (down-regulation in the presence of mimetic **18**) signs; proteins identified from more than one location on the 2D gels are separated by /.

Protein identity	PA no[a]	Regulation		
		intra-cellular	surface	extra-cellular
Amino acid transport and metabolism				
Polyamine transport protein PotF2	PA0300	-	-	
Polyamine transport protein	PA0301	-		
Arginine/ornithine binding protein AotJ	PA0888	---	--	
Branched-chain amino acid transport protein BraC	PA1074	-/--		
Hypothetical ABC-type amino acid transporter	PA5139			-
Probable periplasmic binding protein	PA5153	-		
Arginine deiminase	PA5171			--
Carbohydrate transport and metabolism				
Chitinase	PA2300	++		
Probable binding protein component of ABC sugar transporter	PA3190	--		
Lipid transport and metabolism				
Long-chain fatty acid transport protein	PA1288		--/--	
Acetyl-CoA acetyltransferase	PA2001	+ +		
Acyl carrier protein	PA2966	- - -		
Energy production and conversion				
Malate synthase G	PA0482	+/++		
Lipoamide dehydrogenase	PA1587		+/++	--
Succinyl-CoA synthetase beta chain	PA1588	+++		
Succinyl-CoA synthetase alpha chain SucD	PA1589		+++	
Electron transfer flavoprotein α-subunit EtfA	PA2951		++	
Electron transfer flavoprotein β-subunit EtfB	PA2952		++	
Azurin precursor	PA4922	----	-/--/--/-- -	
Nucleotide transport and metabolism				
Adenylate kinase	PA3686	++		
Inorganic ion transport and metabolism				
Sulfate-binding protein of ABC transporter	PA1493	-		
Catalase	PA4236			-
Periplasmic glucans biosynthesis protein	PA5078			-
Secondary metabolites biosynthesis, transport and catabolism				
ABC-type transport system involved in resistance to organic solvents	PA4453			++
Cellular processes and signaling				
Cell motility				
Flagellin type B FliC	PA1092	--	+	
Flagellar capping protein FliD	PA1094		+	--/--/--/--
Cell wall/membrane biogenesis				
Outer membrane porin OprE precursor	PA0291		--/--	--
Peptidoglycan-associated (lipo)proteins	PA0833			++
Outer membrane porin protein OprD precursor	PA0958		--/--/---	
Outer membrane protein H1 precursor	PA1178		--/-	
Outer membrane protein OprF precursor	PA1777	+/++	++/--/--	
Outer membrane protein OprG precursor	PA4067	--	-/--/---	-/--

Table 4.4 (continued)

Posttranslational modification, protein turnover, Chaperones				
Alkyl hydroperoxide reductase subunit C	PA0139	+ +		
Serine protease MucD precursor	PA0766		++	+
Peptidyl-prolyl cis-trans isomerase SlyD	PA0837	+		
Heat shock protein HtpG	PA1596		+	--
Peptidyl-prolyl cis-trans isomerase A PpiA	PA3227		-	
GroEL protein	PA4385		+/++	
GroES protein	PA4386		++	
DnaK protein	PA4761		+	
Defence mechanisms				
Negative regulator of beta-lactamase expression	PA0807			-
Signal transduction mechanisms				
Twitching motility protein PilH	PA0409		-	
Translation				
30S ribosomal protein S1 RpsA	PA3162		+	--
Elongation factor G FusA1	PA4266		+	-
50S ribosomal protein L7 / L12	PA4271		+++	
50S ribosomal protein L1	PA4273			+
General function prediction only				
Phage tail sheath protein FI	PA0622			-
Phage tail tube protein FII	PA0623			-
Function unknown				
Hypothetical protein	PA0315			++
Predicted membrane protein	PA0320			++
Uncharacterized protein conserved in bacteria	PA0329		+++	
Hypothetical protein	PA0388	-	--	
Uncharacterized conserved protein	PA0423			++/++
Hypothetical protein	PA0572			-
Hypothetical protein	PA0633			-
Uncharacterized protein conserved in bacteria	PA0852			--
Predicted periplasmic/secreted protein	PA0946		+	
Uncharacterized protein conserved in bacteria	PA1657	-		
Predicted periplasmic/secreted protein	PA2659			+++
Probable outer membrane protein	PA2760		--	
Uncharacterized conserved protein	PA3021			-
Hypothetical protein	PA3309			--
Probable endoproteinase Arg-C precursor	PA4175			-
Hypothetical protein	PA4495		++	+
Hypothetical protein	PA4578			++
Hypothetical protein	PA5033			-
Hypothetical protein	PA5178	++		
Hypothetical protein	PA5472		-	

[a] Data generated from peptide mass maps were compared to the translated open reading frames (ORF) for *P. aeruginosa* PAO1 (http://v2.pseudomonas.com).

In order to classify the identified proteins, as well as to allow inference of possible functional roles, the Conserved Domain Database (CDD),[6] the Cluster of orthologous groups database (COG),[7] and the Pseudomonas Genome Database[537][8]

[6] http://www.ncbi.nlm.nih.gov/Structure/cdd/wrpsb.cgi
[7] http://www.ncbi.nlm.nih.gov/Structure/cdd/cdd.shtml
[8] http://v2.pseudomonas.com/search.jsp

were searched using the results of the protein identification. The functional classification of the identified proteins according to the categories of the COG-database, is included in **Table 4.4**, and summarised graphically in **Figure 4.4**.

It can be seen from **Table 4.4** and **Figure 4.4** that the majority of differentially regulated proteins for which functional classes could be assigned from the COG database are involved in central cellular housekeeping functions, such as transport and metabolism of amino acids (7), energy production and conversion (7), cell wall/membrane biogenesis (6), and in the posttranslational modification (PTM) of proteins (7). However, a large proportion of identified protein spots was found to be either functionally poorly characterised or functionally uncharacterised. More precisely, for two proteins down-regulated in the extra-cellular fraction after induction with mimetic **18** (PA0622, PA0623), only general predictions of function as phage tail sheath or tube proteins could be made. Furthermore, the function of 20 of the uniquely identified proteins is still unknown. It is noteworthy that almost all proteins for which no putative function could be assigned were identified either from the extracellular or the surface-bound protein fraction, whereas only three were found in the intracellular fraction of *P. aeruginosa* PAO1.

As already mentioned, several proteins were identified in more than one spot, but additionally, it was also often the case that a given protein species was found to be differentially regulated in more than one sub-cellular fraction. For instance, there were 11 proteins that could be found in two different fractions, and the outer membrane protein OprG (PA4067) was identified in all three sub-cellular fractions. The identification of a protein from separate spots on the same 2D gel is readily explicable by posttranslational modifications (PTM) of the proteins, such as phosphorylation, glycosylation, acetylation and C-terminal amidation on the one hand, or by the aggregation of proteins into homo- respectively hetero-multimeric complexes on the other hand, both being processes which can substantially influence the pI and/or the molecular mass of the protein species. The utility of gel-based proteomics for assessing PTMs has been mentioned, and the high proportion of proteins identified from more than one location on the 2D gels suggests that posttranslational processing might play an important role in the effects of mimetic **18** on *P. aeruginosa* PAO1.

Apart from the obvious possibility that the expression of a given protein might be simultaneously affected by **18** in different sub-cellular fractions, the identification

of a differentially regulated protein species in more than one sub-cellular fraction may also be an artefact of the fractionation protocol. Moreover, and of special interest with respect to AMPs, it is also conceivable that the impairment of membrane structure and/or integrity could lead to the redistribution of protein species between different sub-cellular fractions, for example by releasing intracellular or surface-bound compounds into the surrounding medium. The latter possibilities should be taken into account when considering proteins that are found in sub-cellular fractions in which their presence is not expected based on their functional classes or protein reference maps, if such assignments exist. For example, the 30S ribosomal protein S1 (PA3162) was found to be down-regulated in the extracellular fraction of *P. aeruginosa* PAO1 after induction with mimetic **18**. It has to be mentioned, however, that the ribosomal S1 protein, which is involved in non-specific mRNA binding, is known to be only loosely attached to the 30S subunit.[539]

While the majority of proteins that were found in more than one location on the 2D gels of a given sub-cellular fraction were characterised by variations in the observed pI values, there were, in addition, larger deviations from the theoretically expected molecular masses for several of the outer membrane proteins isolated in this study. For example, the outer membrane protein OprF precursor (PA1777) was identified twice as down-regulated in the surface-bound protein fraction of *P. aeruginosa* PAO1. Both spots corresponding to PA1777 in the control culture were located at positions on the gel that correlate well with the theoretical pI and molecular mass of OprF, being separated only slightly with respect to their pI. However, in the fraction up-regulated by induction with mimetic **18**, PA1777 was identified from a protein spot corresponding to a much lower molecular weight (~ 20 kDa vs. 37.8 kDa) and also at slightly lower pI (~ 4.2 vs. 5.0), than would be expected theoretically. It is worth mentioning that the outer membrane protein OprF precursor (PA1777), or rather some of its post-translationally modified forms, was the only protein species identified to be both up- and down-regulated in the same sub-cellular fraction. Similar behaviour, namely the isolation of protein species from gel locations corresponding to a significantly lower molecular mass than to be expected theoretically, was also found for the outer membrane protein OprG (PA4067). OprG, which was identified as down-regulated simultaneously in all sub-proteomes, was located at positions on the gels corresponding to the theoretical pI/Mr values (pI = 4.9,

M_r = 25.2 kDa), but also at positions corresponding to a lower molecular weight (M_r ~ 15 kDa or ~ 12 kDa).

Several general trends can be extracted from the expression patterns according to the assigned functional classes. For instance, all unique protein species identified to be functionally involved in amino acid transport and metabolism were negatively affected by induction with mimetic **18** (8 out of 8), and furthermore, almost all proteins assigned as playing a role in either energy production and conversion (6 out of 7), or in the post-translational modification of proteins and in protein turnover (9 out of 10) were up-regulated in at least one of the sub-cellular fractions, after induction with **18**.

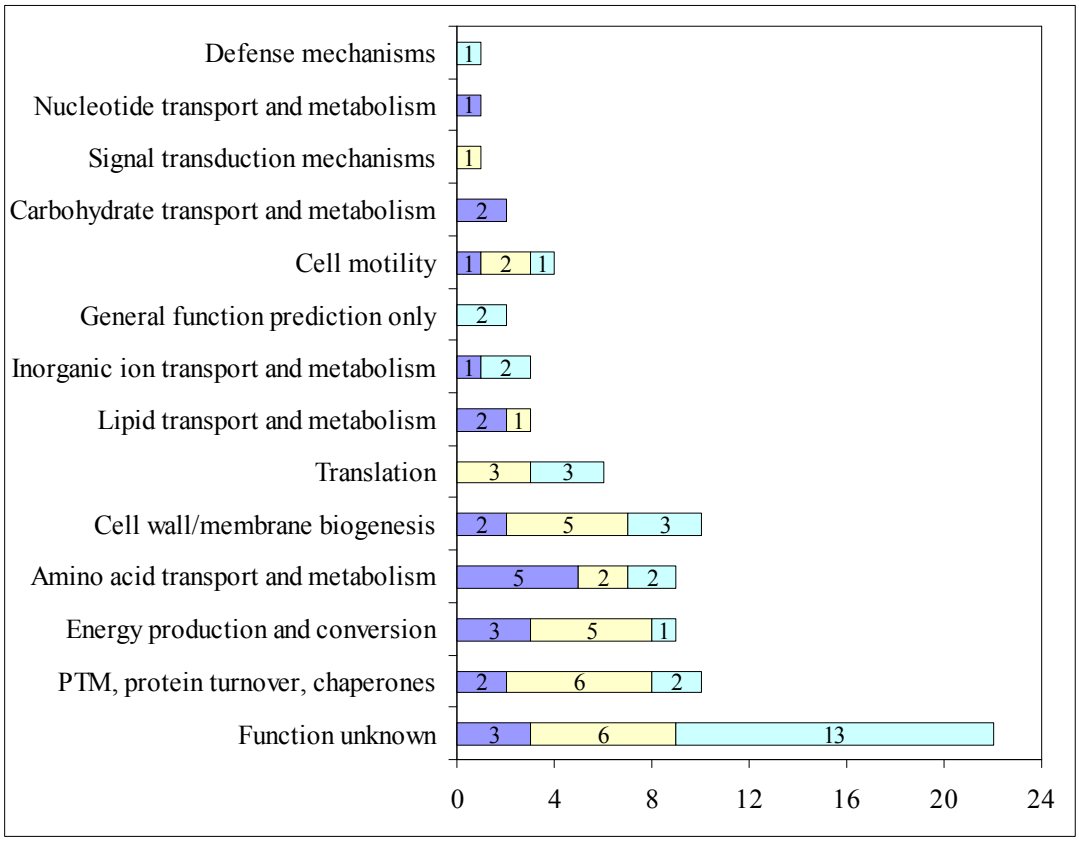

Figure 4.4 Functional classification of the identified protein species differentially expressed by mimetic **18** treated *P. aeruginosa* PAO1. The functional classes correspond to the nomenclature of the COG database, and the occurrence in different sub-cellular fractions is indicated by different colouration of the horizontal bars (blue = intracellular; beige = surface-bound; turquoise = extracellular).

The largest changes in the proteome expression patterns as assessed by visual inspection was the down-regulation of the azurin precursor (PA4922) in the intracellular, as well as in the surface-bound protein fraction of *P. aeruginosa* PAO1.

In total, azurin was identified once in the intracellular, and four times in the surface-bound protein fraction of the *P. aeruginosa* control culture. It is noteworthy that all protein spots from which azurin was identified correlate well with the theoretical M_r and pI value, apart from the spot C25, which shows a decrease in pI of about 1 unit. Azurin is a blue copper protein (cupredoxin) that has been shown to be able to act as an electron donor for nitrite reductase (NIR) in a variety of *in vitro* experiments.[540]

However, it has been demonstrated by the use of strains deficient in azurin, that this protein is not required for denitrification in *P. aeruginosa*.[541] Similar experiments established that azurin plays no obligatory role as electron acceptor for either aromatic amine dehydrogenase or ethanol dehydrogenase, both activities with which the protein has been formerly associated.[541] Furthermore, it has been shown that azurin expression is induced either by transition from the exponential to the stationary growth phase or by anaerobiosis.[541] Based on the sensitivity of an *azu* mutant of *P. aeruginosa* towards reactive oxygen species (ROS), it has been proposed that a functional role of azurin might consist of responding to oxidative stress.[541]

Recently, it was found that azurin was up-regulated together with flagellin (PA1092) and flagellar capping protein (PA1094), in the extracellular protein fraction of either an *rsmY rsmZ* double mutant or a *gacA* mutant of *P. aeruginosa*, which both show reduced synthesis of the quorum sensing signalling molecule *N*-butanoyl-homoserine lactone.[542] Interestingly, the expression of both flagellin and the flagellar capping protein was also found to be affected by mimetic-**18**, although with a different and more diverse pattern than in the above mentioned study. That is, whereas flagellin was down-regulated in the intracellular fraction, both proteins were up-regulated in the surface-bound fraction of *P. aeruginosa* PAO1. Remarkably, the most apparent changes in the expression pattern for the flagellar capping protein FliD, which was found down-regulated in the extracellular fraction, were delineated from four different protein spots that showed a large spread in pI, as well as in molecular mass.

Apart from azurin, all other proteins that were identified as being functionally related to energy production and conversion were found to be up-regulated. In particular, succinyl-CoA synthetase α and β chains (PA 1588, PA1589), which are involved in the tricarboxylic acid cycle, together with a lipoamide dehydrogenase (PA1587) and malate synthase (PA0482) were up-regulated in the intracellular or

surface-bound protein fraction, respectively. Moreover, electron transfer flavoprotein subunits A and B (PA2951, PA2952) were found to be up-regulated in the surface-bound fraction.

The majority of proteins involved in the transport of amino acids, carbohydrates, lipids or other metabolites were found to be down-regulated after induction with mimetic **18**. In particular, transport proteins found to be down-regulated included two polyamine transport proteins (PA0300, PA0301), the arginine/ornithine binding protein AotJ (PA0888),[543] a hypothetical ABC-type sugar transporters (PA5139), a hypothetical ABC-type amino acid transporter (PA3190), a sulphate binding protein (PA1493), a branched amino acid binding protein (PA1074), a long chain fatty acid transport protein (PA1288), and a hypothetical periplasmic binding protein (PA5153). The only transport system found to be up-regulated was an ABC-type transport system involved in resistance to organic solvents (PA4453).

Additionally, the expression profiles of outer membrane proteins after induction with mimetic **18** were also found to be characterised predominantly by down-regulation. For instance, OprE (PA0291; surface and extracellular fraction) and the basic amino acid specific OprD (PA0958; surface fraction) were found to be under-expressed in cell cultures treated with **18**. Notably, OprD has been reported to be involved in the uptake of the antibiotics imipenem and meropenem,[544] and in the response to oxidative stress, as induced by copper.[545] Other down-regulated proteins comprise OprH (PA1178; surface fraction) and OprG (PA4067; all fractions), which belongs to the OmpW outer membrane protein family. On the other hand, OprF (PA1777) was found to be differentially regulated in the intracellular and the surface-bound protein fractions (vide supra). OprF is the major outer membrane protein of *Pseudomonas spp.* and is thought to play a role during growth in environments characterised by low osmolality, in adhesion to supports such as roots or exogenous macromolecules, and in the maintenance of cell shape.[546] Interestingly, it has been demonstrated recently that *P. aeruginosa* OprF binds to interferon-γ, highlighting the possibility that pathogens might be able to sense alterations in the immune function of the host.[547] Finally, a hypothetical membrane protein (PA0833),, belonging to the OmpA family, was also found up-regulated in the extracellular sub-proteome.

The heat shock response is a mechanism elicited in all organisms as a reaction to an increase in temperature as well as to other exogenous stress factors. The heat

shock response consists of the enhanced synthesis of heat shock proteins (HSPs), such as chaperones, chaperonins, proteases which remove misfolded polypeptide chains, or isomerases which aid in the refolding or reformation of native disulfide bonds.[548] From the protein expression profiles, it was found that the group I chaperonins, GroEL and GroES, as well as the chaperone DnaK, the prokaryotic homolog of the eukaryotic Hsp70, were up-regulated. Additionally, the prokaryotic analogue of Hsp90, HtpG was found up-regulated in the surface-bound fraction, yet down-regulated in the extracellular fraction. Furthermore, MucD, an endoprotease presumed to be involved in the proteolysis of misfolded periplasmic proteins,[549] was up-regulated in the surface and extracellular fractions. Two peptidyl-prolyl *cis-trans* isomerases, SlyD and PipA were found to be affected by **18** in a differential manner, that is SlyD was up-regulated intra-cellularly and PipA was down-regulated in the surface-bound fraction. Peptidyl-prolyl *cis-trans* isomerases catalyse the interconversion of *cis-trans* peptide bonds preceding proline residues, and are involved in protein folding.[550] They play a role in the heat-shock response, but are also thought to be involved in processes such as cellular signalling (c.f. **Section 3.2**).[551] Additionally, SlyD has been implicated to be involved in the hydrogenase pathway of *E. coli* by aiding the [NiFe] metallo-centre biosynthesis.[552]

Additionally, the expression of several ribosomal proteins was affected by **18**, notably in the surface-bound and/or extracellular fractions. The most prominent changes with respect to ribosomal proteins were detected for the L7/L12 ribosomal protein. L7 is the *N*-terminally acetylated form of L12, and both proteins are often referred to more generally as L7/L12. Tetramers of L7/L12 make up a flexible protuberance of bacterial ribosomes, also called the ribosomal stalk,[553] and this structure is involved in binding translational factors as well as in GTP hydrolysis.[554] Interestingly, the prokaryotic elongation factor G was also found to be up-regulated by mimetic-**18**. Recently, there have been increasing reports of ribosomal proteins carrying out extra-ribosomal functions,[555, 556] and although such functions have not been associated with L7/L12, the L12 fold has been related to the RRM fold of RNA binding proteins,[557] and to the ovomucoid proteinase inhibitor.[558] Additionally, a 3α-hydroxysteroid dehydrogenase from *Pseudomonas testosteroni* has been found to be homologous to a fusion of the bacterial L10 and L7/L12 genes.[559, 560]

Finally, four more proteins from different functional classes should be mentioned which showed large differences in the protein expression profiles after induction with **18**. Chitinase (PA2300), was found up-regulated in the intracellular fraction, as was acetyl-CoA acetyltransferase (PA2001) and also adenylate kinase (PA3686), which has been shown to be a virulence factor of *P. aeruginosa*.[561] Acyl carrier protein, on the other hand, was found to be down-regulated in the intracellular fraction of *P. aeruginosa*.

4.1.5 Conclusions of the protein expression profiling

The analysis of the protein expression patterns of the three sub-fractions of *P. aeruginosa* PAO1 after induction with mimetic **18** led to several interesting results with respect to possible modes of action of our AMPMs. First of all, it should be mentioned that it was possible to incubate the bacterial cells with a concentration of **18** that did not completely suppress bacterial growth for at least one generation time under the experimental conditions. This situation is to be contrasted with the behaviour of gramicidin S, for which Bandow et al. found that after reaching a threshold concentration, rapid lysis of the bacterial cells occurred, thus complicating the recording of protein expression profiles.[520]

For our protein expression profiles, it was found that a high proportion of the proteins that were shown to be affected by induction with **18** were functionally related to transport and uptake processes of the bacteria, such transport proteins being involved in the uptake of certain amino acids or a variety of outer membrane proteins, which are often implicated in the uptake of small hydrophilic molecules. Additionally, the expression of a variety of so-called heat-shock proteins was found to be significantly up-regulated in the mimetic **18** treated cells.

With respect to possible modes of action for AMPMs, it is of interest to compare the protein expression profiles obtained to the results available from other proteomic and transcriptional analyses. For example, the report by Bandow et al. documents the induction of class I heat shock proteins (GroE, GroEL, and/or GroES) in *B. subtilis* by those inhibitors of protein biosynthesis that affect the fidelity of the translation process, namely the aminoglycosides gentamicin, streptomycin, and kanamycin.[520] Since the expression of class I heat shock proteins in these instances is thought to be induced by the appearance of misfolded proteins, it is conceivable that

any kind of process that leads to the increased formation of corrupted proteins should elicit similar responses. Not surprisingly, therefore, class I HSPs were also found to be induced by puromycin, which causes abortive translation, or diamide (*N*,*N*,*N*',*N*'-tetramethylazodicarboxamide), which causes the formation of non-native inter- and intramolecular disulfide bonds. Similar results of increased expression of HSPs in a concentration-dependent manner after treatment with aminoglycosides have been described for *E. coli*, and based on these findings, HSPs were suggested to be a proteomic signature for impaired ribosome function.[514]

It is interesting to recall, in this respect, that the flexible ribosome stalk, which largely consists of L7/L12, is thought to confer proof reading abilities to the bacterial ribosome and thus to play an important role in the control of translational accuracy.[562] For instance, it has been shown that mutations of evolutionarily conserved residues in the C-terminal domain of *E. coli* L7/L12 lead to increased nonsense codon read-through *in vivo*, and to an increased rate of missense errors *in vitro*.[563] It is noteworthy that L7/L12 was one of the proteins that showed large changes in expression, that is, it was found to be strongly up-regulated in the surface-bound protein fraction after induction with **18**. It should also be recalled that the studies on the incorporation of radio-labelled precursors of macromolecular biosynthesis showed that the rate of incorporation of labelled leucine was not primarily reduced by mimetic **18**, but this result would not be incompatible with defective protein biosynthesis.

However, translating overexpression of HSPs into a proteomic signature for antibiotic action involved in misfolding or defective synthesis of proteins would be too simplistic. Problems in associating antibiotic action with such a proteomic signature arise, for example, since HSPs are also reported to be affected by other factors, such as the physiological state of the bacterial cell or oxidative stress;[564-566] the results of these studies are, however, sometimes not unambiguous. For instance, the amount of heat shock proteins DnaK and GroEL was found to be increased in *E. coli* growing to a high cell density together with alkyl-hydroperoxide reductase, and these changes were attributed to an increased level of misfolded proteins and increased level of oxidative stress caused by the high cell density of the cultures.[566] Similarly, oxidative stress elicited in *Porphyromonas gingivalis* cell cultures grown under hemin limitation, led to increase expression of the heat shock proteins HtpG, GroEL, DnaK.[567]

In contrast to this, a different picture arose from the analysis of the protein expression profiles of *S. aureus* cells in the stationary or exponential growth phase.[564] With respect to heat shock proteins, the authors of this study found that DnaK and the co-chaperones GroE, GroEL, and GroES were all down-regulated, and attributed this effect to the decreased translational activity in stationary phase cells, concomitant with a reduced "protein stress". On the other hand, several proteins to which roles in the response to oxidative stress have been attributed, such as the above mentioned alkyl-hydroperoxide reductase, as well as catalyse, superoxide dismutase, and thioredoxin reductase, were found to be up-regulated.[564] Alkyl hydroperoxide reductase was also found to be up-regulated in the response of *Bacillus subtilis* towards superoxide and peroxide stress,[568] and if one attributes to this protein a function as marker of oxidative stress, then it is of interest to recall that alkyl hydroperoxide reductase was found to be up-regulated in the mimetic **18** treated intracellular protein fraction. Of course, it should be emphasised that most of the published expression profiles were not obtained with *Pseudomonas spp.,* and therefore caution should be taken not to draw too close analogies.

The differential regulation of a variety of different proteins involved in chaperone function and stress response for cells under different growth conditions are also of interest with respect to the observed down-regulation of azurin in the intracellular and surface-bound protein fractions after induction with **18**. That is, since the expression of azurin has been associated with stationary phase growth or anaerobiosis, the absence of the corresponding protein spots/species from mimetic **18** treated cells might arise from higher cell density experienced by the control cultures. On the other hand, the expression patterns of mimetic **18** treated cells with respect to the above mentioned HSPs, alkyl hydroperoxide reductase, and the variety of outer membrane proteins, show no apparent similarity with those obtained from high density or stationary phase cell cultures. Moreover, the publication by Kay et al. also demonstrates that increased expression of azurin can occur under conditions that are not related to high cell density conditions.[542]

Furthermore, interesting conclusions can be drawn from the expression profiles of the outer-membrane proteins that, notably, made up a large fraction of mimetic **18** affected proteins, with respect to the resistance of *P. aeruginosa* towards antimicrobial agents. For example, the protein expression profiles of sarcosine-insoluble outer membrane fractions obtained with strains of *P. aeruginosa* resistant

towards the antibiotics ampicillin, kanamycin, and tetracycline have been studied. [569] It was found that in these cases, OprF was up-regulated in all three resistant strains, whereas OprH was up-regulated in bacteria resistant to the first two antibiotics, and OprD was over-expressed in a strain resistant to tetracycline. Additionally, the outer membrane protein OprG was found to be down-regulated in the strains resistant to kanamycin and tetracycline. It is well established that an increased expression of OprH is connected to resistance of *P. aeruginosa* towards aminoglycoside antibiotics, the cationic peptide antibiotic polymyxin B, or the chelating agent EDTA.[570] In *P. aeruginosa*, the PhoP-PhoQ two-component regulatory system responds to magnesium limited growth conditions by auto-regulating the *oprH-phoP-phoQ* operon. OprH is known to be over-expressed when cells are grown under magnesium limiting conditions,[571] and protein expression profiles of *P. aeruginosa,* determined under magnesium limiting growth conditions, showed a high increase in expression of OprH in the membrane sub-proteome.[572] The PhoP-PhoQ two-component regulatory system has been implied in resistance to the above mentioned cationic antibiotics, as well as to antimicrobial peptides under magnesium limiting growth conditions.[573] Recently, a second two-component regulatory system, PmrA-PmrB has been associated with the response of *P. aeruginosa* to growth under magnesium limiting conditions, and with the regulation of resistance towards cationic antibiotics and antimicrobial peptides, such as LL37 and indolicidin.[574]

The increased resistance of *P. aeruginosa* under magnesium limiting growth conditions is thought to be mediated via induction of a LPS modification system by the PhoP-PhoQ, and/or the PmrA-PmrB regulatory systems, which leads to the synthesis of a less negatively charged lipid A moiety.[575] Interestingly, in *P. aeruginosa* the induction of the *oprH-phoP-phoQ* operon by polyamines such as spermidine,[576] was observed and the *pmrA-pmrB* operon has been shown to be activated by cationic antibiotics and antimicrobial peptides,[574] whereby AMPs that displayed lower MIC values were found to be weaker inducers of the *pmrA-pmrB* operon.

However, it has been found from the evaluation of our protein expression profiles that the regulation of the outer membrane protein OprH was negatively affected by induction with **18**. Moreover, McPhee et al. studied isogenic *phoP* and *pmrA* mutants of *P. aeruginosa* grown under magnesium limiting conditions via transcriptional profiling,[577] and it is noteworthy that none of the 36 gene products

that were reported to be regulated by PmrA could be identified from our protein expression profiles. Similarly, only two out of 19 gene products could be identified from the expression profiles that were described to be regulated by PhoP, with an additional discrepancy being the direction of regulation of OprH. Furthermore, no differential regulation of either PhoP or PhoQ could be detected in our protein expression profiles. Therefore, there is no experimental evidence that would point towards an activation of either the *oprH-phoP-phoQ* or the *pmrA-pmrB* operon by **18**.

These findings are also of special interest with respect to potential therapeutic applications of our AMPMs, since they indicate that these molecules might be less prone to cause resistance towards cationic AMPs or other cationic antibiotics via the above mentioned mechanisms. It is interesting to note that polyphemusins have been demonstrated to be, on the one hand, almost unaffected by PmrA-PmrB mediated resistance, and on the other hand, to show a very low tendency to activate the *pmrA-pmrB* operon, when compared to other AMPs such as indolicidin, or to a linear analogue of polyphemusin.[574] The importance of β-hairpin AMPs such as polyphemusin as starting points for AMPMs was discussed in **Section 1.5**. Finally, it should be mentioned that since AMPs of diverse structure and origins are capable of activating the PhoP-PhoQ regulatory system, presumably by displacing magnesium cations from an acidic patch on the surface of PhoQ,[578] such a mechanism is unlikely to account for the stereospecificity of mimetic **18**.

To summarise, the protein expression profiles of *P. aeruginosa* PAO1 induced with **18** suggest that the AMPM inflicts protein folding stress on *P. aeruginosa* cultures. Furthermore, the amount of protein folding stress might be under estimated, if the presumably higher rate of protein synthesis in the control cultures and/or the higher expression of heat shock proteins in cultures of higher cell density are considered. Due to the lack of a reference database of expression profiles from *P. aeruginosa* challenged by antibiotic stimuli, it is not possible to make a reliable prediction of an actual mode of action for mimetic **18** at this stage. Nevertheless, the expression profiles might prove valuable in rationalising and validating putative targets of mimetic **18** that may be identified from other, independent methodologies (c.f. **Section 4.2-4.3**).

By comparison of the expression profiles seen here to the *B. subtilis* reference database of Bandow et al,[520] impairment of ribosome fidelity emerges as a possible

starting point for further studies. Due to the highly charged nature of **18**, the question of the specificity of a putative AMPM-ribosome interaction is immediately raised, not least because of the acidic character of L7/L12 (pI = 4.7). However, any complete mechanistic interpretation of the anti-pseudomonal activity of **18** has to satisfactorily account for its stereospecificity, and it would also be conceivable that the uptake of mimetic **18** into *P. aeruginosa* depends on a stereospecific interaction with cell wall/membrane components. Such specific uptake could, for example, be mediated by a variety of outer membrane or transport proteins, and a large proportion of proteins belonging to both functional classes were shown to be negatively affected in their expression by **18**. An illustrative example that outer membrane proteins are able to transport polypeptides into bacterial cells is given by the *E. coli* outer membrane protein OmpW. OmpW, which is related to OprG in *P. aeruginosa*, was found to be involved in the uptake of colicin S4, a group A bacteriocin, into susceptible strains of *E. coli*.[579] The often remarkably high selectivities of bacteriocins have been described in **Section 3.3.2**, and interestingly, OprG was found in this work to be down-regulated in all sub-cellular fractions.

4.2 Direct approaches towards target identification

4.2.1 Affinity chromatography of AMPMs

Affinity chromatography (AC) is a widely used chromatographic separation technique based on the reversible interaction of a target macromolecule or a target complex with a specific ligand that has been immobilised on a solid support (affinity matrix). Most frequently, AC is used for the preparative purification of macromolecules, and in such applications purification levels of several thousand-fold are routinely achieved in a single step. Major advantages of AC comprise high selectivity, high resolution, high recovery, and isolation of the target compound(s) in concentrated form.

The main requirement for the successful application of AC is the availability of a ligand specific for the target molecule(s); common examples of frequently used ligand/target combinations are lectins/polysaccharides, complementary base sequences/nucleic acids, glutathione/GST fusion proteins, metal ions such as Ni/poly-His fusion proteins, avidin or streptavidin/biotinylated molecules, and antibody/antigen (immuno-affinity chromatography).

Additionally, AC is used in proteomic studies to increase sensitivity, either by removing from a complex protein mixture (classes of) proteins that might interfere with the 2D-PAGE analysis, or by concentrating (classes of) proteins which are not abundant enough to be detected.[580] Moreover, AC is an integral part of non-gel based quantitative proteomic techniques such as ICAT, in which biotinylated isotope labelled peptide fragments are purified by avidin affinity chromatography before they are analyzed by mass-spectrometric methods.[581]

4.2.1.1 Affinity chromatography and target identification

Apart from the above mentioned applications in the purification of known target molecules or classes of target molecules, AC is also a valuable tool for target identification following phenotypic screening. In this regard, AC seeks to exploit interactions of lead compounds with putative target molecule(s). Several successful examples exist of the application of AC techniques to the target identification

problem. For example, FKBP was discovered by an AC approach to be the molecular target of FK-506, an important immuno-suppressant.[582] Other examples comprise the identification of histone deacetylases as targets for the fungal metabolite trapoxin,[583] or of ATP citrate lyase as a target for the macrolide radicol.[584] The use of biotinylated analogues of the insect Pro/Arg-rich AMP pyrrhocoricin in the identification of DnaK as a putative target for this class of AMPs has been described in detail in **Section 2.1.2.1**.

However, it should be emphasised that successful examples of molecular targets identified by AC described in the literature typically operate with a combination of a high affinity small molecule ligand interacting with at least fairly abundant target molecules. Before examining the AC experiments with AMPMs derived from protegrin-1 in detail, it will be illustrative to summarise briefly the principles of AC, with special emphasis on aspects concerning the use of AC for target identification.

4.2.1.2 Principles of affinity chromatography

A typical AC experiment consists of three basic steps listed below; a theoretical chromatogram illustrating these steps is shown in **Figure 4.5**:

1. equilibration of the affinity matrix.
2. sample application under conditions that favour the binding of the target molecule(s).
3. elution under conditions that favour the dissociation of the ligand target complex(es).

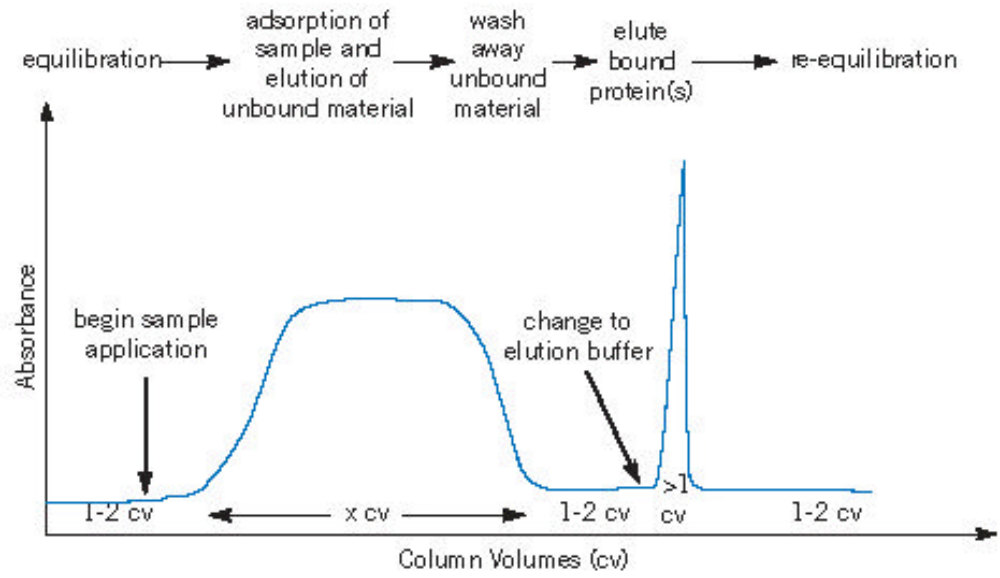

Figure 4.5 Schematic representation of an affinity chromatography experiment.

First of all, the ligand has to be immobilised onto a solid support, in order to create the affinity matrix. This is generally achieved by coupling the ligand covalently to the resin, although attachment via exceptionally strong non-covalent interactions, such as avidin/streptavidin/biotin or antibody/antigen is also possible. Typical methods for immobilising ligands comprise the use of NHS-activated supports (via amino groups), CNBr-activated supports (via amino groups), epoxide functionalised supports (via nucleophiles in general), or the use of amino-functionalised supports (via carboxylic acids).

Of paramount importance for AC is that the ligand retains its activity after the immobilisation step. To achieve this, the incorporation of a spacer arm between the matrix and the ligand is often necessary, especially in such cases where the binding site is located deep inside the target molecule. The steric repulsion from the affinity matrix is expected to be more severe for small molecule ligands and might also be a concern for AMPMs, which are of intermediate size. On the other hand, potential linkers should not be longer than necessary for optimal activity, since they can also lead to unspecific binding of macromolecular components, for example, via hydrophobic interactions.

The potential problem of losing affinity upon immobilisation applies to all chemical genetics/proteomics approaches in which a tag, a label other than an isotope label, or other reactive functionality is introduced into the molecule. Indeed, the problem is more severe for target identification applications, since during purification

of known target molecules, parameters such as the target affinity of the immobilised ligand can readily be verified.

The elution of bound target molecules from the affinity matrix can be achieved by both selective and non-selective methods. Commonly, non-specific elution is achieved by altering the pH, the ionic strength, or the polarity of the buffer system, in order to weaken ligand/target interactions, which can depend on electrostatic interactions, hydrophobic interactions, hydrogen bonding or van der Waals forces. On the other hand, target molecule(s) can be eluted selectively by supplementing the elution buffer with a competitive ligand. These ligands can disrupt ligand/target interactions by binding selectively either to the ligand or to the target molecule, thus leading to displacement of the target molecule from the affinity matrix. Ideally, the free ligand can be used for competitive elution, if it is available in sufficient quantities. The use of ligands with very high affinity might necessitate denaturing elution conditions such as the addition of chaotropic reagents and/or detergents to the buffer system. For example, streptavidin binds biotinylated molecules with such high affinity that they are generally eluted by boiling the affinity matrix in SDS buffer systems. Whereas the use of such harsh conditions can be problematic or impossible if one is interested in the isolation of a functional compound, the isolation of a native target molecule is not necessary for target identification by mass spectrometric or other sequencing methods.

Finally, for target identification by AC it is desirable to include an additional washing step into the experiment that is as stringent as possible, in order to remove proteins that might be bound non-specifically to the affinity matrix. However, again it is not possible to decide *a priori* how extensive the washing step can be made without dissociating the ligand/target interactions.

4.2.1.3 AMPMs as ligands for affinity chromatography

In general, peptidic compounds display several potential attachment points for their capture on solid supports. Whereas the immobilisation of proteins via reactive side-chains is carried out routinely, and is generally applicable because it does normally not introduce large structural alterations to the binding site, the same might not be true for smaller peptides such as the AMPMs. That the introduction of alternative functionality into AMPMs can severely impair their biological activity has

been demonstrated amply by the DANA-labelled library of mimetic-**17** (c.f. **Section 3.8.3.3**).

However, the scaffolds of AMPMs in general and the scaffolds of mimetics **18** and **19** in particular offer a large fraction of residues that might be attached to solid supports. More precisely, both **18** and **19** possess five lysine residues that could be covalently linked to create an affinity matrix. A first indication of the potential feasibility of unselective attachment of AMPMs to solid supports derives from an alanine scan on mimetic **18**, carried out in our group by N. Srinivas.[139] Therein, it was discovered that the anti-pseudomonal activity of the alanine analogues of **18** was insensitive towards alanine substitution except at the two aromatic positions. Apart from replacement of Trp-2 and Trp-8, which led to loss of the anti-pseudomonal activity, all other analogues were comparable in activity to the parent compound and, in fact, mimetic **19** was discovered during these studies as a new antimicrobial lead compound.

However, the alanine scan does not take into account steric influences of the solid support on the MIC values, and therefore a method of immobilisation which allows for site-specific immobilisation of AMPMs might be desirable. A variety of approaches exist for selectively immobilising peptidic compounds containing multiple reactive functionalities. For example, the increased nucleophilicity of hydrazines or thiols, the use of an orthogonal functionality such as an aldehyde, or the use of strong non-covalent interactions such as biotin/streptavidin are possible. Methods of introducing additional functionality into the AMPM framework have been discussed in **Section 3.8**.

For the incorporation of a handle into the scaffold of mimetic-**19** that allows for its site-specific immobilisation, again a strategy employing SPPS was used, with commercially available *N*-α-Fmoc-*N*-γ-(*N*-biotinyl-3-(2-(2-(3-aminopropyloxy)-ethoxy)-ethoxy)-propyl)-L-glutamine (Fmoc-Glu(biotinyl-PEG)-OH; **79**; **Figure 4.6**). **79** was chosen to allow for capture of mimetic **19** onto an avidin or streptavidin-functionalised solid supports, and since biotin represents a versatile functionality that can be used in a variety of applications (vide infra). Moreover, **79** contains a 15 atom hydrophilic PEG spacer arm, that is not prone to unspecific hydrophobic interactions and which also allows for better estimation of steric influences on the anti-pseudomonal activity of mimetic **19**.

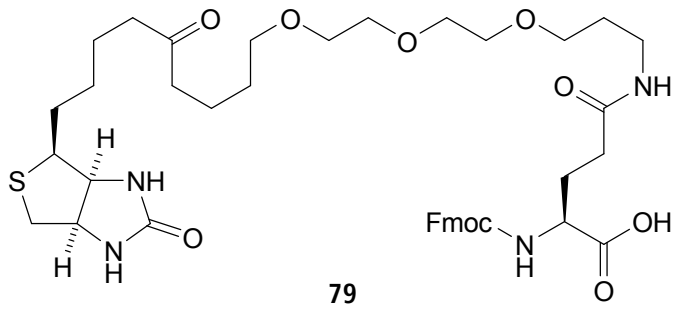

79

Figure 4.6 Fmoc-Glu(biotinyl-PEG)-OH (**79**) used for the synthesis of biotinylated analogues of mimetic **19**.

79 was incorporated into the scaffold of mimetic **19** by single replacement of all residues except Trp-2, Trp-8 and the D-Pro-L-Pro template. The synthesis of the biotinylated analogues was carried out according to our standard protocol for the synthesis of AMPMs outlined in **Section 3.1** and described in detail in **Section 5.2**. The biotin functionality was incorporated into the peptide chain by manually coupling 1.5 equivalents of **79** using 1.45 equivalents of HATU as activating reagent and 3.0 equivalents of DIEA. Crude peptides were purified by RP-HPLC and determined to be of at least 98% purity by analytical HPLC. ESI mass spectrometric and analytical HPLC data are summarised in **Appendix 2**. The biological activities of the biotinylated analogues of mimetic **19** were determined against our panel of test micro-organisms and are summarised in **Table 4.5**. It can be seen, that the scaffold of mimetic **19** is surprisingly tolerant to the introduction of Glu(biotinyl-PEG)-OH. Incorporation of biotin functionality replacing residues Thr-1 and Lys-12, which flank the D-Pro-L-Pro template, leads to analogues (**80** and **89**) with excellent anti-pseudomonal activity. More precisely, the activities are of the same order of magnitude as for **19**. Although for some compounds there is a larger decrease in the biological activity, they all display the same specific activity pattern that is characteristic of the later generation AMPMs (c.f. **Section 3.3**).

Table 4.5 Antimicrobial activities of the biotinylated analogues of mimetic-**19**. The position of the incorporated biotin label is underlined and highlighted in red, and the numbering of amino acid residues is given for the parent compound.

ID[a]	sequence[b]	MIC[c] [µg/mL]				
		E. coli	*P. aeruginosa*		*S. aureus*	
		25922[d]	27853[d]	PAO1[d]	25923[d]	29213[d]
19	^{1}T^{2}W^{3}L^{4}K^{5}K^{6}R^{7}R^{8}W^{9}K^{10}K^{11}A^{12}KpP	64	0.008	0.015	> 64	> 64
80	**B**WLKKRRWKKAKpP	32	0.06	0.06	> 64	> 64
81	TW**B**KKRRWKKAKpP	> 64	> 64	> 64	> 64	> 64
82	TWL**B**KRRWKKAKpP	64	0.125	0.5	> 64	> 64
83	TWLK**B**RRWKKAKpP	> 64	16	64	> 64	> 64
84	TWLKK**B**RWKKAKpP	> 64	0.5	1	> 64	> 64
85	TWLKKR**B**WKKAKpP	64	4	16	> 64	> 64
86	TWLKKRRW**B**KAKpP	> 64	0.25	0.5	> 64	> 64
87	TWLKKRRWK**B**AKpP	64	0.125	0.5	> 64	> 64
88	TWLKKRRWKK**B**KpP	64	2	2	> 64	> 64
89	TWLKKRRWKKA**B**pP	> 64	0.06	0.125	> 64	> 64

[a] Substance identifier; [b] B = Glu(biotinyl-PEG)-OH; [c] MIC = minimal inhibitory concentration.

This pattern is even discernible for compound **85**, which is three orders of magnitude less active than the parent compound. Only compounds **81** and **83**, in which Leu-3 and Lys-5 were replaced respectively, lose the activity pattern. For compound **81**, this corresponds to a decrease in activity of at least four orders of magnitude. Finally, the findings that biotin can be incorporated successfully into the scaffold of mimetic-**19**, especially by replacement of four out of five lysine residues with a biotinylated amino acid containing a 15 atom spacer arm, corroborates the feasibility of unselective coupling of the ligand to the matrix.

4.2.1.4 Affinity chromatography experiments with *P. aeruginosa* PAO1

For AC experiments with *P. aeruginosa* PAO1, cell cultures were grown according to the standard incubation conditions described for the protein expression profiling (c.f. **Section 4.1** and **Section 3.3**). In analogy to the protein expression profiling, three fractions were prepared for analyses. However, due to the denaturing conditions of the prefractionation employed for the proteomics experiments, a different protocol, based on differential centrifugation was used. Briefly, cell cultures were harvested in the mid-logarithmic growth phase, typically after three hours of incubation, corresponding to an OD_{600} of 1.0, and were ruptured either by sonication or via a French pressure cell. Protease inhibitors were added to prevent proteolytic breakdown of proteins, and large cell debris was removed by low speed centrifugation at 5000 g for 10 minutes. The crude cell mixture were further fractionated by centrifugation at 40000 g for 30 minutes to remove the outer membrane fraction and smaller cell debris. A final centrifugation step at 100000 g separated the cytoplasmic membrane and smaller outer membrane fragments from the intracellular fraction. For experiments with membrane preparations, 1% of the non-ionic detergent Triton-X 100™ was added to the buffer systems as a solubilising agent. Since it was found that neither the extracellular nor the membrane fractions lead to the isolation of protein bands on 1D gels, the following discussion will focus on the intracellular fraction of *P. aeruginosa* PAO1. In order to minimise denaturing effects that might impair putative AMPM/target interactions, all operations were carried out on the same day and at 4°C.

For the preparation of affinity columns, mimetics **19** and ent-**18** were coupled to NHS-activated sepharose HiTrap™ columns (1 mL) according to the manufacturer's instructions. Briefly, AMPM ligands were coupled in standard coupling buffer (0.2 M $NaHCO_3$, 0.5 M NaCl, pH 8.3) for 30 minutes at room temperature, and unreacted NHS on the matrix was deactivated with a buffer containing 0.5M ethanolamine, 0.5M NaCl, pH 8.3. The coupling efficiencies were determined by UV spectroscopy and were found to be always ≥ 90%.

In a first set of experiments, 5 mg of mimetic **19** were immobilised onto NHS-activated sepharose and samples of cell lysate of *P. aeruginosa* PAO1, corresponding to 10 mg of protein, as determined by Bradford analysis, were used for the

experiments. To check for unspecific binding of macromolecules to the solid support, a control column, capped with ethanolamine, was used. Unbound proteins were washed out with standard buffer (50 mM phosphate, 100 mM NaCl, pH 7.0), and bound macromolecules were eluted non-selectively with an elution buffer consisting of 50 mM ethanolamine, 100 mM NaCl, pH 9.5. A chromatogram of the affinity purification is depicted in Figure **4.7** and a corresponding 1D-PAGE gel is shown in **Figure 4.8**.

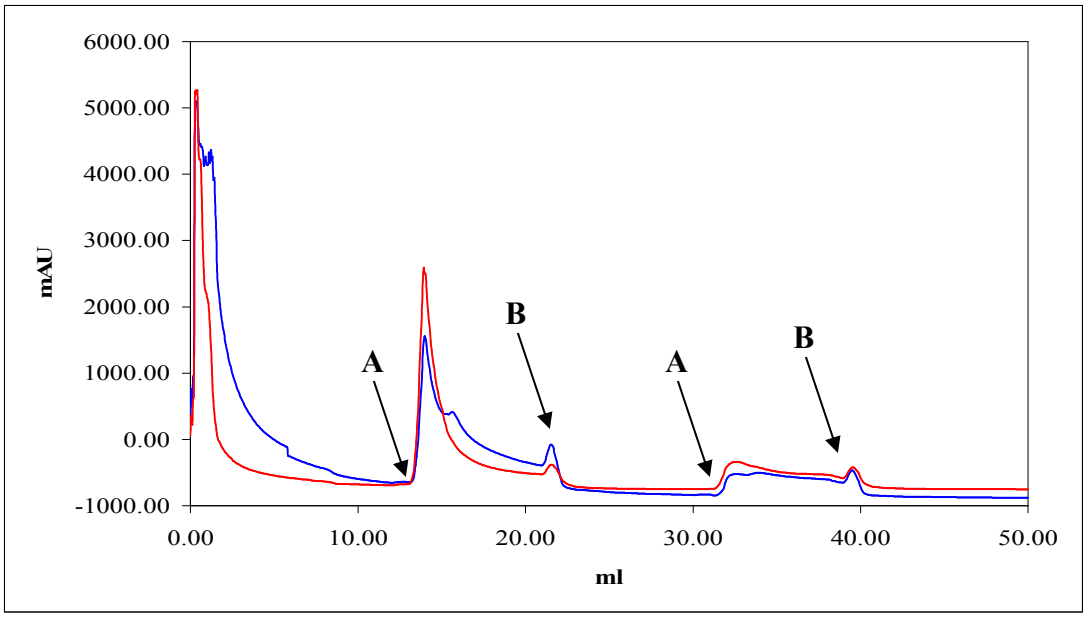

Figure 4.7 Chromatogram of an AC experiment with 5 mg of mimetic-**19** immobilised on 1 ml of NHS-activated Sepharose. Elution buffer (**A**): 50 mM ethanolamine, 100 mM NaCl, pH 9.5; binding buffer (**B**): 50 mM phosphate, 100 mM NaCl, pH 7.0. Conditions: applied protein = 10 mg; flow = 1 mL/min; blue trace = 226 nm; red trace= 254 nm. The arrows mark changes in the buffer system. The second elution step checks for the influence of changing the buffer systems on the UV traces.

It can be seen from this figure that mimetic **19** binds a variety of proteinaceous species on the affinity matrix (lane B), and that the ethanolamine-capped control column (lane C) does not non-specifically retain proteinaceous compounds. For the identification of these proteins and to further increase the resolution, a 2D–PAGE gel was run with an IPG pI gradient from 3 to 10, and the gel is shown in **Figure 4.9**. Protein spots that were subjected to Tryptic digestion and mass spectrometric analysis (c.f. **Section 4.1**) are indicated.

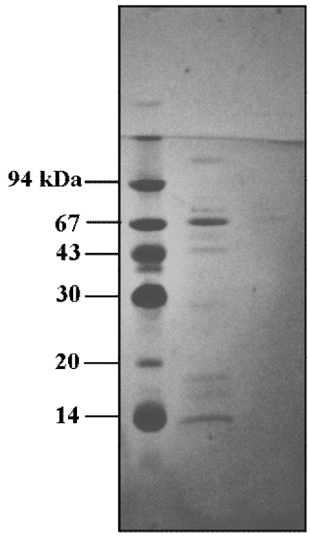

Figure 4.8 Coomassie-stained 1D PAGE corresponding to the AC experiment of **Figure 4.7**. From left to right: (A) molecular mass standards; (B) elution from the affinity matrix created by immobilising 5 mg of mimetic **19**; (C) elution from an ethanolamine capped negative control column.

In total, out of 26 protein spots, 21 could be identified, corresponding to 9 different protein species of *P. aeruginosa* PAO1, and these are summarised in **Table 4.6**. The identified proteins belong to three different classes. Nine spots corresponded to GroEL, a bacterial heat shock protein, three spots corresponded to the α-chain of DNA-directed polymerase and finally, 12 protein spots originated from seven different ribosomal proteins. Most prominent on the 2D gel are spots S23 and S24, which both correspond to ribosomal protein L7/L12. However, it should be mentioned (c.f. **Table 4.6**) that the majority of the identified proteins are negatively charged and highly abundant in the bacterial cells.

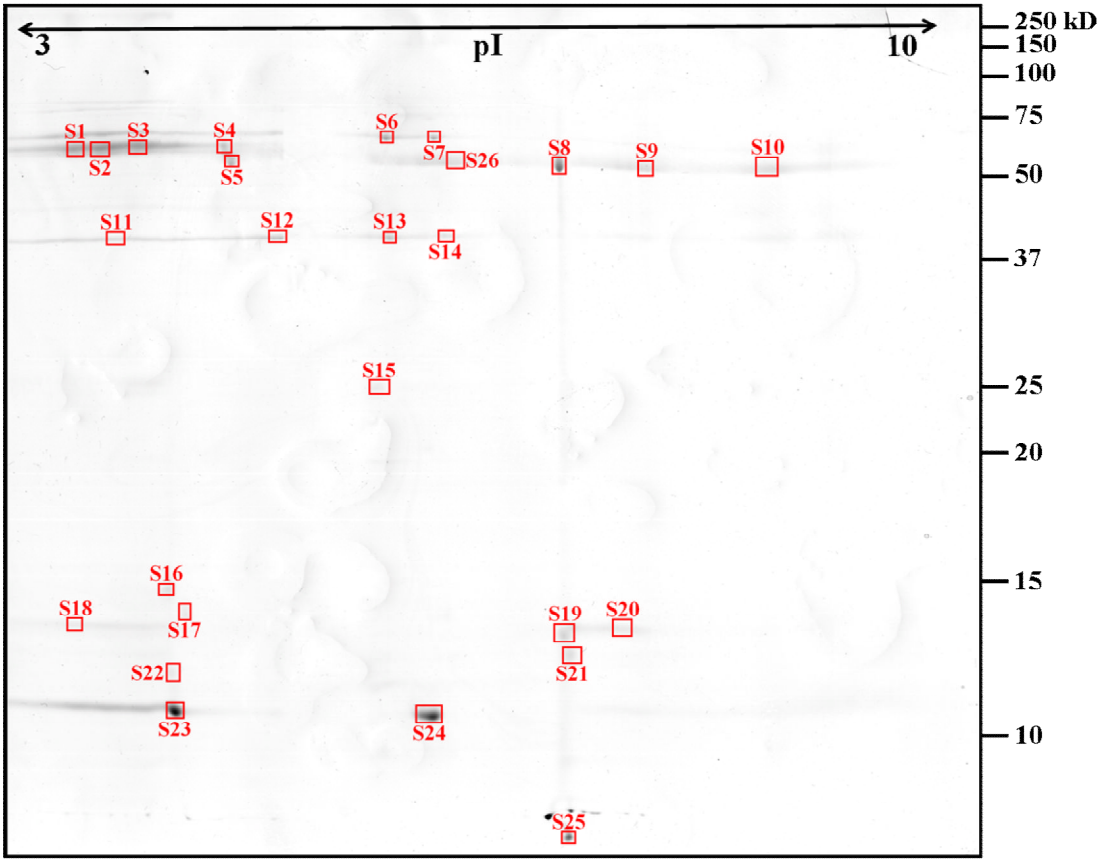

Figure 4.9 Coomassie stained 2D gel of proteins bound to a mimetic-**19** affinity matrix.

Table 4.6 Identification of proteins of the intracellular fraction of *P. aeruginosa* PAO1 retained on a mimetic-**19** affinity column. Missing spot numbers correspond to unidentified proteins.

Spot no[a]	PA no[b]	Protein description	Theoretical pI	Theoretical Mr	Protein score[c]	Sequence coverage [%]
S1	PA4385	GroEL protein	5.0	57.0	462	47
S2	PA4385	GroEL protein	5.0	57.0	333	44
S3	PA4385	GroEL protein	5.0	57.0	412	45
S4	PA4385	GroEL protein	5.0	57.0	211	28
S5	PA4385	GroEL protein	5.0	57.0	701	50
S26	PA4385	GroEL protein	5.0	57.0	219	36
S8	PA4385	GroEL protein	5.0	57.0	701	58
S9	PA4385	GroEL protein	5.0	57.0	341	39
S10	PA4385	GroEL protein	5.0	57.0	244	35
S12	PA4238	DNA-directed RNA polymerase α chain	4.9	36.7	492	57
S13	PA4238	DNA-directed RNA polymerase α chain	4.9	36.7	353	43
S14	PA4238	DNA-directed RNA polymerase α chain	4.9	36.7	413	48
S6	PA3162	30S ribosomal protein S1	4.8	61.9	337	43
S7	PA3162	30S ribosomal protein S1	4.8	61.9	403	47
S17	PA4935	30S ribosomal protein S6	4.9	16.2	168	57
S15	PA4273	50S ribosomal protein L1	9.6	24.0	287	53
S19	PA4932	50S ribosomal protein L9	5.5	15.5	442	63
S20	PA4272	50S ribosomal protein L10	8.9	17.6	154	32
S21	PA4274	50S ribosomal protein L11	9.8	20.0	147	39
S23	PA4271	50S ribosomal protein L7/L12	4.7	12.5	119	65
S24	PA4271	50S ribosomal protein L7/L12	4.7	12.5	124	65

[a] Spot numbers refer to **Figure 4.9**.

[b] Data generated from peptide mass maps were compared to the translated open reading frames (ORF) for P. aeruginosa PAO1 (http://v2.pseudomonas.com).

[c] Probability score of the MASCOT database search based on an implementation of the Mowse algorithm;[538] scores greater than 60 are considered significant ($p<0.05$).

[d] Sequence coverage denotes the percentage of the protein sequence for which matching peptide fragments have been identified.

In order to check the specificity of the retention of the identified protein species, two different approaches were implemented employing the enantiomer of **18**. In one set of experiments, both **19** and ent-**18** were immobilised on NHS-activated Sepharose columns, and bound molecules were eluted non-selectively from the affinity matrices with increasing ionic strength, that is with increasing amounts of NaCl added to the standard buffer. Additionally, the concentration ratio of applied protein to ligand was increased. This is thought to help in suppressing unspecific interactions with the immobilised ligand, as well as resulting in higher sensitivity, and was achieved by decreasing the amount of immobilised ligand from 5 to 1 mg, and by increasing the amount of applied protein from 10 to 30 mg.

Figure 4.10 shows a chromatogram from an AC experiment with immobilised mimetic **19** and elution with increasing ionic strength. It can be seen that elution with buffers containing 0.2M and 0.35M of NaCl led to the release of a significant amount of macromolecules from the affinity matrix. However, the ratio of UV absorption between different wavelengths is not as to be expected for a preparation consisting only of proteinaceous compounds, and thus suggests the presence of nucleic acids.

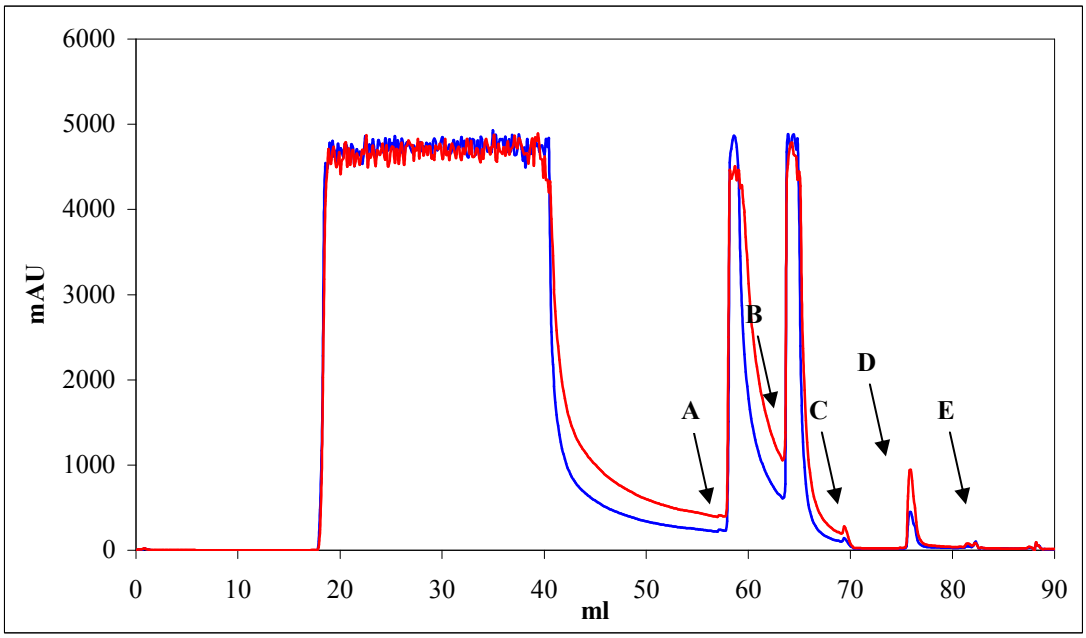

Figure 4.10 Affinity chromatography experiment with 1 mg of immobilised mimetic-**19** and elution with AC standard buffer (50 mM phosphate, 100 mM NaCl, pH 7.0) supplemented with increasing amounts of NaCl. The final concentrations of NaCl in the elution buffer are (A): 0.2M; (B): 0.35M; (C): 0.5M; (D): 1M; (E): 2M.

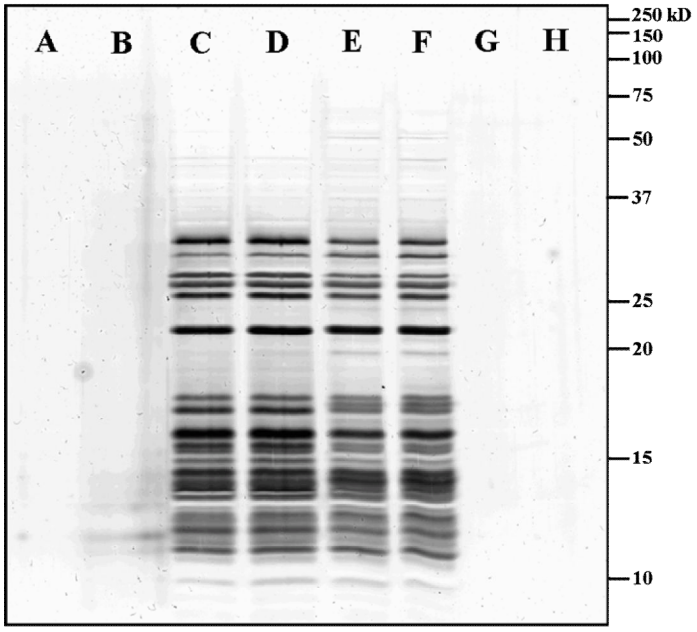

Figure 4.11 Silver stained 1D PAGE of an AC experiment using an elution buffer system of increasing ionic strength to elute macromolecules bound to mimetic-**19** and ent-**18** affinity matrices. From left to right: (**A**) 0.5M NaCl, immobilised ent-**18**; (**B**) 0.5M NaCl, immobilised **19**; (**C**) 0.2M NaCl, immobilised ent-**18**; (**D**) 0.2M NaCl, immobilised **19**; (**E**) 0.35M NaCl, immobilised ent-**18**; (**F**) 0.35M NaCl, immobilised **19**; (**G**) 2M NaCl, immobilised ent-**18**; (**H**) 2M NaCl, immobilised **19**.

A corresponding 1D PAGE gel showing fractions eluted with different ionic strength is shown in **Figure 4.11**. It can be seen that, as to be expected from the chromatogram(s), a large number of bands is detected from fractions collected with elution buffers containing 0.2M, and 0.35M of NaCl. It is noteworthy that these species are concentrated between molecular masses of around 10 to 30 kDa. However, it can also be seen that there are no obvious differences between the 1D gel profiles of mimetic-**19** and the unspecific control compound ent-**18**.

In another set of control experiments, **19** and ent-**18** were used to competitively displace putative target molecules from an affinity matrix composed of immobilised **19**. A silver-stained 1D gel from an experiment with such competitive elution is shown in **Figure 4.12**. Similar to elution using increasing ionic strength, there is a large amount of bands concentrated in a molecular mass region between 10 and 30 kDa. Although the band patterns of the macromolecular fractions eluted with either **19** or ent-**18** added to the binding buffer at concentrations of 1mg/mL show a similar overall appearance, there seem to be discernible differences in the patterns, especially at molecular masses between 10 and 15 kDa. In future work, it will be of interest to analyse these patterns further by 2D-PAGE analysis.

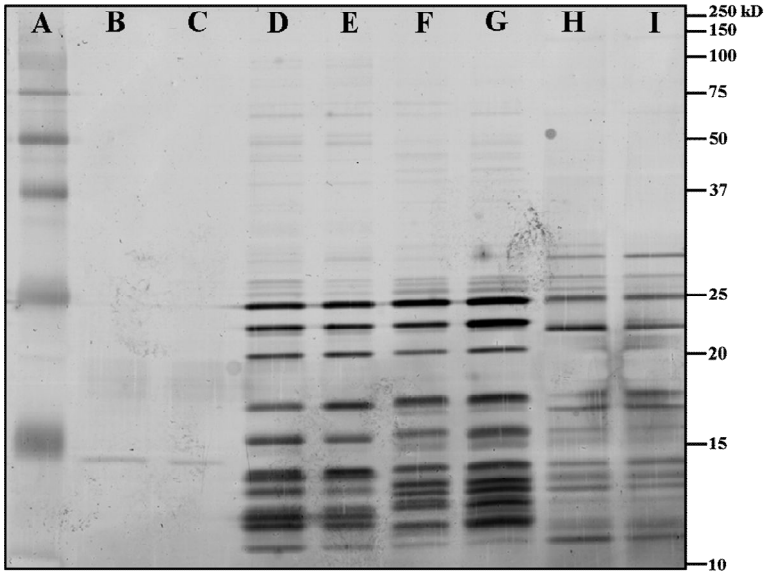

Figure 4.12 Silver stained 1D PAGE of an AC experiment with immobilised mimetic-**19** using competitive elution with either **19** or ent-**18** added to the elution buffer (50 mM phosphate, 100 mM NaCl, pH 7.0). Elution with 3 mL of ent-**18** in elution buffer (**D**), followed by additional 3 mL of ent-**18** in elution buffer (**E**), acidic elution with 50 mM acetate, 100 mM NaCl, pH 4 (**B**), and basic elution with 50 mM ethanolamine, 100 mM NaCl, pH 9.5 (**H**). Elution with 3 mL of **19** in elution buffer(**E**), followed by additional 3 mL of **19** in elution buffer (**F**), acidic elution with 50 mM acetate, 100 mM NaCl, pH 4 (**C**), and basic elution with 50 mM ethanolamine, 100 mM NaCl, pH 9.5 (**I**). Lane **A** corresponds to the molecular mass standards.

4.2.2 Photoaffinity Labelling

Another direct approach towards target identification consists of covalently linking ligands to their target molecule(s), where the ligands are functionalised so as to allow for the isolation and identification of the newly formed adduct. In chemical crosslinking, this can be achieved, for example, by using homo- or hetero-bifunctional linkers, such as EDC and glutardialdehyde, that form bonds with amine or carboxylic acid functionalities of biological macromolecules.[585] Alternatively, in photoaffinity labelling (PAL), formation of a covalent bond is achieved by radiative activation of a photo-reactive moiety creating a highly reactive intermediate species. One advantage of crosslinking experiments compared to AC, with respect to the target identification problem is the potential use of the former method for *in vivo* applications.

The process of designing and using (small) synthetic molecules as chemical probes to covalently modify and identify target proteins, is termed chemical proteomics.[586] Activity-based chemical probes react with classes of enzymes by virtue of the enzymatic reaction mechanism, such as the labelling of cysteine proteases with chemical probes containing epoxide functionalities that are irreversibly attached by bond formation between the active-site cysteine residue and the epoxide.[587] Affinity-based probes, on the other hand, are covalently attached to non-catalytic residues of the target molecule(s), and hence require selective and strong binding to their target molecule(s). Moreover, there is also a third class of chemical probes which are used to covalently modify proteins in an unselective manner. In quantitative non-gel based proteomics, for instance, the ICAT reagent is attached to proteins containing thiol functionality via the general alkylating property of the iodoacetamide moiety of the ICAT reagent.

Typically, a chemical proteomics probe possesses three to four distinct components. These consist firstly of a reactive group for attaching the probe molecule to the target compound, secondly a linker to modulate the reactivity and the specificity of the reactive group, and thirdly a label/tag functionality that allows for identification and/or purification of the newly formed adduct. The use of affinity-based probes as in PAL necessitates a fourth element that is responsible for binding to the target molecule with high affinity, and such elements can also be included in activity-based probes in order to enhance selective binding. Commonly employed tag functionalities are biotin and radioactive or fluorescent labels. One advantage of the

use of biotin tags is the possibility to concentrate biotinylated target molecules from complex protein mixtures via AC, prior to attempting protein identification.

As mentioned, PAL is a direct method for the identification of potential target molecules and in favourable cases this can be achieved at different levels. Apart from the first level of identification, which is concerned with the identity of the target molecule(s), the fragmentation of covalently labelled proteins can permit mapping of the binding site or even the delineation of the site of attachment. As such, PAL is a complementary approach to site directed mutagenesis for the mapping of binding sites, especially in such instances where NMR or X-ray data is not available.[588]

Once again, it is of major importance that the introduction of extra functionality into the ligand in order to create the chemical probe molecules does not impair the biological activity. However, it has been argued that PAL probes which are up to three orders of magnitude less active than the parent compound can still be successfully used in PAL experiments, although this obviously necessitates a high initial activity of the parent compound.[588]

Several examples of the successful application of PAL in target identification schemes have been reported.[589] For instance, the binding of the oxazolidinone antibiotic eperezolid to the ribosome was mapped onto the L27 ribosomal protein, tRNA, ribosome-associated LepA protein, and a conserved base in the peptidyl transferase centre of 23S RNA by the use of a radio-labelled photo-reactive eperezolid analogue.[590] Similarly, an analogue of pioglitazone, an anti-diabetic compound, led to the isolation of a hitherto uncharacterised mitochondrial membrane protein as a putative target for pioglitazones and related compounds.[589] Moreover, photo-reactive analogues of the angiotensin AT-4 have been demonstrated to be efficient tools for the identification of AT4 receptors in various tissues.[591] Finally, Hatanaka et al. described the use of biotinylated diazirine for the analysis of galactosyl transferase binding sites,[592] and recently, the binding site of HIV-1 integrase for coumarin-based inhibitors was identified using photo-reactive analogues.[593]

4.2.2.1 Photo-reactive groups

As mentioned, successful PAL depends on the availability of photo-reactive groups that can be incorporated into the molecular framework of the ligand without

loss of its biological activity. Several requirements for such photo-reactive groups to be useful for PAL experiments in biological systems are summarised below:

1. Excited state with a lifetime shorter than dissociation of the ligand but long enough to allow for covalent linkage.
2. Unambiguous photochemistry to provide desired photo-adducts.
3. Possibility to react with C-H and X-H (X=N, O) bonds.
4. Stability under ambient conditions.
5. High excitation wavelengths.

The last criterion is not stringent for target identification, in which damage to proteins caused by UV irradiation is tolerable as long as it does not interfere with the identification of the target molecule. Three different photo-reactive groups are most frequently used for PAL, and these are based on benzophenone, azide, and diazirine functional groups. The photochemical transformations commonly encountered with these photo-reactive groups are summarised in **Figure 4.13**. Additionally, the use of aromatic diazo compounds has been described for PAL.[594]

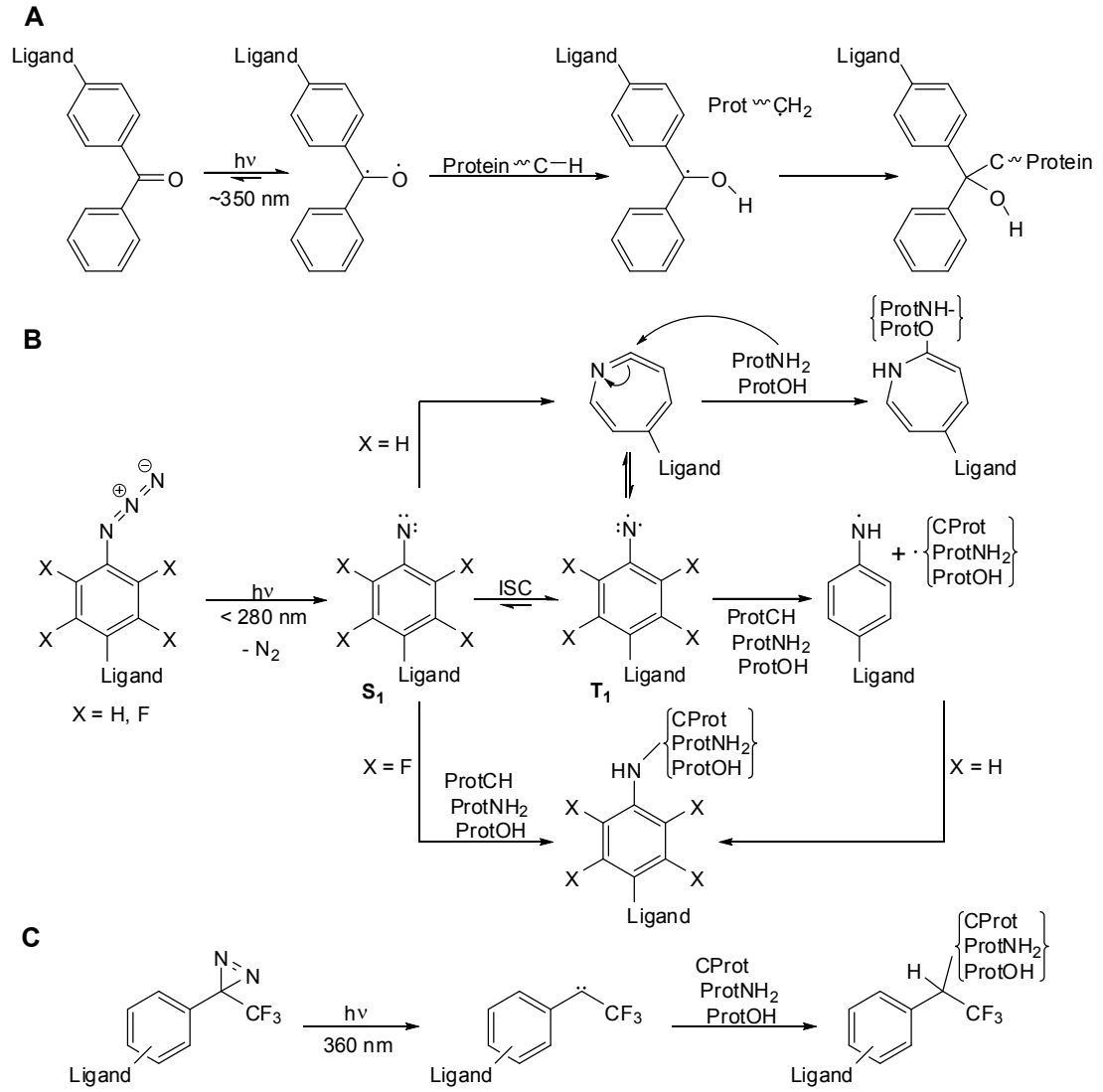

Figure 4.13 Photochemistry of photo-reactive groups used for PAL of biological macromolecules as exemplified with proteins. (A): benzophenone-based probes; (B) aromatic azide-based probes; and (C): diazirine-based probes.

4.2.2.2 Synthesis of PAL probe molecules

For the synthesis of PAL probes of our AMPMs, two commercially available *N*-α-Fmoc-protected amino acids containing either a benzophenone or an aromatic azide photo-reactive moiety were chosen (**Figure 4.14**). Both *N*-α-Fmoc-p-azido-L-Phe-OH (**90**) and *N*-α-Fmoc-p-benzoyl-L-Phe-OH (**91**) can be conveniently introduced into the AMPM scaffold during SPPS.

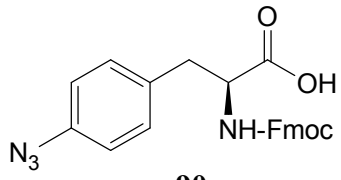

90

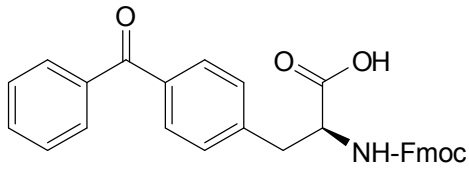

91

Figure 4.14 Commercially available building blocks for the SPPS synthesis of photo-reactive analogues of mimetic-**19**.

Since it was known from the synthesis of DANA-labelled AMPM analogues (c.f. **Section 3.8**), that the incorporation of aromatic amino acids into the scaffold of mimetic **17** under retention of activity was only possible by replacing an aromatic Trp residue, the photo-reactive amino acids **90** and **91** were introduced into positions Trp-2 or Trp-8 of the scaffold of mimetic **19**. The synthesis of photo-reactive analogues was carried out according to the standard protocol for the synthesis of AMPMs outlined in **Section 3.1**) and described in detail in **Section 5.2**, with the only modification that the unnatural amino acids were coupled manually, using 1.5 equivalents of amino acid, 1.45 equivalents of HATU as activating reagent and 3 equivalents of DIEA. Crude peptides were purified by RP-HPLC and determined to be of at least 98% purity by analytical HPLC. ESI mass spectrometric and analytical HPLC data of the photo-reactive analogues of mimetic **19** are summarised in **Appendix 2**. The antimicrobial activity of the synthesised photo-reactive AMPMs against our panel of test organisms are shown in **Table 4.7**, in which a DANA-labelled analogue of **19** is included for comparison.

Table 4.7 Antimicrobial activities of photo-reactive analogues of mimetic-**19**. Photo-reactive and biotinylated amino acids are highlighted in blue and red, respectively. Compound **75** is included for comparison.

ID[a]	sequence[b]	MIC[c] [µg/mL]				
		E. coli	*P. aeruginosa*		*S. aureus*	
		25922[d]	27853[d]	PAO1[d]	25923[d]	29213[d]
19	^{1}T^{2}W^{3}L^{4}K^{5}K^{6}R^{7}R^{8}W^{9}K^{10}K^{11}A^{12}KpP	64	0.008	0.015	> 64	> 64
92	TZLKKRRWKKAKpP	> 64	0.06	0.25	> 64	> 64
93	TWLKKRRZKKAKpP	64	≤ 0.03	0.06	> 64	> 64
94	TOLKKRRWKKAKpP	64	4	8	> 64	64
95	TWLKKRROKKAKpP	64	0.125	0.5	> 64	> 64
96	BZLKKRRWKKAKpP	> 64	0.5	1	64	32
97	BWLKKRRZKKAKpP	> 64	0.125	0.25	> 64	64
98	TWLKKRRZKKABpP	64	1	4	> 64	> 64
99	BOLKKRRWKKAKpP	16	2	2	> 64	32
100	BWLKKRROKKAKpP	64	0.25	0.5	> 64	> 64
77	TWLKKRRDKKAKpP	64	0.125	0.5	> 64	> 64

[a] Substance identifier; [b] B = Glu(biotinyl-PEG), Z = p-azido-Phe, O = p-benzoyl-Phe; D = DANA; [c] MIC = minimal inhibitory concentration; [d] strain or ATCC number.

It can be seen from **Table 4.7**, that both photo-reactive amino acids could be introduced into both Trp positions with retention of the selective anti-pseudomonal activity of the parent compound. Additionally, it is evident that the replacement of tryptophan with p-azido-Phe-OH (**92** and **93**) leads to less decrease in the biological activity than substitution with p-benzoyl-Phe-OH (**94** and **95**). This finding might be explicable by the increased steric bulk of the benzophenone moiety; along these lines the DANA-labelled compound **77** shows almost identical activity compared to **95**. Interestingly, both Trp positions could thus be replaced by either (a) a benzene ring system, (b) a benzophenone moiety, or (c) the aromatic naphthalene system, albeit with a loss of activity of about one order of magnitude.

Moreover, substitution in position 2 was generally found to be more detrimental for the biological activity than in position 8, and this is in agreement with the results obtained from the introduction of DANA into the scaffold of mimetic-**17**. In the latter case replacement of Trp-2 even led to complete loss of the specific activity pattern (c.f. **Section 3.8**).

Finally, in order to obtain probe molecules that could be used in PAL experiments, bi-functionally modified AMPM analogues, carrying both a photo-reactive group as well as a biotin label, were synthesised as outlined in the standard protocol for the synthesis of AMPMs (c.f. **Section 3.1**) and described in detail in **Section 5.2**, with the only modification that the unnatural amino acids were coupled manually, using 1.5 equivalents of amino acid, 1.45 equivalents of HATU as activating reagent and 3 equivalents of DIEA. Crude peptides were purified by RP-HPLC and determined to be of at least 98% purity by analytical HPLC. ESI mass spectrometric and analytical HPLC data of the photo-reactive analogues of mimetic **19** are summarised in **Appendix 2**. The antibacterial activities of the PAL probe molecules were determined against the panel of test organism and are included in **Table 4.3**. For the syntheses the probe molecules, Glu(biotinyl-PEG) was incorporated into position Thr-1, since this was found (c.f. **Table 4.3**) to yield the biotinylated analogue of **19** with the best retention of anti-pseudomonal activity. For Glu(biotinyl-PEG) in position 1, combinations with both photo-reactive groups in either position 2 or position 8 were synthesised. Additionally, replacement of Trp-8 by p-azido-Phe was tested together with replacement of Lys-11 by the biotinylated glutamic acid derivative, since this leads to a PAL probe with decreased positive charge.

Interestingly, the incorporation of the biotin-label into the scaffold of the photo-reactive analogues of mimetic-**19** leads to a higher decrease in anti-pseudomonal activity for both p-azido-Phe functionalised systems than to be expected from the results derived from the library of biotinylated analogues (c.f. **Section 4.2.1**). Moreover, the combination of a biotin label together with p-benzoyl-Phe led to practically no further loss of activity, unlike the combination of the biotin label with the p-azido-Phe photo-reactive group. Nevertheless, the PAL probe with the best anti-pseudomonal activity was obtained by substitution of Thr-1 with Glu(biotinyl-PEG) and of Trp-8 with p-azido-Phe (**97**).

4.2.2.3 PAL with *P. aeruginosa* PAO1

For the PAL experiments, only membrane and intracellular fractions were investigated. Moreover, since PAL allows the *in vivo* labelling of cell cultures, and since the AC experiments with membrane fractions were inconclusive, special

emphasis was put here on the membrane fractions. All experiments described herein are concerned with the biologically most active photo-reactive analogue of mimetic-**19**, namely **97**. For *in vivo* PAL, cultures of *P. aeruginosa* PAO1 were harvested in their mid logarithmic growth phase when they reached an OD_{600} of 0.1. Cells were washed twice in PAL standard buffer (50 mM phosphate, 100 mM NaCl, pH 7.3), and re-suspended in standard buffer to give a cell density of 5×10^9 CFU/mL. 10 mL portions of the cell suspensions were incubated for 30 minutes and at 4°C in Petri dishes of a diameter of 10 cm together with **97** and subsequently irradiated at a wavelength of 254 nm and at a distance of 5 cm. After irradiation, the cell suspensions were fractionated according to the differential centrifugation protocol described for the AC experiments in (c.f. **Section 4.2.1**) to obtain the intracellular and membrane protein fractions. Alternatively, for *in vitro* PAL, cell cultures were first fractionated according to the differential centrifugation protocol, and the intracellular or membrane fractions were re-suspended in standard buffer before the incubation with PAL probes and the subsequent irradiation. In experiments with competitive ligands, either mimetic-**19** or ent-**18** was pre-incubated for 30 minutes with the cell suspensions before addition of the PAL probe.

In order to concentrate biotinylated molecules, from the cell suspensions were incubated with streptavidin immobilised on agarose beads. Streptavidin-bound biotinylated macromolecules were analysed directly by 1D SDS PAGE; the dissociation of the strong biotin-streptavidin complex was achieved by boiling streptavidin beads with SDS PAGE sample buffer. Prior to the concentration steps, PAL samples were dialysed against PAL standard buffer, in order to remove low molecular weight biotinylated compounds. For the detection of biotinylated molecules, a modified Western-blot procedure, based on the amplified alkaline phosphatase Immun-Blot® kit, was used. Briefly, samples from the 1D SDS PAGE were blotted onto PVDF membranes and blocked with 1% BSA. The detection of the biotinylated molecules was achieved by treating the protein blot with a complex of biotinylated alkaline phosphatase/streptavidin (3:1), which possesses one free binding site for attaching to biotinylated species on the PVDF membrane, and which improves the sensitivity as one biotinylated molecule on the membrane is linked to three molecules of alkaline phosphatase. Biotinylated macromolecular bands on the blot were subsequently visualised by a chromogenic enzymatic reaction with BCIP (5-

bromo-4-chloro-3-indolyl phosphate) and NBT (nitro blue tetrazolium) as substrates and with alkaline phosphatase, yielding a purple/blue precipitate.

Firstly, since one focus has been on the identification of putative targets in the membrane fractions of *P. aeruginosa*, several methods for extracting membrane proteins were studied for their applicability in the PAL experiments. Therefore, *P. aeruginosa* PAO1 cells were labelled with **97** *in vivo* as described above, and several different protocols for the extraction of membrane proteins were evaluated. Firstly, three common detergents used to solubilise membrane proteins, namely SDS, Triton-X 100™, and Triton-X 114™ were tested, as well as a method based on extraction with TFE and one method based on extraction with a carbonate buffer system. The extraction protocol employing Triton-X 114™ exploits the low cloud point of the detergent, which leads to phase separation above 20°C and allows for the convenient isolation of hydrophobic proteins in the detergent phase.[595] Extraction with Triton-X 114™ and cooling of the detergent fraction below 4°C also furnishes a precipitate that contains membrane proteins,[596] and which was also analysed in the experiment. Additionally, the different extraction methods were compared to the direct solubilisation of membrane proteins with SDS-PAGE sample buffer.

A modified Western-Blot of the 1D-PAGE, comparing the different extraction methods is shown in **Figure 4.15**. It can be seen that solubilisation of membrane proteins with both Triton-X 100™ or with SDS led to the visualisation of the most bands and was superior to the other extraction methods inasmuch as both were able to visualise more proteins. TFE extraction furnished lower background but was less sensitive in the lower molecular weight range. Finally, both carbonate extraction and analysis of the cold pellet of the Triton-X114™ detergent fraction were unsatisfactory. Despite the larger background, the direct solubilisation with SDS-PAGE offered the highest sensitivity for *in vivo* PAL with membrane fractions. Additionally, it can be seen that TX-100™ can be used in protocols in which membrane proteins are to be extracted under retention of their native activity, and for which the use of non-ionic detergents is highly recommendable.

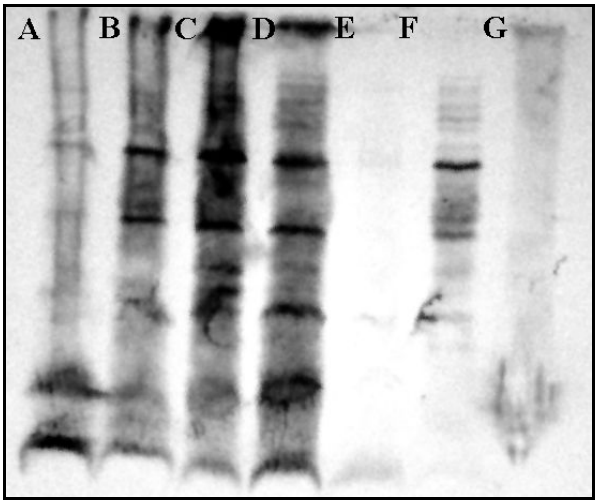

Figure 4.15 Solubilisation of biotinylated proteins of the membrane-fraction of *P. aeruginosa* PAO1. (**A**): Triton-X 114™, (**B**): Triton-X 100™, (**C**) SDS-PAGE sample buffer, (**D**): SDS, (**E**), carbonate extraction, (**F**) TFE extraction, (**G**) Triton-X 114™ cold pellet.

In one set of experiments, the membrane fraction of *P. aeruginosa* PAO1 was studied in an *in vivo* labelling approach with **97** in the presence or absence of **19** or ent-**18**. Briefly, 10 mL suspensions of bacterial cells corresponding to 5×10^9 CFU/mL were irradiated in the presence of 10 μg/mL of **97** after pre-incubation with a fifty-fold excess of either ent-**18** or mimetic-**19**, and the modified Western Blot of the experiment is shown in **Figure 4.16**. It can be seen from this figure that there are no discernible differences between the samples. Additionally, in the case of the concentrated samples, it becomes apparent that a variety of bands are already present in the control, which means that they represent endogenously biotinylated species.

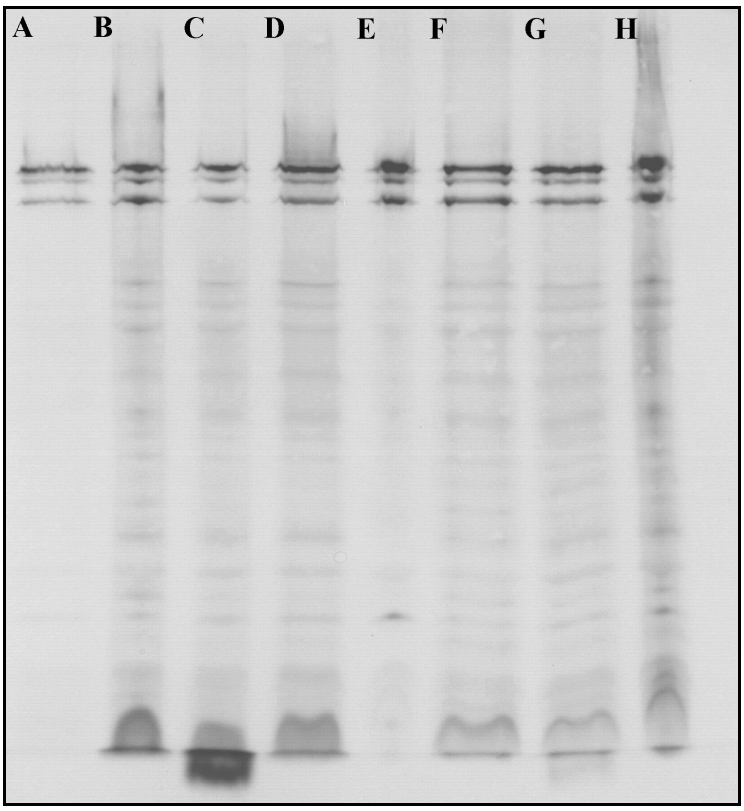

Figure 4.16 *In vivo* PAL of the membrane fraction of *P. aeruginosa* PAO1 with **97**. (**A**): control, (**B**) co-incubation with **19**, (**C**) incubation with **94** alone, (**D**) co-incubation with ent-**18**. Lanes **E**-**H** correspond to lanes **A**-**D** and were concentrated four-fold with the use of Ultrafree®-MC centrifugal filter devices (*Millipore*, Bedford, US) with a molecular weight cut-off of 5 kDa.

Therefore, a protocol with pre-fractionation into intracellular and membrane fractions was used which allows for the removal of endogenous biotin and in which several steps were taken to increase selectivity of a putative ligand/target interaction. Firstly, the concentration of **97** was reduced to 0.05 μg/mL, secondly, the protein concentration was increased two-fold, and thirdly the ionic strength was increased by adjusting the standard PAL buffer to a final NaCl concentration of 350 mM. Furthermore, crude cell lysates were incubated with 0.5 mg/30 mL of RNase A prior to the pre-fractionation protocol, and both fractions were treated with immobilised streptavidin, in order to remove endogenous biotin. Moreover, the ratio of **97** to the competitive inhibitors **19** or ent-**18** was decreased to 1:500. For the solubilisation of PAL membrane fractions after irradiation, 1% of Triton-X 100™ was added to the buffer system.

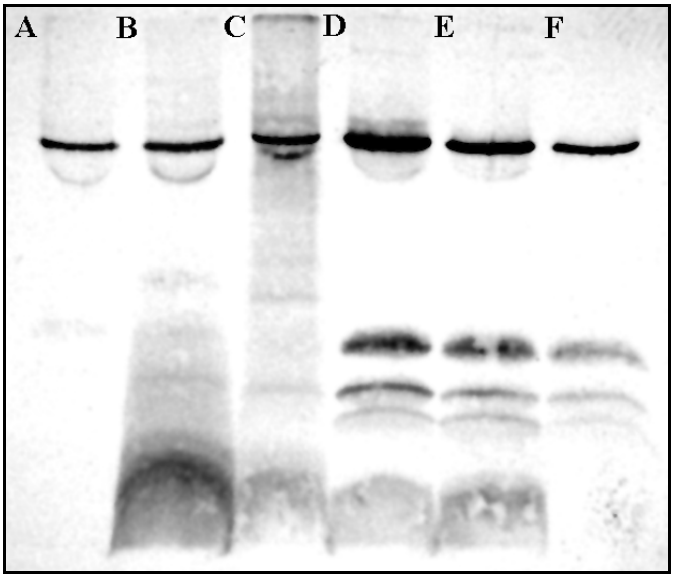

Figure 4.17 PAL experiment with pre-fractionated membrane (**A**-**C**) and intracellular (**D**-**F**) fractions of *P. aeruginosa* PAO1. **A** and **F**: control; **B** and **E**: co-incubation with **19**; **C** and **D**: incubation with **94** alone.

A corresponding modified Western blot is depicted in **Figure 4.17**, from which it can be seen that there are no discernible differences between the three samples in either the intracellular or the membrane fractions, and that endogenous biotin was still present in all samples. Additionally, it can be seen that there is a higher background for the membrane fractions which indicates a large background of labelling.

4.2.3 Conclusions

Several analogues of mimetic-**19** have been developed that show potential for identifying putative target molecules of our AMPMs in *P. aeruginosa*. SAR data such as the alanine scan of mimetic **18**, the biological activities of the series of biotinylated analogues of mimetic-**19**, and input from the fluorescently labelled library of mimetic **17** have been used to guide the synthesis of biotinylated PAL probe molecules. Moreover, the series of biotinylated analogues of mimetic **19** itself confirmed the potential of using **19** and derivatives as ligands in AC experiments. It has been found that the scaffold of **19** was surprisingly tolerant towards the introduction of the sterically demanding biotinylated PEG linker, inasmuch as only the replacement of Lys-5 and Leu-3 lead to complete loss of the biological activity.

A complication for both AC and PAL approaches towards target identification is that lead compounds obtained from phenotypic screening are often only moderately active in the micromolar range. However, mimetic **19** shows excellent anti-pseudomonal activity, with an MIC value that corresponds to a concentration of 4 nM. Moreover, since the most active biotinylated analogues of **19** lose less than one order of magnitude of anti-pseudomonal activity compared to the parent compound, and since the specific activity pattern is retained for four out of five analogues where lysine is replaced by the biotin tag, **19** could be shown to represent an excellent starting point for an AC approach towards target identification.

Additionally, it could be shown that it is possible to synthesise multi-functionalised affinity-based photo-reactive probe molecules that retain good activity against *P. aeruginosa*. These PAL probes are composed of a biotin tag, a hydrophilic spacer arm, a photo-reactive moiety and the peptide scaffold which is responsible for creating target affinity, and which can also function as an additional spacer for separating the photo-reactive group from the biotin tag.

Furthermore, for both target identification approaches, an almost ideal control compound exists, namely the enantiomer of mimetic **18** which can, for example, be used for immobilisation to the affinity support in order to check for non-specific binding events. Similarly **19** and ent-**18** can be assayed for their ability to competitively displace putative target molecules from the affinity matrix or from the PAL probe.

The utility of AC with **19** and ent-**18** coupled to NHS-activated sepharose and of PAL with **97** was evaluated for identifying putative targets of the AMPMs in *P. aeruginosa*. To summarise, it has to be concluded that so far both approaches seem to be prone to unspecific interactions with intracellular and membrane compounds of *P. aeruginosa*. The problems of unspecific binding might arise, for example, from the low abundance of a putative target protein or from possible denaturation during the experiments. This would result in the greatest noticeable effect being non-specific binding mediated by the considerable positive charge of **19**.

Therefore, further work should be carried out to overcome such interactions, especially since the proven stereospecificity of the anti-pseudomonal action must be explicable on the molecular level. For PAL, this might necessitate a change to different photo-reactive groups or the prefractionation of cellular fractions before the labelling experiment, in order to reduce sample complexity. Moreover, re-evaluation

of the membrane fractions using alternative detergent systems might allow for detection of a putative target molecule.

Nevertheless, the experiments towards target identification show that mimetic **19** is a highly versatile scaffold for the introduction of a variety of different functionalities, and that the functionalised analogues have great potential for development into successful chemical proteomic probes. Moreover, the obtained biotinylated analogues of **19** could prove useful for a variety of applications, such as immuno-fluorescence microscopy,[597] or Far-Western blotting.[598]

Furthermore, the mass spectrometric analysis of proteins retained on an affinity matrix based on **19** led to the identification of 9 different proteinaceous species, consisting of seven ribosomal proteins, the bacterial heat shock protein GroEL, and of the α subunit DNA directed RNA polymerase. Although the control experiments with ent-**18** did not yet allow for the identification of a target molecule, it is interesting to note that the most apparent spots from the 2D gel correspond to the ribosomal protein L7/L12 which has also been found to be up-regulated by induction with mimetic **18** in the protein expression profiling experiments (c.f. **Section 4.1**). The role of L7/L12 for the fidelity of bacterial protein synthesis has been mentioned in **Section 4.1**. Moreover, the ribosomal proteins L10 and L11 were identified from the 2D gel, both of which are closely associated with the L12-stalk *in vivo*. That is, L12 tetramers/hexamers bind directly to L10 which, in turn, interacts with 23S rRNA. L11 also binds to 23sRNA in the bacterial ribosome, where it is located at the base of the L7/L12 stalk.[599]

Recently, L7/L12 has been identified from a pull-down assay employing immobilised glutathione fusion of a glucan binding protein in membrane fractions of *Streptococcus mutans*, and has been suggested to be involved in cell division and peptidoglycan biosynthesis.[600] Although the majority of identified proteins are negatively charged and highly abundant in the bacterial cell, L7/L12 was also isolated from a location of the 2D gel that corresponds to a more neutral pI, and which presumably represents the N-terminally acetylated isoforms of the protein. Moreover, both L10 and L11 are positively charged at physiological pH. It is conceivable that ribosomal sub-structures, possibly together with rRNA, are retained on the affinity matrix. On the other hand, only a small fraction of ribosomal proteins were actually

isolated. Therefore, L7/L12 emerges as a promising target for the AMPMs acting selectively against *P. aeruginosa*.

5 Experimental part

5.1 General notes

5.1.1 Chemical synthesis

SOLVENTS AND REAGENTS Ethyl acetate, diethyl ether, DCM, and cyclohexane were redistilled from K_2CO_3 or $CaCl_2$. Dry DCM and dry toluene were obtained by distillation from CaH_2. HMPT was purchased from *Fluka* (Buchs, Switzerland), dried over CaO for 24 hours and distilled from CaH_2 under vacuum. THF was purchased from *Fluka* and distilled from benzophenone/Na under nitrogen. Benzophenone, benzophenone imine, CaH_2, iodine, and lithium shots were purchased from *Fluka* and used without further purification. Glycine *tert*-butyl ester and Fmoc-OSu were purchased from *NovaBiochem* (*EMD Biosciences*, San Diego, US). Lithium HMDS was purchased from Aldrich (Buchs, Switzerland) and used without further purification. 2-Acetyl-6-methoxynaphthalene was purchased from *Lancaster Synthesis* (*Alpha Aeser*, Karlsruhe, Germany) and used without further purification.

MATERIAL AND INSTRUMENTATION Flash chromatography was carried out on silica gel 60 (230-400 mesh, 0.04-0.063 mm) from *Merck* (Darmstadt, Germany) or *CU Chemie Uetikon AG* (Uetikon, Switzerland) Thin layer chromatography (TLC) was performed using *Polygram SIL G/UV$_{254}$* plates from *Machery-Nagel* (Düren, Germany) or *Silica gel 60 F$_{254}$* plates from *Merck* (Darmstadt, Germany). Melting points (m.p.) were measured on a Kofler apparatus connected to a *Nikon YS 100* microscope (Egg, Switzerland). ^{1}H NMR and ^{13}C NMR spectra were measured at 300 MHz on a *Bruker ARX-300* or *Bruker AV-300* spectrometer (*Bruker*, Rheinstetten, Germany) and the chemical shift values are given in ppm relative to the solvent resonances.[601] The coupling constants *J* are given in Hz and resonance multiplicity is described as *s* for singlet, *d* for doublet, *t* for triplet and *m* for multiplet; *br* is used to describe a broad resonance signal. For ^{13}C-NMR spectroscopy, the multiplicities *s*, *d*, *t*, and *q* denote C, CH, CH_2, respectively CH_3, as determined from DEPT-135/90 spectra.[602]

Infrared spectra were measured with a *Perkin-Elmer* Spectrum One FT-IR spectrometer (*Perkin-Elmer*, Shelton, CT) and ν is given in cm^{-1}. The signals and intensities of the bands are described as *br* for broad, *s* for strong, *m* for medium and *w* for weak.

5.2 Peptide synthesis

5.2.1 Synthesis of peptide mimetics

SOLVENTS AND AMINO ACIDS NMP and piperidine were purchased from *Acros Organics* (Geel, Belgium) and used without further purification. DMF was purchased from *Acros Organics* and redistilled under vacuum from ninhydrin, in order to remove amine impurities. DIEA was purchased from *Acros Organics* and redistilled under vacuum first from ninhydrin and subsequently from KOH. HBTU and HOBt were purchased from *Biosolve* (Valkenswaard, Netherlands) and used without further purification. High purity water was obtained from de-ionised water using an *Elgastat® UHP-UF* water purification system (High Wycombe, UK). Amino acids were purchased from *Novabiochem* or *Bachem* (Bubendorf, Switzerland) and 2-chlorotrityl chloride resin (100-200 mesh) with a loading of 1.2 mmol/g was purchased from *Novabiochem.* The following N-α-Fmoc protected L-amino acids were used for routine Fmoc-SPPS of peptide mimetics:

Fmoc-Ser(^{t}Bu)-OH, Fmoc-Gln(Mtt)-OH, Fmoc-Val-OH, Fmoc-Lys(Boc)-OH, Fmoc-Pro-OH, Fmoc-Gly-OH, Fmoc-Phe-OH, Fmoc-Arg(Pbf)-OH, Fmoc-Leu-OH, Fmoc-Tyr(^{t}Bu)-OH, and Fmoc-Thr(^{t}Bu)-OH, as well as Fmoc-D-Pro-OH for synthesis of the D-Pro-L-Pro template. For the synthesis of enantiomeric AMPMs the corresponding *N*-α-Fmoc-protected D-amino acids and Fmoc-L-Pro-OH were used, with the exception of Fmoc-D-Gln(Trt)-OH.

LOADING OF AMINO ACIDS ON THE RESIN For coupling of the first amino acid to 2-chlorotrityl chloride resin, a loading of 0.3 to 0.6 mmol amino acid per gram of resin was typically used. The calculated amount of *N*-α-Fmoc-protected amino acid was dissolved in 10 mL of dry DCM per g of resin, and if necessary, dry DMF was added dropwise to facilitate dissolution. After swelling of the resin in dry DCM

for 30 min, the amino acid solution was treated with 4 equivalents of DIEA and transferred immediately to the resin. The reaction mixture was sealed under nitrogen and agitated on a S50 wrist arm shaker (*CAT*, Germany) for 30 to 90 minutes. After the coupling reaction, the resin was first blocked three times with a solution of DCM/MeOH/DIEA (17:2:1) and subsequently washed three times with dry DCM, twice with dry DMF and twice with dry DCM. The resin was dried overnight under vacuum over KOH. For the determination of the amino acid loading, dry resin corresponding to approximately 1 μmol of Fmoc functionality was weighed into two 3×10 mm quartz UV cells, and treated with 3 mL of a freshly prepared solution of 20% piperidine in dry DMF. The Fmoc deprotection was left for at least one hour at room temperature and the cuvettes were agitated occasionally by inversion of the cuvettes. The UV absorption at 290 nm was measured on a *Cary 3* UV-Vis spectrometer (*Varian*, Palo Alto, US), with the 20% piperidine solution as blank, and re-measured after 30 minutes to check for further increase in the UV absorption. The amino acid loading was then calculated according to the following equation:

$$Fmoc-loading=\frac{A_{290}(sample)-A_{290}(blank)}{1.7\times mg(resin)} \qquad \text{[equation 5.1]}$$

AUTOMATED PEPTIDE SYNTHESIS Peptides were synthesised on an *Applied Biosystems ABI 433A* automated peptide synthesiser (*Applied Biosystems*, Foster City, CA) coupled to a *Perkin-Elmer 785A UV/VIS* detector or a *Perkin-Elmer Series 200 UV/VIS* detector using either the 0.25 mmol or the 0.1 mmol FastMoc® chemistry. In the FastMoc® chemistry, 1 mmol of an *N*-α-Fmoc protected amino acid (i.e. 4 equivalents for a 0.25 mmol scale synthesis) is activated with 0.9 mmol of 0.45M HBTU/HOBt in DMF (2.0 g) together with 2.1 g of NMP and 1 mL of 2M DIEA in NMP for 2 minutes. After transfer of the activated amino acid to the resin, coupling is allowed for either 20 (standard) or 40 minutes (extended coupling) under vortexing. Deprotection is achieved with 18% piperidine in NMP for three minutes and subsequently with 20% piperidine in NMP for seven minutes. The progress of the deprotection reaction is monitored by measuring the UV absorption of *N*-(9-fluorenyl-methyl) piperidine at 301 nm. If the UV absorption obtained for the second deprotection is higher than 3.5% of the preceding value, additional deprotection steps

of 10 minutes each with 20% piperidine in DMF are carried out until the 3.5% criterion is met, or up to a maximum of six additional deprotection steps. In case of a sluggish deprotection profile, the following amino acid is attached with extended coupling. All intermittent washing steps during the automated SPPS are carried out with NMP.

MANUAL COUPLING OF AMINO ACIDS Coupling of non-standard amino acids was carried out manually with 2 equivalents of the *N*-α-Fmoc-protected amino acid activated with 1.9 equivalents of HATU and 4 equivalents of DIEA in 10 mL dry DMF/g of resin. The coupling reactions were carried out for one hour under vigorous agitation with a wrist arm shaker, and completion of the coupling reactions was monitored by Kaiser testing (*Fluka* Kaiser-testkit, Cat. No 60017).[603]

CLEAVAGE FROM THE RESIN The linear, side-chain protected peptides were cleaved from the resin by treating them successively 7 times with 10 mL portions of a 0.8% TFA solution in dry DCM for 2 to 4 minutes each. The TFA solutions were filtered from the resin into a flask containing 14 ml of a solution of 10 % pyridine in MeOH and the combined filtrates were concentrated on a rotary evaporator to about 5% of the initial volume, treated with 200 mL of water and left to precipitate at 4°C for at least four hours. The obtained precipitate was filtered off, washed subsequently three times with water, three times with 5% of $NaHCO_3$, three times with water, three times with 0.05M $NaHSO_4$, twice with water and dried overnight in a desiccator over KOH under vacuum.

CYCLISATION AND DEPROTECTION Linear precursors were cyclised under stirring at room temperature with 1.25 equivalents (with respect to the crude linear precursor) of HATU, 1.25 equivalents of HOAt and 12.5 equivalents of DIEA in dry DMF. For the cyclisation reactions, concentrations of crude linear precursor ranging from 1 to 2.5 mg/mL were used. The progress of the reaction was monitored by LC/MS and after consumption of the starting material the reaction mixture was evaporated to dryness under vacuum, yielding a colourless to slightly yellow resin. The crude cyclised peptides were deprotected in 10 mL of TFA/TIS/water (95:2.5:2.5 v/v/v) under stirring at room temperature for 2 h or until LC/MS analysis showed the

absence of peaks that could be attributed to partially deprotected side-products. The deprotection mixture was concentrated to half its original volume, or until a precipitate formed, and was then partitioned into 50 mL glass centrifuge tubes. Crude peptides were precipitated with 30 mL/tube of diethyl ether cooled to -20°C in an ice-bath and centrifuged at 2000 rpm in a desktop centrifuge (*Megafuge 1.0R*, *Heraeus*, Hanau, Germany). The ether layers were decanted, and the precipitates were washed and centrifuged three times with additional 30 mL portions of diethyl ether. The mass balance of crude peptide mimetics after air-drying overnight were between 90-120%.

PURIFICATION AND ANALYSIS Crude cyclic peptide mimetics were purified by RP-HPLC chromatography with linear gradients of acetonitrile in water (20 to 50%) with added 0.1% of TFA on an ÄKTApurifier 100 system (*Amersham Biosciences*) using either a Vydac C18 (*Grace Vydac*, Hesperia, US) 218TP1022 (10 μm, 300 Å, 22×100 mm), a Zorbax eclipse XDB-C18 (*Agilent*, Santa Clara, US), (7 μm, 125 Å, 21.2×250 mm), or an Interchrom UP10WC4/25M (Interchim, Asnières, France), (10 μm, 300 Å, 21.2×250 mm) preparative column with flow rates between 10 and 20 mL/min and with UV detection at 226 nm, 254 nm, and 278 nm. Typical yields for purified AMPMs were in the range of 30 to 50 %.

Analytical HPLC chromatograms were run with linear gradients of acetonitrile in water (5 to 100%) with added 0.1% of TFA on an ÄKTA purifier 10 system using Vydac C18 218TP104 (4.6×250 mm, 10 μm, 300 Å), Vydac C18 218TP54 (4.6×250 mm, 5 μm, 300 Å), and Zorbax eclipse C18, (4.6×250 mm, 125 Å, 5 μm) analytical columns with a flow rate of 1 mL/min. LC/MS analyses were carried out on an HPLC system consisting of a *Dionex* P580 Pump (Sunnyvale, US), a *Gilson* 215 liquid handler (Middleton, US), and a *Dionex* UVD 170S four channel UV detector, connected to a *ThermoFinnigan* Quadrupole-ESI mass spectrometer (*Thermo Fisher Scientific*, Waltham, US). Columns used were either *Vydac* 218MS5215 (C18, 2.1×150 mm, 5 μm, 300 Å), *Vydac* 214MS5215 (C4, 2.1×150 mm, 5 μm, 300 Å), or *Zorbax* SB-C18 (C18, 2.1×150 mm, 3.5 μm, 80 Å) and chromatograms were run with 0.1% formic acid replacing TFA as ion pairing reagent.

Mass analyses were carried out by the MS-service of the University of Zurich. ESI mass spectra were recorded either on a *Waters Q-tof Ultima API* instrument

(Milford, US), a *Bruker ESQUIRE-LC* quadrupole ion trap instrument or a *Finnigan TSQ-700* instrument. Typical measurement error is 0.1%.

Analytical HPLC and mass spectrometric data of AMP(M)s and analogues as well as of LPS binding mimetics are summarised in **Appendix 2**.

SYNTHESIS OF PROTEGRIN-1 The synthesis of protegrin-1 (**11**) was carried out on the ABI 433A automated peptide synthesiser on a 0.25 mmol scale, using a Rink amide resin with a substitution of (0.66 mmol/g, *Novabiochem*) and FastMoc® chemistry according to the general procedure described above. Fmoc-deprotection of the resin and coupling of the first amino acid were carried out on the synthesiser. The linear protegrin-1 precursor was cleaved from the resin in its fully deprotected form by stirring it overnight with 25 mL of TFA/phenol/thioanisole/EDT (82.5:5:5:2.5). The resin was filtered off and washed twice with TFA and the combined filtrates were concentrated under vacuum until a precipitate formed. Precipitation was completed by addition of ice-cold diethyl ether. The crude material was centrifuged at 2000 rpm in a desktop centrifuge, washed three times with diethyl ether and dried in a desiccator in a rough vacuum over KOH. To achieve disulfide bond-formation, the linear protegrin-1 precursor was dissolved in 0.1 M ammonium bicarbonate at a concentration of 0.1 mg/mL and stirred at room temperature for 2 days. After analytical RP-HPLC showed complete consumption of the linear precursor, the reaction mixture was lyophilized to give crude protegrin-1 (**11**) as a white solid. Crude material was purified by RP- HPLC on an XTerra™ C18 (4.6×100 mm, 5 μm, 125 Å) preparative column (*Waters*, Milford, US) in a gradient of 10-60 % acetonitrile in water +0.1 % TFA over 15 minutes, and checked for the absence of free thiol functionalities via Ellman testing.[604] ESI $[M+H]^+$ = 1078.5 (calc.:1078.5); ESI $[M+2H]^{2+}$ = 719.2 (calc.:719.4)

5.2.2 NMR analysis of peptides

1D and 2D spectra were recorded at 600MHz on a *Bruker DRX-600* or Bruker *AV-600* spectrometer, or at 700MHz on a *Bruker AV-700* spectrometer Unless stated otherwise, spectra were recorded at peptide concentrations of 10 mg/ml in H_2O/D_2O 9:1 with sodium 3-trimethylsilyl(2,2,3,3,-d_4)propanoate (TSP) as internal standard. Water suppression was performed by using the WATERGATE sequence,[605] and

amino acid spin systems were identified from a TOCSY experiment.[606] NOESY experiments were used for both the sequence-specific sequentional resonance assignment and the determination of upper proton-proton distance limits required for structure calculations.[607] The structure calculation was performed by restrained molecular dynamics in torsion angle space by applying the SA protocol implemented in the program DYANA.[317] Restrained energy minimization was performed with the OPAL software,[608] which utilizes AMBER force-field. RMSD values were calculated with the program MOLMOL.[609]

NMR studies in the presence of micelles were recorded at a peptide concentration of 2 mM and at 310 K, pH 5.0, in 300 mM solutions of d_{38}-DPC in 90% H_2O/10% D_2O.

5.3 Bacteriological experiments

CULTURE MEDIA For the preparation of all solutions and media, water was purified using an *Elgastat® UHP-UF* water purification system. Unless noted otherwise, all experiments with bacterial cultures were carried out with Difco™ Mueller Hinton broth (*Becton Dickinson*, Sparks, MD) containing approximately 2.0 g of beef extract powder, 17.5 g of an acid digest of casein and 1.5 g of starch per litre.[610] For solid media, Difco™ Mueller Hinton agar containing an additional 17.0 g/L of agarose was used. All media were prepared according to the manufacturer's instructions and sterilised by autoclaving with a Model FVA steriliser (*Fedegari Autoclavi*, Albuzzano, Italy) for 20 minutes at 121 °C and 1.013×10^5 Pa.

CULTURE CONDITIONS AND GROWTH CONTROL Unless noted otherwise, all bacterial cultures were incubated at 37°C in conical flasks and agitated under orbital shaking at 200 rpm. Overnight bacterial cultures were inoculated with single colonies from agar plates freshly incubated overnight and used in turn to inoculate sterile Muller-Hinton broth, typically at a ratio of ~1:100 (v/v). For growth control, the cell density was estimated photometrically via the turbidity of the bacterial cell suspensions at 600 nm with a Cary 3 UV/Vis spectrometer (*Varian*, Palo Alto, CA). For short-term storage, bacterial strains were stored on Mueller Hinton agar plates at 4°C and were used to inoculate fresh agar plates weekly. For long term storage,

bacterial cultures were stored in 30% glycerol solution at -80°C. The control antibiotics polymyxin B sulphate, rifampicin, tobramycin and aztreonam were purchased from *Sigma* (Buchs, Switzerland); ciprofloxacin was purchased from *Fluka*.

MIC DETERMINATION The determination of the MIC was carried out according to a standard protocol[611] with the modifications of Steinberg et al. to account for unspecific adsorption of AMP(M)s onto reaction vessel surfaces,[312] and with minor modifications as described herein. Lyophylised AMP(M)s and control antibiotics were dissolved in 0.01% HOAc at a concentration of 1 mg/mL. For the routine determination of the MIC, colony material from agar plates incubated freshly overnight was taken with an inoculation loop and transferred into 3 mL of 0.9% NaCl solution. The turbidity of the bacterial suspension was adjusted to McFarland standard 0.5, and 100 µL of this bacterial suspension was transferred into 10 mL of Mueller Hinton broth supplemented with 0.02% BSA. In 96 well microtitre plates, two-fold serial dilutions of the AMP(M)s or of the control antibiotics were prepared in Mueller Hinton broth. The broth was supplemented with 0.02% BSA and the final volume of each dilution was 50 µL. Finally, 50 µL of the bacterial suspension were used to inoculate the microtitre plates to give a final cell density of approximately 5×10^5 CFU/mL in a final volume of 100 µL. Alternatively, for MIC determinations corresponding to higher cell density of the inoculum, overnight cultures of bacteria were diluted ~1:100 into fresh Mueller Hinton broth and incubated for 105 minutes under standard conditions to yield approximately 2×10^8 CFU/mL (for *P. aeruginosa* PAO1). These bacterial suspensions were then used to inoculate the two-fold serial dilutions of test compounds, which were prepared in Mueller Hinton broth supplemented with 0.04% of BSA. The microtitre plates were covered and incubated overnight at 37°C in an orbital shaker at 200 rpm. The MIC was determined by visual inspection as the minimum concentration at which no visible growth occurred after 18 to 20 hours of incubation and is expressed in µg/mL.

HAEMOLYTIC ACTIVITIES The haemolytic activities of AMP(M)s and control compounds against human red blood cells (hRBCs) were tested by a photometric assay as follows. Fresh hRBCs were washed with phosphate buffered

saline (PBS) and centrifuged three times for 10 minutes at 2'000 g in a desk-top centrifuge. Test compounds at concentrations of 100 μg/mL were incubated with 20% (w/v) of hRBCs at 37°C for one hour and at a final erythrocyte concentration of 0.9×10^9/mL. The samples were centrifuged at 2'000 g, the supernatant was diluted twenty-fold in PBS, and the optical density was measured at 540 nm. The values corresponding to 0% and 100% lysis were determined by incubation of hRBCs with PBS or 0.1% Triton X-100 in water, respectively. The OD_{540nm} corresponding to 100% lysis typically ranges from 1.6 to 2.0 and the haemolytic activity obtained for the test compounds is expressed as a percentage relative to the 100% value.

KINETICS OF BACTERIAL KILLING For the recording of killing curves, 50 mL of Mueller Hinton broth, pre-warmed to 37 °C, were inoculated ~1:100 from an overnight culture of *P. aeruginosa* PAO1 to give a starting OD_{600} of approximately 0.05. The cell culture was incubated under standard conditions and after 105 minutes, after which time the cultures typically reach a cell density of 1×10^8 CFU/mL, 10 mL portions were added to sterile 50 mL conical flasks pre-warmed to 37 °C and containing an appropriate amount of test compound. At desired time intervals before and after splitting the bacterial culture, 100 μL samples were withdrawn and diluted serially 1:10 in sterile Mueller Hinton broth. 100 μL of appropriate dilutions of the bacterial suspensions were plated in duplicate on Mueller Hinton agar plates by a spread plate method,[441] and incubated for 20 hours at 37°C. The appropriate dilution factors were determined by preliminary experiments. Bacterial colonies were counted by visual inspection and count rates between 30 and 300 were used to calculate the viable cell count which is expressed as CFU/mL.

POST-ANTIBIOTIC EFFECT For determination of the influence of washing bacterial cultures free of mimetic **18**, 400 mL of a bacterial culture of *P. aeruginosa* PAO1 were grown under standard conditions in a 2 L conical flask. After 105 minutes of incubation, corresponding to approximately 1×10^8 CFU/mL, 50 mL portions of the bacterial suspensions were withdrawn and transferred into 250 mL conical flasks. Of these, two cultures were treated with mimetic **18** while one culture was left as a control. The cultures were incubated under standard conditions for 2 hours before being centrifuged at 5000 g in a Sorvall® GSA rotor (*Kendro,* Zürich,

Switzerland). The control culture and one of the cultures treated with mimetic **18**, were washed and re-suspended twice in 50 mL of sterile Mueller Hinton broth, and finally re-suspended in 50 mL of Mueller-Hinton broth. The other culture induced with mimetic **18** was used as a positive control, and was treated identically to the other samples, but without removal of the original medium. Enumeration of the viable cell count at appropriate time intervals was carried out as described above.

MINIMAL BACTERICIDAL CONCENTRATION For the determination of the MBC, the experimental setup was essentially identical to the one described for the MIC determination in 96 well microtitre plates. However, in addition, the viable cell count for the bacterial cell suspension that was used to inoculate the microtitre plates and the viable cell count for the serial dilutions of test compounds that showed no visible growth after 20 hours of incubation at 37°C were determined as described above and used to calculate the corresponding CFU/mL. The MBC is defined as the minimum concentration of test compound that yields a reduction of at least $3\log_{10}$ in the viable cell count the incubation period.

5.4 Dye-leakage experiments

PREPARATION OF CALCEIN-ENTRAPPED VESICLES In a 25 mL round-bottomed flask, 10 mg of a mixture of 1-palmitoyl-2-oleoyl-*sn*-glycero-3-phosphocholine (POPC, **26**) and 1-palmitoyl-2-oleoyl-*sn*-glycero-3-[phospho-*rac*-(1-glycerol)] (POPG, **27**) (*Genzyme*, Liestal, Switzerland) in the desired ratio were dissolved in 10 mL of DCM/MeOH (1:1 v/v) and evaporated to dryness on a rotary evaporator to provide a lipid film on the surface of the round-bottomed flask. The lipid films were further dried on a lyophiliser for at least 2h, and then hydrated with a 50 mM calcein solution (10 mM Tris, 10 mM NaCl, 0.1 mM EDTA pH 7.4). Agitation with glass beads was used to facilitate the formation of multilamellar vesicles. Solutions of the multilamellar vesicles were then subjected to six freeze–thaw cycles with liquid nitrogen and extruded 13 times through a 100 nm polycarbonate membrane (*Nucleopore*, Pleasanton, CA) using an extruder (*Lipex Biomembranes*, Canada). The size distribution of the obtained LUVs was confirmed by dynamic light-scattering with a model 370 particle sizing system (*Nicomp*, Santa

Barbara, CA). Calcein-entrapped vesicles were separated from free dye by gel filtration through a Sephadex G-25 column (1×25 cm) with standard buffer (10 mM Tris, 100 mM NaCl, 0.1 mM EDTA, pH 7.4), possessing a comparable osmolarity to the 50 mM calcein solution, as eluent. The final phospholipid concentration was determined by phosphorus analysis as described below.

PHOSPHATE DETERMINATION The amount of phosphate was determined by a Bartlett assay[421] modified as follows: a calibration curve ranging from 0 to 80 nmol phosphate was prepared from a 1 mM KH_2PO_4 solution (1 µL = 1 nmol). The standards and the samples were prepared in borosilicate tubes and dried in a *Tecon* heat block at 100°C-120°C. Care has to be taken to increase the temperature slowly to avoid spillage of liquid from the tubes. The dry samples were then treated with 70 µl of a freshly prepared mixture of $H_2SO_4/HClO_4$ (1:1 v/v) and kept at 230-250 °C for 15-30 minutes to combust all phosphorous to inorganic phosphates. The samples were left to cool to room temperature and 1.6 mL of freshly prepared assay solution (0.835% ascorbic acid/0.2% ammonium molybdate) was added. After incubation at 45°C for 30 minutes the absorbance of each sample was measured at 820 nm, using an UV spectrometer with the phosphate-free standard solution as blank. The phosphorous concentration of the sample was then calculated from the calibration curve.

GENERAL PROCEDURE FOR THE DYE LEAKAGE ASSAY The peptide-induced leakage of calcein from the LUVs was monitored by measuring the fluorescence intensity of calcein released into the standard buffer at 20 °C. Dye-entrapped vesicles were diluted in standard buffer (2 mL) to give a final phospholipid concentration of 30 µM. The release of dye was then initiated by addition of an aliquot of peptide and the increase of the calcein fluorescence intensity was recorded for 5 minutes after addition of the test compounds with a *Perkin–Elmer* LS55 luminescence spectrophotometer (*Perkin-Elmer*, Shelton, CT) set to an emission wavelength of λ_{em} = 519 nm. The excitation wavelength was set in the range of λ_{ex} = 430–490 nm to obtain a fluorescence signal within the optimal working range of the photo detector. Slit widths of 4 nm were used throughout. The apparent percentage of calcein release was calculated according to:

$$calcein\ release = \frac{(F_t - F_0)}{(F_{\max} - F_0)} \qquad \text{[equation 5.2]},$$

where F_t is the fluorescence intensity induced by the peptide after 5 minutes of incubation, and F_0 and F_{max} denote the fluorescence intensities before addition of the test compound, and after addition of 0.1% of Triton-X 100™, respectively. Triton-X 100™ was added at the end of each experiment to cause complete disruption of the liposomes.

5.5 Incorporation experiments

RADIO-LABELLED COMPOUNDS L-[4,5-^{3}H]-leucine with a specific activity of 37 MBq/mL (1 mCi/mL), [5,6-^{3}H]-uridine with a specific activity of 37 MBq/mL (1 mCi/mL), [methyl-^{3}H]-thymidine with a specific activity of 37 MBq/mL (1 mCi/mL), [8-^{3}H]-adenine with a specific activity of 37 MBq/mL (1 mCi/mL), and *N*-acetyl-D-[1-^{3}H]-glucosamine with a specific activity of 37 MBq/mL (1 mCi/mL) were purchased from *Amersham* (GE Healthcare Europe, Otelfingen, Switzerland). All radiochemicals were supplied as sterilised aqueous solutions containing 2% ethanol.

GENERAL PROCEDURE FOR CONTINUOUS LABELLING For continuous labelling of trichloroacetic acid (TCA) insoluble fractions of *P. aeruginosa* PAO1 with tritiated precursors of macromolecular biosynthesis, 50 mL of bacterial cell suspension were grown under standard conditions. After 90 minutes of incubation, corresponding to an OD_{600} of 0.2, radioactive label was added to the cell culture to give a final activity of 5 μCi/mL. The cell culture was grown for 15 minutes in the presence of the radioactive label, after which time 1 mL portions were transferred to 10 mL sealable tubes containing the desired amount of test compound (from 1 mg/mL stock solution in 0.01% HOAc and 0.01% HOAc for the control sample). At desired time intervals before and after addition of the test compounds, 50 μL samples were withdrawn and added to 2 mL of ice-cold 10% TCA in 15 mL polypropylene tubes (*Greiner*, Frickenhausen, Germany). The samples were left at 0 °C for at least 50

minutes, warmed to 37 °C for 25 minutes and finally cooled again to 0 °C for at least 10 minutes. The acid insoluble precipitates were filtered through GF/C glass-fibre filters of 24 mm diameter (*Whatman*, Brentford, UK). The tubes were washed out twice with 1 mL of ice-cold 10% TCA and the filters were finally washed with ~5 mL of ice-cold 10% TCA. Filters were dried overnight in an oven at 40 °C. For quantification of radioactivity, the dried filters were measured in Econo 20 mL glass scintillation vials (*Packard*, Meriden, US) with 10 mL of NOCS 104 scintillation cocktail for organic solutes (*Amersham Biosciences*, Sweden) with a *Packard* 2000 CA scintillation analyser, upgraded to 2200 CA.

GENERAL PROCEDURE FOR PULSE-LABELLING For pulse-labelling of the TCA-insoluble fraction of *P. aeruginosa* PAO1, a 50 mL bacterial culture was grown under standard incubation conditions as described for the killing kinetic experiments. After 105 minutes of incubation, the bacterial suspension was split by transferring 10 mL portions to sterile 50 mL conical flasks, pre-warmed to 37 °C, and containing an appropriate amount of test compound from a 1 mg/mL stock solution in 0.01% HOAc. The test cultures were incubated at 200 rpm and 37 °C, and at the desired time intervals before and after splitting of the bacterial culture, 0.2 ml of the samples were withdrawn and added to 0.8 ml of Mueller Hinton broth pre-warmed to 37 °C in 10 mL tubes, containing the appropriate test compound at concentrations identical to the test concentrations, and with a final specific radioactivity of 1 μCi/mL of the radio-labelled precursor. To ensure maximum reproducibility, the radio-labelled precursor was added to a stock solution of Mueller Hinton broth from which the individual 0.8 mL portions containing the appropriate concentration of test compound were prepared. The 1 mL cultures were pulse-labelled by incubation at 37°C and 200 rpm for 6 minutes before they were precipitated with 1 mL ice-cold 20% TCA to give a final concentration of 10% TCA in 2 mL total volume, and the obtained precipitate was further processed as described above for the continuous labelling experiments.

In the case of pulse-labelling with [8-^{3}H]-adenine (**33**), NaOH and EDTA were added immediately after pulse-labelling to give final concentrations of 0.3M and 0.1% (w/v), respectively. The samples were then incubated overnight at 37°C to hydrolyse RNA. After the overnight incubation, the samples were cooled in an ice-bath and precipitated with 1 ml of 20% TCA and further processed as described above.

5.6 LPS binding

PREPARATION OF DANSYLATED POLYMYXIN B To a solution of 40 mg of polymyxin B sulfate in 1.2 mL of 0.1 M $NaHCO_3$, a solution of 10 mg of dansyl chloride in 800 µL of acetone was added dropwise. During addition of the acetone solution, a white precipitate formed and the reaction mixture was left to stand in the dark at room temperature for 2h. The resulting yellow suspension was centrifuged at 2'000 rpm for 8 minutes in a desktop centrifuge, and the supernatant solution was subjected to gel-filtration using a 2.5 x 30 cm column packed with Sephadex G 25 and equilibrated with 0.1 M sodium chloride. The fluorescent fractions were combined and extracted with n-butanol and evaporated to dryness to give crude dansyl polymyxin B as a yellow solid. Crude dansyl polymyxin was purified by RP-HPLC using a Vydac 218TP1022 C18 preparative column and a gradient of 16-33% acetonitrile in water containing 0.1% TFA in 35 minutes to give a mixture of five mono-dansylated products.

For the displacement assays, the concentration of mono-dansylated polymyxin B in solution was determined with a dinitrophenylation assay as follows: Standard solutions of 0 µg/mL, 5 µg/mL, 10 µg/mL, 20 µg/mL, 30 µg/mL, 40 µg/mL, and 50 µg/mL polymyxin B were prepared. To 50 µL of standard or test solution, 200 µL of a 1% (w/v) sodium tetraborate solution in H_2O and 25 µL of a 100 mM solution of 1-fluoro-2,4-dinitrobenzene in ethanol were added, and the samples were left at 37 °C for one hour. 1 mL portions of 2M HCl were added, and the aqueous phases were extracted with 1 mL of n-butanol. The absorbance of the organic phase was measured at 420 nm and the concentration of dansyl-polymyxin was calculated from the calibration curve obtained with the standard solutions.

GENERAL PROCEDURE FOR THE POLYMYXIN-DISPLACEMENT-ASSAY

Lipopolysaccharides from *E. coli* (Serotype 0111:B4) and *P. aeruginosa* (Serotype 10) were purchased from *Sigma*. Stock solutions containing 1 mg/mL of LPS were prepared in 5 mM HEPES buffer, pH 7.0 and stored at -20 °C. Dansyl polymyxin and bacterial LPS were used to prepare an assay solution containing 3 µg of both LPS and dansyl polymyxin. 2 mL of the assay solution were transferred to 3 mL fluorescence cuvettes with a pathlength of 1 cm. The fluorescence spectra were

recorded on a *Perkin Elmer* LS55 luminescence spectrometer with an excitation wavelength of λ_{ex} = 340 nm (slit width 15.0 nm) and an emission wavelength of λ_{em} = 485 nm (slit width 2.5 nm), equipped with a stirrable cell holder. Assay solutions were titrated by addition of appropriate amounts of test compounds (from 1 mg/mL stock solutions) to the stirred assay solution. The I_{50} and I_{max} values for the test compound were calculated from a plot of 1/%inhibition versus 1/concentration as described in **Section 3.7**.

5.7 Fluorescently labelled peptides

5.7.1 Synthesis of Fmoc-DANA-OH (52)

2-ACETYL-6-DIMETHYLAMINONAPHTHALENE (ACEDAN, 48)

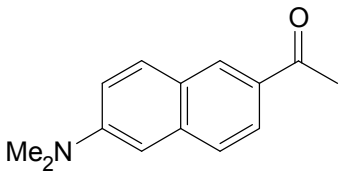

A two-necked, round-bottomed flask was charged with 16 mL of HMPT and dimethylamine was bubbled through the solution until weighing of the flask indicated the absorption of 2.4 g (53 mmol). To the colourless solution, 353 mg (50 mmol) of lithium shots were added and the reaction mixture was stirred at room temperature under argon for 1.5 hours to give a deep red solution. To this, 3.00 g (15 mmol) of 2-acetyl-6-methoxynaphthalene (**47**) were added and the reaction mixture was stirred overnight at room temperature and under argon. The mixture was then cooled in an ice-bath and poured into a cold mixture of 200 ml water and 200 ml ethyl acetate. After thorough mixing, the aqueous phase was separated and extracted twice with 100 ml of ethyl acetate. The combined organic phases were dried over Na_2SO_4 and evaporated to dryness to give 3.15 g (99 %) of crude acedan (**48**). Recrystallisation from ethanol afforded 2.24 g (70 %) of **48** as yellow flakes. M.p. 154-155 °C (from ethanol, lit.[612]: 153.5-155 °C). IR (KBr): 1663 *s* (CO). ^{1}H-NMR (300 MHz; $CDCl_3$): 2.65 (3 H, *s*, acetyl-CH_3), 3.09 (6 H, *s*, N-$(CH_3)_2$), 6.88 (1 H, *m*, Ar-H), 7.16

(1 H, *dd*, *J* 2.6 and 9.1, Ar-H), 7.62 (1 H, *d*, *J* 8.7, Ar-H), 7.78 (1 H, *d*, *J* 9.1, Ar-H), 8.26 (1 H, *dd*, *J* 1.8 and 8.7, Ar-H), 8.26 (1 H, *m*, Ar-H). ^{13}C-NMR (75.5 MHz; $CDCl_3$): 26.3 (*q*), 40.4 (*q*), 105.4 (*d*), 116.2 (*d*), 124.5 (*d*), 125.0 (*s*), 126.1 (*d*), 130.2 (*d*), 130.6 (*d*), 130.8 (*s*), 137.5 (*s*), 150.1 (*s*), 197.5 (*s*). ESI-MS $[M+H]^+$ = 214.2 (calc.: 214.1).

2-(α-IODOACETYL)-6-DIMETHYLAMINONAPHTHALENE (49)

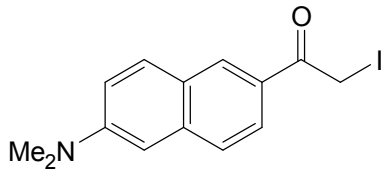

In a 250 ml three-necked, round-bottomed flask equipped with a magnetic stirrer bar and a reaction thermometer, 2.00 g (9.4 mmol) of **48** were dissolved in 25 mL of dry THF to give a clear, slightly yellow solution. Subsequently, the solution was cooled in an acetone/dry ice bath to -78 °C. **48** started to precipitate at a temperature of about -10 °C, giving a white suspension. To this suspension 10.3 mL of a 1.0M solution of lithium bis(trimethylsilyl)amide in THF, that had been pre-cooled to 0 °C, were added dropwise via a syringe. The temperature during the addition was kept below -70 °C, and the reaction mixture was then stirred under argon for 30 minutes to yield a clear solution. Addition of another 0.5 mL of base and stirring for 10 minutes resulted in a clear, slightly orange solution of the enolate. To the enolate, a solution of 2.44 g (9.8 mmol) of iodine in 20 mL of THF that had been pre-cooled to 0 °C was added dropwise via a syringe, keeping the temperature below -70 °C. The reaction mixture was then stirred under argon for one hour at -78 °C in the dark. After quenching with 1 mL of a 1.0 M solution of $NaHSO_4$, the mixture was allowed to warm to 0 °C and a further 17 mL of the $NaHSO_4$ solution were added. After addition of 40 mL of water and 300 mL of ethyl acetate, the layers were separated and the organic phases were washed twice with 50 mL of concentrated $Na_2S_2O_3$ solution, once with 50 mL of water and finally with 50 mL of brine. The resultant orange solution was dried over Na_2SO_4 and evaporated to dryness to yield 3.15 g (9.3 mmol, 99%) of crude **49** as an orange solid. IR (KBr): 1647 *s* (CO). ^{1}H-NMR (300 MHz; $CDCl_3$): 3.11 (6 H, *s*, N-$(CH_3)_2$), 4.42 (1 H, *s*, CH_2I) 6.85 (1 H, *d*, *J*

2.5, Ar-H), 7.15 (1 H, *dd*, *J* 2.5 and 9.1, Ar-H), 7.62 (1 H, *d*, *J* 8.7, Ar-H), 7.79 (1 H, *d*, *J* 9.1, Ar-H), 7.89 (1 H, *dd*, *J* 1.9 and 8.7, Ar-H), 8.35 (1 H, *m*, Ar-H); ^{13}C-NMR (75.5 MHz; $CDCl_3$): 0.8 (*t*), 38.4 (*q*), 103.3 (*d*), 114.3 (*d*), 122.9 (*s*), 123.1 (*d*), 124.4 (*d*), 124.8 (*s*), 128.9 (*d*), 129.1 (*d*), 136.0 (*s*), 148.5 (*s*), 190.2 (*s*). ESI-MS $[M+H]^+$ = 201.3 (calc.: 201.1). ESI-MS $[M+H]^+$ = 340.2 (calc.: 340.0).

PRODAN SCHIFF BASE (51)

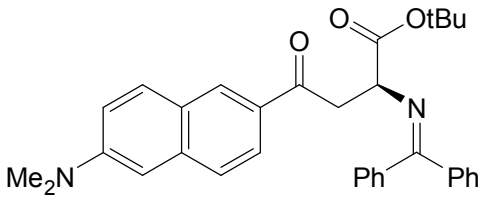

In a 250 mL three-necked, round-bottomed flask equipped with a magnetic stirrer bar and a reaction thermometer, 731 mg (2.47 mmol) of *N*-(diphenylmethylene)glycine tert-butyl ester[613] and 260 mg (0.50 mmol, 20 mol%) of the phase-transfer catalyst *O*-(9)allyl-*N*-(9-anthracenylmethyl)cinchonidinium bromide (**50**) were dissolved in 5 mL of dry DCM to give a clear, colourless solution. The solution was cooled to -78 °C in an acetone/dry ice bath under argon and 4.5 g (27 mol) of caesium hydroxide monohydrate were added portionwise to give a brown suspension. To this suspension, a solution of 900 mg (2.65 mmol) of **49** in 20 mL of dry DCM, pre-cooled to -78 °C was added, keeping the temperature below -60 °C. The reaction mixture was stirred under argon at -78 °C overnight. After HPLC MS analysis showed no more consumption of **49**, even after addition of another 150 mg N-(diphenylmethylene)glycine tert-butyl ester, the reaction mixture was allowed to warm to 0 °C and was diluted with 250 mL of diethyl ether and 50 mL of water. The organic phase was washed three times with 20 mL of water and 20 mL of brine, dried over Na_2SO_4 and evaporated to dryness to yield 1.14 g (85 %) of crude PRODAN Schiff base (**51**) as an orange solid which was used without further purification. ^{1}H-NMR (300 MHz; $CDCl_3$): 1.44 (9 H, *s*, $C(CH_3)_3$), 3.09 (6 H, *s*, N-$(CH_3)_2$), 3.58 (1 H, *dd*, *J* 7.2 and 16.7, CH_2), 3.75 (1 H, *dd*, *J* 5.8 and 16.7, CH_2), 4.69 (1 H, *dd*, *J* 5.8 and 7.2, CH), 6.85 (1 H, *d*, *J* 2.5, Ar-H), 7.14 (1 H, *dd*, *J* 2.5 and 9.1, Ar-H), 7.30 (6 H, *m*, Ar-H), 7.42 (2 H, *m*, Ar-H), 7.58 (3 H, *m*, Ar-H), 7.77 (1 H, *d*, *J* 9.1, Ar-H), 7.89 (1 H,

dd, *J* 1.8 and 8.7, Ar-H), 8.35 (1 H, *m*, Ar-H). ESI-MS $[M+H]^+$ = 507.5 (calc.: 507.3).

DANA-OH (41)

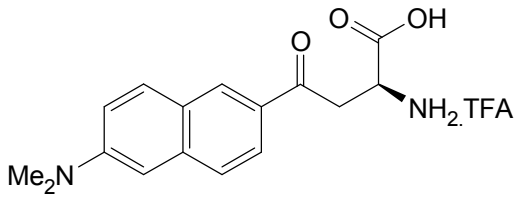

Crude PRODAN Schiff base **51** (720 mg, 1.38 mmol) was dissolved in 10 mL of TFA containing 250 μL of ethanedithiol and was stirred overnight under argon. The TFA solution was concentrated under vacuum to give a dark green highly viscous solution that was partitioned into two 50 mL glass centrifuge tubes and precipitated with ice-cold diethyl ether to afford a yellow-brown solid. The precipitate was washed, centrifuged at 2000 rpm in a desk-top centrifuge at room temperature, and washed twice with diethyl ether to afford 379 mg (96 %) of crude **41** as a dark yellow solid which was used without further purification. For analytical purposes, a small amount of DANA-OH was purified by reversed phase HPLC. ^{1}H-NMR (300 MHz; DMSO-d_6): 3.07 (6 H, *s*, N-$(CH_3)_2$), 3.67 (2 H, *m*, CH_2), 4.20 (1 H, *m*, CH), 6.95 (1 H, *d*, *J* 2.2, Ar-H), 7.28 (1 H, *dd*, *J* 2.5 and 9.2, Ar-H), 7.67 (1 H, *d*, *J* 8.7, Ar-H), 7.81 (1 H, *dd*, *J* 1.6 and 8.7, Ar-H), 7.91 (1 H, *d*, *J* 9.2, Ar-H), 8.47 (1 H, *br*, Ar-H). ESI-MS $[M+H]^+$ = 201.3 (calc.: 201.1). ESI-MS $[M+H]^+$ = 287.1 (calc.: 287.1).

FMOC-DANA-OH (52)

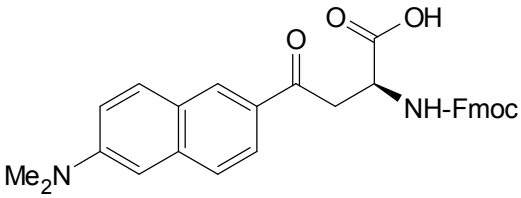

Crude **41** (347 mg, 1.2 mmol) was suspended in 20 mL of water and the pH was adjusted to 8.0 by addition of $NaHCO_3$. A solution of 520 mg (1.54 mmol) of

Fmoc-OSu in 20 mL of acetone was added and the reaction mixture was stirred for 3 hours at room temperature. Since LC/MS analysis of the reaction mixture showed complete consumption of **41**, the solution was diluted with 400 ml of ethyl acetate and acidified with 2.0 M HCl to a pH of 2-3. The aqueous phase was extracted three times with 100 mL of ethyl acetate and the combined organic phases were dried over $NaHCO_3$ and evaporated to dryness to give 585 mg (96 %) of Fmoc-DANA (**52**) as a yellow solid. ^{1}H-NMR (300 MHz; $CDCl_3$): 3.12 (6 H, *s*, N-$(CH_3)_2$), 3.61 (1 H, *dd*, *J* 4 and 18.3 CH) 3.92 (1 H, *dd*, *J* 4 and 18.3, C-H), 4.20 (1 H, *t*, *J* 6.9, C-H), 4.38 (2 H, *m*, *J* 8.7, CH_2), 4.83 (1 H, *m*, C-H), 6.03 (1 H, *d*, *J* 8.1 C-H), 6.93 (1 H, *br*, Ar-H); 7.15-7.39 (5 H, *m*, Ar-H), 7.57 (2 H, *d*, *J* 7.4, Ar-H), 7.64 (1 H, *d*, *J* 8.8, Ar-H), 7.71 (2 H, *m*, Ar-H), 7.79 (1 H, *d*, *J* 9.1, Ar-H), 7.89 (1 H, *d*, *J* 8.5, Ar-H), 8.32 (1 H, *br*, Ar-H). ESI-MS $[M+H]^+$ = 509.3 (calc.: 509.2).

DETERMINATION OF ENANTIOMERIC EXCESS OF DANA-OH (41) For the determination of the enantiomeric excess of **41** according to Marfey,[614] 2.5 mg (9 μmol) of **41** were dissolved in 400 μL of DMF/water (1:1) and the pH of the solution was adjusted to pH 8 by addition of $NaHCO_3$. 3 mg of N_α-(2,4-Dinitro-5-fluorophenyl)-L-valinamide[615] (10 μmol) were added, and the reaction mixture was left to stand at 37 °C for one hour. The mixture was then acidified with 40 μL of 1.0M HCl and subjected to analytical HPLC and LC/MS analysis. Integration of the corresponding peaks gave an enantiomeric excess of 90% ee.

FLUORESCENCE MEASUREMENTS WITH NAAA (78) Fluorescence spectra were recorded on a Perkin Elmer LS 55 luminescence spectrometer, equipped with a stirrable four-cell holder. Quartz cuvettes with a path length of 1 cm and a total volume of 3 ml were used throughout and all measurements were carried out at 20 °C. An acetonitrile stock solution of *N*-acetyl-DANA-NH_2 (NAAA, **78**) was prepared with a concentration of 20 μM and diluted 1:100 into cuvettes containing 2 ml of the appropriate solvent to give a final concentration of the fluorophore of 200 nM. Fluorescence emission spectra were recorded with an excitation wavelength of 360 nm and excitation/emission slit widths of 5.0 nm. All measurements were carried out in triplicate.

5.7.2 Fluorescence measurements

FLUORESCENCE MEASUREMENTS WITH AMPMS Fluorescence spectra of AMPMs in the presence and absence SDS micelles were recorded on a Perkin Elmer LS 55 luminescence spectrometer, equipped with a stirrable four-cell holder and at 20 °C. Quartz cuvettes with a path length of 1 cm and a total volume of 3 ml were used throughout. 2 μM of the appropriate peptide AMPM were titrated into matched quartz cuvettes containing 2 mL of 10 mM Tris-buffer (pH 7.0, 10 mM NaCl) either in the presence or absence of 25 mM SDS. Excitation wavelengths were 295, or 280 nm with a slit width of 5.0 nm.

MEMBRANE PARTITIONING EXPERIMENTS POPC/POPG LUVs were prepared as described for the calcein-entrapped vesicles using a buffer system without calcein (10 mM Tris, 100 mM NaCl, 0.1 mM EDTA, pH 7.4). Fluorescence spectra were measured on a Perkin Elmer LS 55 luminescence spectrometer, equipped with a stirrable four-cell exchanger at 20 °C. Quartz cuvettes with a path length of 1 cm and a total volume of 3 mL were used throughout. The polarization filters in the excitation and emission pathways were set to vertical (excitation) and horizontal (emission) and the spectra were recorded with an excitation wavelength of λ_{ex} = 360 nm with slit widths of 4.0 nm for both excitation and emission. To a solution of the fluorescently labelled peptide at a final peptide concentration of 1 μM, increasing amounts of the POPC/POPG liposomes system were titrated and mixed by inversion. Assay solutions were equilibrated for at least 20 minutes before the fluorescence spectra were recorded. All measurements were carried out in triplicate and all spectra were corrected for the background emission of the buffer system as well as for the background emission of liposome solutions alone.

5.8 Protein expression profiling

FRACTIONATION PROTOCOL 600 mL cultures of *P. aeruginosa* PAO1 were grown under standard incubation conditions in 2 L conical flasks. After 105 minutes of incubation, bacterial cultures were induced with either 0.3 μg/mL of mimetic **18**

from a 1 mg/mL stock solution in 0.01% HOAc or with a corresponding volume of 0.01% HOAc (control). After three hours of incubation, cells were harvested via centrifugation at 5000 rpm with a Sorvall® GS-3 rotor for 30 minutes at 4 °C. Cell pellets were washed twice with 50 mM Tris/HCl, pH 7.5 and centrifuged at 5000 rpm for 15 minutes.

For the isolation of extracellular proteins, the supernatant of the first centrifugation was precipitated with 10% w/v TCA at 4°C overnight. The precipitate was isolated by centrifugation at 5000 rpm in a GS-3 rotor for 1.5 h at 4°C, washed and centrifuged twice with ethanol, and air-dried.

For the isolation of surface-associated proteins, four grams of the bacterial cell pellet were re-suspended in 0.2M glycine/HCl, pH 2.2 and the suspension was stirred at room temperature for 15 minutes. Cells were removed by centrifugation at 5000 rpm with a Sorvall® GSA rotor for 20 minutes at 4 °C and the pH of the supernatant was adjusted to 7.5 by addition of NaOH. Extracted proteins were treated with acetone corresponding to three times the original volume and subsequently precipitated overnight at -20 °C. The obtained precipitate was isolated by centrifugation at 7000 rpm for 30 minutes at 4 °C, washed and centrifuged first with 70% EtOH and subsequently with 70% acetone, and air-dried overnight.

For the isolation of intracellular proteins, cell pellets were taken up in 20 mL of 50 mM Tris/HCl, supplemented with protease inhibitors (*Calbiochem* Protease Inhibitor Cocktail Set I, *EMD Biosciences*, San Diego, US), and broken up by sonicating 5 times for 1 minute with a *Branson* model 450 tip sonicator (Banbury, US) at an amplitude of 40%. To prevent heating, samples were cooled in an ice-bath and pauses of at least two minutes were implemented between the sonication pulse programs. Cell debris was removed by centrifugation at 12000 rpm with a Sorvall® SS34 rotor and the supernatant was split into aliquots of 1 ml and stored at -20°C.

PHENOL EXTRACTION Precipitates from the extracellular or surface-associated fractions were taken up in 50 mM Tris/HCl, pH 7.5 at concentrations of 50 mg/mL. 1 mL aliquots of the different protein fractions were mixed with 1 mL of phenol under vortexing and heated to 70°C for 10 minutes. The samples were cooled on ice for 5 minutes and centrifuged at 5000 rpm in an *Eppendorf* desk-top centrifuge (Hamburg, Germany) for 10 minutes to result in phase separation. The upper aqueous layer was discarded and the phenol layer was washed with 1 mL of water and

centrifuged as described above. After removal of the aqueous layer, 1 mL acetone, pre-cooled to -20°C was added and proteins were precipitated for 3 to 20 hours at -20°C. Precipitated proteins were isolated by centrifugation for 20 minutes at 13200 rpm and the supernatant was discarded. The protein pellet was washed with ice-cold acetone, centrifuged at 13200 rpm, and then air-dried at room temperature.

ISOELECTRIC FOCUSSING For isoelectric focussing, pellets were taken up in rehydration buffer [8M urea, 2% (w/v) CHAPS, 15 mM DTT, 0.5% (v/v) immobilised pH-gradient (IPG) buffer pH 3-10 or 4-7]. The IPG buffers consist of carrier ampholytes formulated for *Amersham* Immobiline™ DryStrip pH-gradients (*GE Healthcare Bio-Sciences*, Uppsala, Sweden). Protein concentrations were determined by a Bradford assay with 5 µL of the protein solution, mixed with 1 mL of Coomassie Plus protein assay reagent (*Pierce*, Rockford, IL) and measured at 595 nm relative to BSA as a standard.

IEF was carried out with immobilised pH gradient (IPG) strips (*Amersham*) with an Ettan™ IPGPhor II™ IEF unit (*Amersham*) and settings according to **Table 5.1**. For each run, 300 to 350 µg of proteins in 450 µL of rehydration buffer were used, which were spread evenly between the electrodes of the ceramic strip-holder (*Amersham*). Immobilised IPG strips were laid onto the protein mixture with care not to entrap air bubbles. IPG strips were covered with mineral oil and with the provided lids.

Table 5.1 Ettan™ IPGPhor II™ settings for the isoelectric focussing of IPG strips.

Basic parameters	
Temperature	20 °C
Maximum current	50 µA per IPG strip
Voltage	**Time**
30 V	13 h (rehydration of the gel-matrix and of application of the sample)
200 V	1h 30min
500 V	1h 30min
1000 V	1h 30 min
Gradient 1000 V → 8000 V	1h
8000 V	5h
Total time	**23.5 h**

SECOND DIMENSION For separation according to the molecular masses, IPG strips were transferred into sealable tubes in which they were agitated gently on an orbital shaker together with 10 mL of equilibration buffer A [**Appendix 3**] for 10 to 15 minutes. After decanting equilibration buffer A, the procedure was repeated with equilibration buffer B [**Appendix 3**]. Equilibrated IPG strips were washed briefly in electrophoresis buffer and applied to the top of the SDS-PAGE gels, where special care was taken that no air bubbles were trapped between the gel and the IPG strips. 2D PAGE gels were of dimensions of 26×20×0.15 cm and contained 12.5% polyacrylamide. The gels were cast manually with 12.5% gel solution [**Appendix 3**] in an Ettan™ DALTtwelve gel caster (*Amersham*) according to the manufacturers instructions, and stored at 4 °C in storage buffer before use [**Appendix 3**].

At the acidic end of the IPG strips, square filter paper was added which had been soaked with 15 µL of *Bio-Rad* Precision Plus Protein Standards (*Bio-Rad*, Hercules, US). IPG strips were fixed to the surface of the PAGE-gel with 2 mL of 1% agarose and the gels were run in an Ettan™ DALTtwelve vertical chamber (*Amersham*) with electrophoresis with 2D electrophoresis buffer [**Appendix 3**], and according to the settings described in **Table 5.2**.

Table 5.2 Instrument settings for the second dimension electrophoretic separation.

Time	Settings of the power source	Remarks
45 to 60min	40 mA constant	Sample application
4 to 6h	90 to 120W constant	Depending on the number of gels

VISUALISATION AND DOCUMENTATION After the electrophoresis run, gels were removed from the gel cassettes and the IPG strips and the agarose were removed. Gels were fixed in fixing solution [**Appendix 3**] for at least one hour at room temperature, washed with water, and proteins were visualised by overnight incubation with colloidal Coomassie Brilliant Blue G-250 staining solution [**Appendix 3**], under gentle agitation on an orbital shaker at room temperature. Stained gels were discoloured by washing with water under gentle agitation for about 24 hours whereby the water was exchanged frequently. Wet gels were scanned

immediately with an ImageScanner™ (*Amersham*) at 300 dpi. Gels were stored at 4 °C in sealed plastic bags in aqueous solution supplemented with NaN_3 to prevent microbial growth.

IDENTIFICATION OF PROTEIN SPOTS For the identification of protein spots, gels were washed with water for 30 minutes to remove NaN_3, and protein spots were picked from the gel by using 1000 µL disposable pipette tips, whose diameter had been cut to match the size of the protein spot, and transferred to 96 well microtitre plates. Unless noted otherwise, the following operations were carried out with 100 µL solutions. Protein spots were destained with 100 mM $(NH_4)HCO_3$, pH 8.0/MeOH (50:50 v/v) for 3 hours at 37 °C, washed twice with water and once with 100 mM NH_4HCO_3, pH 8.0. Gel plugs were then shrunk by dehydrating in 80% acetonitrile for 10 minutes until the gel plugs assumed an opaque appearance. The solvent was then removed by drying at 50 °C for 30 minutes and the gel plugs were re-hydrated in 10 µL of trypsin solution (10 ng/µL of trypsin in 5 mM Tris buffer, pH 7.8-8.0) at room temperature for 15 minutes. After rehydration, the gel plugs were covered with 20 µL of 5mM Tris, pH 7.8-8.0 and proteins were digested for 3 to 6 hours at 37 °C. Protein digests were stored at -20 °C until spotting onto MALDI plates.

MASS SPECTROMETRIC ANALYSIS OF TRYPTIC PROTEIN DIGESTS The supernatant of the digested protein spots was spotted on MALDI plates coated with 0.25 mL of a 1 mg/mL α-cyano-4-hydroxycinnamic acid solution in acetonitrile and air-dried. Subsequently, 50 µL of the sample were added to the MALDI plate and mixed with 0.5 µL of the matrix solution containing 15 mg/mL α-cyano-4-hydroxycinnamic acid in 50% acetonitrile, containing 0.5% TFA). The matrix solutions were then air-dried for 10 minutes.

MALDI plates were measured at the Functional Genomics Centre Zürich (FGCZ), using a 4700 Proteomics Analyzer MALDI-TOF/TOF mass spectrometer (*Applied Biosystems*, Foster City, CA), allowing for the detection of both intact peptides and of fragment ions created in the collision cell of the instrument. The mass spectrometer is equipped with a Nd:YAG-laser working at a frequency of 200 Hz. Mass spectra were recorded in positive ion reflector mode and the mass spectrometer was calibrated by a multilevel external calibration with six peptide samples and

spectra were calibrated internally using the trypsin autolysis fragments corresponding to 842.509 and 2211.101 Da, resulting in an accuracy of the mass determination of 10 ppm or better.

Proteins were identified from their peptide mass maps using the GPS-explorer software (*Applied Biosystems*, Foster City, US) with the integrated MASCOT search engine (Matrix Science, London, UK). A maximum of one missed enzymatic cleavage and modification of cysteines by carboxymethylation and of methionines by partial oxidation were considered during the searches, which were based on the non-redundant NCBI database and the annotated sequence database of *P. aeruginosa* PAO1.[537]

5.9 Affinity chromatography

PREPARATION OF AFFINITY COLUMNS For the preparation of affinity columns, AMPMs were coupled to NHS-activated sepharose HiTrap™ columns (1 mL, *Amersham*) according to the manufacturer's instructions. Briefly, AMPM ligands were coupled in standard coupling buffer (0.2 M $NaHCO_3$, 0.5 M NaCl, pH 8.3) for 30 minutes at room temperature, and unreacted NHS on the matrix was blocked with a buffer containing 0.5M ethanolamine, 0.5M NaCl, pH 8.3. The coupling efficiencies were determined spectrometrically via the UV absorption of the ligand at 280 nm and were found to be always ≥ 90%. Columns were equilibrated with affinity chromatography standard buffer (50 mM potassium phosphate, 100 mM NaCl, pH 7.0), and stored at 4 °C in standard buffer supplemented with 0.1% NaN_3.

FRACTIONATION OF P. AERUGINOSA PAO1 For affinity chromatography experiments with *P. aeruginosa* PAO1, cell cultures were harvested in their mid-logarithmic growth phase, typically at an OD_{600} of 1.0, via centrifugation at 5000 rpm for 30 minutes in a Sorvall® GS-3 rotor, and the cell pellets were washed twice in standard buffer (50 mM potassium phosphate, 100 mM NaCl, pH 7.0)

The cell pellet was taken up in 30 mL of standard buffer and protease inhibitors were added (*Calbiochem* Protease Inhibitor Cocktail Set I). Cells were broken up either by sonicating five times with a tip sonicator as described above, or by passing the bacterial suspension twice through a French pressure cell (*SLM*

Aminco, Urbana, US) cooled to 0 °C. Cell debris was removed by low speed centrifugation at 5000 g for 10 minutes in an SS34 rotor, and the crude cell mixtures were further fractionated by centrifugation at 40000 g for 30 minutes in an SS34 rotor. A final centrifugation step of the supernatant at 100000 g in a *Sorvall* OTD-Combi ultracentrifuge (*Kendro,* Zürich, Switzerland) with the T 865 rotor was carried out to separate the cytoplasmic membrane and smaller outer membrane fragments from the soluble intracellular fraction. For experiments with membrane preparations, 1% of the non-ionic detergent Triton-X 100™ was added to the buffer systems as solubilising agent. Protein concentrations were determined from the UV absorptions at 260 and 280 nm, and by Bradford analysis.[535]

AFFINITY CHROMATOGRAPHY Affinity chromatography experiments with AMPMs coupled to 1 mL of NHS-activated sepharose pre-packed columns were carried out with a P-1 peristaltic pump (*Pharmacia*, Uppsala, Sweden) set to flow rate of 1 mL/min. The outlet of the column was connected to the UV detector of an AKTA purifier 10 system (*Amersham*, Uppsala, Sweden) and the UV absorptions at 226 nm, 254 nm and 278 nm were recorded. The eluate was collected in fractions of 3 mL and the fractions were frozen immediately and stored at -20°C until further analysis.

PAGE ANALYSIS 1D PAGE gels were run either on the Phast™ system using pre-cast Phast gels (*Amersham*, Uppsala, Sweden), or according to standard procedures[616] with manually cast gels of dimensions 18×12×0.1 cm with a stacking gel of 5% polyacrylamide and with 12% or 15% of polyacrylamide gel solutions [**Appendix 3**] in a vertical electrophoresis chamber. Proteins were visualised either by staining with colloidal Coomassie Brilliant Blue G-250 dye,[617] or by silver staining.[616] Separation of protein mixtures by 2D-PAGE and mass spectrometric analysis of excised protein spots was performed as described above for the protein expression profiling experiments.

5.10 Photo-affinity labelling

PAL WITH PHOTO-REACTIVE ANALOGUES OF MIMETIC 19 For the PAL experiments cultures of *P. aeruginosa* were either labelled *in vivo* or *in vitro*. For *in vivo* PAL, *P. aeruginosa* PAO1 cells were harvested in their logarithmic growth phase and washed twice by re-suspending them in standard PAL buffer and centrifugation at 5'000 rpm for 30 minutes. Cells were re-suspended in PAL standard buffer in aliquots of either 5 or 10 mL to give an approximate cell density of 5×10^9 CFU/mL. Alternatively, for *in vitro* PAL, bacterial cell suspensions were pre-fractionated according to the differential centrifugation protocol described for the affinity chromatography experiments.

Bacterial suspensions, or membrane or intracellular fractions of *P. aeruginosa* PAO1 were incubated with 5 or 10 μg/mL of the photo-reactive AMPM in *Sterilin* Petri dishes of 5 or 10 cm diameter (*Bibby Sterilin*, Stone, UK) corresponding to 5 or 10 mL of bacterial suspension for 30 minutes at 4 °C in the dark. Prior to that, labelling mixtures were incubated with 100 or 500-fold excess of competitive ligand (either mimetic **19** or ent-**18**) for 30 minutes at 4 °C in the dark. PAL was carried out for 10 minutes in the Petri dishes with handheld Model UVGL-55 Mineralight™ multiband UV lamps (*UVP*, Upland, US) at a distance of 5 cm from the light sources at 4 °C and under agitation on an orbital shaker at 50 rpm.

For *in vivo* PAL, samples were fractionated according to the protocol described above and biotinylated species were isolated by incubation with streptavidin immobilised on agarose (ImmunoPure® Immobilized Streptavidin Gel, *Pierce*, Rockford, US). In the case of membrane systems, 1% of Triton-X 100™ was added to the buffer systems to aid in solubilisation of membrane proteins. For 1D PAGE analysis, biotinylated species retained on the streptavidin matrix were eluted directly by boiling with SDS sample buffer for 10 minutes with intermittent vortexing.

BLOTTING 1D PAGE gels were run as described for the affinity chromatography experiments and transferred immediately to *Amersham* Hybond™-P PVDF membranes (*Amersham*, Uppsala, Sweden) by semi-dry blotting with either a Multiphor II (*Amersham*, Uppsala, Sweden) semi-dry transfer chamber for 1 h at 0.8 mA/cm^2 or with the PhastTransfer™ semi-dry transfer kit (*Pharmacia*, Uppsala,

Sweden) for 30 minutes at 1 mA/cm^2 with transfer buffer [**Appendix 3**]. For the detection of biotinylated species, a modified Western blot procedure was employed. Unless noted otherwise, the following operations were carried out under gentle agitation on an orbital shaker at 50 rpm.

Immediately after transfer, the membrane was blocked with 5% BSA in TBS buffer [**Appendix 3**] for at least 2 hours, preferably overnight. The blocking solution was decanted and the membrane was washed three times with TTBS buffer [**Appendix 3**]. One hour before washing the membrane with TTBS buffer, the alkaline phosphatase/streptavidin complex was formed by incubating biotinylated alkaline phosphatase with streptavidin in TTBS buffer according to the manufacturer's instructions[***] for one hour in TBS buffer. The membrane was incubated with the complex for one to two hours under gentle agitation on an orbital shaker. The solution was then decanted off, and the membrane was washed with TTBS buffer four times for 10 minutes. For colour development, the membrane was covered with the BCIP/NBT reagent (*Sigma*, Buchs, Switzerland) and incubated for a maximum of 30 minutes. Colour development was stopped by washing twice 10 minutes in double-distilled water.

[***] "Amplified Alkaline Phosphatase Goat Anti-Rabbit Immun-Blot® Assay Kit" instruction manual, catalogue number 170-6412, *Bio-Rad*, Hercules, USA

Appendix 1: Abbreviations

AMP	Antimicrobial peptide
AMPM	Antimicrobial peptide mimetics
APS	Ammonium peroxodisulfate
BCIP	5-Brom-4-chlor-3-indoxylphosphat
BSA	Bovine serum albumin
Boc	*tert*-Butyloxycarbonyl
^{t}Bu	*tert*-Butyl
calc.	Calculated
CFU	Colony forming units
CHAPS	3-((3-Cholamidopropyl)dimethylammonio)-1-propanesulfonate
DCM	dichloromethane
DEPT	Distortionless enhancement by polarization transfer
DIEA	*N*,*N*-Diisopropylethylamine
DME	1,2-Dimethoxyethane
DMF	*N*,*N*-Dimethylformamide
DMSO	Dimethylsulfoxid
DNA	Deoxyribonucleic acid
DPC	Dodecylphosphocholine
DQF-COSY	Double quantum filtered correlated spectroscopy
DTT	Dithiothreitol
EDT	Ethanedithiol
em	Emission
ESI	Electrospray ionisation
ex	Excitation
FGCZ	Functional Genomic Center Zurich
Fmoc	*N*-9H-Fluoren-2-ylmethoxycarbonyl
Fmoc-OSu	*N*-(9H-Fluoren-2-ylmethoxycarbonyl)succinimide
HATU	*O*-(7-Azabenzotriazol-1-yl)-*N,N,N′,N′*-tetramethyluronium hexafluorophosphate
HBTU	*O*-(Benzotriazol-1-yl)-*N,N,N′,N′*-tetramethyluronium hexafluorophosphate
HEPES	4-(2-Hydroxyethyl)piperazine-1-ethanesulfonic acid
HMPT	Hexamethylphosphorous triamide
HOAt	1-Hydroxy-7-azabenzotriazole
HOBt	1-Hydroxybenzotriazole
HPLC	High performance liquid chromatography
IPG	Immobilised pH gradient
MALDI	Matrix-assisted laser desorption/ionisation

MH broth/agar	Mueller-Hinton broth/agar
M.p.	Melting point
MS/MS	Tandem mass spectroscopy
Mtt	Methyltrityl
NBT	Nitro-blue tetrazolium chloride
NCBI	National Center for Biotechnology Information
NHS	*N*-Hydroxysuccinimide
NOESY	Nuclear overhauser enhancement spectroscopy
OD	Optical density
PAGE	Polyacrylamide gel electrophoresis
Pbf	Pentamethyldihydrobenzofuran-5-sulfonyl-
PMF	Peptide mass fingerprinting
RP	Reversed phase
Rpm	Revolutions per minute
R.t.	Room temperature
SA	Simulated annealing
SDS	Sodium dodecylphosphate
SPPS	Solid phase peptide synthesis
TBS	Tris-buffered saline
TCA	Trichloroacetic acid
TEMED	*N*,*N*,*N*',*N*'-Tetramethylethylenediamine
TFA	Trifluoroacetic acid
TFE	Trifluoroethanol
TIS	Triisopropylsilane
TOCSY	Totally correlated spectroscopy
Tris	Tris-(hydroxymethyl-)aminoethane
Trt	Trityl
TSP	3-Trimethylsilylpropionic acid-d_4 sodium salt

Appendix 2: Analytical data

Table A2.1 Summary of the HPLC and ESI mass spectrometric analytical data of AMPMs (**16-19**), LPS binding mimetics (**34-36**), and labelled AMPM-analogues (**70**, **75**, **77-86**, and **89-97**).

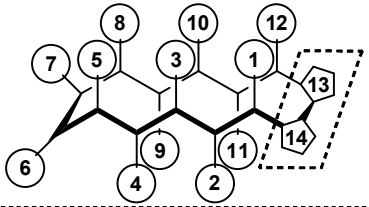

identifier	position[a]														column[b]	conditions[c]	t_R [min][d]	mass[e]
	1	2	3	4	5	6	7	8	9	10	11	12	13	14				
16	Leu	Arg	Leu	Lys	Lys	Arg	Arg	Trp	Lys	Tyr	Arg	Val	pro	Pro	A	A	14.7	940.1 (939.6) $[M+2H]^{2+}$ 627.0 (626.7) $[M+3H]^{3+}$
ent-**16**	leu	arg	leu	lys	lys	arg	arg	trp	lys	tyr	arg	val	Pro	pro	A	A	14.7	940.1 (939.6) $[M+2H]^{2+}$ 626.9 (626.7) $[M+3H]^{3+}$
17	Arg	Trp	Leu	Lys	Lys	Gln	Arg	Trp	Lys	Tyr	Tyr	Arg	pro	Pro	A	A	13.4 and 14.0[f]	994.6 (994.6) $[M+2H]^{2+}$ 663.2 (663.4) $[M+3H]^{3+}$
ent-**17**	arg	trp	leu	lys	lys	gln	arg	trp	lys	tyr	tyr	arg	Pro	pro	A	A	13.4 and 14.0[f]	994.6 (994.6) $[M+2H]^{2+}$ 663.3 (663.4) $[M+3H]^{3+}$
18	Thr	Trp	Leu	Lys	Lys	Arg	Arg	Trp	Lys	Lys	Val	Lys	pro	Pro	A	A	13.2	917.1 (917.6) $[M+2H]^{2+}$ 611.9 (612.1) $[M+3H]^{3+}$
ent-**18**	thr	trp	leu	lys	lys	arg	arg	trp	lys	lys	val	lys	Pro	pro	A	A	13.2	917.6 (917.6) $[M+2H]^{2+}$ 611.9 (612.1) $[M+3H]^{3+}$
19	Thr	Trp	Leu	Lys	Lys	Arg	Arg	Trp	Lys	Lys	Ala	Lys	pro	Pro	A	A	13.1	903.1 (903.6) $[M+2H]^{2+}$ 602.6 (602.7) $[M+3H]^{3+}$
36	Lys	Trp	Lys	Ala	Phe	Lys	Arg	Gln	Leu	Lys	Met	Ser	pro	Pro	B	B	16.8	1727.3 (1727.0) $[M+H]^{+}$ 864.2 (864.0) $[M+2H]^{2+}$
37	Arg	Trp	Lys	Val	Arg	Lys	Ser	Phe	Phe	Lys	Leu	Gln	pro	Pro	B	B	19.4	1799.3 (1799.1) $[M+H]^{+}$ 900.4 (900.0) $[M+2H]^{2+}$
38	Lys	Pro	Thr	Phe	Arg	Arg	Leu	Lys	Trp	Lys	Tyr	Lys	pro	Pro	B	B	16.0	1827.2 (1827.1) $[M+H]^{+}$ 914.3 (914.0) $[M+2H]^{2+}$

Table A2.1 (continued)

identifier	position[a]														column[b]	conditions[c]	t_R [min][d]	mass[e]
	1	2	3	4	5	6	7	8	9	10	11	12	13	14				
72	Arg	Trp	Leu	Lys	Lys	Gln	Arg	Dan	Lys	Tyr	Tyr	Arg	pro	Pro	A	A	13.7	1035.6 (1035.6) $[M+2H]^{2+}$ 690.7 (690.7) $[M+3H]^{3+}$
77	Thr	Trp	Leu	Lys	Lys	Arg	Arg	Dan	Lys	Lys	Ala	Lys	pro	Pro	A	A	13.4	1888.3 (1888.2) $[M+H]^{+}$ 944.8 (944.6) $[M+2H]^{2+}$
80	Biot	Trp	Leu	Lys	Lys	Arg	Arg	Trp	Lys	Lys	Ala	Lys	pro	Pro	A	A	13.5	1131.7 (1131.7) $[M+2H]^{2+}$ 754.7 (754.8) $[M+3H]^{3+}$
81	Thr	Trp	Biot	Lys	Lys	Arg	Arg	Trp	Lys	Lys	Ala	Lys	pro	Pro	A	A	12.9	1125.7 (1125.7) $[M+2H]^{2+}$ 750.7 (750.8) $[M+3H]^{3+}$
82	Thr	Trp	Leu	Biot	Lys	Arg	Arg	Trp	Lys	Lys	Ala	Lys	pro	Pro	A	A	13.9	1118.1 (1118.2) $[M+2H]^{2+}$ 745.7 (745.8) $[M+3H]^{3+}$
83	Thr	Trp	Leu	Lys	Biot	Arg	Arg	Trp	Lys	Lys	Ala	Lys	pro	Pro	A	A	13.6	1118.1 (1118.2) $[M+2H]^{2+}$ 745.7 (745.8) $[M+3H]^{3+}$
84	Thr	Trp	Leu	Lys	Lys	Biot	Arg	Trp	Lys	Lys	Ala	Lys	pro	Pro	A	A	13.5	1104.1 (1104.2) $[M+2H]^{2+}$ 736.4 (736.4) $[M+3H]^{3+}$
85	Thr	Trp	Leu	Lys	Lys	Arg	Biot	Trp	Lys	Lys	Ala	Lys	pro	Pro	A	A	13.5	1104.1 (1104.2) $[M+2H]^{2+}$ 736.4 (736.4) $[M+3H]^{3+}$
86	Thr	Trp	Leu	Lys	Lys	Arg	Arg	Trp	Biot	Lys	Ala	Lys	pro	Pro	A	A	13.5	1118.1 (1118.2) $[M+2H]^{2+}$ 745.7 (745.8) $[M+3H]^{3+}$
87	Thr	Trp	Leu	Lys	Lys	Arg	Arg	Trp	Lys	Biot	Ala	Lys	pro	Pro	A	A	13.4	1118.1 (1118.2) $[M+2H]^{2+}$ 745.7 (745.8) $[M+3H]^{3+}$
88	Thr	Trp	Leu	Lys	Lys	Arg	Arg	Trp	Lys	Lys	Biot	Lys	pro	Pro	A	A	13.1	1146.7 (1146.7) $[M+2H]^{2+}$ 764.6 (764.8) $[M+3H]^{3+}$
89	Thr	Trp	Leu	Lys	Lys	Arg	Arg	Trp	Lys	Lys	Ala	Biot	pro	Pro	A	A	13.7	1118.2 (1118.2) $[M+2H]^{2+}$ 745.7 (745.8) $[M+3H]^{3+}$
92	Thr	Paz	Leu	Lys	Lys	Arg	Arg	Trp	Lys	Lys	Ala	Lys	pro	Pro	A	A	13.1	1808.3 (1888.1) $[M+H]^{+}$
93	Thr	Trp	Leu	Lys	Lys	Arg	Arg	Paz	Lys	Lys	Ala	Lys	pro	Pro	A	A	13.0	1808.3 (1888.1) $[M+H]^{+}$
94	Thr	Bpa	Leu	Lys	Lys	Arg	Arg	Trp	Lys	Lys	Ala	Lys	pro	Pro	A	A	13.4	1871.3 (1871.1) $[M+H]^{+}$ 936.2 (936.1) $[M+2H]^{2+}$
95	Thr	Trp	Leu	Lys	Lys	Arg	Arg	Bpa	Lys	Lys	Ala	Lys	pro	Pro	A	A	13.5	1871.3 (1871.1) $[M+H]^{+}$ 936.2 (936.1) $[M+2H]^{2+}$

Table A2.1 (continued)

identifier	position[a]														column[b]	conditions[c]	t_R [min][d]	mass[e]
	1	2	3	4	5	6	7	8	9	10	11	12	13	14				
96	Biot	Paz	Leu	Lys	Lys	Arg	Arg	Trp	Lys	Lys	Ala	Lys	pro	Pro	A	A	13.8	1133.2 (1132.7) $[M+2H]^{2+}$
97	Biot	Trp	Leu	Lys	Lys	Arg	Arg	Paz	Lys	Lys	Ala	Lys	pro	Pro	A	A	13.6	1132.9 (1132.7) $[M+2H]^{2+}$
98	Thr	Trp	Leu	Lys	Lys	Arg	Arg	Paz	Lys	Lys	Ala	Biot	pro	Pro	A	A	13.8	1119.3 (1119.2) $[M+2H]^{2+}$
99	Biot	Bpa	Leu	Lys	Lys	Arg	Arg	Trp	Lys	Lys	Ala	Lys	pro	Pro	A	A	14.1	2327.7 (2327.4) $[M+H]^{+}$ 1164.6 (1164.2) $[M+2H]^{2+}$
100	Biot	Trp	Leu	Lys	Lys	Arg	Arg	Bpa	Lys	Lys	Ala	Lys	pro	Pro	A	A	13.8	1164.4 (1164.2) $[M+2H]^{2+}$ 776.7 (776.5) $[M+3H]^{3+}$

[a] Dan = DANA (39); Biot = Glu(biotinyl-PEG); Paz = *p*-azido-Phe; Bpa = *p*-benzoyl-Phe.

[b] A = *Grace Vydac* 218TP54 (C18, 4.6×250 mm, 5 μm, 300 Å); B = *Vydac* 218TP54 (C18, 4.6×250 mm, 5 μm, 300 Å).

[c] A = 5% acetonitrile in water, containing 0.1% TFA for 4.2 minutes, followed by a gradient from 5 to 100% acetonitrile in water, containing 0.1% TFA over 25 minutes; B = gradient from 5 to 100% acetonitrile in water, containing 0.1% TFA over 60 minutes

[d] t_R = retention time.

[e] Observed m/z values measured with positive ion mode ESI; calculated values of the basis peaks are given in parentheses.

[f] Two peak pattern.

Appendix 3: Buffers

H_2O used for the preparation of buffers was of double distilled quality. Unless stated otherwise, the concentrations of aqueous solutions of solid compounds are given as weight-volume percentage (% w/v)

Table A3.1 Buffer systems used for gel electrophoresis, affinity chromatography and photoaffinity labelling.

system	contents	amount	remarks
Gel buffer, 4×, pH 8.8	1.5M Tris	182 g	store at 4 °C
	H_2O	ad 1000 mL	
equilibration buffer (stock)	6M urea	180 g	store at 4 °C
	30% glycerol	150 g	
	2% SDS	10 g	
	4× Gel buffer	16.7 mL	
	H_2O	ad 500 mL	
equilibration buffer A	DTT	1 g	prepare freshly; 10 mL per IPG strip
	equilibration buffer (stock)	100 mL	
equilibration buffer B	iodo acetamide	4 g	prepare freshly; 10 mL per IPG strip
	equilibration buffer (stock)	100 mL	
fixing solution	EtOH	800 mL	prepare freshly; 200 mL per gel
	HOAc	200 mL	
	H_2O	ad 2000 mL	
staining solution	$(NH_4)_2SO_4$	100 g	store at r.t. in the dark
	H_3PO_4	20 g	
	MeOH	250 mL	
	Coomassie Brilliant Blue G250	0.625 mg	
	H_2O	ad 1000 mL	
12.5% gel solution	Acrylamide monomer solution	41.7 mL	for 900 mL (14 gels)
	4× Gel buffer	25.0 mL	
	10% SDS	1.0 mL	
	H_2O	31.8 mL	
	10% APS	0.5 mL	
	TEMED	33 µL	
2D Gel storage buffer	4× Gel buffer	250 mL	store at 4 °C
	10% SDS	10 mL	
	H_2O	ad 1000 mL	
2D electrophoresis buffer	25 mM Tris	15.1 g	prepare freshly
	192 mM Glycine	72.1 g	
	0.1% SDS	5 g	
	H_2O	ad 5000 mL	
Fixing solution	EtOH	800 mL	prepare freshly; ca. 200 mL/gel
	HOAc	200 mL	
	H_2O	ad 2000 mL	

Table A3.1 (continued)

2D staining solution (colloidal Coomassie)	$(NH_4)_2SO_4$	100 g	store at r.t. in the dark
	H_3PO_4 (85%)	20 g	
	MeOH	250 mL	
	Coomassie Brilliant Blue G-250 (*Merck*)	0.625 mg	
	H_2O	ad 1000 mL	
1D Gel buffer, pH 8.8	Tris	18.2 g	
	10% SDS	4 mL	
	H_2O	ad 100 mL	
1D Stacking gel buffer, pH 6.8	Tris	6.1 g	
	10% SDS	4 mL	
	H_2O	ad 100 mL	
1D gel solution (12%)	Acrylamide monomer solution	16 mL	for 3 gels
	1D gel buffer	10 mL	
	H_2O	14 mL	
	APS	250 µL	
	TEMED	150 µL	
1D gel solution (15%)	Acrylamide monomer solution	20 mL	for 3 gels
	1D gel buffer	10 mL	
	H_2O	10 mL	
	APS	250 µL	
	TEMED	150 µL	
1D Stacking gel solution (12%)	Acrylamide monomer solution	3.4 mL	for 3 gels
	1D gel buffer	5 mL	
	H_2O	11.6 mL	
	APS	150 µL	
	TEMED	15 µL	
4× Sample buffer, pH 6.8	Glycerol	7.5 mL	for manually cast gels
	β-Mercaptoethanol	2.5 mL	
	SDS	1.2 g	
	1% Bromophenol blue	200 µL	
	Tris	0.4 g	
	H_2O	ad 50 mL	
Transfer buffer, pH 8.3	Tris	3.0 g	
	Glycine	14.4 g	
	MeOH	200 mL	
	H_2O	ad 1000 mL	
10× TBS, pH 7.0	Tris	24.2 g	Filter sterilise
	NaCl	290 g	
	H_2O	ad 1000 mL	
TBS buffer, pH 7.0	10× TBS	100 mL	prepare freshly
	H_2O	ad 1000 mL	
TTBS buffer, pH 7.0	10× TBS	90 mL	prepare freshly
	Tween® 20	450 µL	
	H_2O	ad 900 mL	

Appendix 4: NMR data for 17 and 18

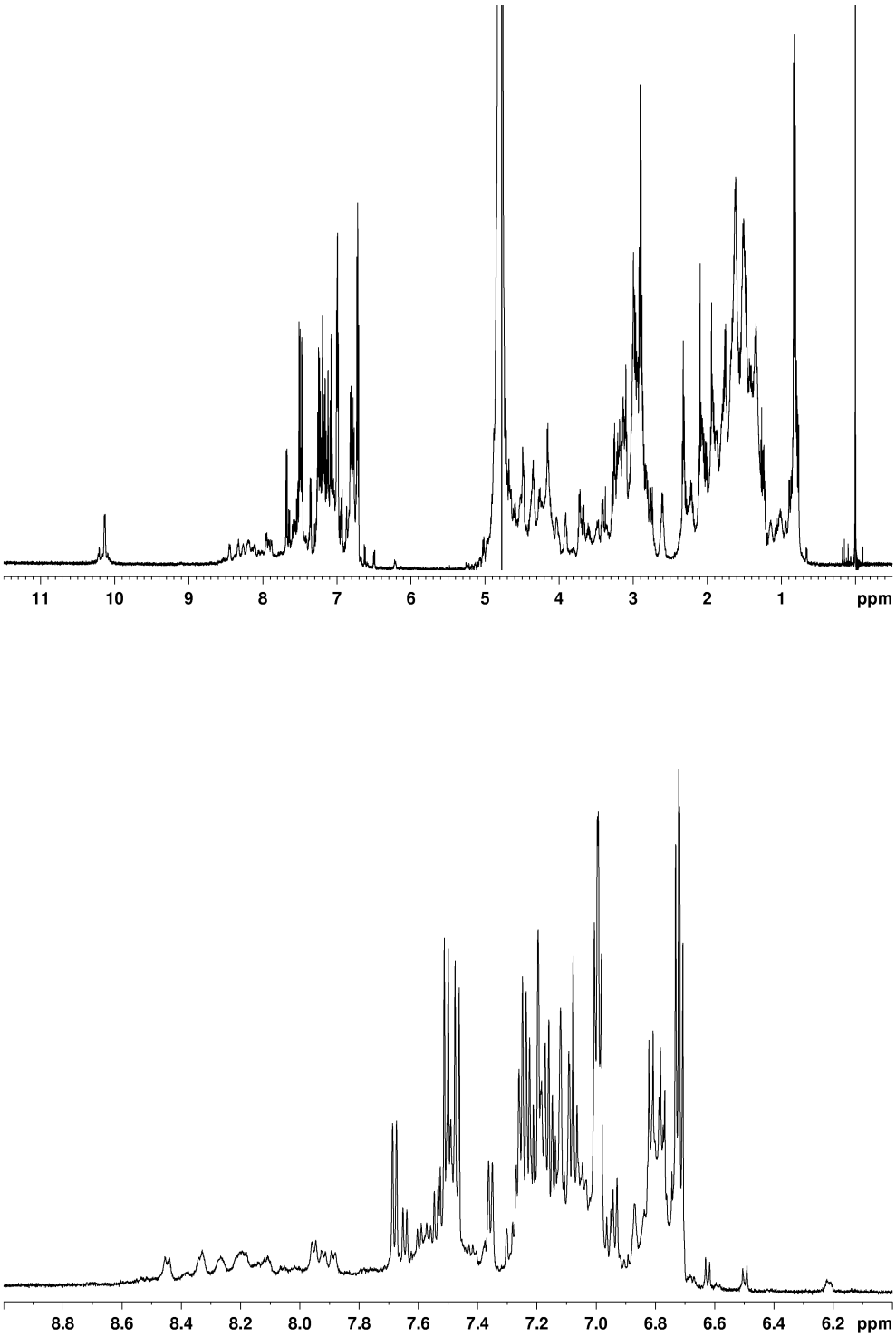

Figure A4.1 *Top*: 600 MHz ^{1}H-NMR spectrum of **17** in H_2O/D_2O (9:1), pH 5, 300K. *Bottom*: expansion of the amide NH region.

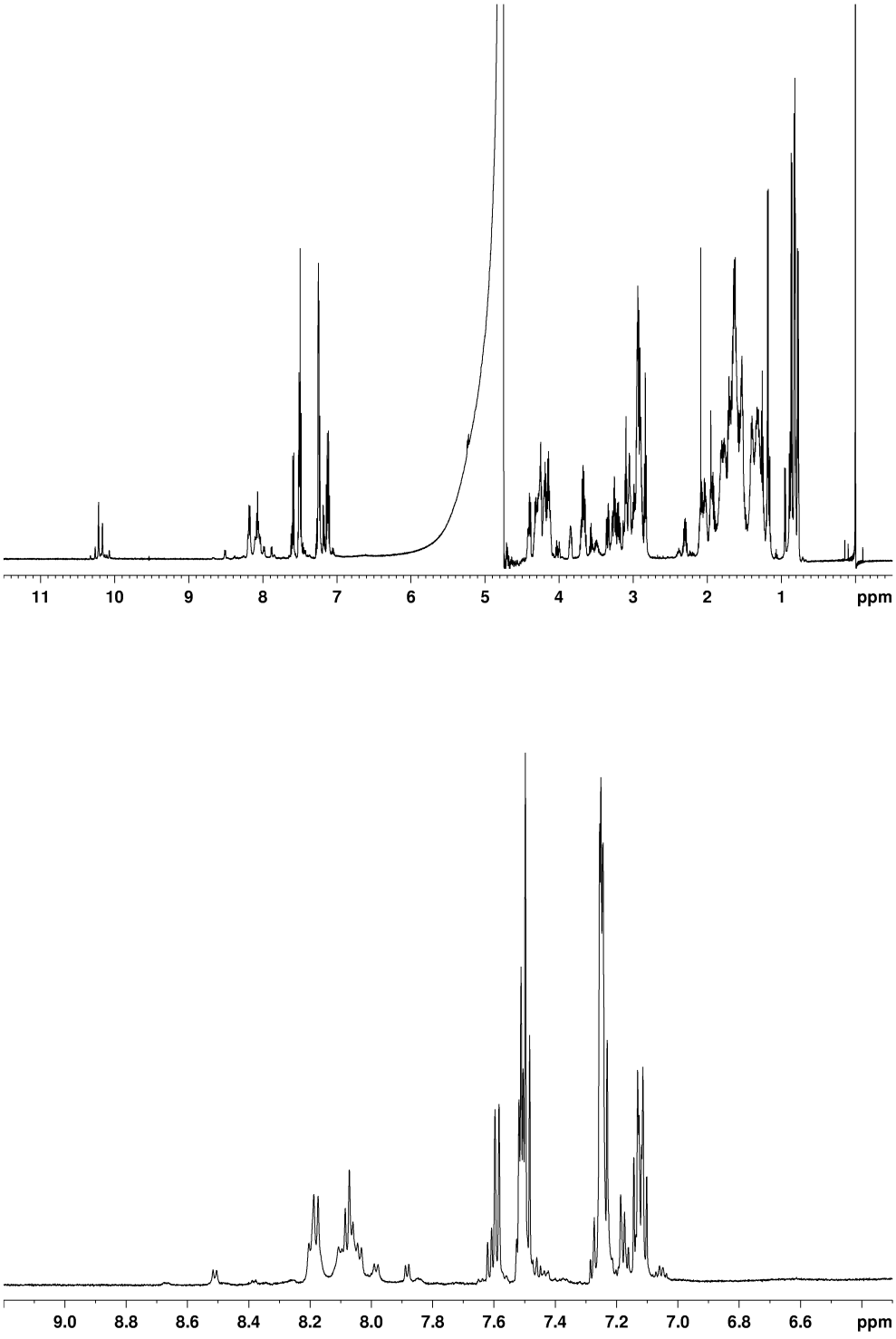

Figure A4.2 *Top*: 600 MHz ^{1}H-NMR spectrum of **18** in H_2O/D_2O (9:1), pH 5, 300K. *Bottom*: expansion of the amide NH region.

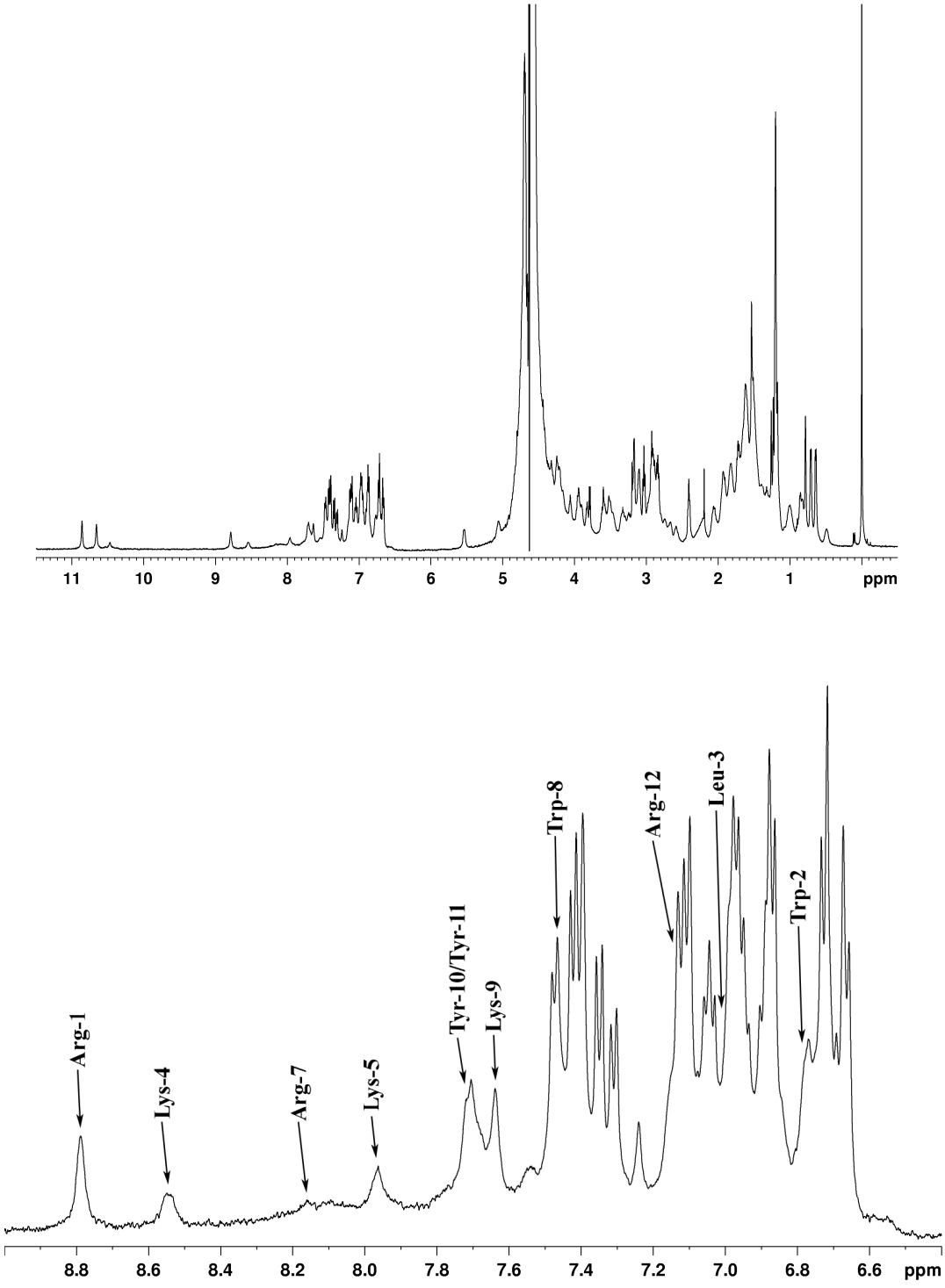

Figure A4.3 *Top*: 600 MHz ^{1}H-NMR spectrum of **17** in a 300 mM solution of DPC-d_{38} in H_2O/D_2O (9:1), pH 5, 300K. *Bottom*: expansion of the amide NH region.

Table A4.1 Chemical shift values obtained for **17** relative to the internal TSP standard at 300K and pH 5 in a 300 mM solution of DPC-d_{38} in H_2O/D_2O (9:1).

Residue	NH	H-C(α)	H-C(β)	Others
Arg[1]	8.81	3.84	1.63, 1.85	CH_2(γ) 1.62, 1.62; CH_2(δ) 3.19, 3.19; NH(ε) -[a]; NH_2(η) -, -
Trp[2]	6.80	4.50	3.25, 3.53	H(δ^1) 7.42; H(ε^3) 7.33; H(ζ^3) 6.92; H(η^2) 6.98; H(ζ^2) 7.37; NH(ε^1) 10.88
Leu[3]	7.00	4.44	1.40, 1.47	CH(γ) 1.18; CH_3(δ) 0.64, 0.71
Lys[4]	8.56	4.26	1.85, 1.95	CH_2(γ) 1.49, 1.49; CH_2(δ) 1.70, 1.70; CH_2(ε) 3.06, 3.06; NH_3^+(ζ) -
Lys[5]	7.99	4.18	1.69, 1.84	CH_2(γ) 1.42, 1.61; CH_2(δ) 1.52, 1.52; CH_2(ε) 2.96, 2.96; NH_3^+(ζ) -
Gln[6]	-	3.98	2.08, 2.08	CH_2(γ) 2.43, 2.43; NH_2(ε) 6.85, 7.48
Arg[7]	8.18	4.08	1.28, 1.69	CH_2(γ) 1.00, 1.00; CH_2(δ) 2.77, 2.91; NH(ε) -; NH_2(η) -, -
Trp[8]	7.49	5.08	2.97, 3.62	H(δ^1) 7.16; H(ε^3) 7.49; H(ζ^3) 6.96; H(η^2) 7.06; H(ζ^2) 7.44; NH(ε^1) 10.68
Lys[9]	7.66	3.95	1.65, 1.75	CH_2(γ) 1.04, 1.18; CH_2(δ) 1.54, 1.54; CH_2(ε) 2.87, 2.87; NH_3^+(ζ) -
Tyr[10]	7.73	4.22	2.60, 2.68	H(δ) 6.69, 6.69; H(ε) 6.75, 6.75
Tyr[11]	7.74	4.33	2.87, 3.25	H(δ) 7.13, 7.13; H(ε) 6.90, 6.90
Arg[12]	7.16	3.92	1.64, 1.64	CH_2(γ) 1.52, 1.64; CH_2(δ) 3.13, 3.13; NH(ε) -; NH_2(η) -, -
DPro[13]	-	5.56	1.95, 2.23	CH_2(γ) 1.93, 1.93; CH_2(δ) 3.49, 3.54
Pro[14]	-	4.26	0.51, 1.68	CH_2(γ) 1.34, 1.54; CH_2(δ) 3.37, 3.60

[a] - = not observed

Table A4.2 Distance restraints derived from $^{1}H,^{1}H$-NOE connectivities for mimetic **17** in 300 mM micellar solution used for SA calculations with the DYANA software packages.

INTRARESIDUAL NOE UPPER-DISTANCE LIMITS			SEQUENTIAL NOE UPPER-DISTANCE LIMITS			MEDIUM and LONG RANGE NOE UPPER-DISTANCE LIMITS		
1 ARG+ HN	1 ARG+ HB2	2.86	1 ARG+ HN	2 TRP HN	3.58	1 ARG+ HA	3 LEU HN	4.14
1 ARG+ HN	1 ARG+ HB3	3.30	1 ARG+ HN	14 PRO HA	2.71	1 ARG+ HA	12 ARG+ QD	6.04
1 ARG+ HN	1 ARG+ QD	6.38	1 ARG+ HN	14 PRO HB2	4.91	2 TRP HN	14 PRO HA	4.11
1 ARG+ HA	1 ARG+ HB2	2.68	1 ARG+ HN	14 PRO HB3	4.91	2 TRP HN	14 PRO QB	5.17
1 ARG+ HA	1 ARG+ HB3	3.05	1 ARG+ HN	14 PRO QB	4.52	3 LEU HN	14 PRO QB	6.07
1 ARG+ HA	1 ARG+ QD	6.38	1 ARG+ HB2	2 TRP HN	3.61	3 LEU HA	5 LYS+ HN	3.48
1 ARG+ HB2	1 ARG+ HE	5.50	1 ARG+ HB3	2 TRP HN	3.45	3 LEU HA	8 TRP HE3	5.50
2 TRP HN	2 TRP HB2	3.48	2 TRP HB2	3 LEU HN	4.32	3 LEU QD1	8 TRP HB3	5.78
2 TRP HN	2 TRP HB3	3.58	2 TRP HB3	3 LEU HN	4.35	3 LEU QD1	8 TRP HD1	6.47
2 TRP HA	2 TRP HB2	2.90	2 TRP HE3	3 LEU HA	4.45	3 LEU QD1	8 TRP HE3	6.19
2 TRP HA	2 TRP HD1	4.63	2 TRP HE3	3 LEU HG	5.38	3 LEU QD1	11 TYR QE	8.66
2 TRP HA	2 TRP HE3	5.50	2 TRP HE3	3 LEU QD1	5.35	3 LEU QD1	14 PRO QD	7.42
2 TRP HB2	2 TRP HD1	3.39	2 TRP HE3	3 LEU QD2	6.53	3 LEU QD2	8 TRP HB3	5.41
2 TRP HB2	2 TRP HE3	4.07	2 TRP HZ3	3 LEU HA	5.50	3 LEU QD2	8 TRP HD1	6.53
2 TRP HB3	2 TRP HE3	3.76	2 TRP HZ3	3 LEU QD1	6.09	3 LEU QD2	8 TRP HE3	6.53
3 LEU HN	3 LEU HG	3.79	2 TRP HZ3	3 LEU QD2	6.53	3 LEU QD2	11 TYR HB3	6.28
3 LEU HN	3 LEU QD1	5.57	3 LEU HA	4 LYS+ HN	2.86	3 LEU QD2	11 TYR QD	8.67
3 LEU HN	3 LEU QD2	5.81	3 LEU QD1	4 LYS+ HN	6.50	3 LEU QD2	11 TYR QE	8.66
3 LEU HA	3 LEU QD1	4.26	4 LYS+ HN	5 LYS+ HN	3.70	3 LEU QD2	12 ARG+ HA	5.29
3 LEU HA	3 LEU QD2	5.72	4 LYS+ HA	5 LYS+ HN	3.36	3 LEU QD2	13 DPR HA	6.22
4 LYS+ HN	4 LYS+ HB2	3.58	7 ARG+ HA	8 TRP HN	3.64	3 LEU QD2	14 PRO HD2	6.16
4 LYS+ HN	4 LYS+ HB3	3.58	7 ARG+ HB2	8 TRP HE3	5.10	3 LEU QD2	14 PRO HD3	6.16
4 LYS+ HN	4 LYS+ QG	5.60	7 ARG+ HB3	8 TRP HE3	5.10	3 LEU QD2	14 PRO QD	5.70
5 LYS+ HN	5 LYS+ HB2	3.30	7 ARG+ QB	8 TRP HD1	6.26	5 LYS+ HN	8 TRP HN	4.54
5 LYS+ HN	5 LYS+ HB3	3.30	7 ARG+ QB	8 TRP HE3	4.69	5 LYS+ HB2	8 TRP HD1	4.69
5 LYS+ HN	5 LYS+ HG2	5.07	7 ARG+ QG	8 TRP HD1	6.38	5 LYS+ HB3	8 TRP HD1	4.69
5 LYS+ HN	5 LYS+ HG3	5.07	7 ARG+ QG	8 TRP HE3	6.38	5 LYS+ QB	8 TRP HD1	4.12
5 LYS+ HN	5 LYS+ QG	4.90	8 TRP HN	9 LYS+ HN	3.08	6 GLN HA	8 TRP HN	4.07
5 LYS+ HN	5 LYS+ QD	5.97	8 TRP HA	9 LYS+ HN	3.42	8 TRP HA	11 TYR QD	6.59
5 LYS+ HA	5 LYS+ HB2	2.90	8 TRP HB2	9 LYS+ HN	4.07	8 TRP HA	11 TYR QE	7.63
5 LYS+ HA	5 LYS+ HB3	2.90	8 TRP HB3	9 LYS+ HN	4.42	8 TRP HB3	11 TYR QD	7.58
5 LYS+ HA	5 LYS+ QD	6.38	9 LYS+ HA	10 TYR HN	3.45	8 TRP HE3	11 TYR HB2	5.31
7 ARG+ HN	7 ARG+ HB2	3.98	9 LYS+ QB	10 TYR HN	4.36	8 TRP HE3	11 TYR QD	6.31
7 ARG+ HN	7 ARG+ HB3	3.98	10 TYR HA	11 TYR HN	3.55	9 LYS+ HA	12 ARG+ HN	3.73
8 TRP HN	8 TRP HB2	3.21	10 TYR HB3	11 TYR QD	7.64	9 LYS+ HA	12 ARG+ QD	6.31
8 TRP HN	8 TRP HB3	3.36	10 TYR HB3	11 TYR QE	7.26	12 ARG+ HA	14 PRO HD2	4.48
8 TRP HA	8 TRP HD1	4.50	10 TYR HB2	11 TYR QD	7.64	12 ARG+ HA	14 PRO HD3	4.48
8 TRP HA	8 TRP HE3	4.00	10 TYR HB2	11 TYR QE	7.63	12 ARG+ HA	14 PRO QD	3.96
8 TRP HB2	8 TRP HD1	3.86	11 TYR HN	12 ARG+ HN	3.08			
8 TRP HB2	8 TRP HE3	3.89	11 TYR HA	12 ARG+ HN	3.21			
9 LYS+ HN	9 LYS+ HB2	3.27	12 ARG+ HN	13 DPR HA	4.48			
9 LYS+ HN	9 LYS+ HB3	3.27	12 ARG+ HA	13 DPR HA	2.55			
9 LYS+ HN	9 LYS+ HG2	4.79	12 ARG+ QB	13 DPR HA	4.76			
9 LYS+ HN	9 LYS+ HG3	4.79	12 ARG+ QG	13 DPR HA	5.54			
9 LYS+ HN	9 LYS+ QG	4.46	13 DPR HA	14 PRO HD2	3.11			
9 LYS+ HN	9 LYS+ QD	6.38	13 DPR HA	14 PRO HD3	3.11			
9 LYS+ HA	9 LYS+ HB2	2.96	13 DPR HB3	14 PRO HD2	4.76			
9 LYS+ HA	9 LYS+ HB3	2.96	13 DPR HB3	14 PRO HD3	4.76			
9 LYS+ HA	9 LYS+ QD	5.45	13 DPR HB2	14 PRO HD2	4.76			
10 TYR HN	10 TYR HB3	3.05	13 DPR HB2	14 PRO HD3	4.76			
10 TYR HN	10 TYR HB2	3.11	13 DPR QB	14 PRO QD	3.86			
10 TYR HA	10 TYR HB3	3.05						
11 TYR HN	11 TYR HB3	3.33						
11 TYR HN	11 TYR HB2	2.99						
11 TYR HA	11 TYR HB3	2.96						
12 ARG+ HN	12 ARG+ QG	4.74						
12 ARG+ HN	12 ARG+ QD	6.38						
12 ARG+ HA	12 ARG+ QG	3.97						
12 ARG+ HA	12 ARG+ QD	5.79						
TOTAL = 61			TOTAL = 51			TOTAL = 38		

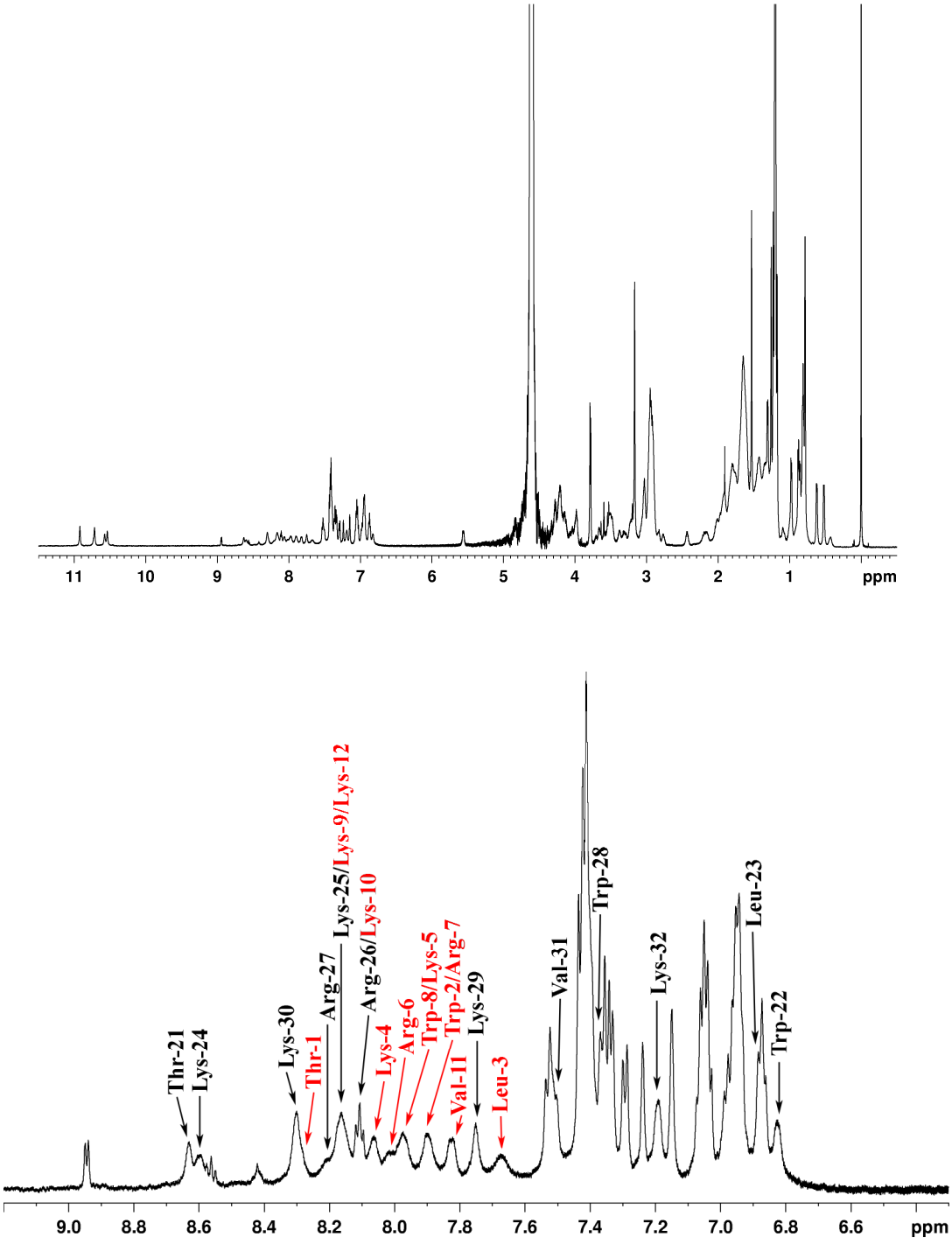

Figure A4.4 *Top*: 600 MHz ^{1}H-NMR spectrum of **18** in a 300 mM solution of DPC-d_{38} in H_2O/D_2O (9:1), pH 5, 300K. *Bottom*: expansion of the amide NH region. For mimetic **18**, amide resonances corresponding to the *cis*- or the *trans*-isomer are depicted in black and red, respectively. The numbering for the *cis*-isomer is derived from the normal numbering system by the addition of the value 20.

Table A4.3 Chemical shift values obtained for the *trans*-isomer of **18** relative to the internal TSP standard at 300K and pH 5in a 300 mM solution of DPC-d_{38} in H_2O/D_2O (9:1). In cases where no unambiguous assignment was possible due to spectral overlap, shift ranges are given.

Residue	NH	CH(α)	CH_n(β)	Others
Thr[1]	8.29	4.20	4.11	CH_3(γ) 1.19
Trp[2]	7.90	4.54	3.23, 3.32	H(δ^1) 7.33; H(ε^3) 7.40; H(ζ^2) 7.42; H(ζ^3) 7.04; H(η^2) 7.06; NH(ε^1) 10.58
Leu[3]	7.67	4.19	1.43, 1.43	CH(γ) 1.54; CH_3(δ) 0.81, 0.85
Lys[4]	8.07	4.15	1.78, 1.83	CH_2(γ) 1.36, 1.36; CH_2(δ) 1.60-1.68, 1.60-1.68; CH_2(ε) 2.91-2.97, 2.91-2.97; NH_3^+(ζ) 1.35
Lys[5]	7.97	4.22	1.68, 1.77	CH_2(γ) 1.35, 1.35; CH_2(δ) 1.60-1.68, 1.60-1.68; CH_2(ε) 2.91-2.97, 2.91-2.97; NH_3^+(ζ) 1.48
Arg[6]	8.02	4.06	1.61, 1.67	CH_2(γ) 1.48, 1.48; CH_2(δ) 3.06, 3.06; NH(ε) -; NH_2(η) -[a], -
Arg[7]	7.91	4.19	1.59, 1.66	CH_2(γ) 1.37, 1.37; CH_2(δ) 3.03, 3.03; NH(ε) -; NH_2(η) -, -
Trp[8]	7.99	4.71	3.22, 3.30	H(δ^1) 7.24; H(ε^3) 7.53; H(ζ^2) 7.42; H(ζ^3) 6.97; H(η^2) 7.06; NH(ε^1) 10.54
Lys[9]	8.17	4.23	1.65, 1.67	CH_2(γ) 1.34, 1.40; CH_2(δ) 1.60-1.68, 1.60-1.68; CH_2(ε) 2.91-2.97, 2.91-2.97; NH_3^+(ζ) -
Lys[10]	8.11	4.23	1.65, 1.75	CH_2(γ) 1.33, 1.38; CH_2(δ) 1.60-1.68, 1.60-1.68; CH_2(ε) 2.91-2.97, 2.91-2.97; NH_3^+(ζ) -
Val[11]	7.83	4.16	2.01	CH_3(γ) 0.81
Lys[12]	8.17	4.62W	1.64, 1.74	CH_2(γ) 1.31, 1.34; CH_2(δ) 1.60-1.68, 1.60-1.68; CH_2(ε) 2.91-2.97, 2.91-2.97; NH_3^+(ζ) -
pro[13]	-	4.60W	1.87, 2.19	CH_2(γ) 1.97, 2.04; CH_2(δ) 3.66, 3.66
Pro[14]	-	4.37	1.51, 2.01	CH_2(γ) 1.77, 1.83; CH_2(δ) 3.48, 3.71

[a] - = not observed

Table A4.4 Chemical shift values obtained for the *cis*-isomer of **18** relative to the internal TSP standard at 300K in a 300 mM solution of DPC-d_{38} in H_2O/D_2O (9:1).

Residue	NH	CH(α)	CH_n(β)	Others
Thr[1]	8.63	4.27	3.80	CH_3(γ) 1.30
Trp[2]	6.83	4.50	3.21, 3.56	H(δ^1) 7.41; H(ε^3) 7.30; H(ζ^2) 7.35; H(ζ^3) 6.87; H(η^2) 6.95; NH(ε^1) 10.93
Leu[3]	6.88	4.33	1.28, 1.34	CH(γ) 0.99; CH_3(δ) 0.52, 0.62
Lys[4]	8.60	4.30	1.83, 1.91	CH_2(γ) 1.45, 1.49; CH_2(δ) 1.70, 1.70; CH_2(ε) 3.02, 3.02; NH_3^+(ζ) -[a]
Lys[5]	8.15	4.22	1.66, 1.75	CH_2(γ) 1.31-1.36, 1.31-1.36; CH_2(δ) 1.60-1.68, 1.60-1.68; CH_2(ε) 2.91-2.97, 2.91-2.97; NH_3^+(ζ) -
Arg[6]	8.11	4.22	1.65, 1.75	CH_2(γ) 1.65-1.75, 1.65-1.75; CH_2(δ) -, -; NH(ε) -; NH_2(η) -, -
Arg[7]	8.22	4.00	1.28, 1.61	CH_2(γ) 0.91, 0.98; CH_2(δ) 2.77, 2.83; NH(ε) -; NH_2(η) -, -
Trp[8]	7.36	4.84	2.91, 3.49	H(δ^1) 7.15; H(ε^3) 7.41; H(ζ^2) 7.43; H(ζ^3) 6.95; H(η^2) 7.04; NH(ε^1) 10.72
Lys[9]	7.75	3.98	1.84, 1.90	CH_2(γ) 1.42, 1.42; CH_2(δ) 1.66, 1.66; CH_2(ε) 2.97, 2.97; NH_3^+(ζ) -
Lys[10]	8.31	4.14	1.79, 1.79	CH_2(γ) 1.43, 1.48; CH_2(δ) 1.70, 1.70; CH_2(ε) 2.91-2.97, 2.91-2.97; NH_3^+(ζ) -
Val[11]	7.51	4.28	2.43	CH_3(γ) 0.88, 0.98
Lys[12]	7.19	3.97	1.53, 1.75	CH_2(γ) 1.08, 1.31; CH_2(δ) -, -; CH_2(ε) -, -; NH_3^+(ζ) -
pro[13]	-	5.56	1.95, 2.15	CH_2(γ) 1.93, 1.93; CH_2(δ) 3.52, 3.52
Pro[14]	-	4.28	0.44, 1.61	CH_2(γ) 1.30, 1.60; CH_2(δ) 3.37, 3.51

[a] - = not observed

Table A4.5 Distance restraints derived from $^{1}H,^{1}H$-NOE connectivities for the *cis*-isomer of mimetic **18** in 300 mM micellar solution used for SA calculations with the DYANA software packages.

21 THR HN	21 THR HB	3.36	21 THR HN	22 TRP HN	3.61	21 THR HN	34 PRO HA	2.87
21 THR HN	21 THR QG2	4.67	21 THR HA	22 TRP HN	3.58	21 THR HN	34 PRO HB2	5.16
22 TRP HN	22 TRP HB3	3.52	21 THR HA	22 TRP HD1	5.38	21 THR HN	34 PRO HB3	5.16
22 TRP HN	22 TRP HB2	3.45	21 THR HB	22 TRP HN	3.73	21 THR HN	34 PRO QB	4.90
22 TRP HN	22 TRP HD1	3.55	21 THR QG2	22 TRP HN	5.78	21 THR HB	23 LEU HN	4.29
22 TRP HA	22 TRP HB3	2.74	21 THR QG2	22 TRP HD1	5.75	22 TRP HN	34 PRO QB	5.21
22 TRP HA	22 TRP HB2	2.49	22 TRP HA	23 LEU HN	3.64	22 TRP HD1	34 PRO HB2	5.28
22 TRP HA	22 TRP HD1	4.26	22 TRP HB3	23 LEU HN	3.86	22 TRP HD1	34 PRO HB2	5.28
22 TRP HA	22 TRP HE3	4.88	22 TRP HB2	23 LEU HN	4.26	22 TRP HD1	34 PRO QB	4.76
22 TRP HB3	22 TRP HD1	3.76	22 TRP HE3	23 LEU HA	3.95	22 TRP HE1	34 PRO HB2	4.91
22 TRP HB3	22 TRP HE3	3.64	22 TRP HE3	23 LEU HG	4.72	22 TRP HE1	34 PRO HB3	4.91
22 TRP HB2	22 TRP HD1	3.45	22 TRP HE3	23 LEU QD1	5.01	22 TRP HE1	34 PRO QB	4.66
23 LEU HN	23 LEU HB2	3.36	22 TRP HE3	23 LEU QD2	6.53	22 TRP HZ2	34 PRO QB	4.90
23 LEU HN	23 LEU HB3	3.36	23 LEU HN	24 LYS+ HN	4.01	22 TRP HZ2	34 PRO QG	4.76
23 LEU HN	23 LEU QB	3.09	23 LEU HA	24 LYS+ HN	2.93	23 LEU HB2	28 TRP HD1	5.50
23 LEU HN	23 LEU HG	3.55	23 LEU QD1	24 LYS+ HN	6.43	23 LEU HB3	28 TRP HD1	5.50
23 LEU HN	23 LEU QD1	4.51	24 LYS+ HN	25 LYS+ HN	3.89	23 LEU QB	28 TRP HD1	5.28
23 LEU HN	23 LEU QD2	5.32	24 LYS+ HA	25 LYS+ HN	3.48	23 LEU QD1	28 TRP HD1	6.19
24 LYS+ HN	24 LYS+ HB2	3.67	24 LYS+ HB2	25 LYS+ HN	4.17	23 LEU QD1	28 TRP HE3	6.19
24 LYS+ HN	24 LYS+ HB3	3.67	24 LYS+ HB3	25 LYS+ HN	4.17	23 LEU QD1	28 TRP HZ3	5.94
24 LYS+ HN	24 LYS+ QB	3.45	24 LYS+ QB	25 LYS+ HN	3.83	23 LEU QD1	32 LYS+ HA	6.53
24 LYS+ HN	24 LYS+ HG2	5.50	27 ARG+ HA	28 TRP HN	3.30	23 LEU QD2	28 TRP HB3	5.57
24 LYS+ HN	24 LYS+ HG3	5.50	27 ARG+ QG	28 TRP HD1	6.38	23 LEU QD2	28 TRP HD1	6.53
24 LYS+ HA	24 LYS+ HB2	2.93	28 TRP HN	29 LYS+ HN	3.39	23 LEU QD2	28 TRP HE3	6.53
24 LYS+ HA	24 LYS+ HB3	2.93	28 TRP HA	29 LYS+ HN	3.36	23 LEU QD2	32 LYS+ HA	4.95
24 LYS+ HA	24 LYS+ QB	2.56	28 TRP HB3	29 LYS+ HN	4.07	23 LEU QD2	33 DPR HA	6.28
24 LYS+ HA	24 LYS+ QD	3.90	28 TRP HB2	29 LYS+ HN	4.38	23 LEU QD2	34 PRO HD2	5.63
25 LYS+ HN	25 LYS+ HB2	3.64	29 LYS+ HN	30 LYS+ HN	3.83	23 LEU QD2	34 PRO HD3	5.63
25 LYS+ HN	25 LYS+ HB3	3.64	29 LYS+ HA	30 LYS+ HN	3.58	23 LEU QD2	34 PRO QD	5.18
25 LYS+ HN	25 LYS+ QB	3.35	30 LYS+ HN	31 VAL HN	3.36	25 LYS+ QB	28 TRP HD1	4.86
27 ARG+ HA	27 ARG+ HB2	2.68	30 LYS+ HA	31 VAL HN	3.33	28 TRP HA	30 LYS+ HN	4.35
27 ARG+ HA	27 ARG+ HB3	2.68	30 LYS+ QB	31 VAL HN	4.64	28 TRP HB3	31 VAL QG2	4.79
27 ARG+ HA	27 ARG+ QB	2.39	31 VAL HN	32 LYS+ HN	2.96	28 TRP HB2	31 VAL QG2	5.29
27 ARG+ HA	27 ARG+ HG2	4.23	31 VAL HA	32 LYS+ HN	3.14	28 TRP HD1	31 VAL QG2	6.16
27 ARG+ HA	27 ARG+ HG3	4.23	31 VAL HB	32 LYS+ HN	4.11	28 TRP HE3	31 VAL QG1	5.54
27 ARG+ HA	27 ARG+ QG	4.03	31 VAL QG1	32 LYS+ HN	6.53	28 TRP HE3	31 VAL QG2	4.54
28 TRP HN	28 TRP HB3	3.30	31 VAL QG2	32 LYS+ HN	5.88	28 TRP HZ3	31 VAL QG1	5.01
28 TRP HN	28 TRP HB2	3.21	32 LYS+ HA	33 DPR HA	2.49	28 TRP HZ3	31 VAL QG2	6.09
28 TRP HN	28 TRP HD1	4.51	33 DPR HA	34 PRO HD2	3.02	29 LYS+ HA	31 VAL HN	3.79
28 TRP HA	28 TRP HB3	2.99	33 DPR HA	34 PRO HD3	3.02	30 LYS+ HA	32 LYS+ HN	4.32
28 TRP HA	28 TRP HD1	3.92	33 DPR HA	34 PRO QD	2.80	31 VAL HA	33 DPR HA	3.95
28 TRP HA	28 TRP HE3	3.02	33 DPR HB3	34 PRO HD2	5.89	32 LYS+ HA	34 PRO HD2	4.11
28 TRP HB3	28 TRP HE3	3.70	33 DPR HB3	34 PRO HD3	5.89	32 LYS+ HA	34 PRO HD3	4.11
28 TRP HB2	28 TRP HD1	3.70	33 DPR HB2	34 PRO HD2	5.89	32 LYS+ HA	34 PRO QD	3.72
28 TRP HB2	28 TRP HE3	4.01	33 DPR HB2	34 PRO HD3	5.89			
29 LYS+ HN	29 LYS+ HB2	3.30	33 DPR QB	34 PRO QD	4.66			
29 LYS+ HN	29 LYS+ HB3	3.30						
29 LYS+ HN	29 LYS+ QB	3.12						
29 LYS+ HN	29 LYS+ QG	5.82						
29 LYS+ HA	29 LYS+ HB2	2.80						
29 LYS+ HA	29 LYS+ HB3	2.80						
29 LYS+ HA	29 LYS+ QB	2.53						
30 LYS+ HN	30 LYS+ HG2	5.00						
30 LYS+ HN	30 LYS+ HG3	5.00						
30 LYS+ HN	30 LYS+ QG	4.41						
31 VAL HN	31 VAL HB	3.42						
31 VAL HN	31 VAL QG2	4.11						
31 VAL HA	31 VAL HB	2.77						
32 LYS+ HN	32 LYS+ HB2	3.08						
32 LYS+ HN	32 LYS+ HB3	3.08						
32 LYS+ HN	32 LYS+ HG2	5.28						
32 LYS+ HN	32 LYS+ HG3	5.28						
32 LYS+ HA	32 LYS+ HG2	4.01						
32 LYS+ HA	32 LYS+ HG3	4.01						
32 LYS+ HA	32 LYS+ QG	3.71						
TOTAL = 62			TOTAL = 46			TOTAL = 39		

Appendix 5: Fluorescence properties of 78

Table A5.1 Fluorescence maxima and relative fluorescence intensities of NAAA (**78**) in various solvent systems.

Solvent	**Fluorescence maximum [nm]**	**Fluorescence intensity [a.u.]**
H_2O	523.60	27.69
TFE	520.69	53.87
MeOH	505.07	213.99
Ethanol	497.59	352.60
^{n}BuOH	492.93	413.84
^{i}PrOH	489.12	423.99
NMP	466.26	439.96
DMSO	469.61	489.60
Acetonitrile	471.53	509.60
DMF	467.02	532.03
Acetone	426.81	555.16
Toluene	434.86	636.91
$CHCl_3$	458.43	674.88
EtOAc	452.67	694.57
DME	455.61	712.60
THF	451.70	720.60
DCM	458.37	757.48
Et_2O	430.70	777.82
$^{i}Pr_2O$	430.37	777.82
Dioxane	438.45	853.46

References

[1] R. G. Finch, *Antibiotic and Chemotherapy*, 8th ed., Churchill Livingstone, Edinburgh, **2003**.
[2] P. Vuillemin, *Association française pour l'avancement des sciences* **1889**, *session 18/partie 2*, 525.
[3] A. Fleming, *Br. J. Exp. Pathol.* **1929**, *10*, 226.
[4] L. Pasteur, J. Joubert, *Comptes rendus hebdomadaires des Séances de l'Académie des Sciences* **1877**, *85*, 101.
[5] J. Tyndall, *Proc. Roy. Soc.* **1875-76**, *24*, 171.
[6] R. Emmerich, O. Löw, *Zeitschrift für Hygiene und Infektionskrankheiten* **1899**, *31*, 1.
[7] S. A. Waksman, *Mycologia* **1947**, *39*, 565.
[8] T. J. Franklin, G. A. Snow, *Biochemistry and molecular biology of antimicrobial drug action*, 6th ed., Springer, New York, **2005**.
[9] P. Ehrlich, *Berliner Klinische Wochenschrift* **1907**, *44*, 9.
[10] A. Cardon de Lichtbuer, PhD thesis, Universität Basel (Basel), **1990**.
[11] G. Domagk, *Deutsche Medizinische Wochenschrift* **1935**, *61*, 250.
[12] E. Chain, H. W. Florey, A. D. Gardner, *Lancet* **1940**, *1*, 1172.
[13] M. S. Barber, U. Giesecke, A. Reichert, W. Minas, *Adv. Biochem. Eng. Biotechnol.* **2004**, *88*, 179.
[14] C. Walsh, *Antibiotics*, ASM, Washington, **2003**.
[15] G. E. Stein, *Pharmacotherapy* **2005**, *25*, 44S.
[16] R. A. Bonomo, D. Szabo, *Clin. Infect. Dis.* **2006**, *43 Suppl 2*, S49.
[17] F. C. Tenover, *Am. J. Med.* **2006**, *119*, S3.
[18] B. H. Normark, S. Normark, *J. Intern. Med.* **2002**, *252*, 91.
[19] D. E. Ehmann, J. E. Demeritt, K. G. Hull, S. L. Fisher, *Biochim. Biophys. Acta* **2004**, *1698*, 167.
[20] C. Freiberg, H. Brotz-Oesterhelt, *Drug Discov. Today* **2005**, *10*, 927.
[21] R. L. Monaghan, J. F. Barrett, *Biochem. Pharmacol.* **2006**, *71*, 901.
[22] B. Spellberg, J. H. Powers, E. P. Brass, L. G. Miller, J. E. Edwards, *Clin. Infect. Dis.* **2004**, *38*, 1279.
[23] H. Jenssen, P. Hamill, R. E. Hancock, *Clin. Microbiol. Rev.* **2006**, *19*, 491.
[24] M. Zasloff, *Nature* **2002**, *415*, 389.
[25] B. Schittek, R. Hipfel, B. Sauer, J. Bauer, H. Kalbacher, S. Stevanovic, M. Schirle, K. Schroeder, N. Blin, F. Meier, G. Rassner, C. Garbe, *Nat. Immunol.* **2001**, *2*, 1133.
[26] P. J. Bergen, J. Li, C. R. Rayner, R. L. Nation, *Antimicrob. Agents Chemother.* **2006**, *50*, 1953.
[27] J. L. Pace, G. Yang, *Biochem. Pharmacol.* **2006**, *71*, 968.
[28] H. Kleinkauf, H. von Dohren, *Crit. Rev. Biotechnol.* **1988**, *8*, 1.
[29] D. R. Storm, K. S. Rosenthal, P. E. Swanson, *Annu. Rev. Biochem.* **1977**, *46*, 723.
[30] D. Shonekan, D. Mildvan, S. Handwerger, *Antimicrob. Agents Chemother.* **1992**, *36*, 1570.
[31] M. Zanetti, *J. Leukoc. Biol.* **2004**, *75*, 39.
[32] M. Paetzel, A. Karla, N. C. Strynadka, R. E. Dalbey, *Chem. Rev.* **2002**, *102*, 4549.
[33] A. E. Shinnar, K. L. Butler, H. J. Park, *Bioorg. Chem.* **2003**, *31*, 425.
[34] D. F. Steiner, *Curr. Opin. Chem. Biol.* **1998**, *2*, 31.
[35] C. I. Cheigh, Y. R. Pyun, *Biotechnol. Lett.* **2005**, *27*, 1641.
[36] V. G. Eijsink, L. Axelsson, D. B. Diep, L. S. Havarstein, H. Holo, I. F. Nes, *Antonie Van Leeuwenhoek* **2002**, *81*, 639.
[37] Y. Q. Tang, J. Yuan, G. Osapay, K. Osapay, D. Tran, C. J. Miller, A. J. Ouellette, M. E. Selsted, *Science* **1999**, *286*, 498.
[38] D. J. Craik, M. Cemazar, C. K. Wang, N. L. Daly, *Biopolymers* **2006**, *84*, 250.

[39] D. J. Craik, *Science* **2006**, *311*, 1563.
[40] H. G. Boman, *Annu. Rev. Immunol.* **1995**, *13*, 61.
[41] R. E. Hancock, *Lancet* **1997**, *349*, 418.
[42] P. A. Raj, E. Marcus, M. Edgerton, *Biochemistry* **1996**, *35*, 4314.
[43] M. Wu, E. Maier, R. Benz, R. E. Hancock, *Biochemistry* **1999**, *38*, 7235.
[44] K. De Smet, R. Contreras, *Biotechnol. Lett.* **2005**, *27*, 1337.
[45] D. I. Chan, E. J. Prenner, H. J. Vogel, *Biochim. Biophys. Acta* **2006**.
[46] P. Bulet, R. Stocklin, L. Menin, *Immunol. Rev.* **2004**, *198*, 169.
[47] K. A. Brogden, *Nat. Rev. Microbiol.* **2005**, *3*, 238.
[48] D. M. Hoover, K. R. Rajashankar, R. Blumenthal, A. Puri, J. J. Oppenheim, O. Chertov, J. Lubkowski, *J. Biol. Chem.* **2000**, *275*, 32911.
[49] R. H. Huang, Y. Xiang, G. Z. Tu, Y. Zhang, D. C. Wang, *Biochemistry* **2004**, *43*, 6005.
[50] R. L. Fahrner, T. Dieckmann, S. S. Harwig, R. I. Lehrer, D. Eisenberg, J. Feigon, *Chem. Biol.* **1996**, *3*, 543.
[51] R. T. Syvitski, I. Burton, N. R. Mattatall, S. E. Douglas, D. L. Jakeman, *Biochemistry* **2005**, *44*, 7282.
[52] N. Mandard, P. Sodano, H. Labbe, J. M. Bonmatin, P. Bulet, C. Hetru, M. Ptak, F. Vovelle, *Eur. J. Biochem.* **1998**, *256*, 404.
[53] C. Xie, A. Prahl, B. Ericksen, Z. Wu, P. Zeng, X. Li, W. Y. Lu, J. Lubkowski, W. Lu, *J. Biol. Chem.* **2005**, *280*, 32921.
[54] Y. Wang, M. E. Henz, N. L. Gallagher, S. Chai, A. C. Gibbs, L. Z. Yan, M. E. Stiles, D. S. Wishart, J. C. Vederas, *Biochemistry* **1999**, *38*, 15438.
[55] A. Rozek, C. L. Friedrich, R. E. Hancock, *Biochemistry* **2000**, *39*, 15765.
[56] W. Humphrey, A. Dalke, K. Schulten, *J. Mol. Graph.* **1996**, *14*, 33.
[57] G. H. Gudmundsson, B. Agerberth, J. Odeberg, T. Bergman, B. Olsson, R. Salcedo, *Eur. J. Biochem.* **1996**, *238*, 325.
[58] B. Lopez-Garcia, P. H. Lee, K. Yamasaki, R. L. Gallo, *J. Invest. Dermatol.* **2005**, *125*, 108.
[59] Y. J. Gordon, L. C. Huang, E. G. Romanowski, K. A. Yates, R. J. Proske, A. M. McDermott, *Curr. Eye Res.* **2005**, *30*, 385.
[60] M. Zasloff, *Proc. Natl. Acad. Sci. U S A* **1987**, *84*, 5449.
[61] A. Mor, V. H. Nguyen, A. Delfour, D. Migliore-Samour, P. Nicolas, *Biochemistry* **1991**, *30*, 8824.
[62] C. Hernandez, A. Mor, F. Dagger, P. Nicolas, A. Hernandez, E. L. Benedetti, I. Dunia, *Eur. J. Cell Biol.* **1992**, *59*, 414.
[63] A. M. Cole, P. Weis, G. Diamond, *J. Biol. Chem.* **1997**, *272*, 12008.
[64] O. A. Mirgorodskaya, A. A. Shevchenko, K. O. Abdalla, I. V. Chernushevich, T. A. Egorov, A. X. Musoliamov, V. N. Kokryakov, O. V. Shamova, *FEBS Lett.* **1993**, *330*, 339.
[65] H. Tamamura, T. Murakami, S. Horiuchi, K. Sugihara, A. Otaka, W. Takada, T. Ibuka, M. Waki, N. Yamamoto, N. Fujii, *Chem. Pharm. Bull.* **1995**, *43*, 853.
[66] Y. Cho, J. S. Turner, N. N. Dinh, R. I. Lehrer, *Infect. Immun.* **1998**, *66*, 2486.
[67] L. Ehret-Sabatier, D. Loew, M. Goyffon, P. Fehlbaum, J. A. Hoffmann, A. van Dorsselaer, P. Bulet, *J. Biol. Chem.* **1996**, *271*, 29537.
[68] T. Nakamura, H. Furunaka, T. Miyata, F. Tokunaga, T. Muta, S. Iwanaga, M. Niwa, T. Takao, Y. Shimonishi, *J. Biol. Chem.* **1988**, *263*, 16709.
[69] T. Miyata, F. Tokunaga, T. Yoneya, K. Yoshikawa, S. Iwanaga, M. Niwa, T. Takao, Y. Shimonishi, *J. Biochem.* **1989**, *106*, 663.
[70] J. C. Pierce, W. L. Maloy, L. Salvador, C. F. Dungan, *Mol. Mar. Biol. Biotechnol.* **1997**, *6*, 248.
[71] L. A. Tziveleka, C. Vagias, V. Roussis, *Curr. Top. Med. Chem.* **2003**, *3*, 1512.
[72] T. Ganz, M. E. Selsted, D. Szklarek, S. S. Harwig, K. Daher, D. F. Bainton, R. I. Lehrer, *J. Clin. Invest.* **1985**, *76*, 1427.
[73] R. I. Lehrer, T. Ganz, D. Szklarek, M. E. Selsted, *J. Clin. Invest.* **1988**, *81*, 1829.

[74] T. L. Chang, J. Vargas, Jr., A. DelPortillo, M. E. Klotman, *J. Clin. Invest.* **2005**, *115*, 765.
[75] S. B. Aley, M. Zimmerman, M. Hetsko, M. E. Selsted, F. D. Gillin, *Infect. Immun.* **1994**, *62*, 5397.
[76] R. Bals, X. Wang, Z. Wu, T. Freeman, V. Bafna, M. Zasloff, J. M. Wilson, *J. Clin. Invest.* **1998**, *102*, 874.
[77] S. Vylkova, X. S. Li, J. C. Berner, M. Edgerton, *Antimicrob. Agents Chemother.* **2006**, *50*, 324.
[78] M. E. Quinones-Mateu, M. M. Lederman, Z. Feng, B. Chakraborty, J. Weber, H. R. Rangel, M. L. Marotta, M. Mirza, B. Jiang, P. Kiser, K. Medvik, S. F. Sieg, A. Weinberg, *Aids* **2003**, *17*, F39.
[79] T. K. Zaalouk, M. Bajaj-Elliott, J. T. George, V. McDonald, *Infect. Immun.* **2004**, *72*, 2772.
[80] B. Yasin, W. Wang, M. Pang, N. Cheshenko, T. Hong, A. J. Waring, B. C. Herold, E. A. Wagar, R. I. Lehrer, *J. Virol.* **2004**, *78*, 5147.
[81] F. Hubert, T. Noel, P. Roch, *Eur. J. Biochem.* **1996**, *240*, 302.
[82] K. P. van den Bergh, P. Proost, J. van Damme, J. Coosemans, E. J. van Damme, W. J. Peumans, *FEBS Lett.* **2002**, *530*, 181.
[83] B. Agerberth, J. Y. Lee, T. Bergman, M. Carlquist, H. G. Boman, V. Mutt, H. Jornvall, *Eur. J. Biochem.* **1991**, *202*, 849.
[84] S. Cociancich, A. Dupont, G. Hegy, R. Lanot, F. Holder, C. Hetru, J. A. Hoffmann, P. Bulet, *Biochem. J.* **1994**, *300 (Pt 2)*, 567.
[85] G. Kragol, R. Hoffmann, M. A. Chattergoon, S. Lovas, M. Cudic, P. Bulet, B. A. Condie, K. J. Rosengren, L. J. Montaner, L. Otvos, Jr., *Eur. J. Biochem.* **2002**, *269*, 4226.
[86] P. Bulet, J. L. Dimarcq, C. Hetru, M. Lagueux, M. Charlet, G. Hegy, A. Van Dorsselaer, J. A. Hoffmann, *J. Biol. Chem.* **1993**, *268*, 14893.
[87] P. Bulet, L. Urge, S. Ohresser, C. Hetru, L. Otvos, Jr., *Eur. J. Biochem.* **1996**, *238*, 64.
[88] P. Casteels, C. Ampe, F. Jacobs, M. Vaeck, P. Tempst, *EMBO J.* **1989**, *8*, 2387.
[89] F. G. Oppenheim, T. Xu, F. M. McMillian, S. M. Levitz, R. D. Diamond, G. D. Offner, R. F. Troxler, *J. Biol. Chem.* **1988**, *263*, 7472.
[90] M. E. Selsted, M. J. Novotny, W. L. Morris, Y. Q. Tang, W. Smith, J. S. Cullor, *J. Biol. Chem.* **1992**, *267*, 4292.
[91] W. E. Robinson, Jr., B. McDougall, D. Tran, M. E. Selsted, *J. Leukoc. Biol.* **1998**, *63*, 94.
[92] A. Giacometti, O. Cirioni, F. Barchiesi, F. Caselli, G. Scalise, *J. Antimicrob. Chemother.* **1999**, *44*, 403.
[93] P. Fehlbaum, P. Bulet, S. Chernysh, J. P. Briand, J. P. Roussel, L. Letellier, C. Hetru, J. A. Hoffmann, *Proc. Natl. Acad. Sci. U S A* **1996**, *93*, 1221.
[94] D. Romeo, B. Skerlavaj, M. Bolognesi, R. Gennaro, *J. Biol. Chem.* **1988**, *263*, 9573.
[95] B. Gallis, J. Mehl, K. S. Prickett, J. A. Martin, J. Merriam, C. J. March, D. P. Cerretti, *Biotechnol. Ther.* **1989**, *1*, 335.
[96] C. B. Park, M. S. Kim, S. C. Kim, *Biochem. Biophys. Res. Commun.* **1996**, *218*, 408.
[97] W. Bellamy, M. Takase, H. Wakabayashi, K. Kawase, M. Tomita, *J. Appl. Bacteriol.* **1992**, *73*, 472.
[98] W. Bellamy, H. Wakabayashi, M. Takase, K. Kawase, S. Shimamura, M. Tomita, *Med. Microbiol. Immunol.* **1993**, *182*, 97.
[99] M. Ikeda, A. Nozaki, K. Sugiyama, T. Tanaka, A. Naganuma, K. Tanaka, H. Sekihara, K. Shimotohno, M. Saito, N. Kato, *Virus Res.* **2000**, *66*, 51.
[100] T. Isamida, T. Tanaka, Y. Omata, K. Yamauchi, K. Shimazaki, A. Saito, *J. Vet. Med. Sci.* **1998**, *60*, 241.
[101] J. M. Graham, J. A. Higgins, *Membrane analysis*, BIOS, Oxford, **1997**.
[102] A. Wiese, T. Gutsmann, U. Seydel, *J. Endotoxin Res.* **2003**, *9*, 67.

[103] P. L. Yeagle, *The structure of biological membranes*, 2nd ed., CRC Press, Boca Raton, **2005**.
[104] S. R. Dennison, J. Howe, L. H. Morton, K. Brandenburg, F. Harris, D. A. Phoenix, *Biochem. Biophys. Res. Commun.* **2006**, *347*, 1006.
[105] K. Matsuzaki, K. Sugishita, N. Fujii, K. Miyajima, *Biochemistry* **1995**, *34*, 3423.
[106] K. Matsuzaki, M. Fukui, N. Fujii, K. Miyajima, *Biochim. Biophys. Acta* **1991**, *1070*, 259.
[107] A. Ramamoorthy, S. Thennarasu, A. Tan, D. K. Lee, C. Clayberger, A. M. Krensky, *Biochim. Biophys. Acta* **2006**, *1758*, 154.
[108] T. Wieprecht, O. Apostolov, M. Beyermann, J. Seelig, *Biochemistry* **2000**, *39*, 442.
[109] E. Glukhov, M. Stark, L. L. Burrows, C. M. Deber, *J. Biol. Chem.* **2005**, *280*, 33960.
[110] D. Kraus, A. Peschel, *Curr. Top. Microbiol. Immunol.* **2006**, *306*, 231.
[111] L. Zhang, A. Rozek, R. E. Hancock, *J. Biol. Chem.* **2001**, *276*, 35714.
[112] A. Peschel, H. G. Sahl, *Nat. Rev. Microbiol.* **2006**, *4*, 529.
[113] S. Frantz, *Nature* **2005**, *437*, 942.
[114] A. Tossi, L. Sandri, A. Giangaspero, *Biopolymers* **2000**, *55*, 4.
[115] J. Chen, T. J. Falla, H. Liu, M. A. Hurst, C. A. Fujii, D. A. Mosca, J. R. Embree, D. J. Loury, P. A. Radel, C. Cheng Chang, L. Gu, J. C. Fiddes, *Biopolymers* **2000**, *55*, 88.
[116] A. Mor, P. Nicolas, *J. Biol. Chem.* **1994**, *269*, 1934.
[117] X. Li, Y. Li, H. Han, D. W. Miller, G. Wang, *J. Am. Chem. Soc.* **2006**, *128*, 5776.
[118] M. Dathe, M. Schumann, T. Wieprecht, A. Winkler, M. Beyermann, E. Krause, K. Matsuzaki, O. Murase, M. Bienert, *Biochemistry* **1996**, *35*, 12612.
[119] I. Zelezetsky, A. Tossi, *Biochim. Biophys. Acta* **2006**.
[120] J. P. Tam, Y. A. Lu, J. L. Yang, *Biochemistry* **2000**, *39*, 7159.
[121] M. Vila-Perello, S. Tognon, A. Sanchez-Vallet, F. Garcia-Olmedo, A. Molina, D. Andreu, *J. Med. Chem.* **2006**, *49*, 448.
[122] J. A. Robinson, *Synlett* **2000**, 429.
[123] M. Favre, K. Moehle, L. Y. Jiang, B. Pfeiffer, J. A. Robinson, *J. Am. Chem. Soc.* **1999**, *121*, 2679.
[124] L. J. Jiang, K. Moehle, B. Dhanapal, D. Obrecht, J. A. Robinson, *Helv. Chim. Acta* **2000**, *83*, 3097.
[125] R. Fasan, R. L. Dias, K. Moehle, O. Zerbe, D. Obrecht, P. R. Mittl, M. G. Grutter, J. A. Robinson, *ChemBioChem* **2006**, *7*, 515.
[126] A. Descours, K. Moehle, A. Renard, J. A. Robinson, *ChemBioChem* **2002**, *3*, 318.
[127] R. L. Dias, R. Fasan, K. Moehle, A. Renard, D. Obrecht, J. A. Robinson, *J. Am. Chem. Soc.* **2006**, *128*, 2726.
[128] Z. Athanassiou, R. L. Dias, K. Moehle, N. Dobson, G. Varani, J. A. Robinson, *J. Am. Chem. Soc.* **2004**, *126*, 6906.
[129] Y. Xu, H. Tamamura, R. Arakaki, H. Nakashima, X. Zhang, N. Fujii, T. Uchiyama, T. Hattori, *AIDS Res. Hum. Retrovir.* **1999**, *15*, 419.
[130] S. Tauro, E. Coutinho, S. Srivastava, *Protein Pept. Lett.* **2003**, *10*, 346.
[131] J. P. Powers, A. Rozek, R. E. Hancock, *Biochim. Biophys. Acta* **2004**, *1698*, 239.
[132] N. Mandard, P. Bulet, A. Caille, S. Daffre, F. Vovelle, *Eur. J. Biochem.* **2002**, *269*, 1190.
[133] S. S. Harwig, A. Waring, H. J. Yang, Y. Cho, L. Tan, R. I. Lehrer, *Eur. J. Biochem.* **1996**, *240*, 352.
[134] K. Matsuzaki, M. Nakayama, M. Fukui, A. Otaka, S. Funakoshi, N. Fujii, K. Bessho, K. Miyajima, *Biochemistry* **1993**, *32*, 11704.
[135] S. Thennarasu, R. Nagaraj, *Biochem. Biophys. Res. Commun.* **1999**, *254*, 281.
[136] B. Romestand, F. Molina, V. Richard, P. Roch, C. Granier, *Eur. J. Biochem.* **2003**, *270*, 2805.
[137] S. C. Shankaramma, Z. Athanassiou, O. Zerbe, K. Moehle, C. Mouton, F. Bernardini, J. W. Vrijbloed, D. Obrecht, J. A. Robinson, *ChemBioChem* **2002**, *3*, 1126.
[138] J. A. Robinson, S. C. Shankaramma, P. Jetter, U. Kienzl, R. A. Schwendener, J. W. Vrijbloed, D. Obrecht, *Bioorg. Med. Chem.* **2005**, *13*, 2055.

[139] N. Srinivas, PhD thesis, University of Zürich (Zürich), **2005**.
[140] S. C. Shankaramma, K. Moehle, S. James, J. W. Vrijbloed, D. Obrecht, J. A. Robinson, *Chem. Commun.* **2003**, 1842.
[141] K. L. Brown, R. E. Hancock, *Curr. Opin. Immunol.* **2006**, *18*, 24.
[142] N. Papo, Y. Shai, *Cell Mol. Life Sci.* **2005**, *62*, 784.
[143] M. G. Scott, H. Yan, R. E. Hancock, *Infect. Immun.* **1999**, *67*, 2005.
[144] M. G. Scott, M. R. Gold, R. E. Hancock, *Infect. Immun.* **1999**, *67*, 6445.
[145] R. I. Lehrer, A. Barton, K. A. Daher, S. S. Harwig, T. Ganz, M. E. Selsted, *J. Clin. Invest.* **1989**, *84*, 553.
[146] N. Papo, Y. Shai, *Peptides* **2003**, *24*, 1693.
[147] P. A. Lambert, *Symp. Ser. Soc. Appl. Microbiol.* **2002**, 46S.
[148] H. V. Westerhoff, D. Juretic, R. W. Hendler, M. Zasloff, *Proc. Natl. Acad. Sci. U S A* **1989**, *86*, 6597.
[149] D. Juretic, R. W. Hendler, F. Kamp, W. S. Caughey, M. Zasloff, H. V. Westerhoff, *Biochemistry* **1994**, *33*, 4562.
[150] K. Matsuzaki, K. Sugishita, M. Harada, N. Fujii, K. Miyajima, *Biochim. Biophys. Acta* **1997**, *1327*, 119.
[151] M. Zasloff, B. Martin, H. C. Chen, *Proc. Natl. Acad. Sci. U S A* **1988**, *85*, 910.
[152] M. Hugosson, D. Andreu, H. G. Boman, E. Glaser, *Eur. J. Biochem.* **1994**, *223*, 1027.
[153] V. C. Kalfa, H. P. Jia, R. A. Kunkle, P. B. McCray, Jr., B. F. Tack, K. A. Brogden, *Antimicrob. Agents Chemother.* **2001**, *45*, 3256.
[154] H. M. Chen, S. C. Chan, J. C. Lee, C. C. Chang, M. Murugan, R. W. Jack, *Microsc. Res. Tech.* **2003**, *62*, 423.
[155] M. R. Yeaman, N. Y. Yount, *Pharmacol. Rev.* **2003**, *55*, 27.
[156] R. Bessalle, H. Haas, A. Goria, I. Shalit, M. Fridkin, *Antimicrob. Agents Chemother.* **1992**, *36*, 313.
[157] M. Dathe, T. Wieprecht, H. Nikolenko, L. Handel, W. L. Maloy, D. L. MacDonald, M. Beyermann, M. Bienert, *FEBS Lett.* **1997**, *403*, 208.
[158] D. Eisenberg, *Annu. Rev. Biochem.* **1984**, *53*, 595.
[159] T. Wieprecht, M. Dathe, M. Beyermann, E. Krause, W. L. Maloy, D. L. MacDonald, M. Bienert, *Biochemistry* **1997**, *36*, 6124.
[160] L. H. Kondejewski, M. Jelokhani-Niaraki, S. W. Farmer, B. Lix, C. M. Kay, B. D. Sykes, R. E. Hancock, R. S. Hodges, *J. Biol. Chem.* **1999**, *274*, 13181.
[161] M. Dathe, J. Meyer, M. Beyermann, B. Maul, C. Hoischen, M. Bienert, *Biochim. Biophys. Acta* **2002**, *1558*, 171.
[162] N. Uematsu, K. Matsuzaki, *Biophys. J.* **2000**, *79*, 2075.
[163] L. Yang, T. A. Harroun, T. M. Weiss, L. Ding, H. W. Huang, *Biophys. J.* **2001**, *81*, 1475.
[164] F. Y. Chen, M. T. Lee, H. W. Huang, *Biophys. J.* **2003**, *84*, 3751.
[165] W. T. Heller, A. J. Waring, R. I. Lehrer, T. A. Harroun, T. M. Weiss, L. Yang, H. W. Huang, *Biochemistry* **2000**, *39*, 139.
[166] S. Ludtke, K. He, H. Huang, *Biochemistry* **1995**, *34*, 16764.
[167] G. Baumann, P. Mueller, *J. Supramol. Struct.* **1974**, *2*, 538.
[168] Z. Oren, Y. Shai, *Biopolymers* **1998**, *47*, 451.
[169] D. M. Ojcius, J. D. Young, *Trends Biochem. Sci.* **1991**, *16*, 225.
[170] Y. Shai, *Biopolymers* **2002**, *66*, 236.
[171] J. D. Lear, Z. R. Wasserman, W. F. DeGrado, *Science* **1988**, *240*, 1177.
[172] D. O. Mak, W. W. Webb, *Biophys. J.* **1995**, *69*, 2323.
[173] K. He, S. J. Ludtke, D. L. Worcester, H. W. Huang, *Biophys. J.* **1996**, *70*, 2659.
[174] R. O. Fox, Jr., F. M. Richards, *Nature* **1982**, *300*, 325.
[175] N. Saint, L. Marri, D. Marchini, G. Molle, *Peptides* **2003**, *24*, 1779.
[176] Y. Shai, *Biochim. Biophys. Acta* **1999**, *1462*, 55.
[177] K. Lohner, E. J. Prenner, *Biochim. Biophys. Acta* **1999**, *1462*, 141.
[178] K. Matsuzaki, K. Sugishita, N. Ishibe, M. Ueha, S. Nakata, K. Miyajima, R. M. Epand, *Biochemistry* **1998**, *37*, 11856.

[179] E. M. Tytler, J. P. Segrest, R. M. Epand, S. Q. Nie, R. F. Epand, V. K. Mishra, Y. V. Venkatachalapathi, G. M. Anantharamaiah, *J. Biol. Chem.* **1993**, *268*, 22112.
[180] E. Y. Chekmenev, B. S. Vollmar, K. T. Forseth, M. N. Manion, S. M. Jones, T. J. Wagner, R. M. Endicott, B. P. Kyriss, L. M. Homem, M. Pate, J. He, J. Raines, P. L. Gor'kov, W. W. Brey, D. J. Mitchell, A. J. Auman, M. J. Ellard-Ivey, J. Blazyk, M. Cotten, *Biochim. Biophys. Acta* **2006**.
[181] F. M. Marassi, S. J. Opella, P. Juvvadi, R. B. Merrifield, *Biophys. J.* **1999**, *77*, 3152.
[182] Y. Pouny, D. Rapaport, A. Mor, P. Nicolas, Y. Shai, *Biochemistry* **1992**, *31*, 12416.
[183] C. Hetru, L. Letellier, Z. Oren, J. A. Hoffmann, Y. Shai, *Biochem. J.* **2000**, *345 Pt 3*, 653.
[184] S. Fernandez-Lopez, H. S. Kim, E. C. Choi, M. Delgado, J. R. Granja, A. Khasanov, K. Kraehenbuehl, G. Long, D. A. Weinberger, K. M. Wilcoxen, M. R. Ghadiri, *Nature* **2001**, *412*, 452.
[185] M. Sharon, Z. Oren, Y. Shai, J. Anglister, *Biochemistry* **1999**, *38*, 15305.
[186] Z. Oren, J. C. Lerman, G. H. Gudmundsson, B. Agerberth, Y. Shai, *Biochem. J.* **1999**, *341 (Pt 3)*, 501.
[187] J. A. Whiles, R. Brasseur, K. J. Glover, G. Melacini, E. A. Komives, R. R. Vold, *Biophys. J.* **2001**, *80*, 280.
[188] B. Bechinger, K. Lohner, *Biochim. Biophys. Acta* **2006**, *1758*, 1529.
[189] J. M. Boon, B. D. Smith, *Med. Res. Rev.* **2002**, *22*, 251.
[190] K. Matsuzaki, O. Murase, N. Fujii, K. Miyajima, *Biochemistry* **1996**, *35*, 11361.
[191] S. J. Ludtke, K. He, W. T. Heller, T. A. Harroun, L. Yang, H. W. Huang, *Biochemistry* **1996**, *35*, 13723.
[192] N. Saint, H. Cadiou, Y. Bessin, G. Molle, *Biochim. Biophys. Acta* **2002**, *1564*, 359.
[193] M. Miteva, M. Andersson, A. Karshikoff, G. Otting, *FEBS Lett.* **1999**, *462*, 155.
[194] A. Pokorny, T. H. Birkbeck, P. F. Almeida, *Biochemistry* **2002**, *41*, 11044.
[195] B. Bechinger, *J. Membr. Biol.* **1997**, *156*, 197.
[196] K. A. Henzler Wildman, D. K. Lee, A. Ramamoorthy, *Biochemistry* **2003**, *42*, 6545.
[197] S. Yamaguchi, T. Hong, A. Waring, R. I. Lehrer, M. Hong, *Biochemistry* **2002**, *41*, 9852.
[198] A. Naito, T. Nagao, K. Norisada, T. Mizuno, S. Tuzi, H. Saito, *Biophys. J.* **2000**, *78*, 2405.
[199] Y. Hori, M. Demura, T. Niidome, H. Aoyagi, T. Asakura, *FEBS Lett.* **1999**, *455*, 228.
[200] A. S. Ladokhin, S. H. White, *Biochim. Biophys. Acta* **2001**, *1514*, 253.
[201] I. Wiedemann, E. Breukink, C. van Kraaij, O. P. Kuipers, G. Bierbaum, B. de Kruijff, H. G. Sahl, *J. Biol. Chem.* **2001**, *276*, 1772.
[202] H. Brotz, G. Bierbaum, K. Leopold, P. E. Reynolds, H. G. Sahl, *Antimicrob. Agents Chemother.* **1998**, *42*, 154.
[203] E. Breukink, I. Wiedemann, C. van Kraaij, O. P. Kuipers, H. Sahl, B. de Kruijff, *Science* **1999**, *286*, 2361.
[204] E. Breukink, B. de Kruijff, *Nat. Rev. Drug Discov.* **2006**, *5*, 321.
[205] R. W. Jack, G. Jung, *Curr. Opin. Chem. Biol.* **2000**, *4*, 310.
[206] M. Couturier, M. Bahassi el, L. Van Melderen, *Trends Microbiol.* **1998**, *6*, 269.
[207] M. A. Delgado, M. R. Rintoul, R. N. Farias, R. A. Salomon, *J. Bacteriol.* **2001**, *183*, 4543.
[208] B. J. MacKay, L. Denepitiya, V. J. Iacono, S. B. Krost, J. J. Pollock, *Infect. Immun.* **1984**, *44*, 695.
[209] J. J. Pollock, L. Denepitiya, B. J. MacKay, V. J. Iacono, *Infect. Immun.* **1984**, *44*, 702.
[210] K. Kavanagh, S. Dowd, *J. Pharm. Pharmacol.* **2004**, *56*, 285.
[211] M. Edgerton, S. E. Koshlukova, T. E. Lo, B. G. Chrzan, R. M. Straubinger, P. A. Raj, *J. Biol. Chem.* **1998**, *273*, 20438.
[212] J. Driscoll, C. Duan, Y. Zuo, T. Xu, R. Troxler, F. G. Oppenheim, *Gene* **1996**, *177*, 29.
[213] X. S. Li, M. S. Reddy, D. Baev, M. Edgerton, *J. Biol. Chem.* **2003**, *278*, 28553.

[214] X. S. Li, J. N. Sun, K. Okamoto-Shibayama, M. Edgerton, *J. Biol. Chem.* **2006**, *281*, 22453.
[215] E. J. Helmerhorst, P. Breeuwer, W. van't Hof, E. Walgreen-Weterings, L. C. Oomen, E. C. Veerman, A. V. Amerongen, T. Abee, *J. Biol. Chem.* **1999**, *274*, 7286.
[216] J. Dong, S. Vylkova, X. S. Li, M. Edgerton, *J. Dent. Res.* **2003**, *82*, 748.
[217] D. Baev, X. Li, M. Edgerton, *Microbiology* **2001**, *147*, 3323.
[218] C. Gyurko, U. Lendenmann, R. F. Troxler, F. G. Oppenheim, *Antimicrob. Agents Chemother.* **2000**, *44*, 348.
[219] S. E. Koshlukova, T. L. Lloyd, M. W. Araujo, M. Edgerton, *J. Biol. Chem.* **1999**, *274*, 18872.
[220] K. De Smet, R. Reekmans, R. Contreras, *Biotechnol. Lett.* **2004**, *26*, 1781.
[221] Y. Wang, R. Roman, S. D. Lidofsky, J. G. Fitz, *Proc. Natl. Acad. Sci. U S A* **1996**, *93*, 12020.
[222] A. Surprenant, F. Rassendren, E. Kawashima, R. A. North, G. Buell, *Science* **1996**, *272*, 735.
[223] S. E. Koshlukova, M. W. Araujo, D. Baev, M. Edgerton, *Infect. Immun.* **2000**, *68*, 6848.
[224] D. Baev, X. S. Li, J. Dong, P. Keng, M. Edgerton, *Infect. Immun.* **2002**, *70*, 4777.
[225] D. Baev, A. Rivetta, S. Vylkova, J. N. Sun, G. F. Zeng, C. L. Slayman, M. Edgerton, *J. Biol. Chem.* **2004**, *279*, 55060.
[226] E. J. Helmerhorst, R. F. Troxler, F. G. Oppenheim, *Proc. Natl. Acad. Sci. U S A* **2001**, *98*, 14637.
[227] D. Wunder, J. Dong, D. Baev, M. Edgerton, *Antimicrob. Agents Chemother.* **2004**, *48*, 110.
[228] E. C. Veerman, K. Nazmi, W. Van't Hof, J. G. Bolscher, A. L. Den Hertog, A. V. Nieuw Amerongen, *Biochem. J.* **2004**, *381*, 447.
[229] A. L. den Hertog, H. W. Wong Fong Sang, R. Kraayenhof, J. G. Bolscher, W. Van't Hof, E. C. Veerman, A. V. Nieuw Amerongen, *Biochem. J.* **2004**, *379*, 665.
[230] A. L. den Hertog, J. van Marle, H. A. van Veen, W. Van't Hof, J. G. Bolscher, E. C. Veerman, A. V. Nieuw Amerongen, *Biochem. J.* **2005**, *388*, 689.
[231] U. S. Sajjan, L. T. Tran, N. Sole, C. Rovaldi, A. Akiyama, P. M. Friden, J. F. Forstner, D. M. Rothstein, *Antimicrob. Agents Chemother.* **2001**, *45*, 3437.
[232] D. M. Rothstein, P. Spacciapoli, L. T. Tran, T. Xu, F. D. Roberts, M. Dalla Serra, D. K. Buxton, F. G. Oppenheim, P. Friden, *Antimicrob. Agents Chemother.* **2001**, *45*, 1367.
[233] A. L. Ruissen, J. Groenink, P. Krijtenberg, E. Walgreen-Weterings, W. van 't Hof, E. C. Veerman, A. V. Nieuw Amerongen, *Biol. Chem.* **2003**, *384*, 183.
[234] A. Basak, B. Ernst, D. Brewer, N. G. Seidah, J. S. Munzer, C. Lazure, G. A. Lajoie, *J. Pept. Res.* **1997**, *49*, 596.
[235] P. Casteels, P. Tempst, *Biochem. Biophys. Res. Commun.* **1994**, *199*, 339.
[236] L. Otvos, Jr., K. Bokonyi, I. Varga, B. I. Otvos, R. Hoffmann, H. C. Ertl, J. D. Wade, A. M. McManus, D. J. Craik, P. Bulet, *Protein Sci.* **2000**, *9*, 742.
[237] J. A. Mackintosh, D. A. Veal, A. J. Beattie, A. A. Gooley, *J. Biol. Chem.* **1998**, *273*, 6139.
[238] M. Gobbo, L. Biondi, F. Filira, R. Rocchi, *J. Pept. Sci.* **2006**, *12*, 132.
[239] M. Castle, A. Nazarian, S. S. Yi, P. Tempst, *J. Biol. Chem.* **1999**, *274*, 32555.
[240] L. Otvos, Jr., I. O, M. E. Rogers, P. J. Consolvo, B. A. Condie, S. Lovas, P. Bulet, M. Blaszczyk-Thurin, *Biochemistry* **2000**, *39*, 14150.
[241] G. Kragol, S. Lovas, G. Varadi, B. A. Condie, R. Hoffmann, L. Otvos, Jr., *Biochemistry* **2001**, *40*, 3016.
[242] L. S. Chesnokova, S. V. Slepenkov, S. N. Witt, *FEBS Lett.* **2004**, *565*, 65.
[243] H. G. Boman, B. Agerberth, A. Boman, *Infect. Immun.* **1993**, *61*, 2978.
[244] S. Vunnam, P. Juvvadi, R. B. Merrifield, *J. Pept. Res.* **1997**, *49*, 59.
[245] A. Patrzykat, C. L. Friedrich, L. Zhang, V. Mendoza, R. E. Hancock, *Antimicrob. Agents Chemother.* **2002**, *46*, 605.

[246] C. Subbalakshmi, N. Sitaram, *FEMS Microbiol. Lett.* **1998**, *160*, 91.
[247] J. Lutkenhaus, *Trends Genet.* **1990**, *6*, 22.
[248] C. L. Friedrich, A. Rozek, A. Patrzykat, R. E. Hancock, *J. Biol. Chem.* **2001**, *276*, 24015.
[249] S. Kobayashi, A. Chikushi, S. Tougu, Y. Imura, M. Nishida, Y. Yano, K. Matsuzaki, *Biochemistry* **2004**, *43*, 15610.
[250] A. Yonezawa, J. Kuwahara, N. Fujii, Y. Sugiura, *Biochemistry* **1992**, *31*, 2998.
[251] M. E. Churchill, A. A. Travers, *Trends Biochem. Sci.* **1991**, *16*, 92.
[252] P. G. Baraldi, A. Bovero, F. Fruttarolo, D. Preti, M. A. Tabrizi, M. G. Pavani, R. Romagnoli, *Med. Res. Rev.* **2004**, *24*, 475.
[253] D. D. Boehr, K. A. Draker, K. Koteva, M. Bains, R. E. Hancock, G. D. Wright, *Chem. Biol.* **2003**, *10*, 189.
[254] R. E. Hancock, A. Rozek, *FEMS Microbiol Lett.* **2002**, *206*, 143.
[255] M. E. Selsted, A. J. Ouellette, *Nat. Immunol.* **2005**, *6*, 551.
[256] D. M. Bowdish, D. J. Davidson, M. G. Scott, R. E. Hancock, *Antimicrob. Agents Chemother.* **2005**, *49*, 1727.
[257] L. A. Duits, B. Ravensbergen, M. Rademaker, P. S. Hiemstra, P. H. Nibbering, *Immunology* **2002**, *106*, 517.
[258] C. L. Wilson, A. J. Ouellette, D. P. Satchell, T. Ayabe, Y. S. Lopez-Boado, J. L. Stratman, S. J. Hultgren, L. M. Matrisian, W. C. Parks, *Science* **1999**, *286*, 113.
[259] C. Moser, D. J. Weiner, E. Lysenko, R. Bals, J. N. Weiser, J. M. Wilson, *Infect. Immun.* **2002**, *70*, 3068.
[260] N. H. Salzman, D. Ghosh, K. M. Huttner, Y. Paterson, C. L. Bevins, *Nature* **2003**, *422*, 522.
[261] A. D. Befus, C. Mowat, M. Gilchrist, J. Hu, S. Solomon, A. Bateman, *J. Immunol.* **1999**, *163*, 947.
[262] S. Yomogida, I. Nagaoka, K. Saito, T. Yamashita, *Inflamm. Res.* **1996**, *45*, 62.
[263] M. Ichinose, M. Asai, K. Imai, M. Sawada, *Immunopharmacology* **1996**, *35*, 103.
[264] Z. Prohaszka, K. Nemet, P. Csermely, F. Hudecz, G. Mezo, G. Fust, *Mol. Immunol.* **1997**, *34*, 809.
[265] R. H. van den Berg, M. C. Faber-Krol, S. van Wetering, P. S. Hiemstra, M. R. Daha, *Blood* **1998**, *92*, 3898.
[266] G. A. Porro, J. H. Lee, J. de Azavedo, I. Crandall, T. Whitehead, E. Tullis, T. Ganz, M. Liu, A. S. Slutsky, H. Zhang, *Am. J. Physiol. Lung Cell. Mol. Physiol.* **2001**, *281*, L1240.
[267] J. Chen, X. M. Xu, C. B. Underhill, S. Yang, L. Wang, Y. Chen, S. Hong, K. Creswell, L. Zhang, *Cancer Res.* **2005**, *65*, 4614.
[268] M. C. Territo, T. Ganz, M. E. Selsted, R. Lehrer, *J. Clin. Invest.* **1989**, *84*, 2017.
[269] J. R. Garcia, F. Jaumann, S. Schulz, A. Krause, J. Rodriguez-Jimenez, U. Forssmann, K. Adermann, E. Kluver, C. Vogelmeier, D. Becker, R. Hedrich, W. G. Forssmann, R. Bals, *Cell Tissue Res.* **2001**, *306*, 257.
[270] J. R. Garcia, A. Krause, S. Schulz, F. J. Rodriguez-Jimenez, E. Kluver, K. Adermann, U. Forssmann, A. Frimpong-Boateng, R. Bals, W. G. Forssmann, *FASEB J.* **2001**, *15*, 1819.
[271] D. Verbanac, M. Zanetti, D. Romeo, *FEBS Lett.* **1993**, *317*, 255.
[272] D. Yang, Q. Chen, A. P. Schmidt, G. M. Anderson, J. M. Wang, J. Wooters, J. J. Oppenheim, O. Chertov, *J. Exp. Med.* **2000**, *192*, 1069.
[273] K. Kurosaka, Q. Chen, F. Yarovinsky, J. J. Oppenheim, D. Yang, *J. Immunol.* **2005**, *174*, 6257.
[274] O. Chertov, D. F. Michiel, L. Xu, J. M. Wang, K. Tani, W. J. Murphy, D. L. Longo, D. D. Taub, J. J. Oppenheim, *J. Biol. Chem.* **1996**, *271*, 2935.
[275] D. Yang, Q. Chen, O. Chertov, J. J. Oppenheim, *J. Leukoc. Biol.* **2000**, *68*, 9.
[276] D. Yang, O. Chertov, S. N. Bykovskaia, Q. Chen, M. J. Buffo, J. Shogan, M. Anderson, J. M. Schroder, J. M. Wang, O. M. Howard, J. J. Oppenheim, *Science* **1999**, *286*, 525.

[277] B. Agerberth, J. Charo, J. Werr, B. Olsson, F. Idali, L. Lindbom, R. Kiessling, H. Jornvall, H. Wigzell, G. H. Gudmundsson, *Blood* **2000**, *96*, 3086.
[278] A. Biragyn, M. Surenhu, D. Yang, P. A. Ruffini, B. A. Haines, E. Klyushnenkova, J. J. Oppenheim, L. W. Kwak, *J. Immunol.* **2001**, *167*, 6644.
[279] F. Niyonsaba, K. Iwabuchi, H. Matsuda, H. Ogawa, I. Nagaoka, *Int. Immunol.* **2002**, *14*, 421.
[280] F. Niyonsaba, K. Iwabuchi, A. Someya, M. Hirata, H. Matsuda, H. Ogawa, I. Nagaoka, *Immunology* **2002**, *106*, 20.
[281] H. J. Huang, C. R. Ross, F. Blecha, *J. Leukoc. Biol.* **1997**, *61*, 624.
[282] M. G. Scott, D. J. Davidson, M. R. Gold, D. Bowdish, R. E. Hancock, *J. Immunol.* **2002**, *169*, 3883.
[283] N. Mookherjee, K. L. Brown, D. M. Bowdish, S. Doria, R. Falsafi, K. Hokamp, F. M. Roche, R. Mu, G. H. Doho, J. Pistolic, J. P. Powers, J. Bryan, F. S. Brinkman, R. E. Hancock, *J. Immunol.* **2006**, *176*, 2455.
[284] D. Delfino, V. V. Cusumano, F. Tomasello, V. Cusumano, *New Microbiol.* **2004**, *27*, 369.
[285] J. W. Larrick, M. Hirata, R. F. Balint, J. Lee, J. Zhong, S. C. Wright, *Infect. Immun.* **1995**, *63*, 1291.
[286] M. G. Vallespi, J. C. Alvarez-Obregon, I. Rodriguez-Alonso, T. Montero, H. Garay, O. Reyes, M. J. Arana, *Int. Immunopharmacol.* **2003**, *3*, 247.
[287] J. Li, M. Post, R. Volk, Y. Gao, M. Li, C. Metais, K. Sato, J. Tsai, W. Aird, R. D. Rosenberg, T. G. Hampton, F. Sellke, P. Carmeliet, M. Simons, *Nat. Med.* **2000**, *6*, 49.
[288] R. Koczulla, G. von Degenfeld, C. Kupatt, F. Krotz, S. Zahler, T. Gloe, K. Issbrucker, P. Unterberger, M. Zaiou, C. Lebherz, A. Karl, P. Raake, A. Pfosser, P. Boekstegers, U. Welsch, P. S. Hiemstra, C. Vogelmeier, R. L. Gallo, M. Clauss, R. Bals, *J. Clin. Invest.* **2003**, *111*, 1665.
[289] F. Niyonsaba, A. Someya, M. Hirata, H. Ogawa, I. Nagaoka, *Eur. J. Immunol.* **2001**, *31*, 1066.
[290] S. van Wetering, S. P. Mannesse-Lazeroms, M. A. Van Sterkenburg, M. R. Daha, J. H. Dijkman, P. S. Hiemstra, *Am. J. Physiol.* **1997**, *272*, L888.
[291] S. van Wetering, S. P. Mannesse-Lazeroms, M. A. van Sterkenburg, P. S. Hiemstra, *Inflamm. Res.* **2002**, *51*, 8.
[292] D. M. Bowdish, D. J. Davidson, Y. E. Lau, K. Lee, M. G. Scott, R. E. Hancock, *J. Leukoc. Biol.* **2005**, *77*, 451.
[293] M. H. Braff, M. A. Hawkins, A. Di Nardo, B. Lopez-Garcia, M. D. Howell, C. Wong, K. Lin, J. E. Streib, R. Dorschner, D. Y. Leung, R. L. Gallo, *J. Immunol.* **2005**, *174*, 4271.
[294] Y. V. Chaly, E. M. Paleolog, T. S. Kolesnikova, Tikhonov, II, E. V. Petratchenko, N. N. Voitenok, *Eur. Cytokine Netw.* **2000**, *11*, 257.
[295] M. G. Vallespi, L. A. Glaria, O. Reyes, H. E. Garay, J. Ferrero, M. J. Arana, *Clin. Diagn. Lab. Immunol.* **2000**, *7*, 669.
[296] D. J. Davidson, A. J. Currie, G. S. Reid, D. M. Bowdish, K. L. MacDonald, R. C. Ma, R. E. Hancock, D. P. Speert, *J. Immunol.* **2004**, *172*, 1146.
[297] A. Biragyn, P. A. Ruffini, C. A. Leifer, E. Klyushnenkova, A. Shakhov, O. Chertov, A. K. Shirakawa, J. M. Farber, D. M. Segal, J. J. Oppenheim, L. W. Kwak, *Science* **2002**, *298*, 1025.
[298] C. J. Murphy, B. A. Foster, M. J. Mannis, M. E. Selsted, T. W. Reid, *J. Cell. Physiol.* **1993**, *155*, 408.
[299] J. Aarbiou, M. Ertmann, S. van Wetering, P. van Noort, D. Rook, K. F. Rabe, S. V. Litvinov, J. H. van Krieken, W. I. de Boer, P. S. Hiemstra, *J. Leukoc. Biol.* **2002**, *72*, 167.
[300] T. Chavakis, D. B. Cines, J. S. Rhee, O. D. Liang, U. Schubert, H. P. Hammes, A. A. Higazi, P. P. Nawroth, K. T. Preissner, K. Bdeir, *FASEB J.* **2004**, *18*, 1306.

[301] J. W. Lillard, Jr., P. N. Boyaka, O. Chertov, J. J. Oppenheim, J. R. McGhee, *Proc. Natl. Acad Sci. U S A* **1999**, *96*, 651.
[302] K. A. Brogden, M. Heidari, R. E. Sacco, D. Palmquist, J. M. Guthmiller, G. K. Johnson, H. P. Jia, B. F. Tack, P. B. McCray, *Oral Microbiol. Immunol.* **2003**, *18*, 95.
[303] L. L. An, Y. H. Yang, X. T. Ma, Y. M. Lin, G. Li, Y. H. Song, K. F. Wu, *Leuk. Res.* **2005**, *29*, 535.
[304] G. S. Tjabringa, J. Aarbiou, D. K. Ninaber, J. W. Drijfhout, O. E. Sorensen, N. Borregaard, K. F. Rabe, P. S. Hiemstra, *J. Immunol.* **2003**, *171*, 6690.
[305] A. Elssner, M. Duncan, M. Gavrilin, M. D. Wewers, *J. Immunol.* **2004**, *172*, 4987.
[306] D. M. Bowdish, D. J. Davidson, D. P. Speert, R. E. Hancock, *J. Immunol.* **2004**, *172*, 3758.
[307] M. G. Scott, A. C. Vreugdenhil, W. A. Buurman, R. E. Hancock, M. R. Gold, *J. Immunol.* **2000**, *164*, 549.
[308] T. Tal, M. Sharabani, I. Aviram, *J. Leukoc. Biol.* **1998**, *63*, 305.
[309] M. Dürr, A. Peschel, *Infect. Immun.* **2002**, *70*, 6515.
[310] W. C. Chan, P. D. White, in *Fmoc Solid Phase Peptide Synthesis: A Practical Approach* (Ed.: B. D. Hames), Oxford University Press, Oxford, **2000**.
[311] A. Aumelas, M. Mangoni, C. Roumestand, L. Chiche, E. Despaux, G. Grassy, B. Calas, A. Chavanieu, *Eur. J. Biochem.* **1996**, *237*, 575.
[312] D. A. Steinberg, M. A. Hurst, C. A. Fujii, A. H. Kung, J. F. Ho, F. C. Cheng, D. J. Loury, J. C. Fiddes, *Antimicrob. Agents Chemother.* **1997**, *41*, 1738.
[313] X. Wang, K. M. Morden, in *Methods in Molecular Biology, Vol. 78* (Ed.: W. M. Shafer), Humana Press, Totowa, **1997**, pp. 85.
[314] D. E. Stewart, A. Sarkar, J. E. Wampler, *J. Mol. Biol.* **1990**, *214*, 253.
[315] E. Vignal, A. Chavanieu, P. Roch, L. Chiche, G. Grassy, B. Calas, A. Aumelas, *Eur. J. Biochem.* **1998**, *253*, 221.
[316] K. Wüthrich, *NMR of proteins and nucleic acids*, Wiley, New York, **1986**.
[317] P. Guntert, C. Mumenthaler, K. Wuthrich, *J. Mol. Biol.* **1997**, *273*, 283.
[318] S. C. Lummis, D. L. Beene, L. W. Lee, H. A. Lester, R. W. Broadhurst, D. A. Dougherty, *Nature* **2005**, *438*, 248.
[319] C. J. Nelson, H. Santos-Rosa, T. Kouzarides, *Cell* **2006**, *126*, 905.
[320] T. Luders, G. A. Birkemo, J. Nissen-Meyer, O. Andersen, I. F. Nes, *Antimicrob. Agents Chemother.* **2005**, *49*, 2399.
[321] C. H. Hsu, C. Chen, M. L. Jou, A. Y. Lee, Y. C. Lin, Y. P. Yu, W. T. Huang, S. H. Wu, *Nucleic Acids Res.* **2005**, *33*, 4053.
[322] F. Smaill, *Can. J. Gastroenterol.* **2000**, *14*, 871.
[323] J. J. Biemer, *Ann. Clin. Lab. Sci.* **1973**, *3*, 135.
[324] D. F. Brown, D. I. Edwards, P. M. Hawkey, D. Morrison, G. L. Ridgway, K. J. Towner, M. W. Wren, *J. Antimicrob. Chemother.* **2005**, *56*, 1000.
[325] M. Ikawa, *Bacteriol. Rev.* **1967**, *31*, 54.
[326] L. Zhang, M. G. Scott, H. Yan, L. D. Mayer, R. E. Hancock, *Biochemistry* **2000**, *39*, 14504.
[327] S. A. Muhle, J. P. Tam, *Biochemistry* **2001**, *40*, 5777.
[328] L. Z. Yan, A. C. Gibbs, M. E. Stiles, D. S. Wishart, J. C. Vederas, *J. Med. Chem.* **2000**, *43*, 4579.
[329] C. Corbier, F. Krier, G. Mulliert, B. Vitoux, A. M. Revol-Junelles, *Appl. Environ. Microbiol.* **2001**, *67*, 1418.
[330] D. Drider, G. Fimland, Y. Hechard, L. M. McMullen, H. Prevost, *Microbiol. Mol. Biol. Rev.* **2006**, *70*, 564.
[331] A. M. Jones, M. E. Dodd, A. K. Webb, *Eur. Respir. J.* **2001**, *17*, 295.
[332] R. A. Rastall, *J. Nutr.* **2004**, *134*, 2022S.
[333] C. A. DeRyke, D. Maglio, D. P. Nicolau, *Expert Opin. Pharmacother.* **2005**, *6*, 873.
[334] R. Eckert, F. Qi, D. K. Yarbrough, J. He, M. H. Anderson, W. Shi, *Antimicrob. Agents Chemother.* **2006**, *50*, 1480.

[335] X. Q. Qiu, H. Wang, X. F. Lu, J. Zhang, S. F. Li, G. Cheng, L. Wan, L. Yang, J. Y. Zuo, Y. Q. Zhou, H. Y. Wang, X. Cheng, S. H. Zhang, Z. R. Ou, Z. C. Zhong, J. Q. Cheng, Y. P. Li, G. Y. Wu, *Nat. Biotechnol.* **2003**, *21*, 1480.
[336] X. Q. Qiu, J. Zhang, H. Wang, G. Y. Wu, *Antimicrob. Agents Chemother.* **2005**, *49*, 1184.
[337] C. Carbon, R. Isturiz, *Drugs* **2002**, *62*, 1289.
[338] D. I. Diekema, R. N. Jones, *Drugs* **2000**, *59*, 7.
[339] A. J. Wright, *Mayo Clin. Proc.* **1999**, *74*, 290.
[340] A. G. Madrigal, L. Basuino, H. F. Chambers, *Antimicrob. Agents Chemother.* **2005**, *49*, 3163.
[341] J. Retsema, A. Girard, W. Schelkly, M. Manousos, M. Anderson, G. Bright, R. Borovoy, L. Brennan, R. Mason, *Antimicrob. Agents Chemother.* **1987**, *31*, 1939.
[342] G. A. Pankey, L. D. Sabath, *Clin. Infect. Dis.* **2004**, *38*, 864.
[343] J. J. Jackson, H. Kropp, *J. Infect. Dis.* **1992**, *165*, 1033.
[344] L. R. Peterson, C. J. Shanholtzer, *Clin. Microbiol. Rev.* **1992**, *5*, 420.
[345] T. Butler, *J. Antimicrob. Chemother.* **2001**, *48*, 903.
[346] F. Soriano, *J. Antimicrob. Chemother.* **1992**, *30*, 566.
[347] M. E. Levison, P. G. Pitsakis, P. L. May, C. C. Johnson, *J. Antimicrob. Chemother.* **1993**, *32*, 577.
[348] V. H. Tam, A. N. Schilling, G. Vo, S. Kabbara, A. L. Kwa, N. P. Wiederhold, R. E. Lewis, *Antimicrob. Agents Chemother.* **2005**, *49*, 3624.
[349] S. Mizunaga, T. Kamiyama, Y. Fukuda, M. Takahata, J. Mitsuyama, *J. Antimicrob. Chemother.* **2005**, *56*, 91.
[350] A. Giacometti, O. Cirioni, F. Barchiesi, M. S. Del Prete, G. Scalise, *Peptides* **1999**, *20*, 1265.
[351] L. Steinstraesser, B. F. Tack, A. J. Waring, T. Hong, L. M. Boo, M. H. Fan, D. I. Remick, G. L. Su, R. I. Lehrer, S. C. Wang, *Antimicrob. Agents Chemother.* **2002**, *46*, 1837.
[352] P. Sood, A. Mandal, B. Mishra, *J. Antimicrob. Chemother.* **1999**, *43*, 425.
[353] R. C. Li, M. C. Tang, *J. Antimicrob. Chemother.* **2004**, *54*, 904.
[354] H. H. Haukland, L. H. Vorland, *J. Antimicrob. Chemother.* **2001**, *48*, 569.
[355] E. T. Kaiser, F. J. Kezdy, *Proc. Natl. Acad. Sci. U S A* **1983**, *80*, 1137.
[356] B. Christensen, J. Fink, R. B. Merrifield, D. Mauzerall, *Proc. Natl. Acad. Sci. U S A* **1988**, *85*, 5072.
[357] G. Flouret, V. Duvigneaud, *J. Am. Chem. Soc.* **1965**, *87*, 3775.
[358] J. M. Stewart, D. W. Woolley, *Nature* **1965**, *206*, 619.
[359] J. S. Morley, H. J. Tracy, R. A. Gregory, *Nature* **1965**, *207*, 1356.
[360] R. R. Neubig, M. Spedding, T. Kenakin, A. Christopoulos, *Pharmacol. Rev.* **2003**, *55*, 597.
[361] E. Fischer, *Ber. Dtsch. Chem. Ges.* **1894**, *27*, 2985.
[362] D. Wade, A. Boman, B. Wahlin, C. M. Drain, D. Andreu, H. G. Boman, R. B. Merrifield, *Proc. Natl. Acad. Sci. U S A* **1990**, *87*, 4761.
[363] R. Bessalle, A. Kapitkovsky, A. Gorea, I. Shalit, M. Fridkin, *FEBS Lett.* **1990**, *274*, 151.
[364] M. M. Shemyakin, Y. A. Ovchinnikov, V. T. Ivanov, A. V. Evstratov, *Nature* **1967**, *213*, 412.
[365] M. M. Shemyakin, Y. A. Ovchinnikov, V. T. Ivanov, *Angew. Chem. Int. Ed. Engl.* **1969**, *8*, 492.
[366] A. Pellegrini, U. Thomas, N. Bramaz, S. Klauser, P. Hunziker, R. von Fellenberg, *J. Appl. Microbiol.* **1997**, *82*, 372.
[367] W. M. Shafer, M. E. Shepherd, B. Boltin, L. Wells, J. Pohl, *Infect. Immun.* **1993**, *61*, 1900.
[368] K. Thevissen, I. E. Francois, L. Sijtsma, A. van Amerongen, W. M. Schaaper, R. Meloen, T. Posthuma-Trumpie, W. F. Broekaert, B. P. Cammue, *Peptides* **2005**, *26*, 1113.

[369] H. Ulvatne, L. H. Vorland, *Scand. J. Infect. Dis.* **2001**, *33*, 507.
[370] H. Tsubery, I. Ofek, S. Cohen, M. Fridkin, *Biochemistry* **2000**, *39*, 11837.
[371] B. Yasin, R. I. Lehrer, S. S. Harwig, E. A. Wagar, *Infect. Immun.* **1996**, *64*, 4863.
[372] M. G. Ryadnov, O. V. Degtyareva, I. A. Kashparov, Y. V. Mitin, *Peptides* **2002**, *23*, 1869.
[373] S. Vunnam, P. Juvvadi, K. S. Rotondi, R. B. Merrifield, *J. Pept. Res.* **1998**, *51*, 38.
[374] R. B. Merrifield, P. Juvvadi, D. Andreu, J. Ubach, A. Boman, H. G. Boman, *Proc. Natl. Acad. Sci. U S A* **1995**, *92*, 3449.
[375] E. L. Merrifield, S. A. Mitchell, J. Ubach, H. G. Boman, D. Andreu, R. B. Merrifield, *Int. J. Pept. Protein Res.* **1995**, *46*, 214.
[376] P. Diaz-Achirica, J. Ubach, A. Guinea, D. Andreu, L. Rivas, *Biochem. J.* **1998**, *330 (Pt 1)*, 453.
[377] J. M. Bland, A. J. De Lucca, T. J. Jacks, C. B. Vigo, *Mol. Cell Biochem.* **2001**, *218*, 105.
[378] J. Alvarez-Bravo, S. Kurata, S. Natori, *Biochem. J.* **1994**, *302 (Pt 2)*, 535.
[379] S. Y. Hong, J. E. Oh, K. H. Lee, *Biochem. Pharmacol.* **1999**, *58*, 1775.
[380] B. C. Chia, J. A. Carver, T. D. Mulhern, J. H. Bowie, *Eur. J. Biochem.* **2000**, *267*, 1894.
[381] M. L. Li, R. W. Liao, J. W. Qiu, Z. J. Wang, T. M. Wu, *Int. J. Antimicrob. Agents* **2000**, *13*, 203.
[382] R. Bucki, J. J. Pastore, P. Randhawa, R. Vegners, D. J. Weiner, P. A. Janmey, *Antimicrob. Agents Chemother.* **2004**, *48*, 1526.
[383] P. E. Kristiansen, G. Fimland, D. Mantzilas, J. Nissen-Meyer, *J. Biol. Chem.* **2005**, *280*, 22945.
[384] H. H. Hauge, J. Nissen-Meyer, I. F. Nes, V. G. Eijsink, *Eur. J. Biochem.* **1998**, *251*, 565.
[385] T. Mantyla, H. Sirola, E. Kansanen, T. Korjamo, H. Lankinen, K. Lappalainen, A. L. Valimaa, I. Harvima, A. Narvanen, *APMIS* **2005**, *113*, 497.
[386] D. Wade, J. Silberring, R. Soliymani, S. Heikkinen, I. Kilpelainen, H. Lankinen, P. Kuusela, *FEBS Lett.* **2000**, *479*, 6.
[387] Y. Chen, A. I. Vasil, L. Rehaume, C. T. Mant, J. L. Burns, M. L. Vasil, R. E. Hancock, R. S. Hodges, *Chem. Biol. Drug Des.* **2006**, *67*, 162.
[388] K. T. Miyasaki, A. L. Bodeau, J. Pohl, W. M. Shafer, *Antimicrob. Agents Chemother.* **1993**, *37*, 2710.
[389] C. Santamaria, S. Larios, S. Quiros, J. Pizarro-Cerda, J. P. Gorvel, B. Lomonte, E. Moreno, *Antimicrob. Agents Chemother.* **2005**, *49*, 1340.
[390] H. Wakabayashi, H. Matsumoto, K. Hashimoto, S. Teraguchi, M. Takase, H. Hayasawa, *Antimicrob. Agents Chemother.* **1999**, *43*, 1267.
[391] R. P. Darveau, J. Blake, C. L. Seachord, W. L. Cosand, M. D. Cunningham, L. Cassiano-Clough, G. Maloney, *J. Clin. Invest.* **1992**, *90*, 447.
[392] Y. Nakajima, J. Alvarez-Bravo, J. Cho, K. Homma, S. Kanegasaki, S. Natori, *FEBS Lett.* **1997**, *415*, 64.
[393] M. Andersson, A. Boman, H. G. Boman, *Cell. Mol. Life Sci.* **2003**, *60*, 599.
[394] T. L. Raguse, E. A. Porter, B. Weisblum, S. H. Gellman, *J. Am. Chem. Soc.* **2002**, *124*, 12774.
[395] A. Elmquist, U. Langel, *Biol. Chem.* **2003**, *384*, 387.
[396] R. A. Veach, D. Liu, S. Yao, Y. Chen, X. Y. Liu, S. Downs, J. Hawiger, *J. Biol. Chem.* **2004**, *279*, 11425.
[397] D. Derossi, S. Calvet, A. Trembleau, A. Brunissen, G. Chassaing, A. Prochiantz, *J. Biol. Chem.* **1996**, *271*, 18188.
[398] J. Oehlke, D. Lorenz, B. Wiesner, M. Bienert, *J. Mol. Recognit.* **2005**, *18*, 50.
[399] B. Haimovich, J. C. Tanaka, *Biochim. Biophys. Acta* **1995**, *1240*, 149.
[400] A. J. Miles, A. P. Skubitz, L. T. Furcht, G. B. Fields, *J. Biol. Chem.* **1994**, *269*, 30939.

[401] M. Nomizu, A. Utani, N. Shiraishi, M. C. Kibbey, Y. Yamada, P. P. Roller, *J. Biol. Chem.* **1992**, *267*, 14118.
[402] C. Li, J. B. McCarthy, L. T. Furcht, G. B. Fields, *Biochemistry* **1997**, *36*, 15404.
[403] D. Gerber, Y. Shai, *J. Mol. Biol.* **2002**, *322*, 491.
[404] N. Sal-Man, D. Gerber, Y. Shai, *J. Mol. Biol.* **2004**, *344*, 855.
[405] T. M. Suchyna, S. E. Tape, R. E. Koeppe, O. S. Andersen, F. Sachs, P. A. Gottlieb, *Nature* **2004**, *430*, 235.
[406] J. Y. Lehtonen, P. K. Kinnunen, *Biophys. J.* **1995**, *68*, 1888.
[407] S. Gudi, J. P. Nolan, J. A. Frangos, *Proc. Natl. Acad. Sci. U S A* **1998**, *95*, 2515.
[408] F. C. Neidhardt, J. L. Ingraham, *Escherichia coli and Salmonella typhimurium, cellular and molecular biology*, ASM, Washington, **1987**.
[409] S. T. Yang, S. Y. Shin, K. S. Hahm, J. I. Kim, *Biochim. Biophys. Acta* **2006**.
[410] S. T. Yang, J. H. Jeon, Y. Kim, S. Y. Shin, K. S. Hahm, J. I. Kim, *Biochemistry* **2006**, *45*, 1775.
[411] K. Matsuzaki, O. Murase, K. Miyajima, *Biochemistry* **1995**, *34*, 12553.
[412] K. Yoshida, Y. Mukai, T. Niidome, C. Takashi, Y. Tokunaga, T. Hatakeyama, H. Aoyagi, *J. Pept. Res.* **2001**, *57*, 119.
[413] K. Matsuzaki, M. Harada, S. Funakoshi, N. Fujii, K. Miyajima, *Biochim. Biophys. Acta* **1991**, *1063*, 162.
[414] E. J. Prenner, R. N. Lewis, M. Jelokhani-Niaraki, R. S. Hodges, R. N. McElhaney, *Biochim. Biophys. Acta* **2001**, *1510*, 83.
[415] A. J. Waring, S. S. L. Harwig, R. I. Lehrer, *Protein Pept. Lett.* **1996**, *3*, 177.
[416] T. Allen, in *Liposome Technology, Vol. 3* (Ed.: G. Gregoriadis), CRC Press Inc., Boca Raton, **1984**, p. 183.
[417] R. W. Williams, R. Starman, K. M. Taylor, K. Gable, T. Beeler, M. Zasloff, D. Covell, *Biochemistry* **1990**, *29*, 4490.
[418] R. R. C. New, *Liposomes*, IRL Press, Oxford, **1990**.
[419] T. C. Vogt, B. Bechinger, *J. Biol. Chem.* **1999**, *274*, 29115.
[420] T. M. Allen, L. G. Cleland, *Biochim. Biophys. Acta* **1980**, *597*, 418.
[421] G. R. Bartlett, *J. Biol. Chem.* **1959**, *234*, 466.
[422] F. Boato, Ph.D thesis, University of Zürich (Zürich), **2006**.
[423] G. Drin, J. Temsamani, *Biochim. Biophys. Acta* **2002**, *1559*, 160.
[424] G. Fujii, M. E. Selsted, D. Eisenberg, *Protein Sci.* **1993**, *2*, 1301.
[425] W. C. Wimley, M. E. Selsted, S. H. White, *Protein Sci.* **1994**, *3*, 1362.
[426] K. Matsuzaki, M. Harada, T. Handa, S. Funakoshi, N. Fujii, H. Yajima, K. Miyajima, *Biochim. Biophys. Acta* **1989**, *981*, 130.
[427] H. Schroder-Borm, R. Willumeit, K. Brandenburg, J. Andra, *Biochim. Biophys. Acta* **2003**, *1612*, 164.
[428] J. Ehrlich, Q. R. Bartz, R. M. Smith, D. A. Joslyn, P. R. Burkholder, *Science* **1947**, *106*.
[429] E. F. Gale, J. P. Folkes, *Biochem. J.* **1953**, *53*, 493.
[430] D. Gottlieb, P. K. Bhattacharyya, H. W. Anderson, H. E. Carter, *J. Bacteriol.* **1948**, *55*, 409.
[431] C. L. Wisseman, Jr., J. E. Smadel, F. E. Hahn, H. E. Hopps, *J. Bacteriol.* **1954**, *67*, 662.
[432] T. D. Brock, *Bacteriol. Rev.* **1961**, *25*, 32.
[433] H. Ryu do, A. Litovchick, R. R. Rando, *Biochemistry* **2002**, *41*, 10499.
[434] A. V. Reyonolds, J. M. Hamilton-Miller, W. Brumfitt, *J. Infect. Dis.* **1976**, *134*, S291.
[435] M. Kidwai, P. Misra, R. Kumar, *Curr. Pharm. Des.* **1998**, *4*, 101.
[436] R. C. Walker, *Mayo Clin. Proc.* **1999**, *74*, 1030.
[437] W. Wehrli, M. Staehelin, *Bacteriol. Rev.* **1971**, *35*, 290.
[438] C. Tribuddharat, M. Fennewald, *Antimicrob. Agents Chemother.* **1999**, *43*, 960.
[439] M. S. Rittenbury, *Surg. Gynecol. Obstet.* **1990**, *171*, S19.
[440] R. N. Brogden, R. C. Heel, *Drugs* **1986**, *31*, 96.

[441] P. Gerhardt, R. G. E. Murray, *Methods for general and molecular bacteriology*, ASM, Washington, D.C., **1994**.
[442] M. F. L'Annunziata, *Handbook of radioactivity analysis*, 2nd ed., Academic Press, San Diego, Calif., **2003**.
[443] R. J. Slater, *Radioisotopes in biology*, 2nd ed., Oxford University Press, Oxford, **2002**.
[444] M. Gottfredsson, H. Erlendsdottir, A. Gudmundsson, S. Gudmundsson, *Antimicrob. Agents Chemother.* **1995**, *39*, 1314.
[445] M. K. Lacy, D. P. Nicolau, C. H. Nightingale, R. Quintiliani, *Clin. Infect. Dis.* **1998**, *27*, 23.
[446] T. S. Elliott, J. B. Ward, H. J. Rogers, *J. Bacteriol.* **1975**, *124*, 623.
[447] D. M. Ferber, R. R. Brubaker, *Contrib. Microbiol. Immunol.* **1979**, *5*, 366.
[448] B. Skerlavaj, D. Romeo, R. Gennaro, *Infect. Immun.* **1990**, *58*, 3724.
[449] H. G. Sahl, H. Brandis, *Zentralbl. Bakteriol. Mikrobiol. Hyg.* **1982**, *252*, 166.
[450] D. J. Netz, C. Bastos Mdo, H. G. Sahl, *Appl. Environ. Microbiol.* **2002**, *68*, 5274.
[451] Y. Rosenfeld, Y. Shai, *Biochim. Biophys. Acta* **2006**, *1758*, 1513.
[452] S. Fidai, S. W. Farmer, R. E. W. Hancock, in *Methods in Molecular Biology, Vol. 78: Antibacterial Peptide Protocols* (Ed.: W. M. Shafer), Humana Press, Totowa, **1997**, pp. 187.
[453] S. G. Wilkinson, *Prog. Lipid Res.* **1996**, *35*, 283.
[454] Y. Kamio, H. Nikaido, *Biochemistry* **1976**, *15*, 2561.
[455] S. Paul, K. Chaudhuri, A. N. Chatterjee, J. Das, *J. Gen. Microbiol.* **1992**, *138*, 755.
[456] C. A. Janeway, Jr., R. Medzhitov, *Annu. Rev. Immunol.* **2002**, *20*, 197.
[457] S. I. Miller, R. K. Ernst, M. W. Bader, *Nat. Rev. Microbiol.* **2005**, *3*, 36.
[458] C. R. Raetz, C. Whitfield, *Annu. Rev. Biochem.* **2002**, *71*, 635.
[459] G. L. Su, R. L. Simmons, S. C. Wang, *Crit. Rev. Immunol.* **1995**, *15*, 201.
[460] L. J. Beamer, S. F. Carroll, D. Eisenberg, *Biochem. Pharmacol.* **1999**, *57*, 225.
[461] A. Hoess, S. Watson, G. R. Siber, R. Liddington, *EMBO J.* **1993**, *12*, 3351.
[462] R. L. Kitchens, P. A. Thompson, *J. Endotoxin Res.* **2005**, *11*, 225.
[463] M. Hirata, J. Zhong, S. C. Wright, J. W. Larrick, *Prog. Clin. Biol. Res.* **1995**, *392*, 317.
[464] J. W. Larrick, M. Hirata, H. Zheng, J. Zhong, D. Bolin, J. M. Cavaillon, H. S. Warren, S. C. Wright, *J. Immunol.* **1994**, *152*, 231.
[465] A. Giacometti, O. Cirioni, R. Ghiselli, F. Mocchegiani, M. S. Del Prete, C. Viticchi, W. Kamysz, L. E. E, V. Saba, G. Scalise, *Antimicrob. Agents Chemother.* **2002**, *46*, 2132.
[466] R. R. Schumann, N. Lamping, A. Hoess, *J. Immunol.* **1997**, *159*, 5599.
[467] J. Andra, M. Lamata, G. Martinez de Tejada, R. Bartels, M. H. Koch, K. Brandenburg, *Biochem. Pharmacol.* **2004**, *68*, 1297.
[468] P. Pristovsek, K. Feher, L. Szilagyi, J. Kidric, *J. Med. Chem.* **2005**, *48*, 1666.
[469] P. Mora, C. Mas-Moruno, S. Tamborero, L. J. Cruz, E. Perez-Paya, F. Albericio, *J. Pept. Sci.* **2006**, *12*, 491.
[470] A. Hoess, R. C. Liddington, *Lipopolysaccharide-binding and neutralizing peptides*, US6384188, **1993**.
[471] R. A. Moore, N. C. Bates, R. E. Hancock, *Antimicrob. Agents Chemother.* **1986**, *29*, 496.
[472] P. R. Schindler, M. Teuber, *Antimicrob. Agents Chemother.* **1975**, *8*, 95.
[473] J. Bader, M. Teuber, *Z. Naturforsch. [C]* **1973**, *28*, 422.
[474] L. H. Kondejewski, S. W. Farmer, D. S. Wishart, C. M. Kay, R. E. Hancock, R. S. Hodges, *J. Biol. Chem.* **1996**, *271*, 25261.
[475] M. Jelokhani-Niaraki, L. H. Kondejewski, S. W. Farmer, R. E. Hancock, C. M. Kay, R. S. Hodges, *Biochem. J.* **2000**, *349 Pt 3*, 747.
[476] H. Tsubery, I. Ofek, S. Cohen, M. Fridkin, *J. Med. Chem.* **2000**, *43*, 3085.
[477] C. Y. Park, S. H. Jung, J. P. Bak, S. S. Lee, D. K. Rhee, *Biologicals* **2005**, *33*, 145.
[478] N. Papo, Y. Shai, *J. Biol. Chem.* **2005**, *280*, 10378.

[479] R. E. Hancock, P. G. Wong, *Antimicrob. Agents Chemother.* **1984**, *26*, 48.
[480] M. T. Albrecht, W. Wang, O. Shamova, R. I. Lehrer, N. L. Schiller, *Respir. Res.* **2002**, *3*, 18.
[481] R. Weissleder, V. Ntziachristos, *Nat. Med.* **2003**, *9*, 123.
[482] G. T. Hermanson, *Bioconjugate Techniques*, Academic Press, San Diego, **1996**.
[483] A. S. Ladokhin, S. Jayasinghe, S. H. White, *Anal. Biochem.* **2000**, *285*, 235.
[484] A. H. Clayton, W. H. Sawyer, *Eur. Biophys. J.* **2002**, *31*, 9.
[485] D. M. Chudakov, S. Lukyanov, K. A. Lukyanov, *Trends Biotechnol.* **2005**, *23*, 605.
[486] B. A. Griffin, S. R. Adams, R. Y. Tsien, *Science* **1998**, *281*, 269.
[487] I. Chen, M. Howarth, W. Lin, A. Y. Ting, *Nat. Methods* **2005**, *2*, 99.
[488] L. Wang, J. Xie, P. G. Schultz, *Annu. Rev. Biophys. Biomol. Struct.* **2006**, *35*, 225.
[489] J. A. Prescher, C. R. Bertozzi, *Nat. Chem. Biol.* **2005**, *1*, 13.
[490] B. E. Cohen, T. B. McAnaney, E. S. Park, Y. N. Jan, S. G. Boxer, L. Y. Jan, *Science* **2002**, *296*, 1700.
[491] M. Nitz, A. R. Mezo, M. H. Ali, B. Imperiali, *Chem. Commun.* **2002**, 1912.
[492] G. D. Sui, P. Kele, J. Orbulescu, Q. Huo, R. M. Leblanc, *Lett. Pept. Sci.* **2001**, *8*, 47.
[493] N. Jotterand, D. A. Pearce, B. Imperiali, *J. Org. Chem.* **2001**, *66*, 3224.
[494] O. N. Burchak, L. Mugherli, F. Chatelain, M. Y. Balakirev, *Bioorg. Med. Chem.* **2006**, *14*, 2559.
[495] M. Taki, T. Hohsaka, H. Murakami, K. Taira, M. Sisido, *FEBS Lett.* **2001**, *507*, 35.
[496] I. Dufau, H. Mazarguil, *Tetrahedron Lett.* **2000**, *41*, 6063.
[497] R. B. Macgregor, G. Weber, *Nature* **1986**, *319*, 70.
[498] E. J. Corey, F. Xu, M. C. Noe, *J. Am. Chem. Soc.* **1997**, *119*, 12414.
[499] K. Shimada, K. Mitamura, M. Morita, K. Hirakata, *J. Liq. Chromatogr.* **1993**, *16*, 3311.
[500] D.-B. Li, unpublished work, **2003**.
[501] A. S. Ladokhin, S. H. White, *J. Mol. Biol.* **1999**, *285*, 1363.
[502] S. H. White, W. C. Wimley, A. S. Ladokhin, K. Hristova, *Methods Enzymol.* **1998**, *295*, 62.
[503] L. M. Loura, R. F. de Almeida, A. Coutinho, M. Prieto, *Chem. Phys. Lipids* **2003**, *122*, 77.
[504] X. S. Zheng, T. F. Chan, H. H. Zhou, *Chem. Biol.* **2004**, *11*, 609.
[505] L. Burdine, T. Kodadek, *Chem. Biol.* **2004**, *11*, 593.
[506] C. P. Hart, *Drug Discov. Today* **2005**, *10*, 513.
[507] R. D. Fleischmann, M. D. Adams, O. White, R. A. Clayton, E. F. Kirkness, A. R. Kerlavage, C. J. Bult, J. F. Tomb, B. A. Dougherty, J. M. Merrick, K. McKenney, G. Sutton, W. Fitzhugh, C. Fields, J. D. Gocayne, J. Scott, R. Shirley, L. I. Liu, A. Glodek, J. M. Kelley, J. F. Weidman, C. A. Phillips, T. Spriggs, E. Hedblom, M. D. Cotton, T. R. Utterback, M. C. Hanna, D. T. Nguyen, D. M. Saudek, R. C. Brandon, L. D. Fine, J. L. Fritchman, J. L. Fuhrmann, N. S. M. Geoghagen, C. L. Gnehm, L. A. McDonald, K. V. Small, C. M. Fraser, H. O. Smith, J. C. Venter, *Science* **1995**, *269*, 496.
[508] M. Margulies, M. Egholm, W. E. Altman, S. Attiya, J. S. Bader, L. A. Bemben, J. Berka, M. S. Braverman, Y. J. Chen, Z. Chen, S. B. Dewell, L. Du, J. M. Fierro, X. V. Gomes, B. C. Godwin, W. He, S. Helgesen, C. H. Ho, G. P. Irzyk, S. C. Jando, M. L. Alenquer, T. P. Jarvie, K. B. Jirage, J. B. Kim, J. R. Knight, J. R. Lanza, J. H. Leamon, S. M. Lefkowitz, M. Lei, J. Li, K. L. Lohman, H. Lu, V. B. Makhijani, K. E. McDade, M. P. McKenna, E. W. Myers, E. Nickerson, J. R. Nobile, R. Plant, B. P. Puc, M. T. Ronan, G. T. Roth, G. J. Sarkis, J. F. Simons, J. W. Simpson, M. Srinivasan, K. R. Tartaro, A. Tomasz, K. A. Vogt, G. A. Volkmer, S. H. Wang, Y. Wang, M. P. Weiner, P. Yu, R. F. Begley, J. M. Rothberg, *Nature* **2005**, *437*, 376.
[509] C. L. De Hoog, M. Mann, *Annu. Rev. Genomics Hum. Genet.* **2004**, *5*, 267.
[510] M. R. Wilkins, C. Pasquali, R. D. Appel, K. Ou, O. Golaz, J. C. Sanchez, J. X. Yan, A. A. Gooley, G. Hughes, I. Humphery-Smith, K. L. Williams, D. F. Hochstrasser, *Biotechnology* **1996**, *14*, 61.

[511] K. Riedel, P. Carranza, P. Gehrig, F. Potthast, L. Eberl, *Proteomics* **2006**, *6*, 207.
[512] S. Heim, M. Ferrer, H. Heuer, D. Regenhardt, M. Nimtz, K. N. Timmis, *Environ. Microbiol.* **2003**, *5*, 1257.
[513] S. J. Cordwell, A. S. Nouwens, N. M. Verrills, J. C. McPherson, P. G. Hains, D. D. Van Dyk, B. J. Walsh, *Electrophoresis* **1999**, *20*, 3580.
[514] R. A. VanBogelen, E. E. Schiller, J. D. Thomas, F. C. Neidhardt, *Electrophoresis* **1999**, *20*, 2149.
[515] R. A. VanBogelen, E. R. Olson, B. L. Wanner, F. C. Neidhardt, *J. Bacteriol.* **1996**, *178*, 4344.
[516] R. A. VanBogelen, F. C. Neidhardt, *Proc. Natl. Acad. Sci. U S A* **1990**, *87*, 5589.
[517] S. Evers, K. Di Padova, M. Meyer, H. Langen, M. Fountoulakis, W. Keck, C. P. Gray, *Proteomics* **2001**, *1*, 522.
[518] H. Gmuender, K. Kuratli, K. Di Padova, C. P. Gray, W. Keck, S. Evers, *Genome Res.* **2001**, *11*, 28.
[519] V. K. Singh, R. K. Jayaswal, B. J. Wilkinson, *FEMS Microbiol. Lett.* **2001**, *199*, 79.
[520] J. E. Bandow, D. Becher, K. Buttner, F. Hochgrafe, C. Freiberg, H. Brotz, M. Hecker, *Proteomics* **2003**, *3*, 299.
[521] C. M. Apfel, H. Locher, S. Evers, B. Takacs, C. Hubschwerlen, W. Pirson, M. G. Page, W. Keck, *Antimicrob. Agents Chemother.* **2001**, *45*, 1058.
[522] S. H. Yun, Y. H. Kim, E. J. Joo, J. S. Choi, J. H. Sohn, S. I. Kim, *Curr. Microbiol.* **2006**, *53*, 95.
[523] C. N. Lok, C. M. Ho, R. Chen, Q. Y. He, W. Y. Yu, H. Sun, P. K. Tam, J. F. Chiu, C. M. Che, *J. Proteome Res.* **2006**, *5*, 916.
[524] A. Görg, W. Weiss, M. J. Dunn, *Proteomics* **2004**, *4*, 3665.
[525] P. H. O'Farrell, *J. Biol. Chem.* **1975**, *250*, 4007.
[526] J. Klose, *Humangenetik* **1975**, *26*, 231.
[527] T. Linn, R. Losick, *Cell* **1976**, *8*, 103.
[528] F. S. Young, F. C. Neidhardt, *J. Bacteriol.* **1978**, *135*, 675.
[529] H. Liu, D. Lin, J. R. Yates, *Biotechniques* **2002**, *32*, 898.
[530] R. Aebersold, M. Mann, *Nature* **2003**, *422*, 198.
[531] K. Riedel, C. Arevalo-Ferro, G. Reil, A. Gorg, F. Lottspeich, L. Eberl, *Electrophoresis* **2003**, *24*, 740.
[532] C. Arevalo-Ferro, M. Hentzer, G. Reil, A. Gorg, S. Kjelleberg, M. Givskov, K. Riedel, L. Eberl, *Environ. Microbiol.* **2003**, *5*, 1350.
[533] C. Arevalo-Ferro, G. Reil, A. Gorg, L. Eberl, K. Riedel, *Syst. Appl. Microbiol.* **2005**, *28*, 87.
[534] C. K. Stover, X. Q. Pham, A. L. Erwin, S. D. Mizoguchi, P. Warrener, M. J. Hickey, F. S. Brinkman, W. O. Hufnagle, D. J. Kowalik, M. Lagrou, R. L. Garber, L. Goltry, E. Tolentino, S. Westbrock-Wadman, Y. Yuan, L. L. Brody, S. N. Coulter, K. R. Folger, A. Kas, K. Larbig, R. Lim, K. Smith, D. Spencer, G. K. Wong, Z. Wu, I. T. Paulsen, J. Reizer, M. H. Saier, R. E. Hancock, S. Lory, M. V. Olson, *Nature* **2000**, *406*, 959.
[535] M. M. Bradford, *Anal. Biochem.* **1976**, *72*, 248.
[536] D. N. Perkins, D. J. Pappin, D. M. Creasy, J. S. Cottrell, *Electrophoresis* **1999**, *20*, 3551.
[537] G. L. Winsor, R. Lo, S. J. Sui, K. S. Ung, S. Huang, D. Cheng, W. K. Ching, R. E. Hancock, F. S. Brinkman, *Nucleic Acids Res.* **2005**, *33*, D338.
[538] D. J. Pappin, P. Hojrup, A. J. Bleasby, *Curr. Biol.* **1993**, *3*, 327.
[539] D. E. Brodersen, P. Nissen, *FEBS J.* **2005**, *272*, 2098.
[540] N. Hasegawa, H. Arai, Y. Igarashi, *Biosci. Biotechnol. Biochem.* **2003**, *67*, 121.
[541] E. Vijgenboom, J. E. Busch, G. W. Canters, *Microbiology* **1997**, *143*, 2853.
[542] E. Kay, B. Humair, V. Denervaud, K. Riedel, S. Spahr, L. Eberl, C. Valverde, D. Haas, *J. Bacteriol.* **2006**, *188*, 6026.
[543] T. Nishijyo, S. M. Park, C. D. Lu, Y. Itoh, A. T. Abdelal, *J. Bacteriol.* **1998**, *180*, 5559.

[544] J. Trias, H. Nikaido, *Antimicrob. Agents Chemother.* **1990**, *34*, 52.
[545] G. M. Teitzel, A. Geddie, S. K. De Long, M. J. Kirisits, M. Whiteley, M. R. Parsek, *J. Bacteriol.* **2006**, *188*, 7242.
[546] J. Bodilis, M. Hedde, N. Orange, S. Barray, *Environ. Microbiol.* **2006**, *8*, 1544.
[547] L. Wu, O. Estrada, O. Zaborina, M. Bains, L. Shen, J. E. Kohler, N. Patel, M. W. Musch, E. B. Chang, Y. X. Fu, M. A. Jacobs, M. I. Nishimura, R. E. Hancock, J. R. Turner, J. C. Alverdy, *Science* **2005**, *309*, 774.
[548] X. Zhang, F. Beuron, P. S. Freemont, *Curr. Opin. Struct. Biol.* **2002**, *12*, 231.
[549] L. F. Wood, D. E. Ohman, *J. Bacteriol.* **2006**, *188*, 3134.
[550] C. Scholz, B. Eckert, F. Hagn, P. Schaarschmidt, J. Balbach, F. X. Schmid, *Biochemistry* **2006**, *45*, 20.
[551] G. Wulf, G. Finn, F. Suizu, K. P. Lu, *Nat. Cell Biol.* **2005**, *7*, 435.
[552] J. W. Zhang, G. Butland, J. F. Greenblatt, A. Emili, D. B. Zamble, *J. Biol. Chem.* **2005**, *280*, 4360.
[553] P. Gonzalo, J. P. Reboud, *Biol. Cell* **2003**, *95*, 179.
[554] S. Chandra Sanyal, A. Liljas, *Curr. Opin. Struct. Biol.* **2000**, *10*, 633.
[555] C. L. Squires, D. Zaporojets, *Annu. Rev. Microbiol.* **2000**, *54*, 775.
[556] M. V. Frolov, J. A. Birchler, *Genetics* **1998**, *150*, 1487.
[557] M. C. Wahl, W. Moller, *Curr. Protein Pept. Sci.* **2002**, *3*, 93.
[558] D. V. Laurents, S. Subbiah, M. Levitt, *Protein Sci.* **1994**, *3*, 1938.
[559] J. H. Abalain, S. Di Stefano, M. L. Abalain-Colloc, H. H. Floch, *J. Steroid Biochem. Mol. Biol.* **1995**, *55*, 233.
[560] M. E. Baker, *J. Steroid Biochem. Mol. Biol.* **1996**, *59*, 365.
[561] A. Markaryan, O. Zaborina, V. Punj, A. M. Chakrabarty, *J. Bacteriol.* **2001**, *183*, 3345.
[562] J. Ninio, *Biochimie* **2006**, *88*, 963.
[563] L. A. Kirsebom, R. Amons, L. A. Isaksson, *Eur. J. Biochem.* **1986**, *156*, 669.
[564] C. Kohler, S. Wolff, D. Albrecht, S. Fuchs, D. Becher, K. Buttner, S. Engelmann, M. Hecker, *Int. J. Med. Microbiol.* **2005**, *295*, 547.
[565] P. Folio, P. Chavant, I. Chafsey, A. Belkorchia, C. Chambon, M. Hebraud, *Proteomics* **2004**, *4*, 3187.
[566] S. H. Yoon, M. J. Han, S. Y. Lee, K. J. Jeong, J. S. Yoo, *Biotechnol. Bioeng.* **2003**, *81*, 753.
[567] S. Okano, Y. Shibata, T. Shiroza, Y. Abiko, *Proteomics* **2006**, *6*, 251.
[568] J. Mostertz, C. Scharf, M. Hecker, G. Homuth, *Microbiology* **2004**, *150*, 497.
[569] X. Peng, C. Xu, H. Ren, X. Lin, L. Wu, S. Wang, *J. Proteome Res.* **2005**, *4*, 2257.
[570] A. Bell, M. Bains, R. E. Hancock, *J. Bacteriol.* **1991**, *173*, 6657.
[571] E. L. Macfarlane, A. Kwasnicka, M. M. Ochs, R. E. Hancock, *Mol. Microbiol.* **1999**, *34*, 305.
[572] T. Guina, M. Wu, S. I. Miller, S. O. Purvine, E. C. Yi, J. Eng, D. R. Goodlett, R. Aebersold, R. K. Ernst, K. A. Lee, *J. Am. Soc. Mass Spectrom.* **2003**, *14*, 742.
[573] E. L. Macfarlane, A. Kwasnicka, R. E. Hancock, *Microbiology* **2000**, *146 (Pt 10)*, 2543.
[574] J. B. McPhee, S. Lewenza, R. E. Hancock, *Mol. Microbiol.* **2003**, *50*, 205.
[575] J. S. Gunn, K. B. Lim, J. Krueger, K. Kim, L. Guo, M. Hackett, S. I. Miller, *Mol. Microbiol.* **1998**, *27*, 1171.
[576] D. H. Kwon, C. D. Lu, *Antimicrob. Agents Chemother.* **2006**, *50*, 1615.
[577] J. B. McPhee, M. Bains, G. Winsor, S. Lewenza, A. Kwasnicka, M. D. Brazas, F. S. Brinkman, R. E. Hancock, *J. Bacteriol.* **2006**, *188*, 3995.
[578] I. E. Brodsky, J. S. Gunn, *Mol. Interv.* **2005**, *5*, 335.
[579] H. Pilsl, D. Smajs, V. Braun, *J. Bacteriol.* **1999**, *181*, 3578.
[580] W. C. Lee, K. H. Lee, *Anal. Biochem.* **2004**, *324*, 1.
[581] M. Azarkan, J. Huet, D. Baeyens-Volant, Y. Looze, G. Vandenbussche, *J. Chromatogr. B* **2006**.
[582] M. W. Harding, A. Galat, D. E. Uehling, S. L. Schreiber, *Nature* **1989**, *341*, 758.

[583] J. Taunton, C. A. Hassig, S. L. Schreiber, *Science* **1996**, *272*, 408.
[584] S. W. Ki, K. Ishigami, T. Kitahara, K. Kasahara, M. Yoshida, S. Horinouchi, *J. Biol. Chem.* **2000**, *275*, 39231.
[585] M. A. Trakselis, S. C. Alley, F. T. Ishmael, *Bioconjug. Chem.* **2005**, *16*, 741.
[586] D. A. Jeffery, M. Bogyo, *Curr. Opin. Biotechnol.* **2003**, *14*, 87.
[587] D. Greenbaum, K. F. Medzihradszky, A. Burlingame, M. Bogyo, *Chem. Biol.* **2000**, *7*, 569.
[588] G. Dorman, G. D. Prestwich, *Trends Biotechnol.* **2000**, *18*, 64.
[589] J. R. Colca, G. G. Harrigan, *Comb. Chem. High. Throughput Screen.* **2004**, *7*, 699.
[590] J. R. Colca, W. G. McDonald, D. J. Waldon, L. M. Thomasco, R. C. Gadwood, E. T. Lund, G. S. Cavey, W. R. Mathews, L. D. Adams, E. T. Cecil, J. D. Pearson, J. H. Bock, J. E. Mott, D. L. Shinabarger, L. Xiong, A. S. Mankin, *J. Biol. Chem.* **2003**, *278*, 21972.
[591] S. G. Bernier, J. M. Bellemare, E. Escher, G. Guillemette, *Biochemistry* **1998**, *37*, 4280.
[592] Y. Hatanaka, M. Hashimoto, Y. Kanaoka, *J. Am. Chem. Soc.* **1998**, *120*, 453.
[593] L. Q. Al-Mawsawi, V. Fikkert, R. Dayam, M. Witvrouw, T. R. Burke, Jr., C. H. Borchers, N. Neamati, *Proc. Natl. Acad. Sci. U S A* **2006**, *103*, 10080.
[594] F. Kotzybahibert, I. Kapfer, M. Goeldner, *Angew. Chem. Int. Ed. Engl.* **1995**, *34*, 1296.
[595] C. Bordier, *J. Biol. Chem.* **1981**, *256*, 1604.
[596] T. M. Cunningham, E. M. Walker, J. N. Miller, M. A. Lovett, *J. Bacteriol.* **1988**, *170*, 5789.
[597] J. P. Powers, M. M. Martin, D. L. Goosney, R. E. Hancock, *Antimicrob. Agents Chemother.* **2006**, *50*, 1522.
[598] R. A. Hall, *Methods Mol. Biol.* **2004**, *261*, 167.
[599] D. Shcherbakov, M. Dontsova, M. Tribus, M. Garber, W. Piendl, *Nucleic Acids Res.* **2006**.
[600] R. O. Mattos-Graner, K. A. Porter, D. J. Smith, Y. Hosogi, M. J. Duncan, *J. Bacteriol.* **2006**, *188*, 3813.
[601] H. E. Gottlieb, V. Kotlyar, A. Nudelman, *J. Org. Chem.* **1997**, *62*, 7512.
[602] M. R. Bendall, D. M. Doddrell, D. T. Pegg, *J. Am. Chem. Soc.* **1981**, *103*, 4603.
[603] E. Kaiser, R. L. Colescott, C. D. Bossinger, P. I. Cook, *Anal. Biochem.* **1970**, *34*, 595.
[604] G. L. Ellman, *Arch. Biochem. Biophys.* **1959**, *82*, 70.
[605] M. Piotto, V. Saudek, V. Sklenar, *J. Biomol. NMR* **1992**, *2*, 661.
[606] C. Griesinger, G. Otting, K. Wuthrich, R. R. Ernst, *J. Am. Chem. Soc.* **1988**, *110*, 7870.
[607] A. Kumar, R. R. Ernst, K. Wuthrich, *Biochem. Biophys. Res. Commun.* **1980**, *95*, 1.
[608] P. Luginbuhl, P. Guntert, M. Billeter, K. Wuthrich, *J. Biomol. NMR* **1996**, *8*, 136.
[609] R. Koradi, M. Billeter, K. Wuthrich, *J. Mol. Graph.* **1996**, *14*, 51.
[610] J. H. Mueller, J. Hinton, *Proc. Soc. Exp. Biol. Med.* **1941**, *48*, 330.
[611] NCCLS, *National Committe for Clinical Laboratory Standards, Approved standard M7-A3*, Villanova, **1993**.
[612] A. Jacobson, A. Petric, D. Hogenkamp, A. Sinur, J. R. Barrio, *J. Am. Chem. Soc.* **1996**, *118*, 5572.
[613] M. J. O'Donnell, R. L. Polt, *J. Org. Chem.* **1982**, *47*, 2663.
[614] P. Marfey, *Carlsberg Res. Comm.* **1984**, *49*, 591.
[615] H. Bruckner, C. Kellerhoehl, *Chromatographia* **1990**, *30*, 621.
[616] R. Westermeier, S. Gronau, *Electrophoresis in practice*, 4th ed., Wiley-VCH, Weinheim, **2005**.
[617] V. Neuhoff, N. Arold, D. Taube, W. Ehrhardt, *Electrophoresis* **1988**, *9*, 255.

Summary

This work was concerned with experiments aimed at elucidating the underlying mechanism(s) of antimicrobial action of a class of antimicrobial peptide mimetics (AMPMs), derived from naturally occurring β-hairpin antimicrobial peptides (AMPs). The latter are emerging as interesting antimicrobial agents, due to their promising activities against important multidrug resistant pathogens and their exqpected low tendency to generate bacterial (cross-) resistance. However, a major drawback in terms of therapeutic applicability is their generally high toxicity and/or high haemolytic activity, which is thought to be intrinsically related to the typical membrane-active (i.e. detergent-like) mode of action of these peptides.

It has been shown previously in our group that the antibacterial and haemolytic activities of prototypal β-hairpin AMPs could be separated from each other by suitable structural modifications. This led to the discovery of **16** as a broad spectrum β-hairpin AMPM based on protegrin-1. Furthermore, several rounds of screening led to later generations of AMPMs with a quite different selectivity as well as excellent activity towards the opportunistic bacterial pathogen *Pseudomonas aeruginosa* (with a minimal inhibitory concentration (MIC) corresponding to 4 nM for mimetic **19**).

It was demonstrated by bacteriological experiments such as the kinetics of bacterial killing, that the anti-pseudomonal activity of the later generation AMPMs, in particular of mimetic **18**, is characterised by a pronounced bacteriostatic effect during the first 2 hours following addition, which is in stark contrast to the behaviour expected for protegrin-like membrane-active AMPs. Additionally, an exceptionally large post antibiotic effect (PAE) of more than six hours was observed for mimetic **18** with *P. aeruginosa* PAO1.

The synthesis of the enantiomers of **16**, **17** and **18** showed that, in contrast to mimetic **16**, the anti-pseudomonal activity of later generation AMPMs depends on a stereospecific interaction of the compounds composed predominantly of L-amino acids with the target organism. Notably, this behaviour is highly unusual in the field of AMPs, except for Pro/Arg-rich insect AMPs such as pyrrhocoricin or apidaecin. Moreover, the greatly diminished broad spectrum antibacterial activity of ent-**17**

points towards the possibility of a residual membrane-lytic mode of action for the later generations of AMPMs.

Dye leakage experiments, in which large unilamellar vesicles composed of various ratios of either zwitterionic or negatively charged phospholipids were employed as model membrane systems, were carried out to study peptide-membrane interactions of **16** and **17**. It was found that both compounds were only able to permeabilise highly negatively charged liposomal systems towards the fluorescent dye calcein. These results are in agreement with the low haemolytic activity of **16** and **17**. However, neither compound was able to permeabilise membrane systems of mixed zwitterionic/negatively charged character.

In another biophysical approach, the *N*-α-Fmoc protected fluorescent amino acid DANA (**41**) was synthesized, which can be incorporated into the molecular framework of peptide mimetics during routine solid phase peptide synthesis. Membrane partitioning, as well as fluorescence microscopy experiments with DANA-labelled analogues of **16** and **17** were used to demonstrate the utility of site-specifically fluorescent labelling in mechanistic studies with peptide mimetics. Furthermore, it was shown by means of a displacement assay with dansylated polymyxin B, that binding to bacterial lipopolysaccharides (LPS) is neither responsible for the stereospecificity of later generation AMPMs nor for their selectivity towards *P. aeruginosa*.

To further investigate possible modes of action of the later generation AMPMs, the incorporation of radioactively labelled precursor molecules into the trichloroacetic acid insoluble fraction of *P. aeruginosa* PAO1 was studied. It was found that mimetic **18** exerted no immediate effect on the incorporation of radioactively labelled leucine, uridine, or adenine into bacterial macromolecules, thus suggesting that neither protein, RNA nor DNA biosynthesis are the primary targets for the class of compounds represented by **18**. Additionally, these experiments further corroborated the notion of an alternative mode of action for the later generation AMPMs, since for a membrane active mode of action an instantaneous cessation of macromolecular biosynthetic processes occurs.

With an alternative mode of action firmly established, both direct and indirect biochemical approaches towards the identification of a putative target of AMPMs in *P. aeruginosa* were followed. In an indirect approach, the protein expression profiles

of *P. aeruginosa* PAO1 grown in the presence and absence of mimetic **18** were recorded, using 2D gel electrophoresis coupled with mass spectrometric analysis for the identification of differentially regulated proteins. During this proteomic analysis, a total of 66 unique protein species whose regulation was affected by **18** could be identified, and out of these, a high proportion consisted of membrane or transport proteins. Additionally, a variety of heat shock proteins was found to be up-regulated in mimetic **18** challenged cell cultures, thus indicating the imposition of protein folding stress.

Furthermore, several analogues of mimetic **19** were synthesised that could be used in direct biochemical approaches towards target identification, such as affinity chromatography and photoaffinity labelling (PAL). More precisely, it was possible to incorporate the biotinylated amino acid H-Glu(biotinyl-PEG)-OH (**79**), as well as the two photo-reactive amino acids H-*p*-azido-Phe-OH (**90**) and *H*-p-benzoyl-Phe-OH (**91**) into the scaffold of mimetic **19** with excellent retention of the anti-pseudomonal activity. Additionally, several bi-functional PAL probes comprising both biotin and photo-reactive functionalities were synthesised, again with good retention of the biological activity of the parent compound.

Finally, affinity chromatography experiments with mimetic **19** immobilised on NHS-activated Sepharose showed that a variety of ribosomal proteins were retained on the affinity matrix. In particular several ribosomal proteins such as L7/L12 and L11, that are associated with the flexible stalk of the bacterial ribosome, were identified. Notably L7/12, which was also identified during the protein expression profiling experiments, is thought to be involved in proof-reading functions of the bacterial ribosome. Therefore, L7/L12 emerges as a promising lead for further investigations into the antimicrobial mechanism of action of β-hairpin AMPMs.

Zusammenfassung

Diese Arbeit befasst sich mit Experimenten zur Aufklärung des antimikrobiellen Wirkmechanismus einer Klasse antimikrobieller Peptidmimetika (AMPM), die auf den β-Haarnadel Strukturen natürlich vorkommender antimikrobiellen Peptiden (AMP) basiert. Letztere Verbindungen werden neuerdings vermehrt als vielsprechende antimikrobielle Wirkstoffe diskutiert, da sie einerseits über ein breites Aktivitätsspektrum gegenüber einer Vielzahl wichtiger Pathogene verfügen, und da ihnen andererseits eine geringe Tendenz zur Verursachung von Resistenzen zugewiesen wird. Allerdings ist ein möglicher therapeutischer Nutzen dieser Peptide, bedingt durch ihre hohe Toxizität und/oder hämolytische Aktivität, welche generell mit dem für diese Verbindungsklasse oftmals typischen lösungsmittelartigen Wirkmechanismus in Verbindung gebracht wird, sehr stark eingeschränkt.

In früheren Arbeiten unserer Gruppe gelang es jedoch, durch Einführung geeigneter struktureller Modifikationen wie dem D-Pro-L-Pro Templat, die antibakteriellen Eigenschaften prototypischer, natürlich vorkommender β-Haarnadel-Peptide von deren hämolytischen Aktivitäten zu trennen. Ausgehend von dem auf Protegrin-1 basierenden AMPM **16** führten mehrere Optimierungsschritte zu drei weiteren Generationen von AMPM, die sowohl eine bemerkenswerte Selektivität als auch eine ausgezeichnete Aktivität gegenüber dem Gram-negativen, opportunistischen Pathogen *Pseudomonas aeruginosa* aufweisen, und mit deren Vertretern **17**, **18** und **19** diese Arbeit sich im Wesentlichen befasste.

Es konnte durch bakteriologische Experimente, wie z. B. der Bestimmung der Kinetiken des bakteriellen Absterbevorgangs gezeigt werden, dass die anti-pseudomonale Aktivität von **18** während der ersten zwei Stunden nach der Induktion der spätereren Generationen von AMPM durch einen ausgeprägt bakteriostatischen Charakter gekennzeichnet ist. Dieses Ergebniss steht in grundsätzlichem Kontrast zu dem für membran-aktive AMP zu erwartetenden Verhalten. Darüber hinaus wurde ein ausgerwöhnlich langer post-antibiotischer Effekt (> 6h) von Mimetikum **18** auf Kulturen von *P. aeruginosa* PAO1 beobachtet.

Die Synthese der Enantiomere von **16**, **17** und **18** ergab, dass die anti-pseudomonale Aktivität der Vertreter späterer Generationen von AMPM, im Gegensatz zu Mimetikum **16**, von der stereospezifischen Wechselwirkung der hauptsächlich aus L-Animosäuren bestehenden AMPM mit dem Zielorganismus abhängt. Interessanterweise handelt es sich dabei um ein auf dem Gebiet der AMP - abgesehen von einigen Vertretern der Klasse Arg/Pro-reicher AMP wie Pyrrhocoricin oder Apidaecin - ungewöhnliches Verhalten. Ausserdem deutet die beochtete, wenngleich auch leicht verminderte breitspektrale Aktivität von ent-**17** auf eine mögliche Mitwirkungung eines membranlytischen Wirkmechanismusses zur antimikrobiellen Aktivität dieser Verbindungen hin.

Um Peptid-Membran Wechselwirkungen von **16** und **17** zu untersuchen, wurden Farbstoff-Freisetzungsversuche mit grossen unilamellaren Vesikeln, bestehend aus varienden Verhältnissen zwitterionischer und negativ geladener Phospholipide, durchgeführt. Dabei zeigte sich, dass beide Verbindungen nur in der Lage waren die aus ausschliesslich negativ geladenen Phospholipidien gebildeten Liposomen gegenüber dem Fluoreszensfarbstoff Calcein zu permeabilisieren, was auch in Übereinstimmung mit ihrer niedrigen hämolytischen Aktivität steht. In einem anderen biophysikalischen Ansatz wurde die fluoreszierende Aminosäure DANA (**41**) sythetisiert, die während der Festphasensynthese in das molekulare Grundgerüst der Peptidmimetika eingebaut werden kann. Membranepartitionierungs-Experimente und Fluoreszenzmikroskopie-Experimente mit DANA markierten Vertretern von **16** und **17** wurden durchgeführt, um den Nutzen dieser Verbindungen für mechanistische Studien mit Peptidmimetika zu verdeutlichen.

Zusätzlich konnte durch Verdrängungs-Experimente mit dansyliertem Polymyxin B gezeigt werden, dass eine bindende Wechselwirkung mit bakteriellen Lipopolysacchariden weder für die Stereospezifität noch für die Selektivität gegenüber *P. aeruginosa* der späteren Generationen der AMPM verantwortlich ist.

Um Hinweise auf mögliche Wirkmechanismen dieser Verbindungen zu erhalten, wurde der Einbau radioaktiv markierter Synthesebausteine der makromolekularen Biosynthese in die in Trichloressigsäure-unlösliche Fraktion von *P. aeruginosa* PAO1 untersucht. Es zeigte sich dabei, dass Mimetikum **18** keinen unmittelbaren Effekt auf den Einbau von radioaktiv markiertem Leucin, Uridin oder Adenin hatte, was darauf schliessen lässt, dass diese Verbindung keinen primären Einfluss auf die Protein, RNA oder DNA Biosynthese ausübt. Ausserdem bestätigten

diese Experimente, dass für Mimetikum **18** ein membran-lytischer Mechanismus, für den ein sofortiges Aussetzen aller makromolekularen biosynthetischen Prozesse erwartet wird, auszuschliessen ist.

Des Weiteren wurden sowohl direkte als auch indirekte Ansätze zur Identifizierung eines möglichen Zielmoleküles in *P. aeruginosa* verfolgt. In einem indirekten Ansatz wurden Zellen des sequenzierten Stammes PAO1 in Gegenwart oder Abwesenheit von Mimetikum **18** angezogen, Expressionsprofile dieser Kulturen mittels zweidimensionaler Gel-elektrophorese analysiert, und unterschiedlich regulierte Proteinspezies durch massenspektrometrischer Methoden identifiziert.

Dieser proteomische Ansatz der auch einen Vorfraktionierungsschritt in intrazelluläre, extrazelluläre und membrangebundene Proteine beinhaltete, führte zur Identifizierung von 66 einzigartiger Proteinspezies, deren Regulation durch das Mimetikum beeinflusst wurde. Diese waren durch eine hohe Anzahl an Membran- und Transportproteinen gekennzeichnet; ausserdem wurde eine Vielzahl von Hitzeschock-Proteinen positiv durch die Zugabe **18** reguliert, was auf einen Einfluss dieser Verbindung auf die Proteinfaltung hindeutet.

Abschliessend wurden mehre Analoge des Mimetikums **19** synthetisiert, die in direkten biochemischen Ansätzen zur Auffindung eines molekularen Zielmoleküls dieser Verbindungen, wie z.B. Affinitätschromatographie oder Photoaffinitätsmarkierung Verwendung finden können. Es gelang dabei, einerseits die biotinylierte Aminosäure **79**, sowohl andererseits eine der beiden photoreaktiven Aminosäuren **90** oder **91** in das Grundgerüst des Mimetikums **19** unter Beibehaltung der selektiven Aktivität einzubauen. Darüber hinaus wurden mehrere Probenmoleküle synthetisiert die sowohl Biotin- als auch photoreaktiv-funktionalisiert sind, und selektive Aktivität gegenüber *P. aeruginosa* aufweisen.

Affinitäts-chromatographische Experimente mit **19** zeigten, dass eine Vielzahl von ribosomalen Proteinen an einer mit diesem Mimetikum gebildeten Sepharose-Affinitätsmatrix zurückgehalten wurden. Einige dieser Proteine werden mit der flexiblen Stielstruktur des bakteriellen Ribosoms verknüpft oder konstituieren diese (L7/L12). Interessanterweise wurden letztere Proteinspezies, welche über ihre Funktion im bakteriellen Ribosom mit Korrekturfähigkeiten bei der Proteinsynthese in Verbindung gebracht werden, auch bei den Untersuchungen der Expressionsprofile identifiziert. Daher tritt L7/L12 as eine interessante Ausgangsspezies für

weiterführende Studien zum Wirkmechanismus der β-Haarnadel AMPM in Erscheinung.

Acknowledgements

I would like to thank my supervisor, *Prof. J. A. Robinson* for giving me the opportunity to work on this fascinating topic, and for his advice, encouragement and the freedom he allowed me throughout the work on my thesis.

I would also like to thank all the people who helped in the completion of this work, particularly:

Prof. Leo Eberl, *Dr. Kathrin Riedel* and *Paula Carranza* from the Department of Microbiology, Institute of Plant Biology, University of Zürich for introducing me to the world of proteomics, and for the help and guidance carrying out the expression profiling experiments.

Annelies Meier for carrying out most of the MIC testing.

Dr. Kerstin Möhle for NMR structure calculations, and for sharing her office with me.

Prof. Reto Schwendener for showing me how to prepare the liposomes used in this work.

Dr. Urs Ziegler for the acquisition of confocal fluorescence microscopy pictures.

The *NMR* and *MS service teams*.

I would also like to thank all members of the *Robinson group*, past and present, as well as all the members of the *Eberl group*, for the great atmosphere in the lab, and for their support, advice, encouragement, and friendship.

Curriculum Vitae

Name	Peter Jetter
Date of birth	2 February 1976
Place of birth	Crailsheim, Germany

Education

2002-2007 *Institute of Organic Chemistry, University of Zürich, Switzerland.*
PhD studies under the supervision of Prof. J. A. Robinson: "Studies on the Mode of Action of a Class of Antimicrobial Peptide Mimetics".

2003-2006 Teaching assistant in chemistry practical classes for biology and teacher students at the University of Zürich.

1996-2001 *Ruprecht-Karls-Universität Heidelberg, Germany.*
Undergraduate studies finished with a diploma thesis in the group of Prof. Dr. G. Helmchen: "Stereoselektive Synthese des (-)-5-Hydroxy-4-hydroxymethyl-hexahydrocyclopenta [*b*]furan-2-ons - ein Baustein zur Synthese von Isoprostanen und verwandten Verbindungen".

1999-2000 *Strathclyde University, Glasgow, UK.*
Erasmus exchange stay in the groups of Prof. Dr. R. E. Mulvey and Dr. J. Reglinski.

1986-1995 *Albert-Schweitzer-Gymnasium Crailsheim, Germany.*
Allgemeine Hochschulreife.

1982-1986 *Leonhard-Sachs-Schule Crailsheim, Germany.*